Oxidative Medicine and Cellular Longevity

Oxidative Stress in Aging Brain: Nutritional and Pharmacological Interventions for Neurodegenerative Disorders

Lead Guest Editor: Anna M. Giudetti
Guest Editors: Michel Salzet and Tommaso Cassano

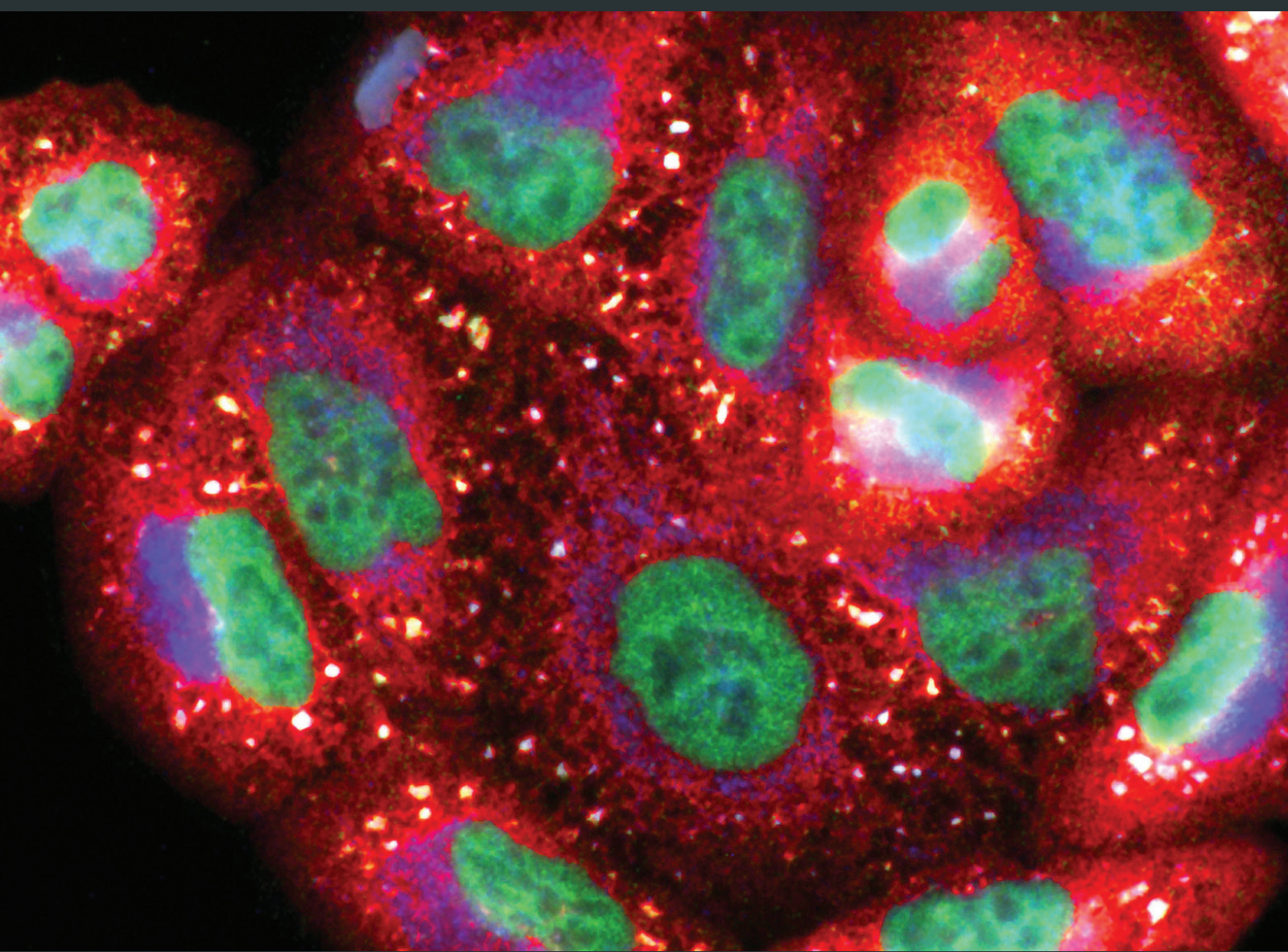

Oxidative Stress in Aging Brain: Nutritional and Pharmacological Interventions for Neurodegenerative Disorders

Oxidative Medicine and Cellular Longevity

Oxidative Stress in Aging Brain: Nutritional and Pharmacological Interventions for Neurodegenerative Disorders

Lead Guest Editor: Anna M. Giudetti
Guest Editors: Michel Salzet and Tommaso Cassano

Editorial Board

Contents

Hindawi
Oxidative Medicine and Cellular Longevity
Volume 2018, Article ID 3416028, 2 pages
https://doi.org/10.1155/2018/3416028

Editorial

Oxidative Stress in Aging Brain: Nutritional and Pharmacological Interventions for Neurodegenerative Disorders

Anna Maria Giudetti,[1] **Michel Salzet**,[2] **and Tommaso Cassano**[3]

[1]*Department of Biological and Environmental Sciences and Technologies, University of Salento, 73100 Lecce, Italy*
[2]*Inserm, U-1192 - Laboratoire Protéomique, Réponse Inflammatoire et Spectrométrie de Masse (PRISM), University of Lille, 59000 Lille, France*
[3]*Department of Clinical and Experimental Medicine, University of Foggia, 71100 Foggia, Italy*

Correspondence should be addressed to Anna Maria Giudetti; anna.giudetti@unisalento.it

Received 17 January 2018; Accepted 17 January 2018; Published 11 February 2018

A large and convincing body of evidence demonstrated that aging is characterized by a progressive decline in the efficiency of physiological functions due to the consequence of free radical-induced damage to cellular macromolecules. Moreover, the age-dependent inability to counterbalance these changes by endogenous antioxidant defenses can further contribute to the oxidative damages.

Many recent concepts of biology or medicine have underlined the importance of nutrition for the maintenance of "physiological" changes during aging or insults stemming from various degenerative diseases. The role of a balanced nutrition to human health is now well documented in different fields such as neuroscience.

Epidemiological analysis of the relations between nutrient consumption and neurodegeneration is complex and it is highly unlikely that a single component might play a major role. In addition, since multiple factors across the human lifespan might influence the brain function in adulthood and in the elderly, multidomain interventions might be more promising in the prevention of the neurodegeneration.

The interactions between lifestyle and brain health have been widely demonstrated, and recent studies have demonstrated the important role of antioxidants and vitamins in the antiaging process and in neurodegenerative disorders, such as Alzheimer's disease (AD) and Parkinson's disease (PD). Moreover, it has been demonstrated that caloric restriction could increase the functional and maximal lifespan, and accumulating evidence demonstrated that the selection of appropriate whole foods or the addition of antioxidants into the diet might be beneficial to increase the functional lifespan, if not the maximal lifespan. One could then argue that caloric selection may be as important as caloric restriction.

Along this line, the current special issue provides appreciable evidence showing that nutritional and pharmacological interventions based on their antioxidant properties might be particularly relevant for the onset and progression of neurodegenerative disorders.

The present volume, at which contributed eminent scholars, includes 10 original research articles and was organized in the attempt to cover the whole field of the interrelationship between oxidative stress, nutritional/pharmacological interventions, and neurodegenerative disorders.

To this regard, an interestingly cross-sectional analysis conducted by L. K. Mischley and colleagues on 1053 individuals affected by idiopathic PD demonstrated that a reduced rate of PD progression is associated to the consumption of different foods, including fresh vegetables, fresh fruit, nuts and seeds, nonfried fish, olive oil, wine, coconut oil, fresh herbs, and spices.

Studies have demonstrated that an altered arginine metabolism is involved in aging and neurodegenerative processes. M. Mazlan and colleagues found a chemical- and region-specific age-related alteration of L-arginine metabolism in the brain of old rats. Moreover, the authors reported that a three-month oral supplementation with vitamin E, in

the form of a tocotrienol-rich fraction, had beneficial effects on memory and motor function in old rats. The authors suggested that such effect was related to a reversion of age-associated changes in arginine metabolites in the entorhinal cortex and cerebellum.

Many efforts and resources have been spent in the last years to find new therapeutic strategies for the treatment of neurodegenerative disorders. Since most of these disorders have oxidative and inflammatory components, studies are geared in the finding of strategies to dampen these processes.

It is widely accepted that the main hallmarks of AD are not only senile plaques and neurofibrillary tangles, but also reactive astrogliosis, which contributes to neuronal loss depriving neurons of the homeostatic support. Palmitoylethanolamide (PEA) is an endogenous fatty acid amide, belonging to the class of nuclear factor agonists. PEA has been demonstrated to bind a nuclear receptor and to exert a great variety of biological functions. PEA has been shown to have anti-inflammatory, antinociceptive, neuroprotective, and anticonvulsant properties. M. R. Bronzuoli and colleagues found that PEA is able to dampen reactive astrogliosis and to promote the glial neuro supportive function, thus furnishing an alternative treatment approach for innovative therapeutic strategy against AD.

The study by S. An and colleagues described in a mouse model of AD the neuroprotective effects of mycelium polysaccharides (AMPS) obtained from *Armillaria mellea*, an edible fungus. In particular, AMPS reduced the apoptosis rate, amyloid beta (Aβ) deposition, oxidative damage, and phospho-Tau aggregations in the hippocampus of a murine model of AD. Moreover, AMPS enhanced horizontal movements in an autonomic activity test, improved endurance times in a rotarod test, and decreased escape latency time in a water maze test.

In the study by A. N. Winter and colleagues, the authors demonstrated that a whey protein supplement significantly protects neurons against diverse inducers of oxidative stress, providing the cystine for the synthesis of the endogenous antioxidant glutathione (GSH). The effect of the supplement was dependent on *de novo* GSH synthesis since the neuroprotection was blocked by the inhibition of γ-glutamyl-cysteine ligase, the first enzyme of the cellular eliminate GSH biosynthetic pathway.

Furthermore, D. Vergara and colleagues reported that resveratrol treatment led to a significant increase of GSH level and a reduction of GSSG/GSH ratio, as well as of reduced free thiol content in fibroblasts from parkin-mutant early-onset PD patients.

P. Priore and colleagues reported that oleic acid (OA) and hydroxytyrosol (HTyr), two different components of extra virgin olive oil, could affect lipid synthesis in C6 glioma cells. In particular, OA and HTyr inhibited both de novo fatty acid and cholesterol synthesis without affecting cell viability. Interestingly, the effect on lipid synthesis was more pronounced when OA and HTyr were coadministered to cells, suggesting a synergistic effect.

In the study by Z. Hou and colleagues, an edible bird's nest (EBN), traditionally used for general well-being, was used to improve the cognitive decline in ovariectomized rats compared to estrogen-treated rats. The results indicated that 12-week treatment with EBN was able to improve learning and memory in ovariectomized female rats without inducing liver toxicity, a side effect observed in the estrogen-treated group. The latter results suggest that EBN might be an effective alternative to estrogen therapy for menopause-induced aging-related memory loss.

It should be considered that the chronic use of drugs, approved to alleviate the symptoms of several neurodegenerative diseases, is often associated with debilitating side effects. Moreover, none of these drugs seems to stop the progression of the degenerative process. In keeping with this, the finding of new natural molecules useful for the treatment/preventions of neurodegenerative disorders acquires considerable significance. From this special issue, it appears evident that many studies are devoted to the finding of natural molecules directed at improving the symptoms of neurodegenerative diseases. In conclusion, the articles in this special issue offer tantalizing hints at the potential for new prevention strategies and treatments for people with neurodegenerative diseases, encompassing a wide variety of techniques and methods. We hope that these studies will inspire new and useful ideas to fill the gaps that remain in this critical area.

Anna Maria Giudetti
Michel Salzet
Tommaso Cassano

Hindawi
Oxidative Medicine and Cellular Longevity
Volume 2018, Article ID 4720532, 14 pages
https://doi.org/10.1155/2018/4720532

Research Article

Palmitoylethanolamide Dampens Reactive Astrogliosis and Improves Neuronal Trophic Support in a Triple Transgenic Model of Alzheimer's Disease: *In Vitro* and *In Vivo* Evidence

Maria Rosanna Bronzuoli,[1] Roberta Facchinetti,[1] Luca Steardo Jr.,[2] Adele Romano,[1] Claudia Stecca,[1] Sergio Passarella,[1] Luca Steardo,[1] Tommaso Cassano,[3] and Caterina Scuderi[1]

[1]*Department of Physiology and Pharmacology "V. Erspamer", Sapienza University of Rome, Rome, Italy*
[2]*Department of Psychiatry, University of Naples SUN, Naples, Italy*
[3]*Department of Clinical and Experimental Medicine, University of Foggia, Foggia, Italy*

Correspondence should be addressed to Tommaso Cassano; tommaso.cassano@unifg.it

Received 25 May 2017; Revised 2 October 2017; Accepted 23 October 2017; Published 16 January 2018

Academic Editor: Bruno Meloni

Alzheimer's disease (AD) is a neurodegenerative disorder responsible for the majority of dementia cases in elderly people. It is widely accepted that the main hallmarks of AD are not only senile plaques and neurofibrillary tangles but also reactive astrogliosis, which often precedes detrimental deposits and neuronal atrophy. Such phenomenon facilitates the regeneration of neural networks; however, under some circumstances, like in AD, reactive astrogliosis is detrimental, depriving neurons of the homeostatic support, thus contributing to neuronal loss. We investigated the presence of reactive astrogliosis in 3×Tg-AD mice and the effects of palmitoylethanolamide (PEA), a well-documented anti-inflammatory molecule, by *in vitro* and *in vivo* studies. *In vitro* results revealed a basal reactive state in primary cortical 3×Tg-AD-derived astrocytes and the ability of PEA to counteract such phenomenon and improve viability of 3×Tg-AD-derived neurons. *In vivo* observations, performed using ultramicronized- (um-) PEA, a formulation endowed with best bioavailability, confirmed the efficacy of this compound. Moreover, the schedule of treatment, mimicking the clinic use (chronic daily administration), revealed its beneficial pharmacological properties in dampening reactive astrogliosis and promoting the glial neurosupportive function. Collectively, our results encourage further investigation on PEA effects, suggesting it as an alternative or adjunct treatment approach for innovative AD therapy.

1. Introduction

Alzheimer's disease (AD) accounts for more than 80% of dementia cases worldwide in elderly people and leads to the progressive loss of mental, behavioral, and learning abilities and to functional decline [1]. Histopathologically, AD is characterized by two major protein deposits affecting mainly hippocampal and cortical regions: extracellular neuritic β-amyloid peptide (Aβ), which induces the creation of senile plaques (SPs), and the production of intracellular neurofibrillary tangles (NFTs) due to tau hyperphosphorylation that occupies much of the cytoplasm of pyramidal neurons [2, 3]. The presence of abnormally activated microglia and astrocytes is a feature of AD of more recent discovery [4]. It is followed by an intense inflammation, closely associated with amyloid deposits in the brain parenchyma [4, 5]. Indeed, studies of post mortem brain tissues from AD patients demonstrated the presence of a generalized astrogliosis, mainly manifested by astrocytic dysfunction, detectable by an increased expression of both glial fibrillary acidic protein (GFAP) and S100B, and accompanied by an increased production of proinflammatory mediators [6]. Many authors name this complex phenomenon as reactive astrogliosis [6, 7]. GFAP is a specific cytoskeletal

marker, whose expression is higher during astrogliosis [8]. S100B is a neurotrophin that, at physiological concentrations (nanomolar), exerts prosurvival effects on neurons and stimulates neurite outgrowth [9]. However, at higher (micromolar) concentrations, S100B becomes neurotoxic, promoting inflammation and neuronal apoptosis [10]. Aβ itself induces the expression of proinflammatory cytokines by glial cells [11] and the induction of proinflammatory enzymes, such as the inducible nitric oxide synthase (iNOS) and the isoenzyme cyclooxygenase type-2 (COX-2). Several lines of evidence suggest that all these factors may contribute to neuronal dysfunction and cell death, either alone or in concert [12]. The reactive astrogliosis has the initial intent of defence of removing injurious stimuli. However, if this phenomenon goes beyond physiological control, it may cause several detrimental effects. Under these circumstances, both neuronal and synaptic loss are detectable, because structural and functional modifications of neurons and astrocytes occur [13, 14]. Alterations of the neuronal marker microtubule-associated protein 2 (MAP-2), as well as modifications of the neurotrophin brain-derived neurotrophic factor (BDNF) content, have also been demonstrated [15, 16]. Considering the crucial actions of BDNF, especially in controlling neuronal survival, differentiation, neurotransmitter release, dendritic remodeling, axon growth, and synaptic plasticity [17, 18], the detrimental consequences of its alterations by reactive astrogliosis may be dramatic.

Based on this evidence, it is reasonable to assume that an early combination of neuroprotective and anti-inflammatory treatments may represent an efficacious approach to counteract AD. In this context, palmitoylethanolamide (PEA), an endogenous lipid mediator, seems to be a promising pharmacological agent. The anti-inflammatory and neuroprotective effects of PEA, as well as its ability to attenuate memory impairment in surgical models of AD, have already been demonstrated [15, 19–22].

In this work, we provide novel evidence on the ability of PEA to counteract reactive astrogliosis and neuronal impairment both *in vitro* and *in vivo*. For the *in vitro* studies, we used primary cortical neurons and astrocytes from 3×Tg-AD mice, a triple transgenic model of AD currently considered the closest to the familial human disease, and from wild-type littermates (non-Tg). The same AD model was used for the *in vivo* experiments, in which male 3-month-old 3×Tg-AD and sex- and age-matched non-Tg mice were subcutaneously implanted with a pellet, releasing either ultramicronized-PEA (um-PEA) or placebo, for three months. This treatment schedule was designed to reproduce a chronic treatment (as needed for this type of disease), administered starting from the early stage of the AD pathology.

In vitro results highlighted an intense activation and inflammation in primary 3×Tg-AD astrocytes, as well as the ability of PEA to counteract them and promote neuronal viability. Moreover, *in vivo* biochemical experiments demonstrated that chronic um-PEA treatment resulted in a beneficial control of the astrocyte activation and neuroinflammation. In addition, um-PEA interestingly increased BDNF levels, confirming its neuroprotective/neurotrophic effects.

Our results confirm the therapeutic potential of PEA, demonstrating its ability to counteract some of the detrimental effects occurring in AD, since the earliest stage of the pathology. PEA is already on the market for the treatment of pain. Therefore, these observations, in addition to the information regarding its safety and tolerability also in humans, prompt us to hypothesize a rapid translation into clinical practice.

2. Materials and Methods

All the procedures involving animals were conducted in conformity with the guidelines of the Italian Ministry of Health (D.L. 26/2014) and performed in compliance with the European Parliament directive 2010/63/EU.

2.1. Animals and Experimental Design. 3×Tg-AD mice [23] expressing APP_{swe}, $PS1_{M146V}$, and tau_{P301L} human transgenes were compared to non-Tg littermates. The background strain of 3×Tg-AD mice was C57BL6/129SvJ hybrid [23]. Animals were group housed and raised in controlled conditions ($22 \pm 2^{\circ}$C temperature, 12 h light/12 h dark cycle, 50%–60% humidity) in an enriched environment, with food and water ad libitum.

For *in vitro* experiments, we used newborn mice at postnatal day (PND) 1 or 2. Astrocytes were isolated from both non-Tg (total pups used = 12) and 3×Tg-AD (total pups used = 24) mice. Neurons were isolated from 3×Tg-AD mice (total pups used = 12).

For *in vivo* experiments, 3-month-old male non-Tg ($n = 18$) and 3×Tg-AD ($n = 18$) mice were used. Animals were surgically implanted with a 90-day-release pellet containing either 28 mg um-PEA, a formulation that improves its bioavailability [24], or placebo (catalogue number NX-999 and NC-111, resp.; Epitech Group SpA). Both pellets were made by Innovative Research of America (Sarasota, Florida) that homogeneously distributed um-PEA in the matrix, keeping its original crystalline form of micrometric size. Therefore, mice received 10 mg/kg/day for 3 consecutive months. Experimental dosage was chosen according to literature [25, 26].

To subcutaneously implant the pellet, mice were anesthetized with ketamine hydrochloride (1 mg/10 g) and xylazine (0.1 mg/10 g). After shaving the shoulder blades, the implantation area was sterilized with 70% alcohol. A dorsal midline incision of 1-2 cm was executed to create a subcutaneous pocket with a blunt probe. One pellet, containing um-PEA or placebo, was placed into the pocket and the surgical incision was closed with sterile absorbable sutures. Non-Tg and 3×Tg-AD mice were then left in their home cages for the next three months, and their weight monitored daily. No weight differences among all experimental groups were detected (data not shown). At the end of the chronic treatment, 6-month-old mice were killed by decapitation, and their brains were rapidly excised and either immediately frozen on dry ice for the immunofluorescence experiments or freshly dissected

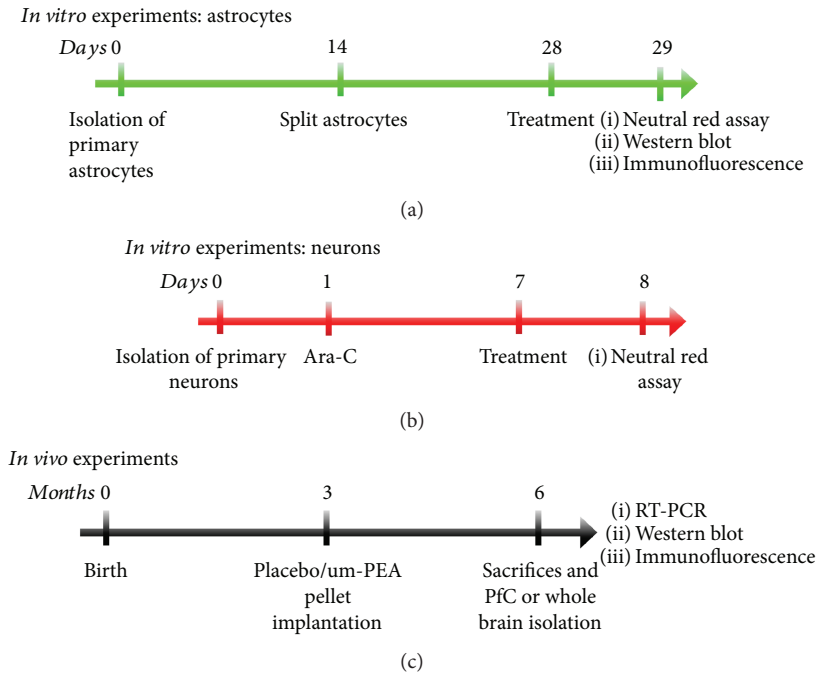

Figure 1: Study designs. Schematic representation of the experimental designs in (a) primary 3×Tg-AD and non-Tg astrocytes, (b) primary 3×Tg-AD neurons, and (c) *in vivo* experiments in 3×Tg-AD and non-Tg mice.

to isolate the frontal cortex (FC) for RT-PCR and Western blot analyses.

The experimental timelines are summarized in Figure 1.

2.2. Astroglial Primary Cultures. Astroglial primary cultures were obtained as previously described [27]. Cortices were isolated from non-Tg and 3×Tg-AD newborn mice (PND 1 or 2) sacrificed by decapitation. Tissues were manually homogenized in Dulbecco's modified Eagle's medium (DMEM) supplemented with 5% inactivated fetal bovine serum (FBS), 100 U/ml penicillin and 100 μg/ml streptomycin and then chemically dissociated with a solution containing 0.25% trypsin, 0.2% ethylenediaminetetraacetic acid (EDTA), and 0.2 mg/ml of DNAse I (all from Sigma-Aldrich, Milan, Italy) to obtain single cells. After a centrifugation at 403 ×g for 5 minutes, the medium was replaced, and surviving cells were counted using a Burker chamber with a 0.2% trypan blue solution and seeded at a density of 3×10^{-6} cells/75 cm^2 flask. Cell cultures were at +37°C in humidified atmosphere containing 5% CO_2. DMEM supplemented with 20% inactivated FBS and 100 U/ml penicillin, and 100 μg/ml streptomycin was replaced 24 h and one week after isolation. Approximately 14-15 days after the dissection, when a monolayer of cells was created, astrocytes were separated from microglia by mechanical shacking. Then, astrocytes were detached from the plates with a solution containing 0.25% trypsin and 0.2% EDTA and then seeded into 10 cm diameter petri dishes at a density of 1×10^6 cells/dish for Western blot analysis, into eight chambers polystyrene culture slides at a density of 3×10^4 cells/chamber (Thermo Fisher Scientific, MA, USA) for immunofluorescence, or into 24-well plates at a density of 1×10^5 cells/well for neutral red viability assay. Experiments were performed 28 days after cells isolation, when astrocytes are considered completely mature [22].

2.3. Neuronal Primary Cultures. Cortices from newborn 3×Tg-AD mice (PND 1 or 2) were used to obtain primary neuronal cultures as previously described [20]. Multiwells were previously coated with poly-L-lysine (Sigma-Aldrich) to allow neurons to adhere to the bottom of the wells. Mice were sacrificed by decapitation and cerebral cortices dissected in Hank's balanced salt solution (HBSS) containing 25 mM 4-(2-hydroxyethyl)-1-piperazineethanesulfonic acid (Hepes), 100 U/ml penicillin, and 100 μg/ml of streptomycin in cold conditions. Tissues were mechanically and chemically homogenized in a solution containing 0.25% trypsin, 0.2% EDTA, and 0.2 mg/ml of DNAse I (all from Sigma). After a centrifugation at 403 ×g for 5 minutes, cells were suspended in neurobasal media supplemented with 2% B27, 100 U/ml penicillin, and 100 μg/ml streptomycin. Then, they were counted using a Burker chamber while suspended in 0.2% trypan blue solution and then seeded in 24-well multiplates at a density of 5×10^{-5} cells/well. Neuronal cultures were maintained at +37°C in humidified atmosphere containing 5% CO_2. Twenty-four hours later, cells were treated with 10 μM of cytosine arabinoside (ara-C) to suppress glial cell growth. One week later, primary 3×Tg-AD-derived neurons were treated with PEA.

2.4. Chemicals and Cell Treatments. Mature astrocytes and neurons derived from 3×Tg-AD mice were treated with PEA (Epitech Group SpA, Saccolongo, Italy), at three different concentrations (0.01, 0.1, and 1 μM), chosen according to our previous works [19, 20, 22]. PEA was suspended in 5% pluronic F-68 (Sigma-Aldrich) and solubilized in 95%

Table 1: Experimental conditions for immunofluorescence.

Primary antibody	Brand primary antibody	Primary antibody dilution	Secondary antibody	Brand secondary antibody
Rabbit α-GFAP	Abcam	1 : 1000 0.5% BSA in TBS/0.25% triton X-100	FITC conjugated goat anti-rabbit IgG (H+L) 1 : 200, 0.5% BSA in TBS/0.25% triton X-100	Jackson ImmunoResearch
Rabbit α-S100B	Novus Biologicals	1 : 250 0.5% BSA in TBS/0.25% triton X-100	TRITC conjugated goat anti-rabbit IgG (H+L) 1 : 200, 0.5% BSA in TBS/0.25% triton X-100	Jackson ImmunoResearch
Mouse α-MAP2	Novus Biologicals	1 : 250 0.5% BSA in TBS/0.25% triton X-100	TRITC conjugated goat anti-mouse IgG (H+L) 1 : 200, 0.5% BSA in TBS/0.25% triton X-100	Jackson ImmunoResearch

DMEM. First, we added pluronic F-68 to PEA powder and sonicated the emulsion for 20 min protecting it from light, and then we included DMEM to complete the solution. Viability assay, Western blot analysis, and immunofluorescence were performed 24 h after treatments.

2.5. Analysis of Astrocyte and Neuronal Viability by Neutral Red Uptake Assay. Astrocyte and neuronal viability was tested 24 h after treatment by neutral red uptake assay, as previously described [27]. Cells were incubated with a neutral red working solution, containing 50 μg/ml in Ca^{2+} and Mg^{2}-free PBS (Sigma-Aldrich), for 3 h at +37°C. Cells were then rinsed in Ca^{2+}- and Mg^{2}-free PBS and the dye removed from the inside of the cells through a rinse in destaining solution (ethanol : deionized water : glacial acetic acid, 50 : 49 : 1 *v*/*v*). The absorbance, whose value is proportional to the number of living cells, was read at 540 nm using a microplate spectrophotometer (Epoch, BioTek, Winooski, VT, USA). The values obtained were referred to control medium-exposed cultures (CTRL) and expressed as percentage variation of CTRL. Three independent experiments were performed in triplicate.

2.6. Immunofluorescence. Both primary astrocytes, 24 h after treatment, and non-Tg and 3×Tg-AD coronal slices (12 μm thickness), deriving from 6-month-old mice containing the FC, were rinsed in PBS and postfixed for 10 minutes at +4°C with 4% paraformaldehyde (PFA) prepared in PBS. Then, samples were blocked with 1% bovine serum albumin (BSA) prepared in PBS/0.25% triton X-100 for 90 minutes at room temperature. Cells were incubated overnight at +4°C in 0.5% BSA in Tris-buffered saline (TBS)/0.25% triton X-100 solution containing the primary antibodies rabbit anti-GFAP (1 : 1000, Abcam, Cambridge, USA) or rabbit anti-S100B (1 : 250, Novus Biologicals, Littleton, CO, USA). FC slices, instead, were incubated overnight at +4°C with mouse anti-MAP2 (1 : 250, Novus Biologicals, Littleton, CO, USA) in 0.5% BSA in TBS/0.25% triton X-100 solution. The following day, cells and tissues were thoroughly rinsed in PBS and then incubated for 2 hours at room temperature with the appropriate secondary antibody (fluorescein- (FITC-) conjugated AffiniPure goat anti-rabbit IgG (H+L), rhodamine- (TRITC-) conjugated AffiniPure goat anti-rabbit IgG (H+L), 1 : 200, or rhodamine- (TRITC-) conjugated AffiniPure goat anti-mouse IgG (H+L); Jackson ImmunoResearch, Suffolk, UK). Nuclei were stained with 4′,6-diamidino-2-phenylindole, dihydrochloride (DAPI) (1 : 75000, Sigma-Aldrich) in 0.5% BSA in TBS/0.25% triton X-100, added to the solution of the secondary antibodies. Samples were rinsed with PBS and coverslipped using Fluoromount aqueous mounting medium (Sigma-Aldrich). Experimental conditions are summarized in Table 1.

Pictures were captured with a wide-field microscope (Eclipse E600; Nikon Instruments, Rome, Italy) and densitometric analysis performed using ImageJ software. Data are expressed as ratio ($\Delta F/F_0$) of the difference between the mean of fluorescence sample and its background (ΔF) and the non-immunoreactive regions (F_0). To prevent the observation of differences among experimental groups due to artifacts, the exposure parameters, such as gain and time, were kept constant during image acquisitions. For each analysis, three replicates were used, and at least three independent experiments were performed.

2.7. RNA Isolation and RT-PCR. Total mRNA from FC of both non-Tg and 3×Tg-AD mice was extracted using the NZY total RNA isolation kit (NZYTech, Lisboa, Portugal) following the manufacturer's protocol. Total mRNA was quantified by Nanodrop 1000 spectrophotometer (Thermo Fisher Scientific, MA, USA). Revers transcription of 1 μg mRNA was performed to obtain cDNA adding oligo(dT) and random primers to the first-strand cDNA synthesis kit (NZYTech, Lisboa, Portugal). All PCRs were performed using the supreme NZYTaq DNA polymerase (NZYTech, Lisboa, Portugal) in the presence of specific primers (Sigma-Aldrich) for the target genes: GFAP, GAPDH, S100B, iNOS, and COX-2. GAPDH was used as reference gene. Three independent experiments were performed in triplicate. Primer sequences and PCR details are reported in Table 2.

2.8. Protein Extraction and Western Blot Analysis. Western blot analysis was performed on protein extracts obtained from primary astrocytic cultures as well as from FC samples, as previously described [15]. Samples were suspended in ice-cold hypotonic lysis buffer containing 50 mM Tris/HCl pH 7.5, 150 mM NaCl, 1 mM EDTA, 1% triton X-100, 1 mM phenylmethylsulfonyl fluoride (PMSF), 10 μg/ml aprotinin, and 0.1 mM leupeptin (all from Sigma-Aldrich). After 40 min of incubation at +4°C, homogenates were centrifuged at 18440 ×g for 30 min and the supernatant collected and stored in aliquots at −80°C until use. An equivalent

Table 2: Primer sequences used for RT-PCR.

Sequence of interest		Primer $5'\rightarrow3'$	Annealing temperature (°C)	Number of cycles
GFAP	Forward	GAAGAGGGACAACTTTGCAC	61	32
	Reverse	GCTCTAGGGACTCGTTCGTG		
S100B	Forward	TAATGTGAGTGGCTGCGGAA	63	32
	Reverse	CCTCACCAAGGGCTAAGCAG		
iNOS	Forward	CAAGCTGATGGTCAAGATCCAGAG	64	40
	Reverse	GTGCCCATGTACCAACCATTGAAG		
COX-2	Forward	GCTGTACAAGCAGTGGCAAA	62	30
	Reverse	CCCCAAAGATAGCATCTGGA		
GAPDH	Forward	GCTACACTGAGGACCAGGTTGTC	64	30
	Reverse	CCATGTAGGCCATGAGGTCCAC		

Table 3: Experimental conditions for Western blot from 3×Tg-AD mice astrocytes and FC.

Primary antibody	Brand primary antibody	Dilution	Secondary antibody	Brand secondary antibody
GFAP	Abcam	1 : 50000 5% milk in TBS-T 0.1%	HRP conjugated goat anti-rabbit IgG 1 : 30000 5% milk in TBS-T 0.1%	Jackson ImmunoResearch
S100B	Novus Biologicals	1 : 1000 5% BSA in TBS-T 0.1%	HRP conjugated goat anti-rabbit IgG 1 : 10000 5% BSA in TBS-T 0.1%	Jackson ImmunoResearch
COX-2	Cell Signaling	1 : 1000 5% milk in TBS-T 0.1%	HRP conjugated goat anti-rabbit IgG 1: 10000 5% milk in TBS-T 0.1%	Jackson ImmunoResearch
iNOS	Sigma-Aldrich	1 : 8000 1% BSA in TBS-T 0.1%	HRP conjugated goat anti-rabbit IgG 1 : 10000 1% BSA in TBS-T 0.1%	Jackson ImmunoResearch
BDNF	Santa Cruz	1 : 500 5% milk in TBS-T 0.1%	HRP conjugated goat anti-rabbit IgG 1 : 10000 5% milk in TBS-T 0.1%	Jackson ImmunoResearch
MAP2	Novus Biologicals	1 : 250 5% BSA in TBS-T 0.1%	HRP conjugated goat anti-rabbit IgG 1 : 10000 5% BSA in TBS-T 0.1%	Jackson ImmunoResearch
$A\beta_{(1-42)}$	Millipore	1 : 1000 5% BSA in TBS-T 0.1%	HRP conjugated goat anti-mouse IgG 1 : 10000 5% BSA in TBS-T 0.1%	Jackson ImmunoResearch
β-actin	Santa Cruz	1 : 1500 5% milk in TBS-T 0.1%	HRP conjugated goat anti-rabbit IgG 1 : 10000 5% milk in TBS-T 0.1%	Jackson ImmunoResearch

amount of each sample (50 μg), calculated by Bradford assay, was resolved through 12% acrylamide SDS-PAGE precast gels (Bio-Rad Laboratories, Segrate, Italy). Then, with a trans-blot SD semidry transfer cell (Bio-Rad Laboratories), proteins were transferred onto nitrocellulose membranes that were then blocked with 5% no-fat dry milk powder or 5% BSA in TBS 0.1% Tween 20 (TBS-T) (Tecnochimica Moderna, Rome, Italy) for 1 h before overnight incubation at +4°C with the appropriate primary antibodies. After appropriate rinses in 0.05% TBS-T, membranes were incubated for 1 h at room temperature with a specific secondary horseradish peroxidase- (HRP-) conjugated antibody. The experimental conditions are summarized in Table 3.

Immunocomplexes were detected by an ECL kit (GE Healthcare Life Sciences, Milan, Italy), exposed to X-ray film (GE Healthcare Life Sciences, Milan, Italy) and quantified using ImageJ software. Protein expression level of β-actin was used as loading control. For each antibody, three replicates were used, and at least three independent experiments were performed.

2.9. Statistical Analysis. Analysis was performed using GraphPad Prism software (GraphPad Software, San Diego, CA, USA). Student's *t*-test was used to compare two groups. One-way analysis of variance (ANOVA) was used to determine statistical differences among experimental groups in *in vitro* experiments. *In vivo* results were analyzed by two-way ANOVA, with genotype and treatment as factors. Bonferroni's post hoc test was used upon detection of a main significant effect. Differences between mean values were considered statistically significant when $P < 0.05$.

3. Results

3.1. 3×Tg-AD Primary Astrocytes Present Reactive Astrogliosis. Reactive astrogliosis is a phenomenon commonly detectable in AD brains and characterized by both astrocyte activation and neuroinflammation [6]. Here, we decided to test parameters connected with such events in both non-Tg and 3×Tg-AD primary astrocytes.

To study astrocyte activation, we tested the expression of GFAP, a specific cytoskeletal marker, and S100B, a neurotrophin that when present at high concentrations becomes neurotoxic [6, 28, 29]. Results obtained from both immunofluorescence and Western blot analysis showed a significantly higher GFAP immunoreactivity in primary 3×Tg-AD astrocytes than non-Tg cells (immunofluorescence: $P < 0.05$; Western blot $P < 0.01$) (Figures 2(a), 2(b), 2(e), and 2(f)), while we did not detect changes in S100B signal ($P > 0.05$) (Figures 2(c), 2(d), 2(e), and 2(g)).

A neuroinflammatory environment is mainly characterized by the production and activation of two inducible enzymes: the prostanoid-generating enzyme COX-2 and iNOS [15]. Here, we tested the expression of these two enzymes in non-Tg and 3×Tg-AD primary astrocytes. Results showed that iNOS expression is significantly higher in transgenic-derived primary astrocytes than non-Tg cells ($P < 0.01$) (Figures 2(e) and 2(h)). We did not find any statistical difference in COX-2 expression between the two experimental groups ($P > 0.05$) (Figures 2(e) and 2(i)).

Collectively, these results show that reactive astrogliosis is detectable in mature 3×Tg-AD cortical astrocytes.

3.2. PEA Improves Neuronal Viability and Counteracts Reactive Astrogliosis In Vitro. To test whether PEA treatment could have any toxic effect on astrocyte and neuronal viability, we performed the neutral red assay. Results showed that PEA did not affect astrocytes or neuronal viability at all concentrations tested ($P > 0.05$) (Figures 3(a) and 3(b)). Surprisingly, the highest PEA concentration significantly improved neuronal viability (+5.35%; $P < 0.001$) (Figure 3(b)).

Next, we tested the ability of PEA, at different concentrations (0.01, 0.1, and 1 μM), to counteract reactive astrogliosis. Western blot analyses showed that PEA treatment prevented GFAP increase in primary astrocytes derived from newborn 3×Tg-AD mice in a concentration-dependent manner ($P < 0.05$) (Figures 3(c) and 3(d)). Results by immunofluorescence confirmed this trend, although only the highest dose of PEA reached statistical significance ($P < 0.05$) (Figures 3(f) and 3(g)). Moreover, by Western blot, we found that 1 μM PEA was able to significantly reduce iNOS expression ($P < 0.05$) (Figures 3(c) and 3(e)).

These results show that PEA has no toxicity in both astrocytes and neurons from 3×Tg-AD mice, at the concentrations tested; rather, it promotes neuron viability. Moreover, PEA counteracts reactive astrogliosis in mature 3×Tg-AD primary astrocytes.

3.3. Chronic Um-PEA Normalizes Reactive Astrogliosis in the Frontal Cortex of 3×Tg-AD Mice. Given the interesting *in vitro* results, and with the aim of further exploring PEA effectiveness in the triple transgenic model of AD, we decided to translate the study *in vivo*. Specifically, we tested the effect of chronic um-PEA treatment on reactive astrogliosis and neuronal functionality in FCs of 6-month-old 3×Tg-AD mice, compared to their age-matched non-Tg littermates.

Confirming our *in vitro* observations, we found astrocyte activation in FC of 3×Tg-AD mice when compared with their age-matched non-Tg littermates. Indeed, we found, by RT-PCR and Western blot, an increase of both GFAP and S100B expression in placebo-treated 3×Tg-AD mice in comparison with placebo-treated non-Tg mice ($P < 0.05$) (Figures 4(a), 4(b), 4(c), 4(f), 4(g), and 4(h)). Um-PEA chronic treatment greatly controlled such astrocytic activation, significantly decreasing GFAP mRNA and protein expression ($P < 0.05$) (Figures 4(a), 4(b), 4(f), and 4(g)). Moreover, the two-way ANOVA showed a significant genotype-by-treatment interaction effect on GFAP transcription ($F_{\text{genotype}\times\text{treatment}(1,23)} = 7.872$, $P = 0.0062$) (Figure 4(g)) and expression ($F_{\text{genotype}\times\text{treatment}(1,23)} = 4.829$, $P = 0.0337$) (Figure 4(g)). Surprisingly, um-PEA also induced a trend toward a decrease (−20%) of S100B protein expression in 3×Tg-AD mice compared to placebo-treated 3×Tg-AD ones (Figures 4(a), 4(c), 4(f), and 4(h)).

Regarding the parameters related to the inflammatory process, RT-PCR and Western blot results showed a significant increase of iNOS transcription ($P < 0.001$) (Figures 4(a) and 4(d)) and expression ($P < 0.05$) (Figures 4(f) and 4(i)) in the FC of placebo-treated 3×Tg-AD mice in comparison with placebo-treated non-Tg animals. Interestingly, chronic um-PEA treatment greatly controlled the induced production of this proinflammatory enzyme (RT-PCR: $P < 0.001$; Western blot: $P < 0.05$) (Figures 4(a), 4(d), 4(f), and 4(i)). In addition, two-way ANOVA showed a significant genotype-by-treatment interaction effect in iNOS transcription ($F_{\text{genotype}\times\text{treatment}(1,23)} = 28.37$, $P < 0.0001$) (Figure 4(d)) and protein expression ($F_{\text{genotype}\times\text{treatment}(1,23)} = 4.894$, $P = 0.0306$) (Figure 4(i)). As in *in vitro* results, neither genotype nor treatment induced changes in COX-2 transcript and protein expression (Figures 4(a), 4(e), 4(f), and 4(j)).

Interestingly, using Western blot experiments, we found a trend toward an increase of $A\beta_{(1-42)}$ (+20%) in the FCs of transgenic mice in comparison with the non-Tg animals. This trend, which follows the observed changes in parameters related to astrocyte activation and neuroinflammation, is in line with the evidence available in literature indicating that 6-month-old 3×Tg-AD mice show $A\beta$ overexpression predominantly in FC layers 4 to 5 [23]. Moreover, chronic um-PEA treatment dampened the expression of $A\beta$ in 3×Tg-AD mice, although this failed to reach significance (−34.23%) (Figures 4(f) and 4(k)). Despite this evidence, further experiments will be required to demonstrate the existence of a causative correlation between the reduction of $A\beta$ load and the control of neuroinflammation.

Combined, our results demonstrate the presence of activated astrocytes and a proinflammatory environment in the FCs of 3×Tg-AD mice at 6 months of age. Additionally, we show that chronic um-PEA treatment efficaciously controls these alterations in the AD brain.

3.4. Chronic um-PEA Normalizes Astrocyte Support to Neuronal Functionality in the Frontal Cortex of 3×Tg-AD Mice. Finally, we wanted to explore if there was any impairment in neuronal functionality guided by astrocytes

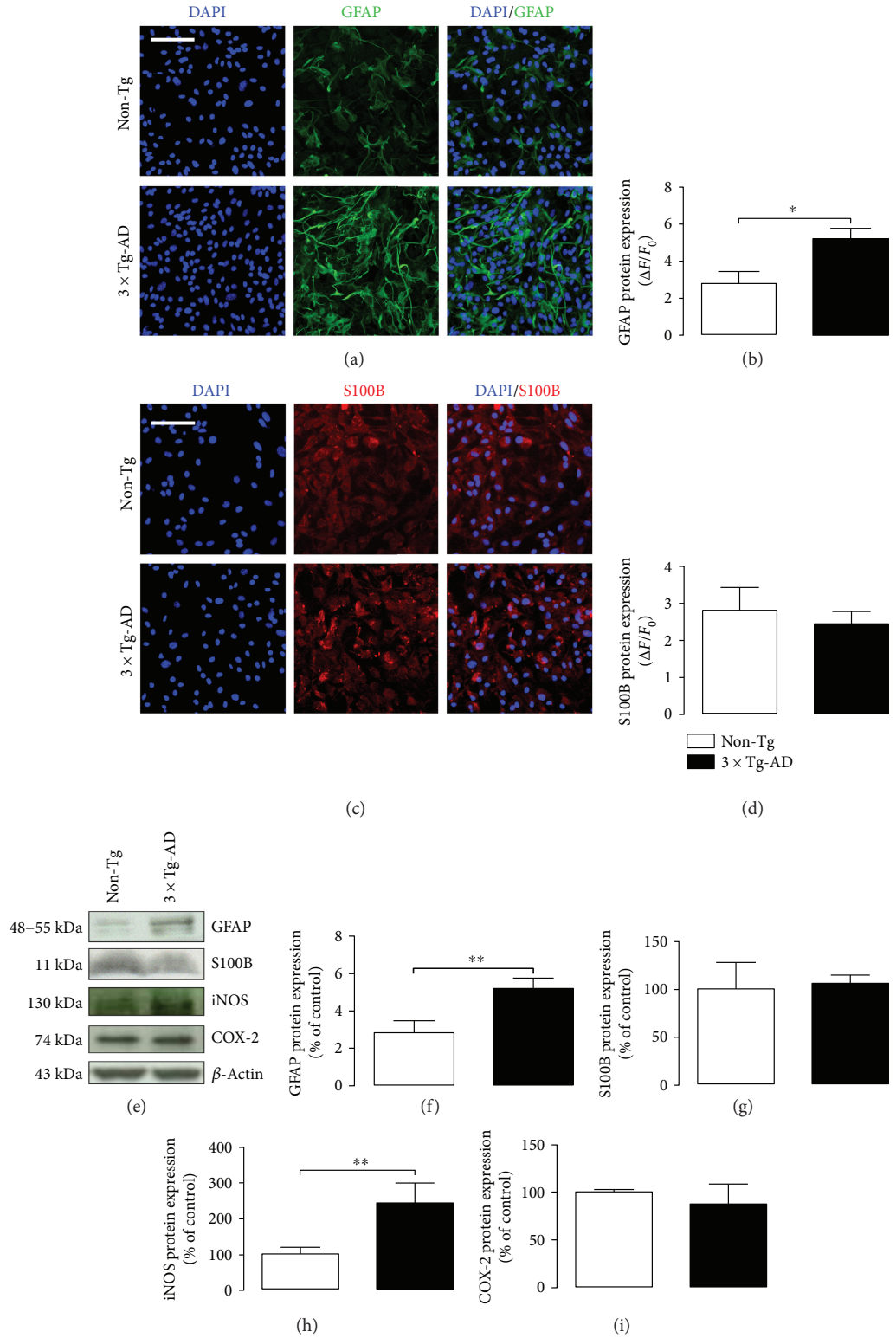

Figure 2: Study of parameters related to reactive astrogliosis in 3×Tg-AD and non-Tg primary astrocytes. (a) Representative fluorescent photomicrographs of GFAP (green) and (b) signal quantification in both non-Tg (white bar) and 3×Tg-AD (black bar) primary astrocytes. (c) Representative fluorescent photomicrographs of S100B (red) and (d) signal quantification in both non-Tg (white bar) and 3×Tg-AD (black bar) primary astrocytes. Nuclei were stained with DAPI (blue). Scale bar is 50 μm. Fluorescence analysis is expressed as $\Delta F/F_0$. (e) Representative bands and Western blot densitometric analysis of (f) GFAP, (g) S100B, (h) iNOS, and (i) COX-2. β-Actin was used as loading control. Results are expressed as percentage of the mean control value (non-Tg cells). Experiments were performed three times in triplicate. Data are presented as mean ± SEM. The statistical analysis was performed by Student's t-test ($^*P < 0.05$ and $^{**}P < 0.01$ versus non-Tg group).

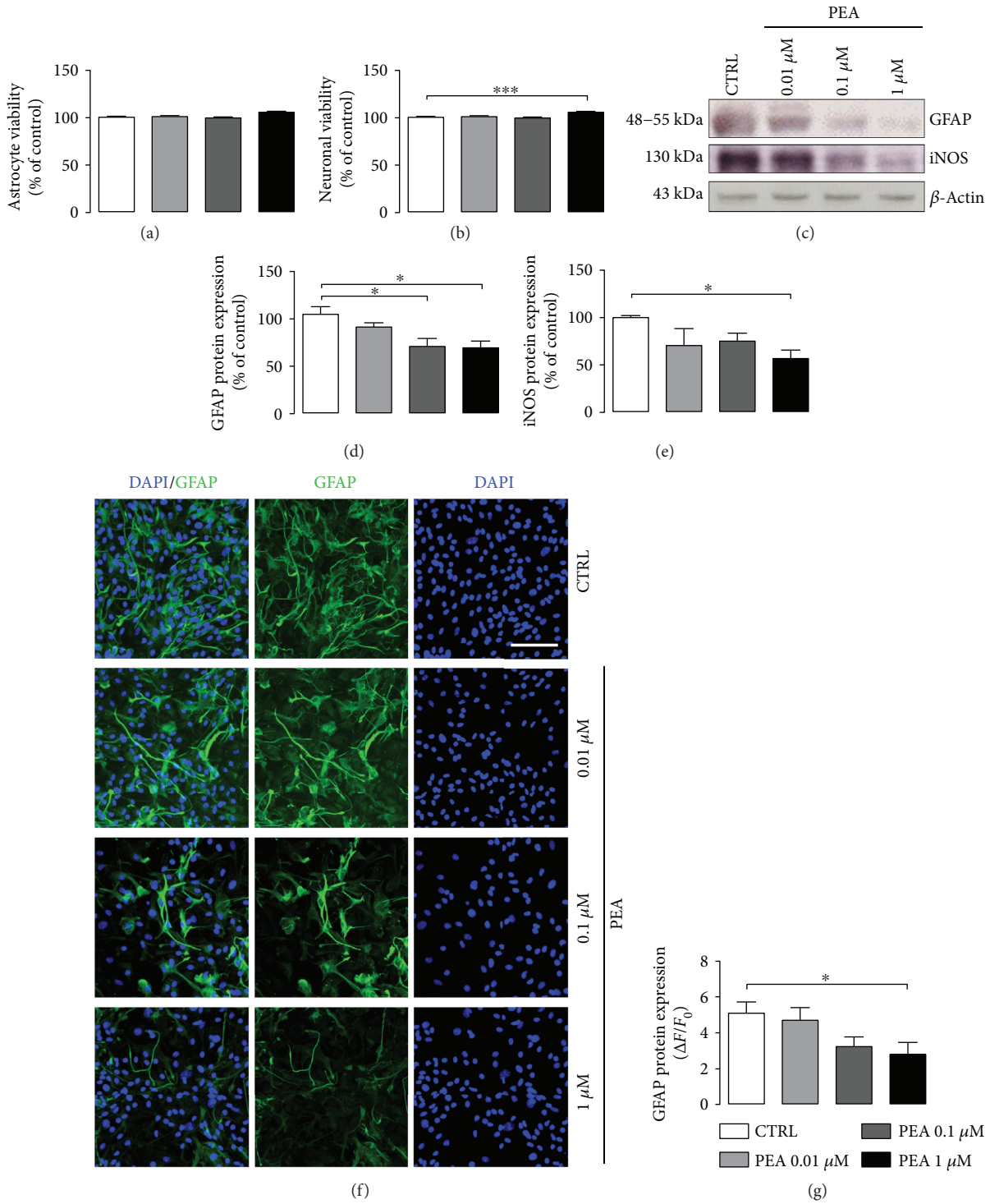

Figure 3: Effect of PEA treatment on astrocyte and neuronal viability and reactive astrogliosis in 3×Tg-AD cells. Evaluation of (a) astrocyte and (b) neuronal viability tested by neutral red uptake assay after 24 h PEA treatment (0.01–0.1–1 μM). (c) Representative immunoreactive signals and Western blot densitometric analysis of (d) GFAP and (e) iNOS. β-Actin was used as loading control. Results are expressed as percentage of the mean control value (CTRL). (f) Representative fluorescent photomicrographs of GFAP (green) staining in 3×Tg-AD primary astrocytes. Nuclei were stained with DAPI (blue). Scale bar is 50 μm. (g) Fluorescence analysis is expressed as $\Delta F/F_0$. Experiments were performed three times in triplicate. Data are presented as mean ± SEM. The statistical analysis was performed by one-way ANOVA followed by Bonferroni's post hoc multiple comparison test ($^{*}P < 0.05$ and $^{***}P < 0.001$ versus CTRL group).

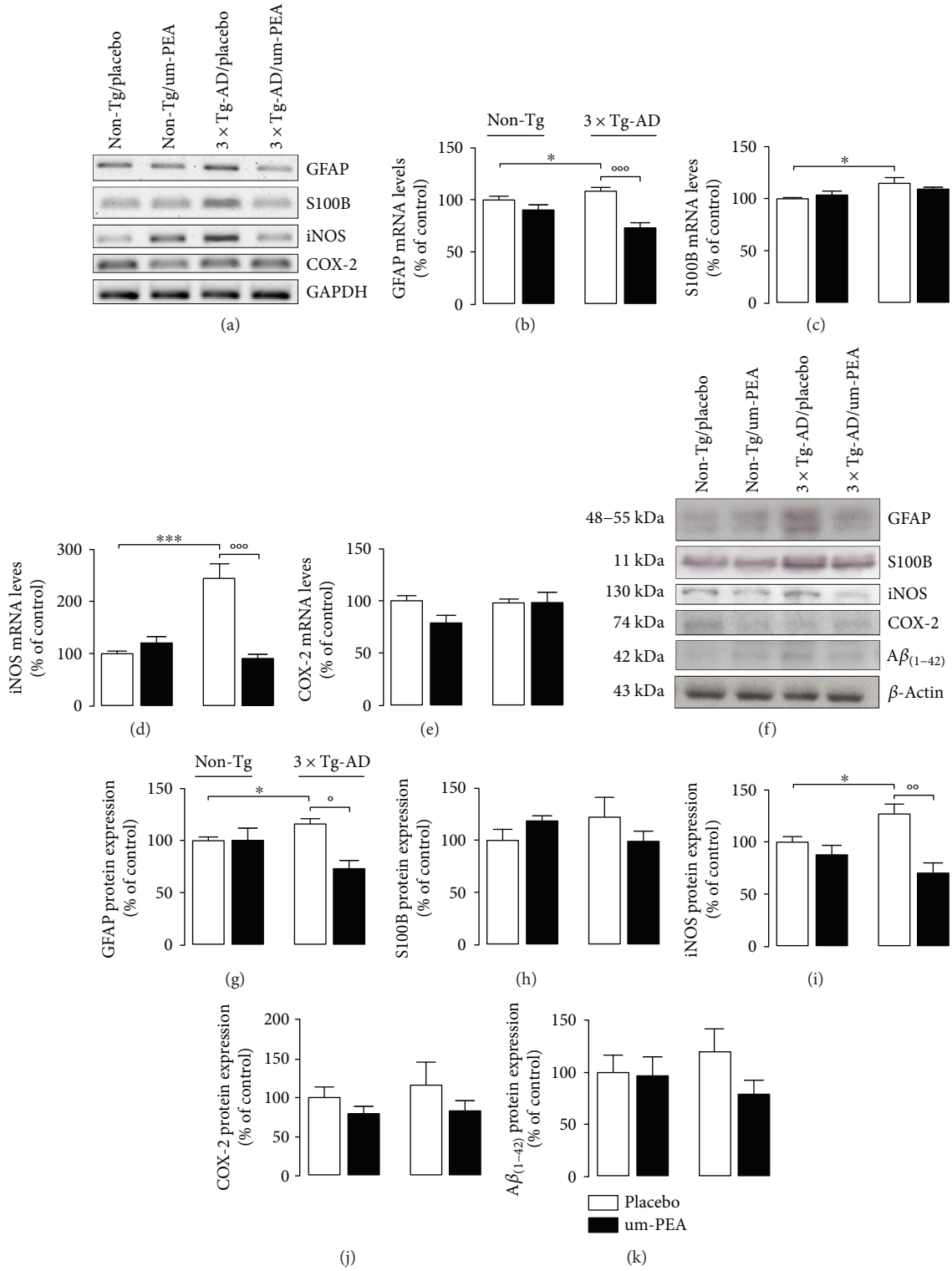

Figure 4: Effect of chronic um-PEA on reactive astrogliosis and $A\beta_{(1-42)}$ expression in the FC of 3×Tg-AD and non-Tg mice. (a) Representative bands from RT-PCR performed in FC homogenates for GFAP, S100B, iNOS, and COX-2, and (b–e) densitometric analysis of the corresponding signals normalized to GAPDH. (f) Representative immunoreactive species and Western blot densitometric analysis of (g) GFAP, (h) S100B, (i) COX-2, (j) iNOS, and (k) $A\beta_{(1-42)}$. β-Actin was used as loading control. Results are expressed as percentage of the mean control value (non-Tg/placebo). Experiments were performed three times in triplicate. Data are presented as mean ± SEM. The statistical analysis was performed by two-way ANOVA followed by Bonferroni's post hoc multiple comparison test ($^{*}P < 0.05$ and $^{***}P < 0.001$ versus non-Tg/placebo group; $^{\circ}P < 0.05$, $^{\circ\circ}P < 0.01$, and $^{\circ\circ\circ}P < 0.001$ versus 3×Tg-AD/placebo group).

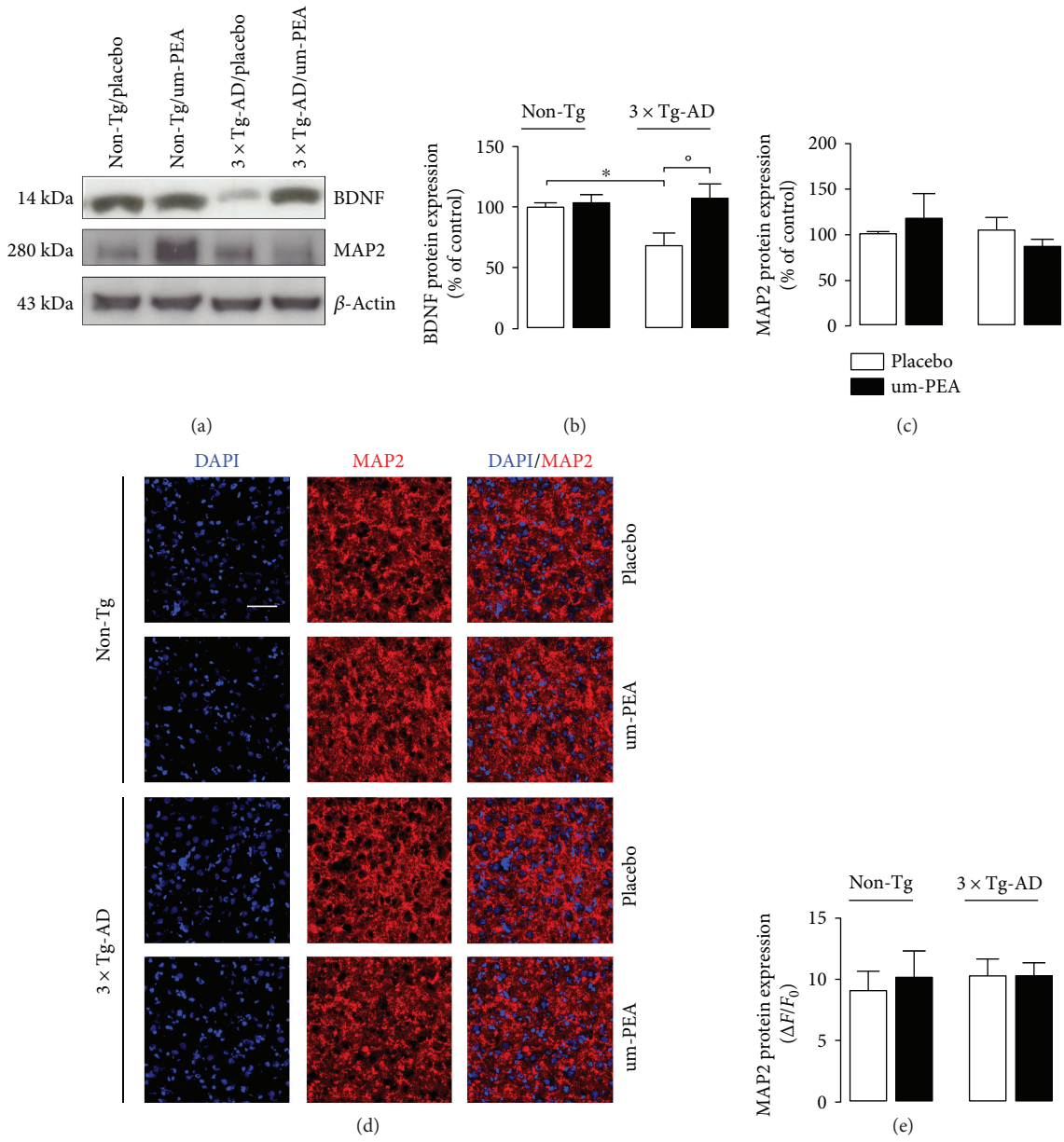

Figure 5: Effect of chronic um-PEA on neuronal support and survival in FC of 3×Tg-AD and non-Tg mice. (a) Representative immunoreactive species and Western blot densitometric analysis of (b) BDNF and (c) MAP2. β-Actin was used as loading control. Results are expressed as percentage of the mean control value (non-Tg/placebo). (d) Representative fluorescent photomicrographs of MAP2 (red) staining in FC of 6-month-old non-Tg and 3×Tg-AD mice, placebo- or um-PEA-treated. Nuclei were stained with DAPI (blue). Scale bar is 50 μm. (e) Fluorescence analysis is expressed as $\Delta F/F_0$. Experiments were performed three times in triplicate. Data are presented as mean ± SEM. The statistical analysis was performed by two-way ANOVA followed by Bonferroni's post hoc multiple comparison test ($^*P < 0.05$ versus non-Tg/placebo group; $^\circ P < 0.05$ versus 3×Tg-AD/placebo group).

that is responsible for BDNF production [30]. To address this goal, we tested both BDNF and MAP2 expression. Western blot analysis showed an impaired production of BDNF in the FC of placebo-treated 3×Tg-AD animals compared to placebo-treated non-Tg littermates. Interestingly, um-PEA significantly counteracted such decrease ($P < 0.05$) (Figures 5(a) and 5(b)). Surprisingly, these modifications did not affect neuronal survival. Indeed, by both Western blot and immunofluorescence, we did not observe modifications in MAP2 expression in placebo-treated transgenic mice in comparison with placebo-treated non-Tg animals (Figures 5(a), 5(c), 5(d), and 5(e)).

Altogether, these results demonstrate the presence of reduced trophic support to FC neurons in 6-month-old 3×Tg-AD mice; this has not yet impaired neuronal viability. Chronic um-PEA treatment restores the neuronal trophic support.

4. Discussion

Astrocytes represent the crucial element of a defensive system of CNS. Cerebral insults trigger reactive astrogliosis, which represents a conserved defensive reprogramming of astroglial cells. It is a very heterogeneous phenomenon that limits damage and facilitates postlesion regeneration of neural networks [31–33], although it may become neurotoxic in some circumstances [34]. In fact, astrogliosis involves complex biochemical and functional remodelling and produces multiple reactive cellular phenotypes. The common feature of pathological astroglial change is the morphological cellular remodelling towards atrophy or hypertrophy [35, 36]. This sometimes occurs at early pathological stages preceding (and possibly precipitating) neuronal death. Such an early activation is observed in AD, when astrocytes, in proximity of plaques and β-amyloid deposits, acquire a reactive phenotype detectable by an increased expression of intermediate filaments and overproduction of proinflammatory mediators [23, 35, 37]. By this way, astrocytes contribute to neurodegeneration, becoming interesting targets for the development of innovative therapies [38–41]. Here, we provide the first *in vitro* evidence of the presence of a basal reactive state in primary astrocytes derived from 3×Tg-AD mice cortices, as well as of the capability of PEA to counteract such a phenomenon and improve neuronal viability. We also obtained important data on the beneficial pharmacological properties of this compound by testing the effect of a chronic treatment with um-PEA in 3×Tg-AD mice. Our *in vivo* results indicate that, during the mild stage of the disease, both reactive astrogliosis and neuroinflammation are already detectable in the FCs of transgenic animals, and that chronic um-PEA is able to alleviate both indices.

Several clinical studies have shown that an impairment of hippocampus, entorhinal cortex, posterior cingulate gyrus, amygdala, and parahippocampal gyrus occur in early AD [42–45]. When AD becomes severe, atrophy progresses from the hippocampus to the FC [46]. Interestingly, our results revealed the absence of neuronal atrophy in 6-month-old 3×Tg-AD mice (age that corresponds to a mild stage of pathology), but detected the early presence of reactive astrogliosis, confirming that such phenomenon is precocious and comes before neuronal loss in this animal model.

Since glial cells, previously considered only space-filling support cells of the CNS, are indeed highly involved in the maintenance of CNS homeostasis, we wondered whether cells in the FC were abnormally activated during the mild stage of the disease, before atrophy occurs. To this aim, we first performed an *in vitro* screening of 3×Tg-AD cortical astrocytes and compared them with non-Tg-derived cells, for signs of astrocyte activation and inflammation. In the absence of any exogenous insult, 3×Tg-AD primary astrocytes showed a basal reactive and proinflammatory phenotype, as demonstrated by the increased expression of GFAP and iNOS, a cytoskeletal astrocyte marker and a proinflammatory inducible enzyme, respectively. Since reactive gliosis may occur before plaque formation, these results suggest that astrocytes can contribute to AD progression before the development of the main AD hallmarks [40]. Since some astrocytes express little or no GFAP [47], we used an additional astrocytic marker, such as S100B, a Ca^{2+}-binding protein. S100B is a neurotrophic factor that improves neuronal survival during CNS development [48]. In adulthood, levels of S100B increase after brain damage and can be neurotoxic and proinflammatory [49]. We did not find any genotypic difference in S100B expression, in our experimental condition. Therefore, it is possible that this protein maintains trophic functionality in the cell population analysed in the absence of an actual injury. Moreover, to further evaluate the inflammatory component in this animal model, we studied a proinflammatory enzyme, COX-2, responsible for prostanoid formation. Its involvement in the cascade of events leading to neurodegeneration in AD is still controversial [50]. COX-2 expression did not change in 3×Tg-AD cortical astrocytes, confirming the hypothesis that COX-2 induction could be connected with neurotoxicity [51], but this was not assessed in this *in vitro* study.

In the last few years, increasing evidence has confirmed the effectiveness of PEA treatment against inflammation in different models of neurodegeneration [15, 21, 52, 53]. Here, we tested the effectiveness of this compound on those parameters that we found to be influenced by the 3×Tg-AD genotype. Therefore, first we demonstrated the absence of astrocytic and neuronal toxicity of PEA at three different concentrations (0.01, 0.1, and 1 μM). Then, we performed the neutral red assay, a viability test, in both primary astrocytes and primary neurons, confirming that PEA is not cytotoxic and fosters neuronal viability at the highest concentration investigated. This result agrees with the already proven neuroprotective effects of PEA in different preclinical models of neurological disorders [15, 54, 55]. In a surgical rat model of AD, we recently demonstrated the ability of PEA to counteract the reactive gliosis caused by $A\beta_{(1-42)}$ hippocampal infusion [15]. Here, we demonstrated that PEA exerts this pharmacological effect in a transgenic model of AD, expanding the range of pathological targets treatable with this compound. In fact, the present *in vivo* experiments confirmed the therapeutic potential of chronic PEA administration. Moreover, such experiments were designed to simulate a clinic-like treatment schedule; for this reason, 3-month-old 3×Tg-AD and sex- and age-matched non-Tg animals were chronically treated for three months with placebo or um-PEA, a crystalline form on micrometric size, which improves its pharmacokinetics properties [24, 56]. Consistent with our *in vitro* observations, in the FC of 3×Tg-AD mice, we detected the presence of reactive gliosis in the mild stage of the disease, as shown by the increased transcription and expression of both GFAP and iNOS. The expression of both S100B and COX-2 were not affected by the genotype. Only S100B mRNA was increased in transgenic cortices. Interestingly, chronic um-PEA treatment dampened such alterations, confirming its effectiveness against reactive gliosis *in vivo*. Another interesting result was the detection of lower levels of BDNF in the FC of transgenic mice in comparison with non-Tg littermates, and, even more significant, the discovery of the ability of chronic um-PEA at increasing the expression of BDNF. Despite the fact that we found a

decreased expression of BDNF together with the presence of reactive gliosis, known to be able to amplify CNS damages [14, 47], we did not detect any impairment of neuronal viability in FC of 3×Tg-AD mice. Such evidence was surprising because it is widely accepted that at 6 months of age these transgenic mice show early symptoms of AD-like pathology and behavioural alterations [23, 57–59]. However, since CNS impairment in AD travels broadly from hippocampus to FC, we can speculate that the massive alteration of this brain region has not occurred as yet, and neurons can somehow survive these insults. In fact, Castello and colleagues demonstrated that BDNF reduction does not exacerbate Aβ and tau pathology, but is a consequence of the pathology itself [60]. If this is true, the improvement in BDNF production that we found in mice after chronic um-PEA treatment can be a positive sign of the control that such a molecule has on the pathology in its entirety, and not only against reactive gliosis.

5. Conclusions

In the present study, we expand the knowledge on glial activity in a triple transgenic model of AD that closely mimics the main features of the pathology. Here, we provide the first evidence that 3×Tg-AD mice present signs of reactive gliosis in the FC at an early stage of the disease. Moreover, we demonstrate for the first time that acute PEA *in vitro*, as well as chronic um-PEA *in vivo*, may counteract such phenomenon, improving the trophic support to neurons, in absence of astrocytes and neuronal toxicity. By the virtue of its safety [61], and considering the growing body of evidence regarding its efficacy, we foresee a possible translation of the results collected in animal models into the clinical practice, in the near future.

Conflicts of Interest

The authors report no financial interests or potential conflicts of interest.

Acknowledgments

This research was supported by the Italian Ministry of Education, University and Research (MIUR) to Luca Steardo (PON01-02512 and PRIN Protocol 2009NKZCNX) and Sapienza University of Rome to Caterina Scuderi (Protocol C26A15X58E) and Maria Rosanna Bronzuoli (Protocol C26N15BHZZ).

References

[1] R. Anand, K. D. Gill, and A. A. Mahdi, "Therapeutics of Alzheimer's disease: past, present and future," *Neuropharmacology*, vol. 76, pp. 27–50, 2014.

[2] H. Braak and E. Braak, "Neuropil threads occur in dendrites of tangle—bearing nerve cells," *Neuropathology and Applied Neurobiology*, vol. 14, no. 1, pp. 39–44, 1988.

[3] P. Merz, H. Wisniewski, R. Somerville, S. A. Bobin, C. L. Masters, and K. Iqbal, "Ultrastructural morphology of amyloid fibrils from neuritic and amyloid plaques," *Acta Neuropathology*, vol. 60, no. 1-2, pp. 113–124, 1983.

[4] J. J. Rodríguez, M. Olabarria, A. Chvatal, and A. Verkhratsky, "Astroglia in dementia and Alzheimer's disease," *Cell Death & Differentiation*, vol. 16, no. 3, pp. 378–385, 2009.

[5] H. Akiyama, S. Barger, S. Barnum, B. Bradt, J. Bauer, and G. M. Cole, "Inflammation and Alzheimer's disease," *Neurobiology of Aging*, vol. 21, no. 3, pp. 383–421, 2000.

[6] A. Verkhratsky, M. Olabarria, H. N. Noristani, C. Y. Yeh, and J. J. Rodriguez, "Astrocytes in Alzheimer's disease," *Neurotherapeutics*, vol. 7, no. 4, pp. 399–412, 2010.

[7] A. Verkhratsky, M. V. Sofroniew, A. Messing et al., "Neurological diseases as primary gliopathies: a reassessment of neurocentrism," *ASN Neuro*, vol. 4, no. 3, article AN20120010, 2012.

[8] Z. Yang and K. K. W. Wang, "Glial fibrillary acidic protein: from intermediate filament assembly and gliosis to neurobiomarker," *Trends in Neurosciences*, vol. 38, no. 6, pp. 364–374, 2015.

[9] G. Esposito, C. Scuderi, J. Lu, C. Savani, D. De Filippis, and T. Iuvone, "S100B induces tau protein hyperphosphorylation via Dickopff-1 up-regulation and disrupts the Wnt pathway in human neural stem cells," *Journal of Cellular and Molecular Medicine*, vol. 12, no. 3, pp. 914–927, 2008.

[10] L. J. van Eldik and M. S. Wainwright, "The Janus face of glial-derived S100B: beneficial and detrimental functions in the brain," *Restorative Neurology and Neuroscience*, vol. 21, no. 3-4, pp. 97–108, 2003.

[11] C. Lindberg, E. Hjorth, C. Post, B. Winblad, and M. Schultzberg, "Cytokine production by a human microglial cell line: effects of ßamyloid and α-melanocyte-stimulating hormone," *Neurotoxicity Research*, vol. 8, no. 3-4, pp. 267–276, 2005.

[12] G. C. Brown and A. Bal-Price, "Inflammatory neurodegeneration mediated by nitric oxide, glutamate, and mitochondria," *Molecular Neurobiology*, vol. 27, no. 3, pp. 325–355, 2003.

[13] J. E. Burda and M. V. Sofroniew, "Reactive gliosis and the multicellular response to CNS damage and disease," *Neuron*, vol. 81, no. 2, pp. 229–248, 2014.

[14] L. Steardo Jr., M. R. Bronzuoli, A. Iacomino, G. Esposito, L. Steardo, and C. Scuderi, "Does neuroinflammation turn on the flame in Alzheimer's disease? Focus on astrocytes," *Frontiers in Neuroscience*, vol. 9, p. 259, 2015.

[15] C. Scuderi, C. Stecca, M. Valenza et al., "Palmitoylethanolamide controls reactive gliosis and exerts neuroprotective functions in a rat model of Alzheimer's disease," *Cell Death & Disease*, vol. 5, no. 9, article e1419, 2014.

[16] S. E. O'Bryant, V. Hobson, J. R. Hall et al., "Brain-derived neurotrophic factor levels in Alzheimer's disease," *Journal of Alzheimer's Disease*, vol. 17, no. 2, pp. 337–341, 2009.

[17] A. N. Voineskos, J. P. Lerch, D. Felsky, S. Shaikh, T. K. Rajji, and D. Miranda, "The brain-derived neurotrophic factor Val66Met polymorphism and prediction of neural risk for Alzheimer disease," *Archives of General Psychiatry*, vol. 68, no. 2, pp. 198–206, 2011.

[18] V. K. Sandhya, R. Raju, R. Verma et al., "A network map of BDNF/TRKB and BDNF/p75NTR signaling system," *Journal of Cell Communication and Signaling*, vol. 7, no. 4, pp. 301–307, 2013.

[19] C. Scuderi, G. Esposito, A. Blasio, M. Valenza, P. Arietti, and L. Steardo Jr., "Palmitoylethanolamide counteracts reactive astrogliosis induced by β-amyloid peptide," *Journal of*

Cellular and Molecular Medicine, vol. 15, no. 12, pp. 2664–2674, 2011.

[20] C. Scuderi, M. Valenza, C. Stecca, G. Esposito, M. R. Carratù, and L. Steardo, "Palmitoylethanolamide exerts neuroprotective effects in mixed neuroglial cultures and organotypic hippocampal slices via peroxisome proliferator-activated receptor-α," *Journal of Neuroinflammation*, vol. 9, no. 1, 2012.

[21] G. D'Agostino, R. Russo, C. Avagliano, C. Cristiano, R. Meli, and A. Calignano, "Palmitoylethanolamide protects against the amyloid-β25-35-induced learning and memory impairment in mice, an experimental model of Alzheimer disease," *Neuropsychopharmacology*, vol. 37, no. 7, pp. 1784–1792, 2012.

[22] M. C. Tomasini, A. C. Borelli, S. Beggiato, L. Ferraro, T. Cassano, and S. Tanganelli, "Differential effects of palmitoylethanolamide against amyloid-β induced toxicity in cortical neuronal and astrocytic primary cultures from wild-type and 3xTg-AD mice," *Journal of Alzheimer's Disease*, vol. 46, no. 2, pp. 407–421, 2015.

[23] S. Oddo, A. Caccamo, J. D. Shepherd et al., "Triple-transgenic model of Alzheimer's disease with plaques and tangles: intracellular Aβ and synaptic dysfunction," *Neuron*, vol. 39, no. 3, pp. 409–421, 2003.

[24] S. Petrosino and V. Di Marzo, "The pharmacology of palmitoylethanolamide and first data on the therapeutic efficacy of some of its new formulations," *British Journal of Pharmacology*, vol. 174, no. 11, pp. 1349–1365, 2017.

[25] B. Costa, S. Conti, G. Giagnoni, and M. Colleoni, "Therapeutic effect of the endogenous fatty acid amide, palmitoylethanolamide, in rat acute inflammation: inhibition of nitric oxide and cyclo-oxygenase systems," *British Journal of Pharmacology*, vol. 137, no. 4, pp. 413–420, 2002.

[26] S. L. Grillo, J. Keereetaweep, M. A. Grillo, K. D. Chapman, and P. Koulen, "*N*-Palmitoylethanolamine depot injection increased its tissue levels and those of other acylethanolamide lipids," *Drug Design, Development and Therapy*, vol. 7, pp. 747–752, 2013.

[27] C. Scuderi, C. Stecca, M. R. Bronzuoli et al., "Sirtuin modulators control reactive gliosis in an in vitro model of Alzheimer's disease," *Frontiers in Pharmacology*, vol. 5, p. 89, 2014.

[28] J. Baudier, C. Delphin, D. Grunwald, S. Khochbin, and J. J. Lawrence, "Characterization of the tumor suppressor protein p53 as a protein kinase C substrate and a S100b-binding protein," *Proceedings of the National Academy of Sciences of the United States of America*, vol. 89, no. 23, pp. 11627–11631, 1992.

[29] C. Scotto, J. C. Deloulme, D. Rousseau, E. Chambaz, and J. Baudier, "Calcium and S100B regulation of p53-dependent cell growth arrest and apoptosis," *Molecular and Cellular Biology*, vol. 18, no. 7, pp. 4272–4281, 1998.

[30] Y. Sato, Y. Chin, T. Kato et al., "White matter activated glial cells produce BDNF in a stroke model of monkeys," *Neuroscience Research*, vol. 65, no. 1, pp. 71–78, 2009.

[31] V. Parpura, M. T. Heneka, V. Montana et al., "Glial cells in (patho)physiology," *Journal of Neurochemistry*, vol. 121, no. 1, pp. 4–27, 2012.

[32] A. Verkhratsky, R. Zorec, J. J. Rodríguez, and V. Parpura, "Astroglia dynamics in ageing and Alzheimer's disease," *Current Opinion in Pharmacology*, vol. 26, pp. 74–79, 2016.

[33] M. Pekny and M. Pekna, "Reactive gliosis in the pathogenesis of CNS diseases," *Biochimica et Biophysica Acta (BBA) - Molecular Basis of Disease*, vol. 1862, no. 3, pp. 483–491, 2016.

[34] S. A. Liddelow, K. A. Guttenplan, L. E. Clarke et al., "Neurotoxic reactive astrocytes are induced by activated microglia," *Nature*, vol. 541, no. 7638, pp. 481–487, 2017.

[35] M. Olabarria, H. N. Noristani, A. Verkhratsky, and J. J. Rodriguez, "Concomitant astroglial atrophy and astrogliosis in a triple transgenic animal model of Alzheimer's disease," *Glia*, vol. 58, no. 7, pp. 831–838, 2010.

[36] V. C. Jones, R. Atkinson-Dell, A. Verkhratsky, and L. Mohamet, "Aberrant iPSC-derived human astrocytes in Alzheimer's disease," *Cell Death & Disease*, vol. 8, no. 3, article e2696, 2017.

[37] A. Verkhratsky, V. Parpura, M. Pekna, M. Pekny, and M. Sofroniew, "Glia in the pathogenesis of neurodegenerative diseases," *Biochemical Society Transactions*, vol. 42, no. 5, pp. 1291–1301, 2014.

[38] P. C. Chen, M. R. Vargas, A. K. Pani et al., "Nrf2-mediated neuroprotection in the MPTP mouse model of Parkinson's disease: critical role for the astrocyte," *Proceedings of the National Academy of Sciences of the United States of America*, vol. 106, no. 8, pp. 2933–2938, 2009.

[39] J. Bradford, J. Y. Shin, M. Roberts et al., "Mutant huntingtin in glial cells exacerbates neurological symptoms of Huntington disease mice," *Journal of Biological Chemistry*, vol. 285, no. 14, pp. 10653–10661, 2010.

[40] C. Acosta, H. D. Anderson, and C. M. Anderson, "Astrocyte dysfunction in Alzheimer disease," *Journal of Neuroscience Research*, vol. 95, no. 12, pp. 2430–2447, 2017.

[41] M. R. Bronzuoli, A. Iacomino, L. Steardo, and C. Scuderi, "Targeting neuroinflammation in Alzheimer's disease," *Journal of Inflammation Research*, vol. 9, pp. 199–208, 2016.

[42] M. Basso, J. Yang, L. Warren et al., "Volumetry of amygdala and hippocampus and memory performance in Alzheimer's disease," *Psychiatry Research: Neuroimaging*, vol. 146, no. 3, pp. 251–261, 2006.

[43] D. P. Devanand, G. Pradhaban, X. Liu et al., "Hippocampal and entorhinal atrophy in mild cognitive impairment: prediction of Alzheimer disease," *Neurology*, vol. 68, no. 11, pp. 828–836, 2007.

[44] C. Pennanen, M. Kivipelto, S. Tuomainen et al., "Hippocampus and entorhinal cortex in mild cognitive impairment and early AD," *Neurobiology of Aging*, vol. 25, no. 3, pp. 303–310, 2004.

[45] H. Wolf, A. Hensel, F. Kruggel et al., "Structural correlates of mild cognitive impairment," *Neurobiology of Aging*, vol. 25, no. 7, pp. 913–924, 2004.

[46] R. I. Scahill, J. M. Schott, J. M. Stevens, M. N. Rossor, and N. C. Fox, "Mapping the evolution of regional atrophy in Alzheimer's disease: unbiased analysis of fluid-registered serial MRI," *Proceedings of the National Academy of Sciences of the United States of America*, vol. 99, no. 7, pp. 4703–4707, 2002.

[47] M. V. Sofroniew and H. V. Vinters, "Astrocytes: biology and pathology," *Acta Neuropathologica*, vol. 119, no. 1, pp. 7–35, 2010.

[48] A. Bhattacharyya, R. W. Oppenheim, D. Prevette, B. W. Moore, R. Brackenbury, and N. Ratner, "S100 is present in developing chicken neurons, and Schwann cells, and promotes neuron survival in vivo," *Journal of Neurobiology*, vol. 23, no. 4, pp. 451–466, 1992.

[49] H. Zetterberg, D. H. Smith, and K. Blennow, "Biomarkers of mild traumatic brain injury in cerebrospinal fluid and blood," *Nature Reviews Neurology*, vol. 9, no. 4, pp. 201–210, 2013.

[50] L. Minghetti, "Cyclooxygenase-2 (COX-2) in inflammatory and degenerative brain diseases," *Journal of Neuropathology and Experimental Neurology*, vol. 63, no. 9, pp. 901–910, 2004.

[51] M. A. Meraz-Ríos, D. Toral-Rios, D. Franco-Bocanegra, J. Villeda-Hernández, and V. Campos-Peña, "Inflammatory process in Alzheimer's disease," *Frontiers in Integrative Neuroscience*, vol. 7, p. 59, 2013.

[52] E. Esposito, D. Impellizzeri, E. Mazzon, I. Paterniti, and S. Cuzzocrea, "Neuroprotective activities of palmitoylethanolamide in an animal model of Parkinson's disease," *PLoS One*, vol. 7, no. 8, article e41880, 2012.

[53] A. Rahimi, M. Faizi, F. Talebi, F. Noorbakhsh, F. Kahrizi, and N. Naderi, "Interaction between the protective effects of cannabidiol and palmitoylethanolamide in experimental model of multiple sclerosis in C57BL/6 mice," *Neuroscience*, vol. 290, pp. 279–287, 2015.

[54] S. D. Skaper, A. Buriani, R. Dal Toso et al., "The ALIAmide palmitoylethanolamide and cannabinoids, but not anandamide, are protective in a delayed postglutamate paradigm of excitotoxic death in cerebellar granule neurons," *Proceedings of the National Academy of Sciences of the United States of America*, vol. 93, no. 9, pp. 3984–3989, 1996.

[55] D. M. Lambert, S. Vandevoorde, G. Diependaele, S. J. Govaerts, and A. R. Robert, "Anticonvulsant activity of *N*-palmitoylethanolamide, a putative endocannabinoid, in mice," *Epilepsia*, vol. 42, no. 3, pp. 321–327, 2001.

[56] D. Impellizzeri, G. Bruschetta, M. Cordaro et al., "Micronized/ultramicronized palmitoylethanolamide displays superior oral efficacy compared to nonmicronized palmitoylethanolamide in a rat model of inflammatory pain," *Journal of Neuroinflammation*, vol. 11, no. 1, p. 136, 2014.

[57] K. R. Stover, M. A. Campbell, C. M. Van Winssen, and R. E. Brown, "Analysis of motor function in 6-month-old male and female 3xTg-AD mice," *Behavioural Brain Research*, vol. 281, pp. 16–23, 2015.

[58] S. Oddo, A. Caccamo, M. Kitazawa, B. P. Tseng, and F. M. LaFerla, "Amyloid deposition precedes tangle formation in a triple transgenic model of Alzheimer's disease," *Neurobiology of Aging*, vol. 24, no. 8, pp. 1063–1070, 2003.

[59] L. M. Billings, S. Oddo, K. N. Green, J. L. McGaugh, and F. M. LaFerla, "Intraneuronal Aβ causes the onset of early Alzheimer's disease-related cognitive deficits in transgenic mice," *Neuron*, vol. 45, no. 5, pp. 675–688, 2005.

[60] N. A. Castello, K. N. Green, and F. M. LaFerla, "Genetic knockdown of brain-derived neurotrophic factor in 3xTg-AD mice does not alter aβ or tau pathology," *PLoS One*, vol. 7, no. 8, article e39566, 2012.

[61] E. R. Nestmann, "Safety of micronized palmitoylethanolamide (microPEA): lack of toxicity and genotoxic potential," *Food Science & Nutrition*, vol. 5, no. 2, pp. 292–309, 2017.

Hindawi
Oxidative Medicine and Cellular Longevity
Volume 2017, Article ID 9076052, 10 pages
https://doi.org/10.1155/2017/9076052

Research Article

Oleic Acid and Hydroxytyrosol Inhibit Cholesterol and Fatty Acid Synthesis in C6 Glioma Cells

Paola Priore,[1,2] Antonio Gnoni,[3] Francesco Natali,[1] Mariangela Testini,[1] Gabriele V. Gnoni,[1] Luisa Siculella,[1] and Fabrizio Damiano[1]

[1]*Laboratory of Biochemistry and Molecular Biology, Department of Biological and Environmental Sciences and Technologies, University of Salento, Via Prov.le Lecce-Monteroni, 73100 Lecce, Italy*
[2]*CNR-NANOTEC, Institute of Nanotechnology c/o Campus Ecotekne, University of Salento, Via Monteroni, 73100 Lecce, Italy*
[3]*Department of Basic Medical Sciences, Neurosciences and Sense Organs, University of Bari "Aldo Moro", Policlinico P.zza G. Cesare 11, 70100 Bari, Italy*

Correspondence should be addressed to Luisa Siculella; luisa.siculella@unisalento.it

Received 26 May 2017; Revised 8 September 2017; Accepted 5 December 2017; Published 24 December 2017

Academic Editor: Tommaso Cassano

Recently, the discovery of natural compounds capable of modulating nervous system function has revealed new perspectives for a healthier brain. Here, we investigated the effects of oleic acid (OA) and hydroxytyrosol (HTyr), two important extra virgin olive oil compounds, on lipid synthesis in C6 glioma cells. OA and HTyr inhibited both de novo fatty acid and cholesterol syntheses without affecting cell viability. The inhibitory effect of the individual compounds was more pronounced if OA and HTyr were administered in combination. A reduction of polar lipid biosynthesis was also detected, while triglyceride synthesis was marginally affected. To clarify the lipid-lowering mechanism of these compounds, their effects on the activity of key enzymes of fatty acid biosynthesis (acetyl-CoA carboxylase-ACC and fatty acid synthase-FAS) and cholesterologenesis (3-hydroxy-3-methylglutaryl-CoA reductase-HMGCR) were investigated in situ by using digitonin-permeabilized C6 cells. ACC and HMGCR activities were especially reduced after 4 h of 25 μM OA and HTyr treatment. No change in FAS activity was observed. Inhibition of ACC and HMGCR activities is corroborated by the decrease of their mRNA abundance and protein level. Our results indicate a direct and rapid downregulatory effect of the two olive oil compounds on lipid synthesis in C6 cells.

1. Introduction

Extra virgin olive oil (EVOO), the principal source of fat in the Mediterranean diet, represents the topic of many studies because several epidemiological data suggest that it positively affects human health, reducing the incidence of cancer, hypertension, and cardiovascular diseases [1, 2]. Besides these well-recognized effects, recent clinical studies support the efficacy of the Mediterranean diet and of its main fat also against the cognitive decline associated with ageing as well as against the onset and progression of a number of neurodegenerative diseases. In such neurological contexts, several data highlight the role of the natural compounds whose EVOO is rich [3, 4].

The EVOO health effects can be ascribed to a plethora of molecules contained in both its saponifiable (fatty acids) and unsaponifiable (mainly cholesterol) fractions. Initially, the beneficial properties of EVOO were attributed to its high content in oleic acid (OA). OA consumption was claimed to promote cardiovascular disease prevention and to influence the expression of homeostatic and metabolic genes that protect tissues from oxidative and inflammatory processes associated with ageing, degenerative diseases, and cancer [5–9]. In a previous study carried out on rat C6 glioma cells [5], it has been shown that, among a number of various fatty acids, OA was the most effective downregulator of lipid synthesis.

In the last decade, a flurry of scientific findings has highlighted that many of the EVOO beneficial effects can be accounted not only for the monounsaturated nature of its predominant fatty acid OA but also for the bioactivity of EVOO minor compounds, which can act on cells through both indirect and direct mechanisms, the latter modulating gene expression [6, 8–10]. Among the minor constituents of EVOO, the phenolic compound hydroxytyrosol (2,(3,4-dihydroxyphenyl)-ethanol, HTyr) is considered one of the most effective antioxidants. Consumption of HTyr has certain health benefits, and the responsible mechanisms for these effects have been mainly attributed to its ability to scavenge reactive oxygen species and to enhance endogenous antioxidant systems [11]. In previous studies carried out on rat primary hepatocytes [12, 13], we found that HTyr (alone or as a part of a crude extract) stands out for its capacity to modulate also some enzyme activities relevant for lipid metabolism.

After white adipose tissue, the brain is the organ with the highest lipid content of the body. The biosynthesis and deposition of lipids play a pivotal role in maintaining the brain structure and function. Alterations in lipid metabolism are the cause of or are associated with many neurological diseases [14, 15].

Attenuation of age- and disease-associated cognitive decline by olive oil or by its minor compounds has been observed in cellular, animal, and human models [16–18]. In most of these studies, a reduction of oxidative damage and a modulation of antioxidant defences were shown. However, besides the antioxidant and anti-inflammatory activity, other mechanisms might underlie the beneficial effects of EVOO minor compounds on brain development and homeostasis [3, 16–18].

Considering the need for chemotherapeutic intervention against neurological disorders [19] and the putative role of fatty acids and antioxidants in this field [7, 15, 20], further studies are required to gain insight into the impact of EVOO compounds on neurodegenerative processes. C6 glioma cells present a large repertoire of astrocyte-expressing enzymatic activities [21, 22] and exhibit a prevalent astrocyte-like phenotype when cultured in serum-rich medium [23]. Thus, they are considered a useful cellular model to study cerebral dysfunction [20, 24].

To our knowledge, this is the first study in which the effect of EVOO constituents on lipid metabolism in glial cells has been investigated. In detail, this study was focused on the effects of the cosupplementation of OA and HTyr on cholesterol and fatty acid syntheses in glial cells.

2. Materials and Methods

2.1. Materials. Rat C6 glioma cells were from the American Type Culture Collection. Dulbecco's modified eagle's high-glucose medium (DMEM), foetal bovine serum (FBS), penicillin/streptomycin, phosphate buffer solution (PBS), and 3-[4,5-dimethylthiazol-2-yl]-2,5-diphenyltetrazolium bromide (MTT) were obtained from Gibco-Invitrogen Ltd. (Paisley, UK); [1-^{14}C]acetate was obtained from GE Healthcare (Little Chalfont, UK); [1-^{14}C]acetyl-CoA, [3-^{14}C]3-hydroxy-3-methylglutaryl-CoA ([3-^{14}C]HMG-CoA) were obtained from PerkinElmer (Boston, MA). Primary antibodies for acetyl-CoA carboxylase (ACC), fatty acid synthase (FAS), and α-tubulin were obtained from Cell Signaling Technologies (Boston, MA). The antibody against 3-hydroxy-3-methylglutaryl-CoA reductase (HMGCR) as well as horseradish peroxidase-conjugated IgGs was obtained from Santa Cruz Biotechnology (Dallas, TX). All other reagents, obtained from Sigma-Aldrich, were of analytical grade.

2.2. Cell Culture. C6 cells were maintained in DMEM supplemented with 10% FBS and 1% penicillin/streptomycin, at 37°C in a humidified atmosphere of 5% CO_2. Unless otherwise specified in the text, C6 cells were seeded in 6-well plates (Corning Inc., Corning, NY) at a density of 5×10^5 cells per well and cultured in 10% FBS-supplemented medium. 24 h after plating, the medium was changed and, following further 24 h, OA sodium salt and HTyr were added for 4 h, singularly or in coincubation, to the DMEM medium, obtaining 25 μM final concentration. OA stock solution was 10 mM in DMEM and HTyr stock solution was 100 mM dissolved in dimethyl sulfoxide (DMSO). For each determination, untreated control cells were also considered.

2.3. Cell Viability Assay. Cell proliferation and viability were assessed by the MTT assay. To this purpose, C6 cells were cultured at a density of 5×10^3 cells/well in a 96-well plate (Corning Inc., Corning, NY) and after 24 h, the serum-rich medium was refreshed. Following further 24 h, cells were incubated for 4 h with OA and/or HTyr, using for each sample three concentrations: 25 μM, 50 μM, and 100 μM of OA and/or the HTyr. Then, cell monolayers were incubated for 3 h with 1 mg/mL MTT. Mitochondria of living cells transform the yellow-coloured tetrazolium compound to its purple formazan derivative. Formazan crystals formed in the cells were dissolved in 100 μL DMSO, and the absorbance was measured at 570 nm using a Multiskan FC ELISA reader (Thermo Fisher Scientific, Waltham, MA). The viability is calculated as percentage of absorbance relative to control cells.

2.4. Rate of Fatty Acid and Cholesterol Synthesis. Acetyl-CoA is the precursor for both fatty acid and cholesterol synthesis. Lipogenic activity was monitored by the incorporation of [1-^{14}C]acetate (16 mM, 0.96 mCi/mol) into total fatty acids and cholesterol essentially as in Gnoni et al. [25]. Cells were incubated for 4 h with 25 μM OA and/or 25 μM HTyr. Labelled acetate was added 1 h before ending the experiment.

To terminate the lipogenic assay, the medium was aspirated and the cells were washed three times with ice-cold PBS to remove unreacted acetate, and the reaction was stopped by 1.5 mL of 0.5 N NaOH.

The cells were scraped off, transferred to a test tube, and saponified with ethanolic KOH. Sterols and fatty acids were extracted and counted for radioactivity as reported [25].

2.5. Chromatographic Analysis of Radiolabelled Lipid Fractions. Radiolabelled acetate incorporation into phospholipids and neutral lipids was analyzed. At the end of the

incubation period, the cells were washed with ice-cold PBS and the reaction was blocked with 2 mL of KCl:CH_3OH (1 : 2, *v*/*v*). Total lipids were extracted according to Bligh and Dyer [26] and resolved by thin layer chromatography on silica gel plates, using as developing system $CHCl_3$: CH_3OH : 28% NH_4OH (65 : 25 : 4) and exane : ethyl ether : acetic acid (80 : 20 : 1) for phospholipids and neutral lipid analysis, respectively. Lipid spots were visualized with iodine vapour and scraped into counting vials for radioactivity measurement [5].

2.6. Chromatographic Analysis of Radiolabelled Fatty Acids. HPLC analysis of the extracted fatty acids was performed as reported [5]. 20 μL of sample was injected into a Beckman Coulter System Gold Programmable Solvent Module 125 and furnished with a C18 ODS column (4.6 × 250 mm) and Diode Array Detector 168 (Beckman Coulter, Milan, IT). Two mobile phases were used for elution: solvent A, constituted by acetonitrile : water (4 : 1) and ran for 45 min and solvent B, constituted by acetonitrile and ran for another 15 min. Flow rate was 2 mL/min and detection was at 242 nm. Eluted fractions were collected for radioactivity measurement.

2.7. Assay of Lipogenic Enzyme Activities. ACC activity was determined as the incorporation of radiolabelled acetyl-CoA into fatty acid in an assay coupled with FAS activity. This method circumvents interferences linked to the classical bicarbonate assay [27]. ACC and FAS activities were determined in digitonin-permeabilized C6 cells. Cell permeabilization, achieved by using an assay mix containing 400 μg/mL digitonin [5], represents an appropriate tool to investigate enzyme activities directly in situ (i.e., in a more or less natural environment).

FAS activity was assayed by measuring the incorporation of [1-^{14}C]acetyl-CoA into fatty acids essentially as described above for ACC activity, except that 0.2 mM malonyl-CoA was included and ATP, butyryl-CoA and FAS were omitted in the digitonin-containing assay mixture [28]. The assay was carried out at 37°C for 10 min.

Both the lipogenic assays were stopped by the addition of 100 μL of 10 M NaOH. The samples were saponified by adding 5 mL of CH_3OH and boiling for 45–60 min in capped tubes. After acidification with 200 μL of 12 M HCl, fatty acids were extracted and counted for the radioactivity as in [5].

The activities of ACC and FAS are expressed as nanomoles of [1-^{14}C]acetyl-CoA incorporated into fatty acids per minute per milligram of protein.

2.8. Activity Assay of 3-Hydroxy-3-Methylglutaryl-CoA Reductase (HMGCR). HMGCR is the rate-controlling enzyme in the biosynthesis of cholesterol. The HMGCR activity assay was carried out essentially as described in [5]. Briefly, C6 cells were seeded at a density of 2×10^6 cells per 100 mm diameter Petri dish. After 48 h, 25 μM OA and HTyr were added singularly or in coincubation to the medium for 4 h. Then, the medium was discarded and the cells were scraped into a buffer containing 50 mM Tris-HCl (pH 7.4) and 150 mM NaCl. After centrifugation (900 ×g, 3 min, room temperature), the pellet was frozen in liquid nitrogen and kept at −80°C until use.

Cell extracts were prepared from the pellets which were thawed, resuspended, and subsequently used for HMGCR activity assay [5]. The reaction started by the addition of [3-^{14}C]HMG-CoA (75 μM, 1.8 Ci/mol). After 120 min at 37°C, the reaction was stopped by the addition of 20 μL of 7 M HCl. Conversion to mevalonolactone occurred following an additional 60 min incubation at 37°C and the radioactive product was isolated by TLC, using toluene : acetone (1 : 1) as the mobile phase. Spots were collected and counted for the radioactivity. As internal standard, [^{3}H]mevalonolactone was used.

2.9. Isolation of RNA from C6 Cells and Real-Time qPCR Analysis. Total RNA from C6 cells was isolated using the SV Total RNA Isolation System kit (Promega), following the manufacturer's instructions. The reverse transcriptase reaction (20 μl) was carried out using 5 μg of total RNA, 100 ng of random hexamers, and 200 units of SuperScript III RNase H-Reverse Transcriptase (Life Technologies—Thermo Fisher Scientific, Waltham, MA) [29].

Quantitative gene expression analysis was performed using SYBR® Select Master Mix for CFX (Life Technologies—Thermo Fisher Scientific, Waltham, MA) and 18S rRNA for normalization. The primers used for quantitative real-time PCR analysis were as follows (5′ to 3′): rFASNfor CTCTGGTGGTGTCTACATTTC; rFASNrev GAGCTCTT TCTGCAGGATAG; rACCfor CTTGGAGCAGAGAACC TTCG; rACCrev; CCTGGATGGTTCTTTGTCCC; rHMG CRfor CTCACAGGATGAAGTAAGGG; rHMGCRrev CT GAGCTGCCAAATTGGACG [30]

2.10. Western Blotting Analysis. Cells grown in 6-well dishes were treated with OA and/or HTyr as indicated above and lysed as previously described [12]. The extracts were boiled for 5 min and samples containing an equal amount of total protein (25 μg) were loaded on 10% SDS-polyacrylamide gels. Following electrophoresis, the proteins were transferred onto a nitrocellulose membrane [13]. To detect ACC, FAS, and HMGCR, membranes were incubated with the specific primary antibodies for 1.5 h at room temperature and then for 1 h with appropriate horseradish peroxidase-conjugated IgG (dilution 1 : 5000). Signals were detected by enhanced chemiluminescence using the Amersham ECL plus kit (GE Healthcare, Milan, Italy). Beta-actin detection was used for signal normalization.

3. Statistical Analysis

Data are the means ± S.D. for the indicated number of experiments. The results were computed with Excel (Microsoft 10). Comparisons among groups were made using one-way analysis of variance (ANOVA). The differences between mean values were tested, using Bonferroni post hoc test. All statistical analyses were performed by GraphPad Prism 6 software (GraphPad Software Inc., La Jolla, CA). Differences were considered statistically significant at $P < 0.05$.

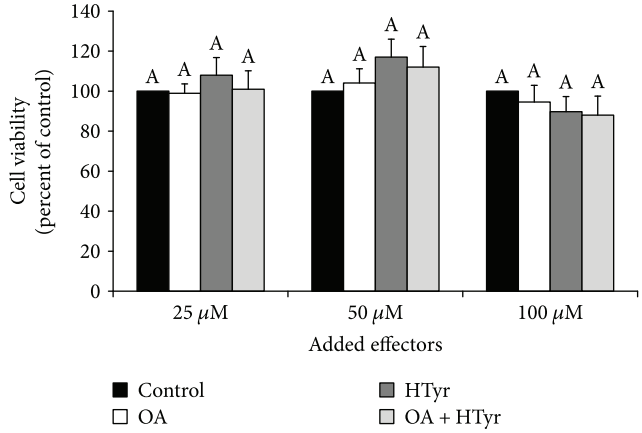

Figure 1: Effect of oleic acid and/or hydroxytyrosol on C6 cell viability. C6 cells were incubated for 4 h with 25 μM, 50 μM, and 100 μM OA, HTyr, or their combination in serum-rich medium. Cell viability was estimated by an MTT assay. Values, expressed as % of control, are means ± S.D. of five experiments. Within the same group, samples bearing different letters differ significantly ($P < 0.05$). Control: untreated cells; OA: oleic acid; HTyr: hydroxytyrosol.

4. Results

4.1. Cell Viability. MTT test showed that C6 cells incubated with OA or HTyr (25 μM, 50 μM, and 100 μM for 4 h), had the same viability of the control cells at each tested concentration (Figure 1). Also, the coincubation of OA and HTyr did not exert any cytotoxic effect. These findings were corroborated by morphological observation, protein assay, and trypan blue exclusion (data not shown). Thus, all further experiments were performed on cells treated with 25 μM OA, 25 μM HTyr, or their combination and incubated for 4 h in order to exclude putative nonspecific toxic effect while at the same time using the lowest effective concentration.

4.2. Effect of OA, HTyr, and Their Combination on Cholesterol and Fatty Acid Syntheses. Acetate in the cell is transformed into acetyl-CoA, which represents a common precursor for both fatty acid and cholesterol synthesis. Hence, both these metabolic pathways were simultaneously followed by using labelled acetate as a precursor.

Bar graphs in Figure 2 show a significant reduction of [1-^{14}C]acetate incorporation into total cholesterol (Figure 2(a)) and fatty acids (Figure 2(b)). In particular, when C6 cells were incubated for 4 h with OA or HTyr, a decrease by 24% and 18%, respectively, of [1-^{14}C]acetate incorporation into cholesterol was observed. This inhibition was much more evident (−36% versus untreated cells) if OA and HTyr were added in combination to the cells.

With respect to cholesterologenesis, fatty acid synthesis was greater affected by EVOO compounds under investigation. Incubation of C6 cells singularly with OA, or HTyr led to a reduction of the radiolabelled acetate incorporation into fatty acids by about 56% and 23%, respectively, compared to that measured in control cells. Analogously to cholesterol synthesis, fatty acid synthesis inhibition was more pronounced (−68% versus untreated cells) after 4 h of OA and HTyr coincubation of C6 cells.

4.3. Effect of EVOO Components on Radiolabelled Acetate Incorporation into Phospholipids and Neutral Lipids. Since newly synthesized fatty acids are mainly incorporated into complex lipids, the effect of OA and HTyr addition to C6 glioma cells on [1-^{14}C]acetate incorporation into polar and neutral lipids was tested (Table 1). A general decrease of labelled precursor incorporation into all phospholipids, particularly into phosphatidylcholine, the most abundant phospholipid in C6 glioma cells, was observed mainly when cells were incubated for 4 h with OA and HTyr in combination. Among neutral lipids, unesterified fatty acids, cholesterol, and cholesterol ester were the fractions showing significant reduction in radioactivity incorporation due to the EVOO compound addition. Interestingly, only slight reduction in the incorporation of labelled acetate into triglycerides (TG) was detected after additions of OA and HTyr.

4.4. Analysis of Newly Synthesized Radiolabelled Fatty Acids. In order to investigate the effect of OA and HTyr additions to C6 cells on the individual fatty acids synthesized from labelled acetate, an HPLC analysis of the total fatty acid extract was carried out.

Figure 3 shows that, in agreement with previous results [5], in control cells, the incorporation of labelled acetate into the individual fatty acids was in the following order: palmitic acid (C16:0) > stearic acid (C18:0) > oleic acid (C18:1). Only a small amount of radioactivity was incorporated into other fatty acids (data not shown). A reduction of about 50% of the radiolabelled incorporation into palmitic, stearic, and oleic acid was observed upon OA addition to the cells, while a near 30% decrease was evidenced upon HTyr treatment. The inhibitory effect of [1-^{14}C]acetate incorporation into the fatty acids was more pronounced (about 70%) when both OH and HTyr were contemporaneously added to the medium culture.

4.5. Modulation of Activity of ACC, FAS, and HMGCR by OA, HTyr, and Their Combination. Palmitic acid and to a lesser extent stearic acid are the main final products of the de novo fatty acid synthesis.

In order to determine the enzymatic steps of lipid biosynthetic pathways affected by the addition of OA, HTyr, and their combination, experiments were carried out to assay the activities of the key enzymes ACC and FAS for de novo fatty acid synthesis and HMGCR for cholesterol synthesis. All enzymatic activities were measured by in situ assays using digitonin-permeabilized C6 cells.

4 h incubation of C6 cells with 25 μM of OA or HTyr caused a reduction of ACC activity by about 45% and 19%, respectively (Figure 4). A further decrement (−56% versus untreated cells) was measured when these compounds were coincubated.

OA or HTyr lowered HMGCR activity by 29% and 16%, respectively. During coincubation, the inhibition was more pronounced. In fact, HMGCR activity reached 61% of

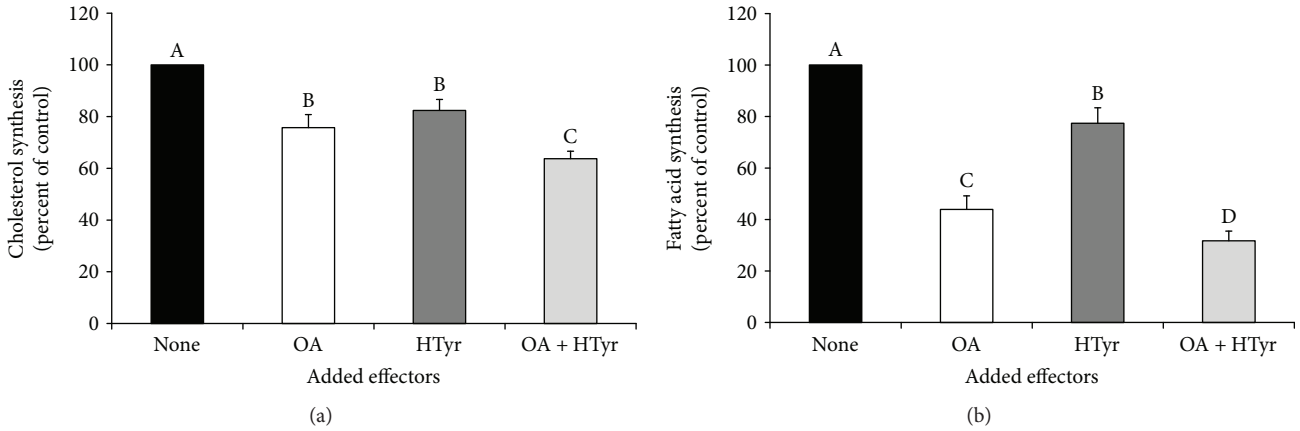

Figure 2: Modulation of cholesterol and fatty acid syntheses by oleic acid and/or hydroxytyrosol. After an initial 48 h plating, C6 glioma cells, growing in serum-rich medium, were incubated for 4 h with 25 μM OA and/or 25 μM HTyr. During the last hour of incubation, labelled acetate was added and its incorporation into cholesterol (a) and fatty acids (b) was followed. Data, nmol [1-^{14}C]acetate/h/mg protein, are expressed as % of control and are means ± S.D. of six independent experiments. In each experiment, determinations were carried out in triplicate. In control cells, rates of cholesterol and fatty acid synthesis were 1.43 ± 0.07 and 8.67 ± 0.49 nmol [1-^{14}C]acetate inc/h/mg protein, respectively. Samples bearing different letters differ significantly ($P < 0.05$). None: no addition to the cells; OA: oleic acid; HTyr: hydroxytyrosol.

Table 1: Effect of OA and HTyr and their combination on [1-^{14}C]acetate incorporation into various lipid fractions in C6 cells

Added effectors	None	OA	HTyr	OA + HTyr
Polar lipids				
CL + PE	2151 ± 151^{a}	1377 ± 85^{b}	1742 ± 121^{c}	1119 ± 75^{d}
PC	15,908 ± 875^{a}	5596 ± 308^{b}	12,781 ± 703^{c}	3487 ± 192^{d}
SM	741 ± 67^{a}	463 ± 37^{b}	640 ± 37^{a}	270 ± 19^{c}
PS + PI	3781 ± 246^{a}	1439 ± 101^{b}	2533 ± 165^{c}	962 ± 65^{d}
Neutral lipids				
MG	289 ± 20^{a}	231 ± 11^{b,c}	252 ± 11^{b}	214 ± 7^{c}
DG	711 ± 136^{a}	587 ± 24^{a}	623 ± 27^{a}	562 ± 35^{a}
Cholesterol	2155 ± 194^{a}	1724 ± 155^{b}	1896 ± 170^{a,b}	1509 ± 136^{b}
Unesterified fatty acids	239 ± 14^{a}	200 ± 12^{a,b}	187 ± 11^{b}	123 ± 8^{b}
TG	1123 ± 73^{a}	1048 ± 68^{a,b}	999 ± 65^{a,b}	921 ± 60^{b}
CE	896 ± 63^{a}	659 ± 46^{b,c}	725 ± 47^{a,b}	587 ± 23^{c}

C6 cells were incubated with 25 μM oleic acid (OA) and/or 25 μM hydroxytyrosol (HTyr) for 4 h, and labeled acetate was added 1 h before ending the incubation. Total lipids were extracted. Phospholipids and neutral lipids were resolved by TLC, and the radioactivity associated with the different lipid fractions was counted. CL: cardiolipin; PE: phosphatidylethanolamine; PC: phosphatidylcholine; SM: sphingomyelin; PS: phosphatidylserine; PI: phosphatidylinositol; MG: monoglycerides; DG: diglycerides; TG: triglycerides; CE: cholesterol esters. Values are expressed as cpm/mg protein ± SD, $n = 5$. Within the same group, samples bearing different letters differ significantly ($P < 0.05$).

that observed in control cells in presence of 25 μM OA and 25 μM HTyr.

Notably, FAS activity was not significantly affected by either incubation conditions.

The reduced activity of ACC and of HMGCR is in accordance with the results of Figure 2, regarding the reduction of total synthesis of fatty acids (Figure 2(a)) and cholesterol (Figure 2(b)) starting from [1-^{14}C]acetate.

4.6. Regulation of ACC, FAS, and HMGCR Expression by OA, HTyr and OA + HTyr. Next, the molecular mechanisms responsible for the modulation exerted by OA or HTyr on the above-reported enzyme activities were investigated. To this aim, the abundance of mRNAs encoding for ACC, FAS, and HMGCR was quantified by real-time qPCR analysis, and the amount of the corresponding encoded protein was determined by Western blotting.

In treated cells, a decrease of ACC mRNA abundance was observed (Figure 5(a)). After OA incubation, ACC mRNA level decreased by about 42% with respect to that measured in control cells; HTyr singularly added to the cell culture medium exerted minor inhibitory effect. In all the experimental conditions tested, no significant change in the abundance of FAS mRNA was detected (Figure 5(a)). After 4 h incubation with 25 μM OA alone or in combination with 25 μM HTyr, the amount of HMGCR mRNA lowered by about 18% and 22%, respectively (Figure 5(a)). Results obtained for ACC, FAS, and HMGCR mRNA abundance

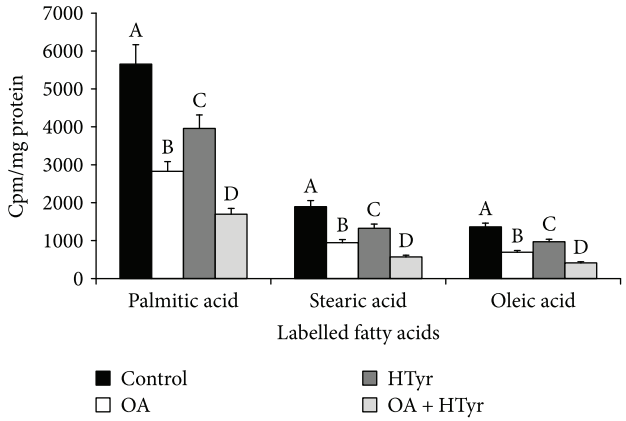

Figure 3: Effect of oleic acid, hydroxytyrosol, or their combination on [1-^{14}C]acetate incorporation into individual fatty acids. The effects of 25 μM OA, 25 μM HTyr, and their combination on the incorporation of labelled acetate into different fatty acids were assayed. After 4 h of incubation, the radiolabelled neosynthesized fatty acids were extracted and separated by HPLC. Eluted fractions, corresponding to the different fatty acids, were collected for radioactivity measurement. Data, expressed as cpm/mg protein, represent means ± S.D. of six experiments. Within the same group, samples bearing different letters differ significantly ($P < 0.05$). OA: oleic acid; HTyr: hydroxytyrosol.

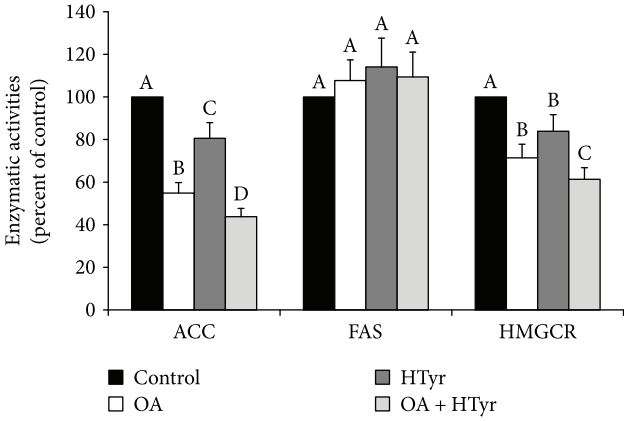

Figure 4: Oleic acid and/or hydroxytyrosol modulation of ACC, FAS, and HMGCR activities. After 4 h incubation with 25 μM of OA, HTyr, or OA + HTyr, the indicated enzyme activities were assayed in digitonin-permeabilized C6 cells. Values, expressed as percentage of control, are means ± SD of five independent experiments. Control-specific activities were ACC, 0.178 ± 0.011 [1-^{14}C]acetyl-CoA inc/min/mg protein; FAS, 0.051 ± 0.003 nmol [1-^{14}C]acetyl-CoA inc/min/mg protein; HMGCR, 33.6 ± 1.9 pmol [3-^{14}C]HMG-CoA inc/min/mg protein. Within the same group, samples bearing different letters differ significantly ($P < 0.05$). OA: oleic acid; HTyr: hydroxytyrosol.

were confirmed also by the Western blotting analysis of the respective protein contents (Figure 5(b)).

5. Discussion

The Mediterranean diet has been considered the healthier dietary regimen, related to a reduced risk of several pathologies

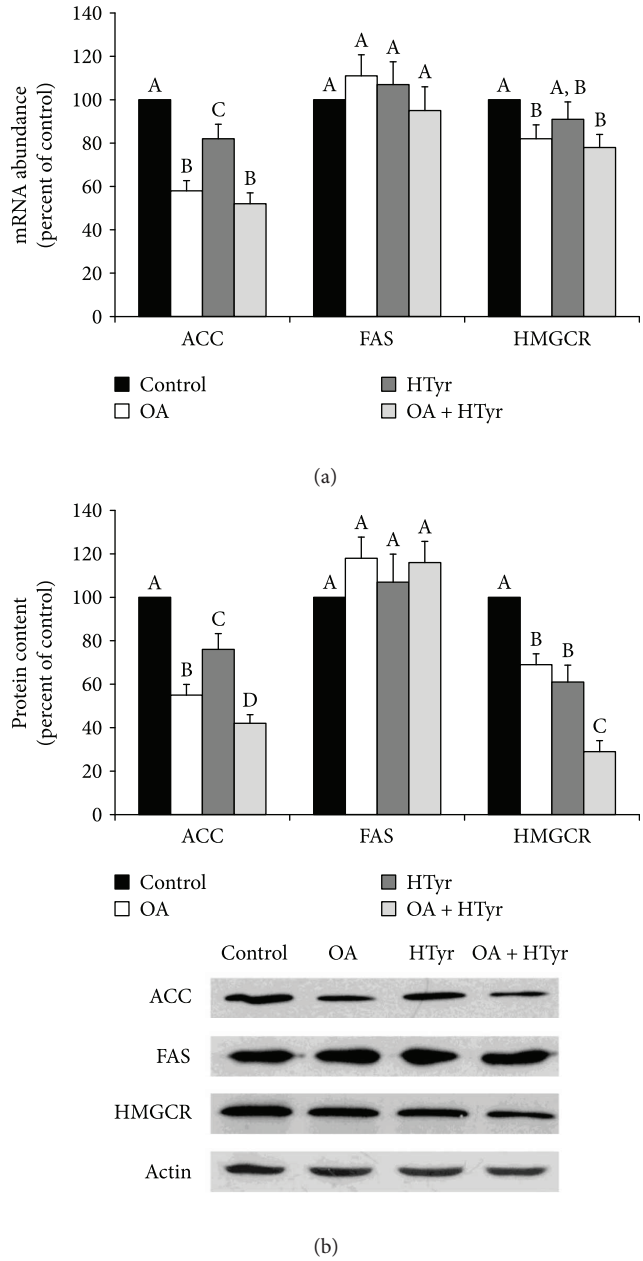

Figure 5: Effect of oleic acid, hydroxytyrosol, or their combination on ACC, FAS, and HMGCR mRNA abundance and protein content in C6 glioma cells. C6 cells were incubated with 25 μM of OA, HTyr, or OA + HTyr for 4 h in serum-rich medium. (a) The abundance of ACC, FAS, and HMGCR mRNA was determined by RT-qPCR and normalized with respect to 18S rRNA, used as a reference. Normalized values are expressed in histograms as percentage of the control. Values are means ± S.D. of triplicate samples from each of four independent experiments. (b) C6 cells were lysed and protein content was isolated. ACC, FAS, and HMGCR were then assessed by Western blotting and quantified by densitometry. The protein contents are expressed as percentage of the control and are means ± SD of three independent experiments. Within the same group, samples bearing different letters differ significantly ($P < 0.05$). OA: oleic acid; HTyr: hydroxytyrosol.

such as metabolic disorders and cardiovascular diseases [1, 2, 6, 31, 32]. A key component of the Mediterranean diet is the EVOO, which is characterized by the presence of bioactive phytonutrients, with antioxidant and anti-inflammatory properties, and of monounsaturated fatty acid (OA) as fat source.

Studies from a number of research groups have established that variations in dietary fatty acids or in the intake of phenolic compounds are able to influence cellular metabolism and regulatory processes in neuronal and glial cells [3, 5, 17, 24], supporting mounting evidence that EVOO active components could have a great potential to reduce the incidence of neurodegenerative diseases [3, 18, 33]. It has to be stressed that most of these studies focused mainly on the antioxidant and anti-inflammatory activities of fatty acids [7] and of phenolic compounds [20], without taking into account their possible direct action on metabolism, such as lipid biosynthesis.

Lipids are fundamental components of neuronal membranes and are essential for brain function. Cholesterol and fatty acids are particularly present in the synaptic membranes and play a key role in the membrane fluidity and in the formation of specialized microdomains, lipid rafts, essential for synaptic transmission [34].

Brain lipids can derive from blood and/or can be endogenously synthesized. Fatty acids can cross the blood-brain barrier by a complex process, involving diffusional and protein-mediated transport, which occurs predominantly by fatty acid transport protein-1 and protein-4 (FATP-1 and FATP-4) in humans and mouse [34]. Lipid synthesis is inefficient in neurons but not in glia cells. *In vitro* studies have demonstrated that astrocytes, the most abundant glia cells, synthesize and release lipids that are complexed to apolipoprotein E- (ApoE-) containing lipoproteins [35]. Consequently, neuronal functions are negatively affected by perturbed lipid metabolism which has been observed in several neurological disorders, such as Niemann-Pick's disease [36], Alzheimer's disease [37], Huntington's disease [38], Parkinson's disease [39], and amyotrophic lateral sclerosis [40].

Despite the crucial role of EVOO bioactive compounds in brain function and metabolism, little is known about their action on lipogenesis in glial cells [5].

This work primarily shows that both fatty acid and cholesterol syntheses are rather active in cultured glioma C6 cells when [1-^{14}C]acetate is used as common precursor for both the metabolic pathways, thus adding further support to previous findings [5]. Notably, in human malignant glial cells, compared with their normal counterparts, a very active de novo fatty acids and cholesterol syntheses have been reported [41].

The present study represents the first report of a direct and rapid effect of EVOO main compounds (OA and HTyr) on lipid synthesis in rat glioma cells. We show that in C6 cells, the addition of OA and HTyr causes a fast (within 4 h) inhibition of radiolabelled acetate incorporation into both cholesterol and fatty acid fractions. A rapid effect of EVOO components on both these pathways has been described in different cell cultures [12, 13]. Beside the OA, a monounsaturated fatty acid, which represents the most abundant fatty acid (about 70%) in EVOO, polyunsaturated fatty acids (such as linoleic acid), and saturated fatty acid (mainly palmitic acid) are significantly present in the fatty acid fraction of EVOO. However, Natali et al. reported that OA was the most effective in reducing lipid synthesis in C6 cells [5].

Compared to control cells, the radiolabelled precursor incorporation into cholesterol decreased by about 30% in cells incubated with 25 μM OA and 25 μM HTyr (Figure 2(a)). This result can be explained, at least in part, by the reduction of HMGCR activity (Figure 4) and the regulatory enzyme of cholesterol synthesis, which is reasonably related to changes in the HMGCR expression. Indeed, the expression of HMGCR at both mRNA and protein levels was noticeably reduced in C6 cells upon treatment with both OA and HTyr.

However, the reduction of cholesterologenesis by EVOO active compounds was often less pronounced, compared with fatty acid synthesis, especially in the case of the OA and HTyr coincubation.

Incubation of C6 cells with OA or HTyr singularly or in combination caused a reduction of [1-^{14}C]acetate incorporation into fatty acids and of their subsequent esterification into complex lipids. The strongest inhibition of labelled acetate incorporation into the phospholipid fractions, mainly into phosphatidylcholine, was observed upon OA and HTyr coincubation (Table 1).

Unlike phospholipids, TG synthesis in C6 cells seems to be poorly affected by EVOO compounds. The opposite trend has been reported to occur in rat hepatocytes, where EVOO components, almost without effect on phospholipid synthesis, greatly reduced acetate incorporation into TG [12, 13]. These findings are in agreement with the role of hepatic cells in TG synthesis [42] and with the assumption that dietary phenolic compounds may have a protective role against hepatic steatosis [12, 13]. Phospholipids and cholesterol are important components of biological membranes. Thus, the remarkable decrease we observed in the present study of the phospholipids and cholesterol syntheses exerted by OA and HTyr led us to suppose that EVOO components might modulate in C6 cells the shift towards membrane biogenesis instead of an accumulation of cellular neutral lipids. Actually, this hypothesis is corroborated by previous studies which indicated that fatty acids exogenously added to C6 cells may represent specific means of controlling gliomatous growth [5, 43, 44].

Coincubation with OA and HTyr greatly reduced the incorporation of [1-^{14}C]acetate into the individual fatty acids, in particular into palmitic acid (Figure 3), the principal final product of the de novo fatty acid synthesis. This metabolic pathway is catalyzed by two enzymatic systems working in sequence: ACC and FAS. The activity of ACC, first committing step in fatty acid biosynthesis, was reduced in C6 cells treated with OA together with HTyr. Then, the reduced ACC activity in OA-/HTyr-treated C6 cells could explain, at least in part, the decrease in the [1-^{14}C]acetate incorporation into the whole fatty acid fraction observed in Figure 2. The molecular mechanism of this reduction was

deepened, and our results clearly indicate that coincubation of OA and HTyr reduced either ACC mRNA abundance or protein level. Conversely, in our experimental condition, that is, 4 h of treatment, OA and/or HTyr incubation showed practically no effect on FAS activity and on FAS mRNA abundance and protein level. With regard to the apparent insensitivity of FAS to 4 h OA and HTyr incubation, it is worth noting that while ACC is regulated by both short- and long-term mechanisms, only the latter is involved in FAS modulation [12, 45].

A great body of evidence indicates HTyr as a potent antioxidant, and its ability to decrease reactive oxygen species (ROS) in both *in vitro* and *in vivo* experiments has been well documented (for review, see [46]). Recent works have highlighted that ROS promote the expression of sterol regulatory element-binding proteins (SREBPs) [47, 48] and transcription factors involved in the upregulation of key enzymes of lipogenesis and cholesterologenesis [31, 49, 50]. In fly, treatment with an antioxidant reduces ROS, suppresses lipid droplet accumulation, and delays neurodegeneration [48]. The present study shows that, in addition to the reported antioxidant effect, HTyr supplementation to C6 cells determines an early and direct decreasing effect on fatty acid synthesis and cholesterologenesis. This effect can be at least partially ascribed to a molecular mechanism that involves the downregulation of the expression of ACC and HMGCR. This decrease is more evident when OA is added to the cells together with HTyr, indicating in most cases an additive effect of these EVOO components on lipid metabolism. Thus, also this aspect should be considered in determining the beneficial action of EVOO components, OA and HTyr, in brain dysfunction when alterations of lipid metabolism take place.

An important matter concerns the bioavailability of EVOO phenolic compounds. HTyr is dose-dependently absorbed in humans [51, 52]. Data on plasma phenol concentrations that can be achieved in humans after consumption of olive oil are poor and controversial [52]. This may be due to a number of factors: (i) the very variable levels of phenols found in EVOO (50–800 mg/kg) [53], (ii) the level of dietary intake of olive oil, and (iii) the method and the time chosen for plasma phenol quantification [53]. Most of HTyr is present in plasma and urine in conjugated forms, mainly glucuroconjugates, suggesting extensive first-pass intestinal/hepatic metabolism of the ingested HTyr [54]. However, a plasma concentration of HTyr up to 15 μM has been measured in humans during the first 4 h after ingestion of 40 mL of olive oil containing a considerable amount of phenols (366 mg/kg) [55]. Moreover, it has been established that HTyr is able to cross the blood-brain barrier, although it presents a low brain uptake [3]. Considering the above, the question of EVOO phenol bioavailability in the brain remains a matter of debate and the physiological relevance of these *in vitro* findings needs to be tested in appropriate animal models and in humans. However, even if the HTyr concentration used in the present study (25 μM) could be considered a pharmacological dose, the present study indicates an early and direct downregulatory effect of HTyr on fatty acids and cholesterol syntheses.

6. Conclusions

Correct lipid homeostasis is essential for cell survival and performance. Thus, brain fatty acid and cholesterol synthesis are critically challenged in several neurodegenerative diseases. The modulation of the activity and expression of the key enzymes of these metabolic pathways by OA and HTyr suggest a putative role in the prevention of neurological diseases, where dysfunction of lipid metabolism is involved. In this context, the reduced ACC and HMGCR expression and activity we observed in glial cells treated with such compounds may be considered of importance.

Conflicts of Interest

The authors declare that there is no conflict of interest regarding the publication of this article.

Acknowledgments

This work was in part supported by Ministero della Salute Project GR-2013-02355646.

References

[1] E. Toledo, J. Salas-Salvadó, C. Donat-Vargas et al., "Mediterranean diet and invasive breast cancer risk among women at high cardiovascular risk in the PREDIMED trial: a randomized clinical trial," *JAMA Internal Medicine*, vol. 175, no. 11, pp. 1752–1760, 2015.

[2] M. Á. Martínez-González, M. Ruiz-Canela, A. Hruby, L. Liang, A. Trichopoulou, and F. B. Hu, "Intervention trials with the Mediterranean diet in cardiovascular prevention: understanding potential mechanisms through metabolomic profiling," *The Journal of Nutrition*, vol. 146, no. 4, pp. 913S–919S, 2016.

[3] J. Rodríguez-Morató, L. Xicota, M. Fitó, M. Farré, M. Dierssen, and R. de la Torre, "Potential role of olive oil phenolic compounds in the prevention of neurodegenerative diseases," *Molecules*, vol. 20, no. 3, pp. 4655–4680, 2015.

[4] L. Fernández del Río, E. Gutiérrez-Casado, A. Varela-López, and J. Villalba, "Olive oil and the hallmarks of aging," *Molecules*, vol. 21, no. 2, p. 163, 2016.

[5] F. Natali, L. Siculella, S. Salvati, and G. V. Gnoni, "Oleic acid is a potent inhibitor of fatty acid and cholesterol synthesis in C6 glioma cells," *The Journal of Lipid Research*, vol. 48, no. 9, pp. 1966–1975, 2007.

[6] P. Priore, A. Cavallo, A. Gnoni, F. Damiano, G. V. Gnoni, and L. Siculella, "Modulation of hepatic lipid metabolism by olive oil and its phenols in nonalcoholic fatty liver disease," *IUBMB Life*, vol. 67, no. 1, pp. 9–17, 2015.

[7] E. Lei, K. Vacy, and W. C. Boon, "Fatty acids and their therapeutic potential in neurological disorders," *Neurochemistry International*, vol. 95, pp. 75–84, 2016.

[8] M. Piroddi, A. Albini, R. Fabiani et al., "Nutrigenomics of extra-virgin olive oil: a review," *BioFactors*, vol. 43, no. 1, pp. 17–41, 2017.

[9] R. Fabiani, "Anti-cancer properties of olive oil secoiridoid phenols: a systematic review of *in vivo* studies," *Food & Function*, vol. 7, no. 10, pp. 4145–4159, 2016.

[10] C. C. Tangney and H. E. Rasmussen, "Polyphenols, inflammation, and cardiovascular disease," *Current Atherosclerosis Reports*, vol. 15, no. 5, p. 324, 2013.

[11] F. Visioli, G. Bellomo, and C. Galli, "Free radical-scavenging properties of olive oil polyphenols," *Biochemical and Biophysical Research Communications*, vol. 247, no. 1, pp. 60–64, 1998.

[12] P. Priore, L. Siculella, and G. V. Gnoni, "Extra virgin olive oil phenols down-regulate lipid synthesis in primary-cultured rat-hepatocytes," *The Journal of Nutritional Biochemistry*, vol. 25, no. 7, pp. 683–691, 2014.

[13] P. Priore, D. Caruso, L. Siculella, and G. V. Gnoni, "Rapid down-regulation of hepatic lipid metabolism by phenolic fraction from extra virgin olive oil," *European Journal of Nutrition*, vol. 54, no. 5, pp. 823–833, 2015.

[14] W. J. Lukiw, M. Pappolla, R. P. Pelaez, and N. G. Bazan, "Alzheimer's disease—a dysfunction in cholesterol and lipid metabolism," *Cellular and Molecular Neurobiology*, vol. 25, no. 3-4, pp. 475–483, 2005.

[15] A. Romano, J. B. Koczwara, C. A. Gallelli et al., "Fats for thoughts: an update on brain fatty acid metabolism," *The International Journal of Biochemistry & Cell Biology*, vol. 84, pp. 40–45, 2017.

[16] C. Féart, C. Samieri, V. Rondeau et al., "Adherence to a Mediterranean diet, cognitive decline, and risk of dementia," *JAMA*, vol. 302, no. 6, pp. 638–648, 2009.

[17] V. Pitozzi, M. Jacomelli, M. Zaid et al., "Effects of dietary extra-virgin olive oil on behaviour and brain biochemical parameters in ageing rats," *British Journal of Nutrition*, vol. 103, no. 11, pp. 1674–1683, 2010.

[18] D. Pantano, I. Luccarini, P. Nardiello, M. Servili, M. Stefani, and F. Casamenti, "Oleuropein aglycone and polyphenols from olive mill waste water ameliorate cognitive deficits and neuropathology," *British Journal of Clinical Pharmacology*, vol. 83, no. 1, pp. 54–62, 2017.

[19] S. Torres, M. Lorente, F. Rodríguez-Fornés et al., "A combined preclinical therapy of cannabinoids and temozolomide against glioma," *Molecular Cancer Therapeutics*, vol. 10, no. 1, pp. 90–103, 2011.

[20] I. Matias, A. S. Buosi, and F. C. A. Gomes, "Functions of flavonoids in the central nervous system: astrocytes as targets for natural compounds," *Neurochemistry International*, vol. 95, pp. 85–91, 2016.

[21] J. J. Volpe, K. Fujimoto, J. C. Marasa, and H. C. Agrawal, "Relation of C-6 glial cells in culture to myelin," *The Biochemical Journal*, vol. 152, no. 3, pp. 701–703, 1975.

[22] F. A. McMorris, "Norepinephrine induces glial-specific enzyme activity in cultured plasma glioma cells," *Proceedings of the National Academy of Sciences of the United States of America*, vol. 74, no. 10, pp. 4501–4504, 1977.

[23] K. A. Nave and G. Lemke, "Induction of the myelin proteolipid protein (PLP) gene in C6 glioblastoma cells: functional analysis of the PLP promotor," *The Journal of Neuroscience*, vol. 11, no. 10, pp. 3060–3069, 1991.

[24] A. Quincozes-Santos, L. D. Bobermin, A. Latini et al., "Resveratrol protects C6 astrocyte cell line against hydrogen peroxide-induced oxidative stress through heme oxygenase 1," *PLoS One*, vol. 8, no. 5, article e64372, 2013.

[25] G. V. Gnoni, M. J. H. Geelen, C. Bijleveld, E. Quagliariello, and S. G. van den Bergh, "Short-term stimulation of lipogenesis by triiodothyronine in maintenance cultures of rat hepatocytes," *Biochemical and Biophysical Research Communications*, vol. 128, no. 2, pp. 525–530, 1985.

[26] E. G. Bligh and W. J. Dyer, "A rapid method of total lipid extraction and purification," *Canadian Journal of Biochemistry and Physiology*, vol. 37, no. 1, pp. 911–917, 1959.

[27] M. J. H. Geelen, "The use of digitonin-permeabilized mammalian cells for measuring enzyme activities in the course of studies on lipid metabolism," *Analytical Biochemistry*, vol. 347, no. 1, pp. 1–9, 2005.

[28] P. Priore, A. M. Giudetti, F. Natali, G. V. Gnoni, and M. J. H. Geelen, "Metabolism and short-term metabolic effects of conjugated linoleic acids in rat hepatocytes," *Biochimica et Biophysica Acta (BBA) - Molecular and Cell Biology of Lipids*, vol. 1771, no. 10, pp. 1299–1307, 2007.

[29] F. Damiano, R. Tocci, G. V. Gnoni, and L. Siculella, "Expression of citrate carrier gene is activated by ER stress effectors XBP1 and ATF6α, binding to an UPRE in its promoter," *Biochimica et Biophysica Acta (BBA) - Gene Regulatory Mechanisms*, vol. 1849, no. 1, pp. 23–31, 2015.

[30] L. Siculella, R. Tocci, A. Rochira, M. Testini, A. Gnoni, and F. Damiano, "Lipid accumulation stimulates the cap-independent translation of SREBP-1a mRNA by promoting hnRNP A1 binding to its 5′-UTR in a cellular model of hepatic steatosis," *Biochimica et Biophysica Acta (BBA) - Molecular and Cell Biology of Lipids*, vol. 1861, no. 5, pp. 471–481, 2016.

[31] E. Scoditti, N. Calabriso, M. Massaro et al., "Mediterranean diet polyphenols reduce inflammatory angiogenesis through MMP-9 and COX-2 inhibition in human vascular endothelial cells: a potentially protective mechanism in atherosclerotic vascular disease and cancer," *Archives of Biochemistry and Biophysics*, vol. 527, no. 2, pp. 81–89, 2012.

[32] E. Scoditti, A. Nestola, M. Massaro et al., "Hydroxytyrosol suppresses MMP-9 and COX-2 activity and expression in activated human monocytes via PKCα and PKCβ1 inhibition," *Atherosclerosis*, vol. 232, no. 1, pp. 17–24, 2014.

[33] N. Scarmeas, Y. Stern, M. X. Tang, R. Mayeux, and J. A. Luchsinger, "Mediterranean diet and risk for Alzheimer's disease," *Annals of Neurology*, vol. 59, no. 6, pp. 912–921, 2006.

[34] R. W. Mitchell, N. H. On, M. R. Del Bigio, D. W. Miller, and G. M. Hatch, "Fatty acid transport protein expression in human brain and potential role in fatty acid transport across human brain microvessel endothelial cells," *Journal of Neurochemistry*, vol. 117, no. 4, pp. 735–746, 2011.

[35] J. Zhang and Q. Liu, "Cholesterol metabolism and homeostasis in the brain," *Protein & Cell*, vol. 6, no. 4, pp. 254–264, 2015.

[36] M. Madra and S. L. Sturley, "Niemann-Pick type C pathogenesis and treatment: from statins to sugars," *Clinical Lipidology*, vol. 5, no. 3, pp. 387–395, 2010.

[37] N. Sato and R. Morishita, "The roles of lipid and glucose metabolism in modulation of β-amyloid, tau, and neurodegeneration in the pathogenesis of Alzheimer disease," *Frontiers in Aging Neuroscience*, vol. 7, p. 199, 2015.

[38] R. C. Block, E. R. Dorsey, C. A. Beck, J. T. Brenna, and I. Shoulson, "Altered cholesterol and fatty acid metabolism in Huntington disease," *Journal of Clinical Lipidology*, vol. 4, no. 1, pp. 17–23, 2010.

[39] M. Doria, L. Maugest, T. Moreau, G. Lizard, and A. Vejux, "Contribution of cholesterol and oxysterols to the pathophysiology of Parkinson's disease," *Free Radical Biology & Medicine*, vol. 101, pp. 393–400, 2016.

[40] N. D. Perera and B. J. Turner, "AMPK signalling and defective energy metabolism in amyotrophic lateral sclerosis," *Neurochemical Research*, vol. 41, no. 3, pp. 544–553, 2016.

[41] P. Prasanna, A. Thibault, L. Liu, and D. Samid, "Lipid metabolism as a target for brain cancer therapy: synergistic activity of lovastatin and sodium phenylacetate against human glioma cells," *The Journal of Neurochemistry*, vol. 66, no. 2, pp. 710–716, 1996.

[42] M. Tuohetahuntila, M. R. Molenaar, B. Spee et al., "ATGL and DGAT1 are involved in the turnover of newly synthesized triacylglycerols in hepatic stellate cells," *Journal of Lipid Research*, vol. 57, no. 7, pp. 1162–1174, 2016.

[43] J. E. C. Sykes and M. Lopes-Cardozo, "Effect of exogenous fatty acids on lipid synthesis, marker-enzymes, and development of glial cells maintained in serum-free culture," *Glia*, vol. 3, no. 6, pp. 495–501, 1990.

[44] F. Leonardi, L. Attorri, R. D. Benedetto et al., "Effect of arachidonic, eicosapentaenoic and docosahexaenoic acids on the oxidative status of C6 glioma cells," *Free Radical Research*, vol. 39, no. 8, pp. 865–874, 2005.

[45] C. F. Semenkovich, "Regulation of fatty acid synthase (FAS)," *Progress in Lipid Research*, vol. 36, no. 1, pp. 43–53, 1997.

[46] F. Echeverría, M. Ortiz, R. Valenzuela, and L. A. Videla, "Hydroxytyrosol and cytoprotection: a projection for clinical interventions," *The International Journal of Biochemistry & Cell Biology*, vol. 18, no. 5, article e930, 2017.

[47] A. M. Giudetti, F. Damiano, G. V. Gnoni, and L. Siculella, "Low level of hydrogen peroxide induces lipid synthesis in BRL-3A cells through a CAP-independent SREBP-1a activation," *The International Journal of Biochemistry & Cell Biology*, vol. 45, no. 7, pp. 1419–1426, 2013.

[48] L. Liu, K. Zhang, H. Sandoval et al., "Glial lipid droplets and ROS induced by mitochondrial defects promote neurodegeneration," *Cell*, vol. 160, no. 1-2, pp. 177–190, 2015.

[49] W. Shao and P. J. Espenshade, "Expanding roles for SREBP in metabolism," *Cell Metabolism*, vol. 16, no. 4, pp. 414–419, 2012.

[50] F. Damiano, A. Rochira, R. Tocci, S. Alemanno, A. Gnoni, and L. Siculella, "HnRNP A1 mediates the activation of the IRES-dependent SREBP-1a mRNA translation in response to endoplasmic reticulum stress," *Biochemical Journal*, vol. 449, no. 2, pp. 543–553, 2013.

[51] F. Visioli, C. Galli, F. Bornet et al., "Olive oil phenolics are dose-dependently absorbed in humans," *FEBS Letters*, vol. 46, no. 2-3, pp. 159-160, 2000.

[52] R. de la Torre, "Bioavailability of olive oil phenolic compounds in humans," *Inflammopharmacology*, vol. 16, no. 5, pp. 245–247, 2008.

[53] F. Visioli and C. Galli, "Olive oil: more than just oleic acid," *The American Journal of Clinical Nutrition*, vol. 72, no. 3, p. 853, 2000.

[54] E. Miro-Casas, M. I. Covas, M. Farre et al., "Hydroxytyrosol disposition in humans," *Clinical Chemistry*, vol. 49, no. 6, pp. 945–952, 2003.

[55] M. I. Covas, K. de la Torre, M. Farré-Albaladejo et al., "Postprandial LDL phenolic content and LDL oxidation are modulated by olive oil phenolic compounds in humans," *Free Radical Biology & Medicine*, vol. 40, no. 4, pp. 608–616, 2006.

Hindawi
Oxidative Medicine and Cellular Longevity
Volume 2017, Article ID 8526438, 16 pages
https://doi.org/10.1155/2017/8526438

Review Article

Polyphenols and Oxidative Stress in Atherosclerosis-Related Ischemic Heart Disease and Stroke

Yu-Chen Cheng,[1] Jer-Ming Sheen,[1] Wen Long Hu,[1,2,3] and Yu-Chiang Hung[1,4]

[1]*Department of Chinese Medicine, College of Medicine, Kaohsiung Chang Gung Memorial Hospital and Chang Gung University, Kaohsiung, Taiwan*
[2]*Kaohsiung Medical University College of Medicine, Kaohsiung, Taiwan*
[3]*Fooyin University College of Nursing, Kaohsiung, Taiwan*
[4]*School of Chinese Medicine for Post Baccalaureate, I-Shou University, Kaohsiung, Taiwan*

Correspondence should be addressed to Yu-Chiang Hung; hungyuchiang@gmail.com

Received 31 July 2017; Revised 16 October 2017; Accepted 18 October 2017; Published 26 November 2017

Academic Editor: Anna M. Giudetti

Good nutrition could maintain health and life. Polyphenols are common nutrient mainly derived from fruits, vegetables, tea, coffee, cocoa, mushrooms, beverages, and traditional medicinal herbs. They are potential substances against oxidative-related diseases, for example, cardiovascular disease, specifically, atherosclerosis-related ischemic heart disease and stroke, which are health and economic problems recognized worldwide. In this study, we reviewed the risk factors for atherosclerosis, including hypertension, diabetes mellitus, hyperlipidemia, obesity, and cigarette smoking as well as the antioxidative activity of polyphenols, which could prevent the pathology of atherosclerosis, including endothelial dysfunction, low-density lipoprotein oxidation, vascular smooth muscle cell proliferation, inflammatory process by monocytes, macrophages or T lymphocytes, and platelet aggregation. The strong radical-scavenging properties of polyphenols would exhibit antioxidative and anti-inflammation effects. Polyphenols reduce ROS production by inhibiting oxidases, reducing the production of superoxide, inhibiting OxLDL formation, suppressing VSMC proliferation and migration, reducing platelet aggregation, and improving mitochondrial oxidative stress. Polyphenol consumption also inhibits the development of hypertension, diabetes mellitus, hyperlipidemia, and obesity. Despite the numerous *in vivo* and *in vitro* studies, more advanced clinical trials are necessary to confirm the efficacy of polyphenols in the treatment of atherosclerosis-related vascular diseases.

1. Introduction

Atherosclerosis-related ischemic heart disease (IHD) and stroke are the leading cause of morbidity or mortality worldwide for decades [1, 2]. Oxidative stress [3–5] is found to be associated with some risk factors [6, 7] of atherosclerosis, such as hypertension, diabetes mellitus, hyperlipidemia, obesity, and cigarette smoking. Numerous relevant studies investigating disease ontology and seeking for effective diagnostic measures and therapies exist. Some researchers found that nutrient antioxidants could help inhibit atherosclerosis process [8–11]. Following, we make a brief introduction of oxidative stress and polyphenols.

1.1. Oxidative Stress. Reactive oxygen species (ROS) are generated as metabolic by-products by biological systems, including superoxide radicals ($\bullet O_2^-$), hydrogen peroxide (H_2O_2), and hydroxyl radicals ($\bullet OH$) [12]. Nitric oxide (NO) plays an important role in vessel dilatation and inflammation. Normally, NO is produced by endothelial nitric oxide synthase (eNOS) in the vessel endothelium. But in the inflammatory process, inducible nitric oxide synthase (iNOS) expresses in macrophages and smooth muscle cells and also produces NO. When $\bullet O_2^-$ contacts to NO, they rapidly react to form the highly reactive molecule peroxynitrite ($ONOO^-$). $\bullet O_2^-$ is rapidly dismutated to the more stable ROS, H_2O_2, by superoxide dismutase (SOD), which is then

converted to H_2O and O_2 by either catalase or glutathione peroxidase [13].

ROS [14] may also play a vital role in the progressive pathology of atherosclerosis, which involves endothelial dysfunction, oxidized low-density lipoprotein (OxLDL) [15], vascular smooth muscle cell (VSMC) proliferation, inflammatory process by monocytes, macrophages, or T lymphocytes, and platelet aggregation. ROS origin from a variety of sources such as NO synthase (NOS), xanthine oxidases, the cyclooxygenases, nicotinamide adenine dinucleotide phosphate (NADPH) oxidase isoforms, and metal-catalyzed reactions [16]. Low-density lipoprotein (LDL) activates endothelial NADPH oxidase, predominantly through a signaling pathway that leads to cytosolic phospholipase A2 (PLA2) activation [17] and promoting ROS formation. Once ROS-induced OxLDL crossed the damaged endothelium into the intima, monocytes differentiate into macrophages, which would in turn take up OxLDL and subsequently become foam cells. These lipid-containing foam cells in the arterial wall can evolve into atherosclerotic plaques or atheromas. Ruptured plaques could result in IHD, stroke, and even death. Hence, reducing the mortality rate due to atherosclerosis is crucial.

1.2. Polyphenol. Polyphenols are common nutrient antioxidants, mainly derived from fruits, vegetables, tea, coffee, cocoa, mushrooms, beverages, and traditional medicinal herbs such as *Salvia miltiorrhiza* [18–20]. The classification of polyphenols mainly includes flavonoids (60%), phenolic acids (30%), and other polyphenols (including stilbenes and lignans) [21], attached at least one aromatic ring with one or more hydroxyl functional groups [22]. Flavonoids, the most studied group of polyphenol, are divided into six subclasses: flavonols, flavones, flavanones, flavanols, anthocyanins, and isoflavones. Phenolic acids are divided into two subclasses, benzoic acid and cinnamic acid. Stilbenes in plants act as antifungal phytoalexins and are rare in human diet. Resveratrol, found in grapes and red wine, is the well-known polyphenol in stilbene group. Lignans are rich in flax, sesame, and many grains [23, 24].

The bioavailability of polyphenols predominantly depends on gut microflora activity [25]. After intake, polyphenols are subjected to three main types of conjugation: methylation, sulfation, and glucuronidation. These metabolic reactions contribute to polyphenols' chemopreventive activities [22]. Polyphenols clearly improve the status of different oxidative stress biomarkers [25]. Previous studies had noted that flavonoids could scavenge superoxide anion and peroxynitrite. They also would exert some antioxidative activity by effectively regulating oxidative stress-mediated enzyme activity [26] and by chelation of the transition metals involved in radical-forming processes [27]. Through direct interactions with receptors or enzymes involved, cells respond to polyphenols which may trigger a series of redox-dependent reactions and result in modification of the redox status of the cells [28–30].

Polyphenols are potential substances against cancers and cardiovascular, metabolic [31], and neurodegenerative diseases [32] through their abilities of antioxidation and antimutation. The metabolism of polyphenols can neutralize free radicals by donating an electron or hydrogen atom to suppress the generation of free radicals or deactivate the active species and precursors of free radicals. Polyphenols, as metal chelators, chelate metal transition such as Fe^{2+} and directly reduce the rate of Fenton reaction, thus preventing oxidation caused by highly reactive hydroxyl radicals (•OH) [33, 34]. As the well antioxidative abilities of polyphenols, they may play important roles and interact with some cell receptor and intracellular signaling and/or gene expression regulation during atherosclerotic progressions. This review aims to present a novel focus on the role of antioxidative polyphenols and oxidative stress in atherosclerosis-related IHD and stroke.

2. Materials and Methods

The current review focuses on the role of polyphenols and oxidative stress in atherosclerosis-related IHD and stroke. The keywords were entered "polyphenol and oxidative stress and atherosclerosis, or polyphenol and oxidative stress and ischemic heart disease, or polyphenol and oxidative stress and stroke." Literature searches were performed using the Medicine, PubMed, EMBASE, Cochrane library, CINAHL, and Scopus databases. We exclude papers from nonabove databases or non-English-writing articles.

3. Results and Discussion

3.1. Polyphenols and Oxidative Stress Associated with Risk Factors of Atherosclerosis

3.1.1. Hypertension. Hypertension is closely associated with atherosclerosis, which is related to IHD and stroke. One of the underlying mechanisms for the enhanced atherogenesis in hypertensive patients is oxidative stress [5]. Polyphenols from red wine reduce blood pressure elevations by increasing nitric oxide synthase (NOS) activity; decreasing end-organ damage, for example, myocardial fibrosis and aortic thickening; and decreasing protein synthesis in the heart and aorta [35, 36].

Angiotensin II (AngII) is a significant factor in blood pressure regulation and is also involved in the process of atherosclerosis and in the remodeling through repairing processes of the myocardium following myocardial infarction [37]. AngII-induced hypertension is associated with blunted endothelium-dependent vasodilation. The increasing ROS formation in the arterial wall through nicotinamide adenine dinucleotide phosphate (NADPH) oxidase activation via type 1 AngII receptors leads to increased oxidative stress [38]. Moreover, AngII also induces the migration and proliferation of cultured VSMCs [39] and increases cytosolic Ca^{2+} levels, which was found to stimulate the DNA-binding activity of the transcription factor nuclear factor kappa B (NF-κB) in cultured human neutrophils [40]. Furthermore, polyphenols can block AngII-stimulated upregulation of several NADPH oxidase (NOX) subunits, including NOX 1 and p22phox (an essential component of NOX), and the associated oxidative stress [38]. Based on these mechanisms,

some researches revealed that systolic blood pressure in hypertensive patients is improved after ingesting polyphenol-rich foods [41, 42]. Combining dietary flavonoids and a pharmacological antihypertensive therapy based on telmisartan or captopril may improve blood pressure, lipid profile, obesity, and inflammation in young hypertensive patients of both sexes [43].

In a randomized, single-blinded, and controlled trial with a 4-year follow-up, consumption of extravirgin olive oil significantly decreased diastolic blood pressure; however, no differences in systolic blood pressure changes were observed [44]. A similar result was also reported in a randomized, controlled study of tea flavonoids [45].

The relationship between oxidative stress and hypertension is noteworthy. Some animal studies have found that high blood pressure would be associated with increased oxidative stress [46]. However, the effects of polyphenol on blood pressure were still inconsistent [42, 47, 48]. Further clinical studies on polyphenol in hypertension will be necessary.

3.1.2. Diabetes Mellitus. Increasing ROS levels are an important trigger for insulin resistance [49, 50]. Hyperglycemia induces oxidative stress in patients with diabetes, and the overproduction of ROS contributes to the development of cardiovascular diseases (CVD) [51]. In the presence of hyperglycemia, vascular remodeling is augmented by uncoupled eNOS [52], endothelial superoxide levels that inhibit vascular smooth muscle and Na^+-K^--ATPase activity increase [53], and transient receptor potential cation channel subfamily V member 4 that regulates vascular function is downregulated [54].

Gut microbiota lipopolysaccharide (LPS) may translocate into the bloodstream and subsequently contribute to adipose tissue inflammation and oxidative stress, which in turn leads to insulin resistance [55]. Polyphenols reduce LPS proinflammatory action by increasing the production of adiponectin and peroxisome proliferator-activated receptor gamma (PPARγ), which is known as a key anti-inflammatory and insulin-sensitizing mediators [56]. Moreover, LPS increases intracellular ROS levels and the expression of genes encoding ROS-producing enzymes, including NOX2, NOX4, and iNOS. Polyphenols reverse these effects and upregulate manganese superoxide dismutase (MnSOD) and catalase antioxidant enzyme gene expression [56].

Diabetic vasculopathy is characterized by abnormal angiogenesis [57]. Excessive concentrations of vascular endothelial growth factor (VEGF) and its receptor expressions drive angiogenesis and cause complications, such as increased tumor growth and atherosclerotic plaques. Polyphenol inhibits angiogenesis by downregulating VEGF [56]. For example, curcumin could inhibit VEGF expression in streptozotocin-induced diabetic retina [58, 59] and chlorogenic acid could reduce retinal vascular hyperpermeability and leakage on diabetic retinopathy through decreasing VEGF levels [60] in a rat model.

Diabetes is a metabolic disease, and some comorbidities are related to IHD and stroke, such as hyperlipidemia, obesity, and hypertension. One randomized, placebo-controlled, double-blind study revealed that taking polyphenol-rich dark chocolate is effective in improving triglyceride levels in hypertensive patients with diabetes and in decreasing blood pressure and fasting blood sugar [42]. In another study, after a short-term polyphenol-rich dark chocolate administration, a significantly increasing insulin sensitivity and decreasing blood pressure in healthy subjects were noted [48].

3.1.3. Hyperlipidemia. Hyperlipidemia is the most important risk factor for atherosclerosis [61, 62]. Increased transcytosis of lipoproteins is the initial event in atherogenesis. ROS generated by activated inflammatory cells and the production of oxidized lipoproteins are key points for atherosclerotic plaque erosion and rupture [63]. Theaflavins may compete with nicotinamide adenine dinucleotide phosphate (NADPH) which is a substrate of b-ketoacyl reductase of fatty acid synthase. They could significantly reduce EGF-induced biosynthesis of triglycerides, cholesterol, and fatty acids through downregulating the epidermal growth factor (EGF) receptor/phosphatidylinositol-3-kinase (PI3K)/protein kinase B(Akt)/Sp-1 signal transduction pathways [64].

AMP-activated protein kinase (AMPK) is an essential therapeutic target for obesity [65]. Theaflavins may modulate AMPK and ROS pathways to inhibit acetyl-CoA carboxylase activities [66]. They could improve the activation of forkhead box O3A (FoxO3A) which is a common target transcription factor for AMPK signaling. Another, theaflavins may upregulate MnSOD against oxidative stress to alleviate atherosclerosis and diabetic nephropathy [67].

Because there are more thearubigins and theaflavins in black tea than in green tea, black tea extract could be more able to inhibit the emulsion of lipid droplets and reduce the surface area to decrease fat digestion [68, 69]. In the processes of lipid metabolism, black tea polyphenol also could inhibit pancreatic lipase to reduce lipids hydrolyzed and lipid absorption [70, 71].

Additionally, data show a good lipid excretion ability after polyphenol consumption. In subjects who had high-lipid diet, intake of polyphenol-enriched oolong tea increased lipid excretion in the feces [72]. Hosoyamada and Yamada reported that a combination of fish oil and apple polyphenol in rats with a high-cholesterol diet showed decreasing serum and liver lipid concentrations and decreasing serum oxidative stress and promoted fecal bile acid excretion [73].

3.1.4. Obesity. Obesity is one of the most common nutritional diseases worldwide. According to the World Health Organization (WHO), obesity is a body mass index ≥ 30. In 2014, >1.9 billion adults, 18 years and older, were overweight. Of these, >600 million were obese [74]. Moreover, obesity could also lead to serious diseases, such as CVD, type 2 diabetes, and cancer [75]. A 10 kg higher body weight is associated with a 3.0 mmHg increase in systolic and 2.3 mmHg increase in diastolic blood pressure. These increases translate into an approximately 12% increased risk for coronary heart disease and 24% increased risk for stroke [76, 77]. An epidemiological study revealed that obesity elevates systemic oxidative stress in humans [78].

Obesity results from a lipid metabolic imbalance and leads to fat accumulation in adipose tissues [79]. The adipose

tissue is a significant source of TNF-?, IL-6, resistin, leptin, angiotensinogen, and adiponectin [80]. In adipocytes, oxidative stress induces the production of the abovementioned proinflammatory adipokines as well as leptin and resistin, which play a role in maintaining insulin resistance [49, 81]. The relationship between obesity and insulin resistance has been recognized for decades [82]. One potential strategy to reduce inflammation and insulin resistance is consuming polyphenol-rich foods, such as grapes or their by-products, which have anti-inflammatory properties [31].

Green tea polyphenols may reduce leptin levels in the subcutaneous tissue of high-fat-diet-induced obese rats [43]. On the contrary, they could increase percentage of fat-free mass and glutathione peroxidase protein expression and decreased percentage of fat mass, serum insulin-like growth factor I, leptin, adiponectin, and proinflammatory cytokines in obese rats [83]. Nevertheless, black tea with polyphenols is more effective in reducing body weight. They may inhibit lipid and saccharide digestion and absorption and reduce calorie intake [71]. The other articles revealed that black tea with polyphenols could promote lipid metabolism by activating AMPK, attenuating lipogenesis and enhancing lipolysis. They would lower lipid accumulation by suppressing the differentiation and proliferation of preadipocytes and by reducing oxidative stress [79].

3.1.5. Cigarette Smoking. Cigarette smoking is associated with vascular endothelial dysfunction [84], which is primarily related to the ROS in tobacco smoke (TS) [85, 86], nicotine, and inflammation. Smoking enhances oxidative stress not only through ROS production but also through weakening of the antioxidant defense systems [87–89]. TS contributes to a proatherosclerotic environment by triggering a complex proinflammatory response and mediates the recruitment of leukocytes through cytokine signaling [90]. Thus, smokers are 2–4 times more likely to suffer from coronary heart disease and stroke [91–93].

Smoking could induce the differentiation of monocytes into macrophages and a strong vascular proinflammatory response through upregulating endothelial proinflammatory genes, increasing the levels of proinflammatory cytokines, and activating matrix metalloproteinase. Being a strong vascular inflammatory primer, TS can accelerate the dysfunction of blood-brain barrier (BBB) and the loss of cerebral blood flow such as during ischemic stroke [85]. TS-induced toxicity at BBB endothelial cells is strongly correlated with the tar and NO levels in the cigarettes rather than the nicotine content [86].

Cigarette smoking promotes glucose intolerance, increases the risk of developing type 2 diabetes mellitus, and thus is a leading high risk of cerebrovascular and neurological disorders like stroke via ROS generation, inflammation, and BBB impairment [94]. One trial revealed that metformin (an antidiabetic drug) activates counteractive mechanisms primarily associated with the nuclear factor erythroid 2-related factor pathway, which drastically reduces cigarette smoking toxicity at the cerebrovascular level [95].

Cigarette smoking causes oxidative stress, hypertension, and endothelial dysfunction. Polyphenol-rich foods, which are good antioxidants, could prevent these conditions. Antioxidant supplementation reduced the oxidation and inflammation induced by TS in animals and cells [94, 96]. One randomized controlled trial involving young volunteers demonstrated that blueberry (*Vaccinium corymbosum*) modulates peripheral arterial dysfunction induced by acute cigarette smoking [97]. Moreover, resveratrol prevents cigarette smoking-induced ROS and carbonyl formation in human keratinocytes [98]. Apple polyphenol, the main sources of flavonoids, not only significantly and dose-dependently reduced cigarette smoking-induced accumulation of inflammatory cells and gene/protein expression of proinflammatory factors but also reversed oxidative stress in the lungs via P38 mitogen-activated protein kinase (MAPK) signaling pathway [99]. p38α MAPK was first recognized for its role in inflammation by regulating the biosynthesis of proinflammatory cytokines, namely, IL-1 and TNF-α, in endotoxin-stimulated monocytes [100]. Tea polyphenols can antagonize cigarette smoking-induced airway epithelial cell apoptosis through the effective removal of ROS, thereby promoting Bcl-2 mRNA expression and inhibiting the expression of Bax mRNA [101].

3.2. Polyphenols and Oxidative Stress Associated with Pathology of Atherosclerosis

3.2.1. Endothelial Dysfunction. Lining the interior surface of vessel cells, endothelial cells could play an essential role in homeostasis, immune, inflammation, cell adhesion, and regulation of thrombosis and fibrinolysis [50, 102]. They maintain vascular tone by regulating various vasodilator factors such as NO and vasoconstrictive factors such as endothelin-1 (ET-1).

Endothelial dysfunction is often associated with increased oxidative stress [50] and impaired mitochondrial activity [103]. Oxidative stress would alter endothelial signal transduction and redox-regulated transcription factors to increase vascular endothelial permeability and catalyze leukocyte adhesion [104]. Shortly after then, endothelial dysfunction can lead to pathologic process of atherosclerosis [105, 106].

Some articles showed hydroxytyrosol and the polyphenol extract from extravirgin olive oil may reverse the decreased endothelial NO synthase phosphorylation, intracellular NO levels, and increased ET-1 synthesis by the stimulation of ROS production with high glucose and linoleic and oleic acid levels. In addition, they also could revert the reduced NO and increased ET-1 levels by acetylcholine inducing with high glucose and free fatty acids [107]. Dark chocolate with high flavonoid consumption may ameliorate endothelium-dependent dilation of the brachial artery and increase plasma epicatechin concentrations in healthy adults [108]. Red wines and grapes could elevate the level of cyclic GMP which is the mediator of nitric oxide-induced vascular smooth muscle relaxation through exhibiting endothelium-dependent relaxation of blood vessels and increasing biological activity of NO [109] (Figure 1).

3.2.2. Oxidized Low-Density Lipoprotein. The oxidation of low-density lipoprotein (LDL) is a complex process in which

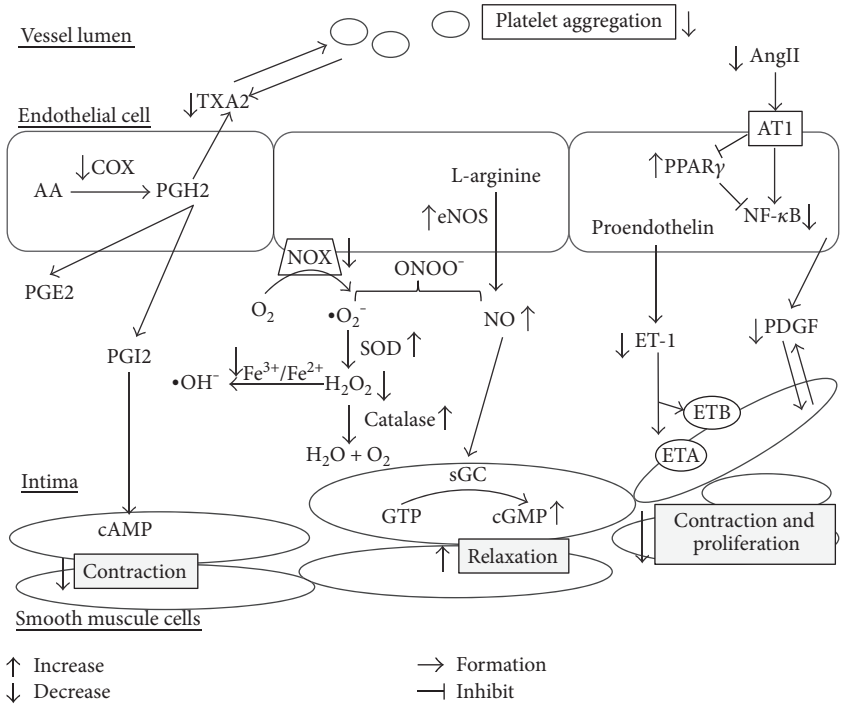

Figure 1: Effects of polyphenols in endothelial cells and smooth muscle cells. AA: arachidonic acid; COX: cyclooxygenase; PGE2/H2/I2: prostaglandin E2/H2/I2; TXA2: thromboxane A2; eNOS: endothelial nitric oxide synthase; NO: nitric oxide; ET-1: endothelin-1; ETA/B: endothelin A/B receptor; LDL: low-density lipoprotein; PDGF: platelet-derived growth factor; NOX: NADPH oxidase; SOD: superoxidase dismutase; H_2O_2: hydrogen peroxide; GTP: guanosine triphosphate; sGC: soluble guanylate cyclase; cGMP: cyclic guanosine monophosphate; AngII: angiotensin II; AT1: angiotensin II receptor type 1; PPARγ: peroxisome proliferator-activated receptor γ; NF-κB: nuclear factor kappa B.

both the protein and the lipids undergo oxidative changes and form complex products. Oxidative stress and LDL oxidation might play a vital role in atherosclerosis, which has been studied for several years. Strong evidence about the close relationship between OxLDL and atherosclerosis exists [110–112].

All these reactions are oxidative in nature, and they are not uniformly amenable to inhibition by traditional antioxidants. Vitamin E or simple phenols, such as tyrosine or estradiol, actually enhance peroxidase-mediated LDL oxidation. Antioxidative ability and concentrations of antioxidants are positively related [113]. Maiolino et al. reviewed the results of randomized clinical trials employing antioxidants and reported that despite demonstrating no benefits in healthy populations, antioxidant use suggests a benefit in high-risk patients [114].

The term "French paradox" is first used in the newsletter of the International Organization of Vine and Wine in 1986. It says a high-fat diet with a low incidence of coronary atherosclerosis is due to moderate consumption of red wine. In 1991, Serge Renaud, a scientist from Bordeaux University, France, made a series of studies that strongly support the result [115]. In vitro studies of phenolic substances in red wine and normal human LDL showed that red wine inhibits copper-catalyzed LDL oxidation [116]. An in vitro study by Chen et al. implied that (−)-epicatechin gallate-enriched *Hibiscus sabdariffa* leaf polyphenols upregulate the autophagic pathway, which in turn led to reduction of OxLDL induced by human umbilical vein endothelial cell injury and apoptosis [117]. Suzuki-Sugihara et al. found that green tea catechins are incorporated into LDL particles in nonconjugated forms after the incubation of green tea extract and reduced the oxidizability of LDL [118] (Figure 2).

3.2.3. Vascular Smooth Muscle Cell Proliferation. VSMCs contribute to the pathogenesis of atherosclerotic lesions; their proliferation and migration are critical events for progressive intimal thickening and arterial wall sclerosis development. Platelet-derived growth factor (PDGF) is the most potent chemotactic and mitogenic agent for VSMCs at the atherosclerotic lesions. They are released by platelets, endothelial cells, and VSMCs themselves. PI3K [119] and MAPK pathway [120, 121] activation as a response to PDGF is implicated in VSMC motility.

Attenuation of the signals leading to VSMC proliferation and migration could also be a consequence of PDGF β receptor inhibition by red wine polyphenols [122]. Polyphenol fractions of different molecular weights, for example, 200–400 for monomeric components (anthocyanosides, catechins, and flavonoids) and 1600–2000 for oligomeric proanthocyanidins, showed similar antiproliferative effects [123]. VSMC migration and matrix metalloproteinase-2 (MMP-2) activation are related to atherosclerosis formation. Pterostilbene, a polyphenol compound in blueberries, inhibits VSMC migration, and MMP-2 activation could be mediated via Erk1/2 phosphorylation [124]. Brain-derived neurotrophic factor (BDNF) is considered an

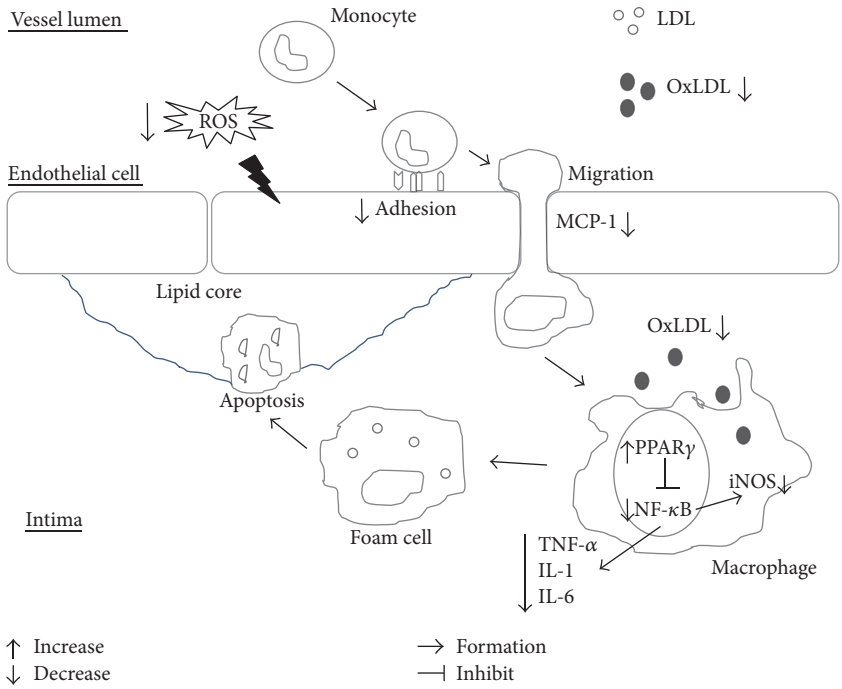

Figure 2: Effects of polyphenols in LDL and inflammatory process with monocytes and macrophages. ROS: reactive oxygen species; LDL: low-density lipoprotein; OxLDL: oxidized low-density lipoprotein; MCP-1: monocyte chemoattractant protein 1; iNOS: inducible nitric oxide synthase; TNF-α: tumor necrosis factor-α; IL-1: interleukin-1; IL-6: interleukin-6; PPARγ: peroxisome proliferator-activated receptor γ; NF-κB: nuclear factor kappa B.

essential element in maintaining stable cerebral blood flow. Resveratrol increases serum BDNF concentrations and reduces VSMC contractility via a NOS-3-independent mechanism [125].

As discussed in Section 3.1.1, AngII-induced production of inflammatory factors and VSMC proliferation play a vital role in the progression of atherosclerotic plaques. The activation of PPARγ effectively attenuates AngII-induced inflammation and intercellular ROS production. Curcumin downregulates the expression of p47phox (a key subunit of NADPH oxidase), inhibits the expression of IL-6 and TNF-α, decreases the production of NO, and suppresses the proliferation of VSMCs by elevating PPARγ activity and suppressing oxidative stress [126] (Figure 1).

3.2.4. Inflammatory Process with Monocytes, Macrophages, and T Lymphocytes. Macrophages play a key role in atherogenesis through their proinflammatory action, which involves the production of IL-1 and tumor necrosis factor, and following more specific adaptive responses mediated by T cells [127, 128]. Macrophage cells pretreated with TF3 could reduce cell-mediated LDL oxidation by decreasing superoxide release from macrophages [33].

The unsaturated aldehyde acrolein is proatherogenic. Acrolein exposure increases intracellular oxidative stress and stimulates cholesterol and triglyceride accumulation via enhanced biosynthesis rates and overexpression of key regulators of cellular lipid biosynthesis. Acrolein also demonstrates a major shift in the gut microbiota composition wherein a significantly increased prevalence of Ruminococcaceae and Lachnospiraceae, of which the *Coprococcus* genus was significantly and positively correlated with serum, aortic, and macrophage lipid levels and peroxidation, was noted. These proatherogenic effects of acrolein on serum, aortas, macrophages, and the gut microbiota were substantially abolished by pomegranate juice [129]. Polyphenol-rich pomegranate juice inhibits macrophage foam cell formation. Moreover, Sarkar et al. reported that ellagic acid, a phenolic lactone, inhibits tautomerase activity of human macrophage migration inhibitory factor (MIF) by inhibiting MIF-induced NF-κB nuclear translocation [130]. Hydroxytyrosol, a major olive oil antioxidant polyphenol in cardioprotective Mediterranean diets, could suppress MMP-9 and COX-2 activity and expression in activated human monocytes via PKCα and PKCβ1 inhibition [131]. Short-term oral administration of polyphenol-rich extract resulted in a modest anti-inflammatory effect in subjects with clustered metabolic risk factors by reducing inflammatory chemokines, for example, monocyte chemoattractant protein 1, and MIF [132]. Ford et al. compared the effects of 31 polyphenols and 6 polyphenol mixtures on proinflammatory cytokine release by Jurkat T lymphocytes and revealed that resveratrol, isorhamnetin, curcumin, vanillic acid, and specific polyphenol mixtures reduced proinflammatory cytokine release from T lymphocytes. Therefore, polyphenols may decrease proinflammatory mediators especially in chronic inflammation [133] (Figure 2).

3.2.5. Platelet Aggregation. Platelet could maintain the hemostasis of the circulatory system [134]. The major

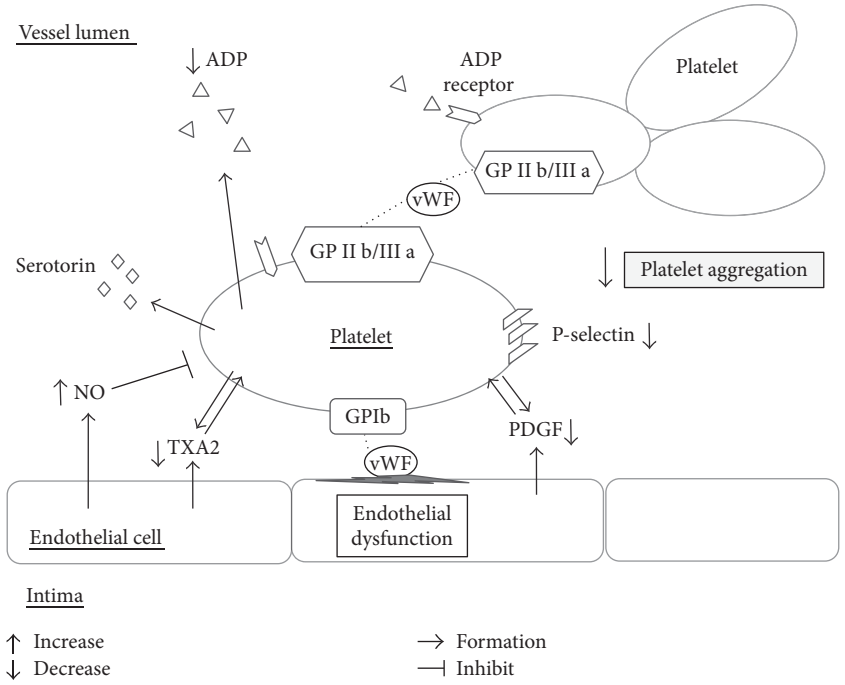

Figure 3: Effects of polyphenols in platelets. ADP: adenosine diphosphate; NO: nitric oxide; TXA2: thromboxane A2; GP1b: glycoprotein Ib; GPIIb/IIIa: glycoprotein IIb/IIIa; vWF: Von Willebrand factor; PDGF: platelet-derived growth factor.

platelet activation pathways mediated by agonists involve the arachidonic acid pathway, adenosine diphosphate (ADP) pathway, serotonin pathway, and NO pathway, and the action of free radicals on molecules is involved in platelet aggregation [135].

Polyphenols, such as resveratrol, have antithrombotic effects, which could be attributed to reduced susceptibility to platelet activation and aggregation, reduced synthesis of prothrombotic mediators (eicosanoid synthesis), and decreased gene expression of tissue factor. Resveratrol has been shown to inhibit, in a concentration-dependent manner, platelet aggregation induced by collagen, ADP, and thrombin. Mattiello et al. compared the effect of pomegranate juice and that of the polyphenol-rich extract from pomegranate fruit on platelet aggregation, calcium mobilization, thromboxane A2 production, and hydrogen peroxide formation induced by collagen and arachidonic acid. Both the pomegranate juice and extract reduced all platelet responses, with the latter showing a stronger effect [136]. Other flavonoids have antiplatelet aggregation effects mainly through the inhibition of the arachidonic acid-based pathway [134].

Cocoa and dark chocolate have been shown to prevent platelet aggregation by reducing ADP-, adrenaline-, and epinephrine-induced glycoprotein IIb/IIIa (GPIIb/IIIa) membrane activation; ADP-induced P-selectin membrane expression; and phospholipase A2 (PLA2) and cyclooxygenase activity [137–140]. One trial found that in smokers, dark chocolate dose-dependently inhibits platelet function by lowering oxidative stress. The platelet ROS, 8-iso-PGF2α, and NOX2 activation were significantly decreased after dark chocolate consumption [141] (Figures 3 and 4) (Table 1).

3.3. Clinical Evidence of Polyphenols and Oxidative Stress in Atherosclerosis-Related Ischemic Heart Disease and Stroke

3.3.1. Polyphenols and Oxidative Stress Associated with Atherosclerosis. Isoflavone in soybeans has antiatherosclerotic property to reduce risk of coronary artery disease and stroke in women [142], but not in men [143]. Interestingly, a randomized controlled trial in the USA showed that isoflavone soy protein supplementation did not significantly reduce subclinical atherosclerosis progression in postmenopausal women but could possibly reduce subclinical atherosclerosis in women at low risk for CVD who were <5 years postmenopausal [144].

A prospective study of forty healthy volunteer women consumed 200 g of açai (one polyphenol-rich fruit which is native to the Brazilian Amazon region) pulp/day for 4 weeks and the result showed açai consumption increased the transfer of cholesteryl esters to high-density lipoprotein and decreased ROS and OxLDL [145].

Cardio-ankle vascular index reflects arterial stiffness which related to atherosclerosis [146]. In a double-blind, randomized, placebo-controlled study, 50 patients with type 2 diabetes mellitus received supplement of a 100 mg resveratrol tablet or placebo daily for 12 weeks. After resveratrol consumption, systolic blood pressure and cardio-ankle vascular index significantly decreased [147].

Plasminogen activator inhibitor type 1 levels are associated with thrombus formation and increased risk of

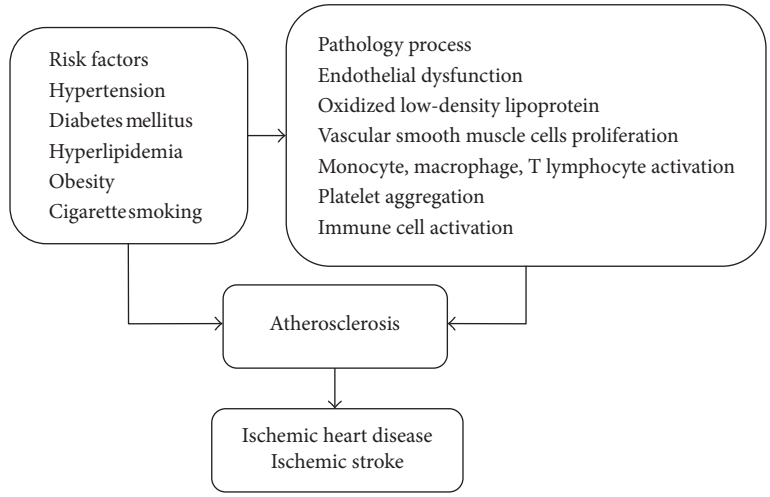

Figure 4: Risk factors and pathology process of atherosclerosis leading to ischemic heart disease or ischemic stroke.

atherosclerosis [148]. One prospective study about nineteen healthy young volunteers, who received oral polyphenol-rich rosemary extracts for 21 days, revealed oral rosemary extracts supplementation improved serum plasminogen activator inhibitor type 1 activity and endothelial dysfunction [149].

3.3.2. Polyphenols and Oxidative Stress Associated with Ischemic Heart Disease. Lekakis et al., in his randomized controlled study of 30 male patients with coronary heart disease, demonstrated that grape polyphenol extract increases flow-mediated dilatation, peaking at 60 min, which was significantly higher than the baseline values or than that of water intake (placebo) [150]. A double-blinded, placebo-controlled, randomized, 3-month study evaluated the efficacy of resveratrol treatment in 40 Caucasian postmyocardial infarction (MI) patients with coronary artery disease. The resveratrol group received 10 mg resveratrol capsule daily for 3 months. Results showed that resveratrol improved left ventricle diastolic function and endothelial function, lowered LDL cholesterol level, and exhibited protection against unfavorable hemorheological changes in patients with coronary artery disease [151]. Several population studies reported an inverse association between flavonoid intake and risk of coronary disease [152–154].

Green tea polyphenols can inhibit $H_2O_2^-$ induced oxidative stress through the Akt/GSK-3β/caveolae pathways in cardiac cells. They could prevent the activation of NF-κb and the inhibition on PI3K/Akt signaling for the acute MI stress. Moreover, green tea polyphenols also could improve mitochondria dysfunction associated with alterations of lipid metabolism, the adaptor 14-3-3 ε protein signaling, and chaperone-induced stress response during post-MI remodeling [155].

In a UK women's cohort study, total fruit intake, especially polyphenol-rich fruit group such as grapes and citrus, was associated with lower risk of CVD and coronary heart disease mortality, with a 6-7% risk reduction for every 80 g/day portion consumed [156]. The other results of the PREDIMED multicenter, randomized, primary prevention trial noted that the MeDiet supplemented with nuts, which is rich in unsaturated fat and polyphenols, can be a sustainable and ideal diet for cardiovascular disease prevention [157].

3.3.3. Polyphenols and Oxidative Stress Associated with Ischemic Stroke. According to the WHO, cerebrovascular diseases are the second leading cause of death worldwide and the major cause of disability in adults [158]. Stroke represents 3-4% of the healthcare spending in developed countries [159]. Hence, early protection that would minimize the damage is crucial. The key factor mediating stroke-related damage is oxidative stress. Nutritional intervention, such as polyphenol-enriched diets, has been proposed as preventive and therapeutic agents.

Resveratrol provides protection from cerebral ischemic injury by regulating the expression of silent mating type information regulation 2 homolog 1 (SIRT1). Wan et al. proved that resveratrol provides neuroprotection by inhibiting phosphodiesterase and regulating the cAMP, AMPK, and SIRT1 pathways, which reduces ATP energy consumption during ischemia [160]. Recent findings in animal models and humans showed that polyphenols may have a role in regulating neurotrophin levels, particularly nerve growth factor (NGF) and BDNF, suggesting that polyphenols may also have protective effects through the potentiation of neurotrophin action. NGF and BDNF also act in glucose and energy metabolism and in pancreatic beta cell and cardiovascular homeostasis as metabotropic factors [161]. Salvianolic acid is an active polyphenol component in Danshen (*Salvia miltiorrhiza*) against ischemia/reperfusion injury, and we explored whether the neuroprotection was dependent on mitochondrial connexin43 via the PI3K/Akt pathway. Our previous population-based studies demonstrated that Danshen is the most common herbal drug used to treat ischemic stroke [162].

Wang et al. published a meta-analysis confirming that diets rich in flavonols (intake of 20 mg/day) was associated with a 14% decrease in the risk of developing stroke, specifically among men [163]. Goetz et al. reported the association

Table 1: Mechanisms of polyphenols in preventing atherosclerosis formation.

Pathology of atherosclerosis	Polyphenols/polyphenol-rich food	Preventing mechanism	Reference
Endothelial dysfunction	Hydroxytyrosol and EVOO polyphenol extract	↑ eNOS phosphorylation, ↑ NO ↓ ET-1 synthesis ↓ ROS	[107]
	High- versus low-dose flavonoid dark chocolate (213 mg versus 46 mg procyanidins)	↑ endothelium-dependent flow-mediated dilation of the brachial artery ↑ plasma epicatechin concentrations ↔ LDL oxidation, total antioxidant capacity, 8-isoprostanes, blood pressure, lipid parameters, body weight, or body mass index	[108]
	Red wines and grapes	↑ NO activity ↑ cGMP ⊕ vascular smooth muscle relaxation	[109]
OxLDL	Red wine	⊖ copper-catalyzed oxidation of LDL	[116]
	(−)-Epicatechin gallate-enriched *Hibiscus sabdariffa* leaf polyphenols	↓ OxLDL-dependent apoptosis	[117]
	Green tea catechins	Incorporated into LDL particles in nonconjugated forms ↓ oxidizability of LDL	[118]
VSMC proliferation	Red wine	⊖ inhibition of PDGF β receptor ↓ VSMC proliferation and migration	[122]
	Pterostilbene, polyphenol compound in blueberries	↓ VSMC migration ⊖ MMP-2 activation via Erk1/2 phosphorylation	[124]
	Resveratrol	↑ serum BDNF concentrations ↓ VSMC contractility via a NOS-3-independent mechanism	[125]
	Curcumin	↓ expression of p47phox ⊖ expression of IL-6 and TNF-α ↓ iNOS activity, ↓ NO ⊖ VSMC proliferation ↑ PPARγ activity ⊖ oxidative stress ↓ AngII-induced inflammatory responses	[126]
Monocyte/macrophage and T lymphocytes inflammatory process	Tea flavonoids (theaflavin digallate, theaflavin, epigallocatechin gallate, epigallocatechin, and gallic acid)	↓ cell-mediated LDL oxidation ↓ macrophages release superoxide and iron ions	[33]
	Pomegranate juice	⊖ acrolein increases macrophage lipid accumulation and alters the gut microbiota composition	[129]
	Ellagic acid	⊖ tautomerase activity of human macrophage MIF ⊖ NF-κB nuclear translocation	[130]
	Polyphenol-rich extract	↓ MCP-1 ↓ macrophage MIF	[132]
	Resveratrol, isorhamnetin, curcumin, vanillic acid, and specific (poly)phenol mixtures	↓ IL-6, interferon-γ induced protein 10 and TNF-α release	[133]
Platelet aggregation	Pomegranate juice or the polyphenol-rich extract from pomegranate fruit	⊖ collagen- and arachidonic acid-induced platelet aggregation ↓ collagen- and arachidonic acid-induced calcium mobilization ↓ thromboxane A2 production ↓ H_2O_2 formation	[136]
	Cocoa and dark chocolate	↓ ADP-, adrenaline- and, epinephrine-induced GPIIb/IIIa membrane activation ↓ ADP-induced P-selectin membrane expression ↓ PLA2 and COX activity ↓ ROS, 8-iso-PGF2α, and NOX2 activation	[137–141]

↑: increase; ↓: decrease; ↔: no change; ⊖: inhibit; ⊕: promote. EVOO: extra virgin olive oil; eNOS: endothelial nitric oxide synthase; NO: nitric oxide; ET-1: endothelin-1; LDL: low-density lipoprotein; ROS: reactive oxygen species; Erk: extracellular-signal-regulated kinase; PDGF: platelet-derived growth factor; VSMCs: vascular smooth muscle cells; MMP-2: matrix metalloproteinase-2; BDNF: brain-derived neurotrophic factor; MIF: migration inhibitory factor; MCP-1: monocyte chemoattractant protein 1; H_2O_2: hydrogen peroxide; ADP: adenosine diphosphate; GPIIb/IIIa: glycoprotein IIb/IIIa; PLA2: phospholipase A2; COX: cyclooxygenase; 8-iso-PGF2α: 8-isoprostane-prostaglandin F2α; NOX2: NADPH oxidase 2.

between flavonoid intake and incident ischemic stroke in a biracial, national cohort using updated flavonoid composition tables and assessed the differences in flavonoid intake by sex, race, and region of residence. The result revealed that greater consumption of flavanones was inversely associated with incident ischemic stroke [164]. We also noted that *Salvia miltiorrhiza* is rich in polyphenol with antioxidant effects by inhibiting oxidases, the production of superoxide, the oxidative modification of low-density lipoproteins, and ameliorating mitochondrial oxidative stress in aging-associated cardiovascular diseases and stroke [165].

4. Conclusion

In the result of the study, polyphenol or polyphenol-rich diets exhibit antioxidative and anti-inflammation effects. Polyphenols reduce ROS production through inhibiting oxidases, reducing the production of superoxide, inhibiting OxLDL formation, inhibiting VSMC proliferation and migration, reducing platelet aggregation, and ameliorating mitochondrial oxidative stress. Polyphenol consumption also improves developing into hypertension, diabetes mellitus, hyperlipidemia, and obesity. However, in accordance with in vitro and in vivo laboratory evidence, well-designed clinical studies are necessary to confirm the efficacy of polyphenols in the treatment of atherosclerosis-related IHD and stroke.

Abbreviations

IHD: Ischemic heart disease
ROS: Reactive oxygen species
$\bullet O_2^-$: Superoxide radicals
H_2O_2: Hydrogen peroxide
NO: Nitric oxide
eNOS: Endothelial nitric oxide synthase
iNOS: Inducible nitric oxide synthase
OxLDL: Oxidized low-density lipoprotein
LDL: Low-density lipoprotein
VSMCs: Vascular smooth muscle cells
NOS: Nitric oxide synthase
AngII: Angiotensin II
NADPH: Nicotinamide adenine dinucleotide phosphate
NF-κB: Nuclear factor kappa B
NOX: NADPH oxidase
LPS: Lipopolysaccharide
PPARγ: Proliferator-activated receptor gamma
MnSOD: Manganese superoxide dismutase
VEGF: Vascular endothelial growth factor
FAS: Fatty acid synthase
EGF: Epidermal growth factor
PI3K: Phosphatidylinositol-3-kinase
Akt: Protein kinase B
AMPK: AMP-activated protein kinase
TF3: Theaflavin-3,3′-digallate
FoxO3A: Forkhead box O3A
WHO: World Health Organization
BBB: Blood-brain barrier
Nrf2: Nuclear factor erythroid 2-related factor
IL-1: Interleukin-1
TNF-α: Tumor necrosis factor-α
MAPK: Mitogen-activated protein kinase
ET-1: Endothelin-1
PDGF: Platelet-derived growth factor
MMP-2: Matrix metalloproteinase-2
BDNF: Brain-derived neurotrophic factor
MIF: Migration inhibitory factor
MCP-1: Monocyte chemoattractant protein 1
ADP: Adenosine diphosphate
GPIIb/IIIa: Epinephrine-induced glycoprotein IIb/IIIa
PLA2: Phospholipase A2
MI: Myocardial infarction
CVD: Cardiovascular disease
MeDiet: Mediterranean diet
EVOO: Extravirgin olive oil
SIRT1: Silent mating type information regulation 2 homolog 1
NGF: Nerve growth factor.

Conflicts of Interest

The authors declare no conflict of interest.

Authors' Contributions

Yu-Chen Cheng drafted the manuscript. Jer-Ming Sheen, Wen Long Hu, and Yu-Chiang Hung supervised the drafting of the manuscript. Yu-Chen Cheng and Yu-Chiang Hung contributed equally to this work. All the authors read and approved the final draft of the manuscript.

References

[1] W. Herrington, B. Lacey, P. Sherliker, J. Armitage, and S. Lewington, "Epidemiology of atherosclerosis and the potential to reduce the global burden of atherothrombotic disease," *Circulation Research*, vol. 118, no. 4, pp. 535–546, 2016.

[2] S. Barquera, A. Pedroza-Tobías, C. Medina et al., "Global overview of the epidemiology of atherosclerotic cardiovascular disease," *Archives of Medical Research*, vol. 46, no. 5, pp. 328–338, 2015.

[3] N. Inoue, "Stress and atherosclerotic cardiovascular disease," *Journal of Atherosclerosis and Thrombosis*, vol. 21, no. 5, pp. 391–401, 2014.

[4] I. Olmez and H. Ozyurt, "Reactive oxygen species and ischemic cerebrovascular disease," *Neurochemistry International*, vol. 60, no. 2, pp. 208–212, 2012.

[5] U. Forstermann, N. Xia, and H. Li, "Roles of vascular oxidative stress and nitric oxide in the pathogenesis of atherosclerosis," *Circulation Research*, vol. 120, no. 4, pp. 713–735, 2017.

[6] R. Mia-Jeanne van and E. Pretorius, "Obesity, hypertension and hypercholesterolemia as risk factors for atherosclerosis leading to ischemic events," *Current Medicinal Chemistry*, vol. 21, no. 19, pp. 2121–2129, 2014.

[7] J. Frohlich and A. Al-Sarraf, "Cardiovascular risk and atherosclerosis prevention," *Cardiovascular Pathology*, vol. 22, no. 1, pp. 16–18, 2013.

[8] N. Torres, M. Guevara-Cruz, L. A. Velazquez-Villegas, and A. R. Tovar, "Nutrition and atherosclerosis," *Archives of Medical Research*, vol. 46, no. 5, pp. 408–426, 2015.

[9] G. Vilahur and L. Badimon, "Antiplatelet properties of natural products," *Vascular Pharmacology*, vol. 59, no. 3-4, pp. 67–75, 2013.

[10] M. Massaro, E. Scoditti, M. A. Carluccio, and R. De Caterina, "Nutraceuticals and prevention of atherosclerosis: focus on ω-3 polyunsaturated fatty acids and Mediterranean diet polyphenols," *Cardiovascular Therapeutics*, vol. 28, no. 4, pp. e13–ee9, 2010.

[11] E. Brglez Mojzer, M. Knez Hrncic, M. Skerget, Z. Knez, and U. Bren, "Polyphenols: extraction methods, antioxidative action, bioavailability and anticarcinogenic effects," *Molecules*, vol. 21, no. 7, 2016.

[12] G. Pizzino, N. Irrera, M. Cucinotta et al., "Oxidative stress: harms and benefits for human health," *Oxidative Medicine and Cellular Longevity*, vol. 2017, Article ID 8416763, 13 pages, 2017.

[13] K. K. Griendling and G. A. FitzGerald, "Oxidative stress and cardiovascular injury: part I: basic mechanisms and in vivo monitoring of ROS," *Circulation*, vol. 108, no. 16, pp. 1912–1916, 2003.

[14] N. Panth, K. R. Paudel, and K. Parajuli, "Reactive oxygen species: a key hallmark of cardiovascular disease," *Advances in Medicine*, vol. 2016, Article ID 9152732, 12 pages, 2016.

[15] S. H. Choi, D. Sviridov, and Y. I. Miller, "Oxidized cholesteryl esters and inflammation," *Biochimica et Biophysica Acta (BBA) - Molecular and Cell Biology of Lipids*, vol. 1862, no. 4, pp. 393–397, 2017.

[16] M. M. Elahi, Y. X. Kong, and B. M. Matata, "Oxidative stress as a mediator of cardiovascular disease," *Oxidative Medicine and Cellular Longevity*, vol. 2, no. 5, pp. 259–269, 2009.

[17] R. W. O'Donnell, D. K. Johnson, L. M. Ziegler, A. J. DiMattina, R. I. Stone, and J. A. Holland, "Endothelial NADPH oxidase: mechanism of activation by low-density lipoprotein," *Endothelium*, vol. 10, no. 6, pp. 291–297, 2003.

[18] F. L. Song, R. Y. Gan, Y. Zhang, Q. Xiao, L. Kuang, and H. B. Li, "Total phenolic contents and antioxidant capacities of selected Chinese medicinal plants," *International Journal of Molecular Sciences*, vol. 11, no. 6, pp. 2362–2372, 2010.

[19] S. Dragland, H. Senoo, K. Wake, K. Holte, and R. Blomhoff, "Several culinary and medicinal herbs are important sources of dietary antioxidants," *The Journal of Nutrition*, vol. 133, no. 5, pp. 1286–1290, 2003.

[20] Y. Cai, Q. Luo, M. Sun, and H. Corke, "Antioxidant activity and phenolic compounds of 112 traditional Chinese medicinal plants associated with anticancer," *Life Sciences*, vol. 74, no. 17, pp. 2157–2184, 2004.

[21] V. Neveu, J. Perez-Jimenez, F. Vos et al., "Phenol-explorer: an online comprehensive database on polyphenol contents in foods," *Database*, vol. 2010, article bap024, 2010.

[22] C. Manach, A. Scalbert, C. Morand, C. Remesy, and L. Jimenez, "Polyphenols: food sources and bioavailability," *The American Journal of Clinical Nutrition*, vol. 79, no. 5, pp. 727–747, 2004.

[23] K. B. Pandey and S. I. Rizvi, "Plant polyphenols as dietary antioxidants in human health and disease," *Oxidative Medicine and Cellular Longevity*, vol. 2, no. 5, pp. 270–278, 2009.

[24] R. Tsao, "Chemistry and biochemistry of dietary polyphenols," *Nutrients*, vol. 2, no. 12, pp. 1231–1246, 2010.

[25] G. Williamson and C. Manach, "Bioavailability and bioefficacy of polyphenols in humans. II. Review of 93 intervention studies," *The American Journal of Clinical Nutrition*, vol. 81, no. 1, pp. 243S–255S, 2005.

[26] S. Ramos, "Cancer chemoprevention and chemotherapy: dietary polyphenols and signalling pathways," *Molecular Nutrition & Food Research*, vol. 52, no. 5, pp. 507–526, 2008.

[27] M. Biesaga, "Influence of extraction methods on stability of flavonoids," *Journal of Chromatography A*, vol. 1218, no. 18, pp. 2505–2512, 2011.

[28] A. Scalbert, I. T. Johnson, and M. Saltmarsh, "Polyphenols: antioxidants and beyond," *The American Journal of Clinical Nutrition*, vol. 81, no. 1, pp. 215S–217S, 2005.

[29] B. Halliwell, J. Rafter, and A. Jenner, "Health promotion by flavonoids, tocopherols, tocotrienols, and other phenols: direct or indirect effects? Antioxidant or not?," *The American Journal of Clinical Nutrition*, vol. 81, Supplement 1, pp. 268s–276s, 2005.

[30] J. O. Moskaug, H. Carlsen, M. C. Myhrstad, and R. Blomhoff, "Polyphenols and glutathione synthesis regulation," *The American Journal of Clinical Nutrition*, vol. 81, Supplement 1, pp. 277s–283s, 2005.

[31] C. C. Chuang and M. K. McIntosh, "Potential mechanisms by which polyphenol-rich grapes prevent obesity-mediated inflammation and metabolic diseases," *Annual Review of Nutrition*, vol. 31, pp. 155–176, 2011.

[32] E. Middleton Jr.C. Kandaswami and T. C. Theoharides, "The effects of plant flavonoids on mammalian cells: implications for inflammation, heart disease, and cancer," *Pharmacological Reviews*, vol. 52, no. 4, pp. 673–751, 2000.

[33] H. Yoshida, T. Ishikawa, H. Hosoai et al., "Inhibitory effect of tea flavonoids on the ability of cells to oxidize low density lipoprotein," *Biochemical Pharmacology*, vol. 58, no. 11, pp. 1695–1703, 1999.

[34] N. R. Perron and J. L. Brumaghim, "A review of the antioxidant mechanisms of polyphenol compounds related to iron binding," *Cell Biochemistry and Biophysics*, vol. 53, no. 2, pp. 75–100, 2009.

[35] I. Bernatova, O. Pechanova, P. Babal, S. Kysela, S. Stvrtina, and R. Andriantsitohaina, "Wine polyphenols improve cardiovascular remodeling and vascular function in NO-deficient hypertension," *American Journal of Physiology - Heart and Circulatory Physiology*, vol. 282, no. 3, pp. H942–H948, 2002.

[36] O. Pechanova, I. Bernatova, P. Babal et al., "Red wine polyphenols prevent cardiovascular alterations in L-NAME-induced hypertension," *Journal of Hypertension*, vol. 22, no. 8, pp. 1551–1559, 2004.

[37] F. Fyhrquist, K. Metsarinne, and I. Tikkanen, "Role of angiotensin II in blood pressure regulation and in the pathophysiology of cardiovascular disorders," *Journal of Human Hypertension*, vol. 9, Supplement 5, pp. S19–S24, 1995.

[38] M. Sarr, M. Chataigneau, S. Martins et al., "Red wine polyphenols prevent angiotensin II-induced hypertension and endothelial dysfunction in rats: role of NADPH oxidase," *Cardiovascular Research*, vol. 71, no. 4, pp. 794–802, 2006.

[39] C. M. Lin, S. W. Hou, B. W. Wang, J. R. Ong, H. Chang, and K. G. Shyu, "Molecular mechanism of (−)-epigallocatechin-3-gallate on balloon injury-induced neointimal formation and leptin expression," *Journal of Agricultural and Food Chemistry*, vol. 62, no. 6, pp. 1213–1220, 2014.

[40] R. El Bekay, M. Álvarez, J. Monteseirín et al., "Oxidative stress is a critical mediator of the angiotensin II signal in human neutrophils: involvement of mitogen-activated protein kinase, calcineurin, and the transcription factor NF-κB," *Blood*, vol. 102, no. 2, pp. 662–671, 2003.

[41] K. Ried, T. R. Sullivan, P. Fakler, O. R. Frank, and N. P. Stocks, "Effect of cocoa on blood pressure," *The Cochrane Database of Systematic Reviews*, no. 8, article Cd008893, 2012.

[42] A. Rostami, M. Khalili, N. Haghighat et al., "High-cocoa polyphenol-rich chocolate improves blood pressure in patients with diabetes and hypertension," *ARYA Atherosclerosis*, vol. 11, no. 1, pp. 21–29, 2015.

[43] M. M. de Jesus Romero-Prado, J. A. Curiel-Beltran, M. V. Miramontes-Espino, E. G. Cardona-Munoz, A. Rios-Arellano, and L. B. Balam-Salazar, "Dietary flavonoids added to pharmacological antihypertensive therapy are effective in improving blood pressure," *Basic & Clinical Pharmacology & Toxicology*, vol. 117, no. 1, pp. 57–64, 2015.

[44] E. Toledo, F. B. Hu, R. Estruch et al., "Effect of the Mediterranean diet on blood pressure in the PREDIMED trial: results from a randomized controlled trial," *BMC Medicine*, vol. 11, p. 207, 2013.

[45] D. Grassi, R. Draijer, C. Schalkwijk et al., "Black tea increases circulating endothelial progenitor cells and improves flow mediated dilatation counteracting deleterious effects from a fat load in hypertensive patients: a randomized controlled study," *Nutrients*, vol. 8, no. 11, 2016.

[46] E. Grossman, "Does increased oxidative stress cause hypertension?," *Diabetes Care*, vol. 31, Supplement 2, pp. S185–S189, 2008.

[47] N. C. Ward, J. M. Hodgson, K. D. Croft, V. Burke, L. J. Beilin, and I. B. Puddey, "The combination of vitamin C and grape-seed polyphenols increases blood pressure: a randomized, double-blind, placebo-controlled trial," *Journal of Hypertension*, vol. 23, no. 2, pp. 427–434, 2005.

[48] D. Grassi, C. Lippi, S. Necozione, G. Desideri, and C. Ferri, "Short-term administration of dark chocolate is followed by a significant increase in insulin sensitivity and a decrease in blood pressure in healthy persons," *The American Journal of Clinical Nutrition*, vol. 81, no. 3, pp. 611–614, 2005.

[49] N. Houstis, E. D. Rosen, and E. S. Lander, "Reactive oxygen species have a causal role in multiple forms of insulin resistance," *Nature*, vol. 440, no. 7086, pp. 944–948, 2006.

[50] N. Suganya, E. Bhakkiyalakshmi, D. V. Sarada, and K. M. Ramkumar, "Reversibility of endothelial dysfunction in diabetes: role of polyphenols," *British Journal of Nutrition*, vol. 116, no. 2, pp. 223–246, 2016.

[51] B. Lipinski, "Pathophysiology of oxidative stress in diabetes mellitus," *Journal of Diabetes and its Complications*, vol. 15, no. 4, pp. 203–210, 2001.

[52] N. Sasaki, T. Yamashita, T. Takaya et al., "Augmentation of vascular remodeling by uncoupled endothelial nitric oxide synthase in a mouse model of diabetes mellitus," *Arteriosclerosis, Thrombosis, and Vascular Biology*, vol. 28, no. 6, pp. 1068–1076, 2008.

[53] S. Gupta, E. Chough, J. Daley et al., "Hyperglycemia increases endothelial superoxide that impairs smooth muscle cell Na^+-K^+-ATPase activity," *American Journal of Physiology-Cell Physiology*, vol. 282, no. 3, pp. C560–C5C6, 2002.

[54] K. Monaghan, J. McNaughten, M. K. McGahon et al., "Hyperglycemia and diabetes downregulate the functional expression of TRPV4 channels in retinal microvascular endothelium," *PLoS One*, vol. 10, no. 6, article e0128359, 2015.

[55] J. M. Gomes, J. A. Costa, and R. C. Alfenas, "Metabolic endotoxemia and diabetes mellitus: a systematic review," *Metabolism*, vol. 68, pp. 133–144, 2017.

[56] F. Le Sage, O. Meilhac, and M. P. Gonthier, "Anti-inflammatory and antioxidant effects of polyphenols extracted from *Antirhea borbonica* medicinal plant on adipocytes exposed to *Porphyromonas gingivalis* and *Escherichia coli* lipopolysaccharides," *Pharmacological Research*, vol. 119, pp. 303–312, 2017.

[57] L. P. Aiello and J. S. Wong, "Role of vascular endothelial growth factor in diabetic vascular complications," *Kidney International*, vol. 58, Supplement 77, pp. S113–S119, 2000.

[58] T. Mrudula, P. Suryanarayana, P. N. Srinivas, and G. B. Reddy, "Effect of curcumin on hyperglycemia-induced vascular endothelial growth factor expression in streptozotocin-induced diabetic rat retina," *Biochemical and Biophysical Research Communications*, vol. 361, no. 2, pp. 528–532, 2007.

[59] T. Sawatpanich, H. Petpiboolthai, B. Punyarachun, and V. Anupunpisit, "Effect of curcumin on vascular endothelial growth factor expression in diabetic mice kidney induced by streptozotocin," *Journal of the Medical Association of Thailand*, vol. 93, Supplement 2, pp. S1–S8, 2010.

[60] J. Y. Shin, J. Sohn, and K. H. Park, "Chlorogenic acid decreases retinal vascular hyperpermeability in diabetic rat model," *Journal of Korean Medical Science*, vol. 28, no. 4, pp. 608–613, 2013.

[61] A. W. Zieske, G. T. Malcom, and J. P. Strong, "Natural history and risk factors of atherosclerosis in children and youth: the PDAY study," *Pediatric Pathology & Molecular Medicine*, vol. 21, no. 2, pp. 213–237, 2002.

[62] M. L. Kortelainen and T. Sarkioja, "Visceral fat and coronary pathology in male adolescents," *International Journal of Obesity*, vol. 25, no. 2, pp. 228–232, 2001.

[63] M. Hulsmans and P. Holvoet, "The vicious circle between oxidative stress and inflammation in atherosclerosis," *Journal of Cellular and Molecular Medicine*, vol. 14, no. 1-2, pp. 70–78, 2010.

[64] J. K. Lin and S. Y. Lin-Shiau, "Mechanisms of hypolipidemic and anti-obesity effects of tea and tea polyphenols," *Molecular Nutrition & Food Research*, vol. 50, no. 2, pp. 211–217, 2006.

[65] M. Daval, F. Diot-Dupuy, R. Bazin et al., "Anti-lipolytic action of AMP-activated protein kinase in rodent adipocytes," *The Journal of Biological Chemistry*, vol. 280, no. 26, pp. 25250–25257, 2005.

[66] C. L. Lin, H. C. Huang, and J. K. Lin, "Theaflavins attenuate hepatic lipid accumulation through activating AMPK in human HepG2 cells," *Journal of Lipid Research*, vol. 48, no. 11, pp. 2334–2343, 2007.

[67] H.-J. Ko, C.-Y. Lo, B.-J. Wang, R. Y.-Y. Chiou, and S.-M. Lin, "Theaflavin-3,3′-digallate, a black tea polyphenol, stimulates lipolysis associated with the induction of mitochondrial uncoupling proteins and AMPK–FoxO3A–MnSOD pathway in 3T3-L1 adipocytes," *Journal of Functional Foods*, vol. 17, pp. 271–282, 2015.

[68] Y. Shishikura, S. Khokhar, and B. S. Murray, "Effects of tea polyphenols on emulsification of olive oil in a small intestine model system," *Journal of Agricultural and Food Chemistry*, vol. 54, no. 5, pp. 1906–1913, 2006.

[69] M. A. Vermeer, T. P. Mulder, and H. O. Molhuizen, "Theaflavins from black tea, especially theaflavin-3-gallate, reduce the incorporation of cholesterol into mixed micelles," *Journal of Agricultural and Food Chemistry*, vol. 56, no. 24, pp. 12031–12036, 2008.

[70] S. Uchiyama, Y. Taniguchi, A. Saka, A. Yoshida, and H. Yajima, "Prevention of diet-induced obesity by dietary black tea polyphenols extract in vitro and in vivo," *Nutrition*, vol. 27, no. 3, pp. 287–292, 2011.

[71] H. Ashigai, Y. Taniguchi, M. Suzuki et al., "Fecal lipid excretion after consumption of a black tea polyphenol containing beverage-randomized, placebo-controlled, double-blind, crossover study," *Biological & Pharmaceutical Bulletin*, vol. 39, no. 5, pp. 699–704, 2016.

[72] T. F. Hsu, A. Kusumoto, K. Abe et al., "Polyphenol-enriched oolong tea increases fecal lipid excretion," *European Journal of Clinical Nutrition*, vol. 60, no. 11, pp. 1330–1336, 2006.

[73] Y. Hosoyamada and M. Yamada, "Effects of dietary fish oil and apple polyphenol on the concentration serum lipids and excretion of fecal bile acids in rats," *Journal of Nutritional Science and Vitaminology*, vol. 63, no. 1, pp. 21–27, 2017.

[74] "Obesity and overweight: WHO fact sheet," 2016, http://who.int/mediacentre/factsheets/fs311/en/.

[75] J. M. Genkinger, C. M. Kitahara, L. Bernstein et al., "Central adiposity, obesity during early adulthood, and pancreatic cancer mortality in a pooled analysis of cohort studies," *Annals of Oncology*, vol. 26, no. 11, pp. 2257–2266, 2015.

[76] R. H. Eckel and R. M. Krauss, "American Heart Association call to action: obesity as a major risk factor for coronary heart disease," *Circulation*, vol. 97, no. 21, pp. 2099-2100, 1998.

[77] P. Poirier, T. D. Giles, G. A. Bray et al., "Obesity and cardiovascular disease," *Arteriosclerosis, Thrombosis, and Vascular Biology*, vol. 26, no. 5, pp. 968–976, 2006.

[78] H. K. Vincent and A. G. Taylor, "Biomarkers and potential mechanisms of obesity-induced oxidant stress in humans," *International Journal of Obesity*, vol. 30, no. 3, pp. 400–418, 2006.

[79] H. Pan, Y. Gao, and Y. Tu, "Mechanisms of body weight reduction by black tea polyphenols," *Molecules*, vol. 21, no. 12, 2016.

[80] B. L. Wajchenberg, "Subcutaneous and visceral adipose tissue: their relation to the metabolic syndrome," *Endocrine Reviews*, vol. 21, no. 6, pp. 697–738, 2000.

[81] S. de Ferranti and D. Mozaffarian, "The perfect storm: obesity, adipocyte dysfunction, and metabolic consequences," *Clinical Chemistry*, vol. 54, no. 6, pp. 945–955, 2008.

[82] B. B. Kahn and J. S. Flier, "Obesity and insulin resistance," *Journal of Clinical Investigation*, vol. 106, no. 4, pp. 473–481, 2000.

[83] C. L. Shen, J. J. Cao, R. Y. Dagda et al., "Green tea polyphenols benefits body composition and improves bone quality in long-term high-fat diet-induced obese rats," *Nutrition Research*, vol. 32, no. 6, pp. 448–457, 2012.

[84] H. W. Chen, M. L. Chien, Y. H. Chaung, C. K. Lii, and T. S. Wang, "Extracts from cigarette smoke induce DNA damage and cell adhesion molecule expression through different pathways," *Chemico-Biological Interactions*, vol. 150, no. 3, pp. 233–241, 2004.

[85] M. Hossain, T. Sathe, V. Fazio et al., "Tobacco smoke: a critical etiological factor for vascular impairment at the blood-brain barrier," *Brain Research*, vol. 1287, pp. 192–205, 2009.

[86] P. Naik, N. Fofaria, S. Prasad et al., "Oxidative and pro-inflammatory impact of regular and denicotinized cigarettes on blood brain barrier endothelial cells: is smoking reduced or nicotine-free products really safe?," *BMC Neuroscience*, vol. 15, p. 51, 2014.

[87] A. Sobczak, D. Golka, and I. Szoltysek-Boldys, "The effects of tobacco smoke on plasma alpha- and gamma-tocopherol levels in passive and active cigarette smokers," *Toxicology Letters*, vol. 151, no. 3, pp. 429–437, 2004.

[88] M. Dietrich, G. Block, E. P. Norkus et al., "Smoking and exposure to environmental tobacco smoke decrease some plasma antioxidants and increase γ-tocopherol in vivo after adjustment for dietary antioxidant intakes," *The American Journal of Clinical Nutrition*, vol. 77, no. 1, pp. 160–166, 2003.

[89] B. Isik, A. Ceylan, and R. Isik, "Oxidative stress in smokers and non-smokers," *Inhalation Toxicology*, vol. 19, no. 9, pp. 767–9, 2007.

[90] T. Masubuchi, S. Koyama, E. Sato et al., "Smoke extract stimulates lung epithelial cells to release neutrophil and monocyte chemotactic activity," *The American Journal of Pathology*, vol. 153, no. 6, pp. 1903–1912, 1998.

[91] I. M. Cojocaru, M. Cojocaru, V. Sapira, and A. Ionescu, "Evaluation of oxidative stress in patients with acute ischemic stroke," *Romanian journal of internal medicine = Revue roumaine de medecine interne*, vol. 51, no. 2, pp. 97–106, 2013.

[92] T. Mannami, H. Iso, S. Baba et al., "Cigarette smoking and risk of stroke and its subtypes among middle-aged Japanese men and women: the JPHC study cohort I," *Stroke*, vol. 35, no. 6, pp. 1248–1253, 2004.

[93] J. S. Gill, M. J. Shipley, S. A. Tsementzis et al., "Cigarette smoking. A risk factor for hemorrhagic and nonhemorrhagic stroke," *Archives of Internal Medicine*, vol. 149, no. 9, pp. 2053–2057, 1989.

[94] M. Hossain, P. Mazzone, W. Tierney, and L. Cucullo, "In vitro assessment of tobacco smoke toxicity at the BBB: do antioxidant supplements have a protective role?," *BMC Neuroscience*, vol. 12, p. 92, 2011.

[95] S. Prasad, R. K. Sajja, M. A. Kaisar et al., "Role of Nrf2 and protective effects of metformin against tobacco smoke-induced cerebrovascular toxicity," *Redox Biology*, vol. 12, pp. 58–69, 2017.

[96] J. K. Willcox, S. L. Ash, and G. L. Catignani, "Antioxidants and prevention of chronic disease," *Critical Reviews in Food Science and Nutrition*, vol. 44, no. 4, pp. 275–295, 2004.

[97] C. Del Bo, M. Porrini, D. Fracassetti, J. Campolo, D. Klimis-Zacas, and P. Riso, "A single serving of blueberry (V. corymbosum) modulates peripheral arterial dysfunction induced by acute cigarette smoking in young volunteers: a randomized-controlled trial," *Food & Function*, vol. 5, no. 12, pp. 3107–3116, 2014.

[98] C. Sticozzi, F. Cervellati, X. M. Muresan, C. Cervellati, and G. Valacchi, "Resveratrol prevents cigarette smoke-induced keratinocytes damage," *Food & Function*, vol. 5, no. 9, pp. 2348–2356, 2014.

[99] M. J. Bao, J. Shen, Y. L. Jia et al., "Apple polyphenol protects against cigarette smoke-induced acute lung injury," *Nutrition*, vol. 29, no. 1, pp. 235–243, 2013.

[100] J. C. Lee, J. T. Laydon, P. C. McDonnell et al., "A protein kinase involved in the regulation of inflammatory cytokine biosynthesis," *Nature*, vol. 372, no. 6508, pp. 739–746, 1994.

[101] C. Qing, P. Chen, and X. Xiang, "Effect of tea polyphenols on oxidative damage and apoptosis in human bronchial epithelial cells induced by low-dose cigarette smoke condensate," *Zhong nan da xue xue bao Yi xue ban = Journal of Central South University Medical sciences*, vol. 35, no. 2, pp. 123–128, 2010.

[102] W. C. Aird, "Phenotypic heterogeneity of the endothelium: I. Structure, function, and mechanisms," *Circulation Research*, vol. 100, no. 2, pp. 158–173, 2007.

[103] H. Lum and K. A. Roebuck, "Oxidant stress and endothelial cell dysfunction," *American Journal of physiology Cell physiology*, vol. 280, no. 4, pp. C719–C741, 2001.

[104] S. M. Davidson and M. R. Duchen, "Endothelial mitochondria: contributing to vascular function and disease," *Circulation Research*, vol. 100, no. 8, pp. 1128–1141, 2007.

[105] A. J. Flammer, T. Anderson, D. S. Celermajer et al., "The assessment of endothelial function: from research into clinical practice," *Circulation*, vol. 126, no. 6, pp. 753–767, 2012.

[106] H. A. Hadi, C. S. Carr, and J. Al Suwaidi, "Endothelial dysfunction: cardiovascular risk factors, therapy, and outcome," *Vascular Health and Risk Management*, vol. 1, no. 3, pp. 183–198, 2005.

[107] C. E. Storniolo, J. Rosello-Catafau, X. Pinto, M. T. Mitjavila, and J. J. Moreno, "Polyphenol fraction of extra virgin olive oil protects against endothelial dysfunction induced by high glucose and free fatty acids through modulation of nitric oxide and endothelin-1," *Redox Biology*, vol. 2, pp. 971–977, 2014.

[108] M. B. Engler, M. M. Engler, C. Y. Chen et al., "Flavonoid-rich dark chocolate improves endothelial function and increases plasma epicatechin concentrations in healthy adults," *Journal of the American College of Nutrition*, vol. 23, no. 3, pp. 197–204, 2004.

[109] D. F. Fitzpatrick, S. L. Hirschfield, T. Ricci, P. Jantzen, and R. G. Coffey, "Endothelium-dependent vasorelaxation caused by various plant extracts," *Journal of Cardiovascular Pharmacology*, vol. 26, no. 1, pp. 90–95, 1995.

[110] D. Steinberg, S. Parthasarathy, T. E. Carew, J. C. Khoo, and J. L. Witztum, "Beyond cholesterol: modifications of low-density lipoprotein that increase its atherogenicity," *New England Journal of Medicine*, vol. 320, no. 14, pp. 915–924, 1989.

[111] D. Steinberg, "The LDL modification hypothesis of atherogenesis: an update," *Journal of Lipid Research*, vol. 50, pp. S376–SS81, 2009.

[112] D. Steinberg and J. L. Witztum, "Oxidized low-density lipoprotein and atherosclerosis," *Arteriosclerosis, Thrombosis, and Vascular Biology*, vol. 30, no. 12, pp. 2311–2316, 2010.

[113] N. Santanam and S. Parthasarathy, "Paradoxical actions of antioxidants in the oxidation of low density lipoprotein by peroxidases," *Journal of Clinical Investigation*, vol. 95, no. 6, pp. 2594–2600, 1995.

[114] G. Maiolino, G. Rossitto, P. Caielli, V. Bisogni, G. P. Rossi, and L. A. Calo, "The role of oxidized low-density lipoproteins in atherosclerosis: the myths and the facts," *Mediators of Inflammation*, vol. 2013, Article ID 714653, 13 pages, 2013.

[115] B. Simini, "Serge Renaud: from French paradox to Cretan miracle," *The Lancet*, vol. 355, no. 9197, p. 48, 2000.

[116] E. N. Frankel, J. Kanner, J. B. German, E. Parks, and J. E. Kinsella, "Inhibition of oxidation of human low-density lipoprotein by phenolic substances in red wine," *The Lancet*, vol. 341, no. 8843, pp. 454–457, 1993.

[117] J. H. Chen, M. S. Lee, C. P. Wang, C. C. Hsu, and H. H. Lin, "Autophagic effects of Hibiscus sabdariffa leaf polyphenols and epicatechin gallate (ECG) against oxidized LDL-induced injury of human endothelial cells," *European Journal of Nutrition*, vol. 56, no. 5, pp. 1963–1981, 2017.

[118] N. Suzuki-Sugihara, Y. Kishimoto, E. Saita et al., "Green tea catechins prevent low-density lipoprotein oxidation via their accumulation in low-density lipoprotein particles in humans," *Nutrition Research*, vol. 36, no. 1, pp. 16–23, 2016.

[119] C. Knall, G. S. Worthen, and G. L. Johnson, "Interleukin 8-stimulated phosphatidylinositol-3-kinase activity regulates the migration of human neutrophils independent of extracellular signal-regulated kinase and p38 mitogen-activated protein kinases," *Proceedings of the National Academy of Sciences of the United States of America*, vol. 94, no. 7, pp. 3052–7, 1997.

[120] Y. Imai and D. R. Clemmons, "Roles of phosphatidylinositol 3-kinase and mitogen-activated protein kinase pathways in stimulation of vascular smooth muscle cell migration and deoxyriboncleic acid synthesis by insulin-like growth factor-I," *Endocrinology*, vol. 140, no. 9, pp. 4228–4235, 1999.

[121] J. C. Hedges, M. A. Dechert, I. A. Yamboliev et al., "A role for p38(MAPK)/HSP27 pathway in smooth muscle cell migration," *Journal of Biological Chemistry*, vol. 274, no. 34, pp. 24211–24219, 1999.

[122] S. Rosenkranz, D. Knirel, H. Dietrich, M. Flesch, E. Erdmann, and M. Bohm, "Inhibition of the PDGF receptor by red wine flavonoids provides a molecular explanation for the "French paradox"," *The FASEB Journal*, vol. 16, no. 14, pp. 1958–1960, 2002.

[123] M. Dell'Agli, A. Busciala, and E. Bosisio, "Vascular effects of wine polyphenols," *Cardiovascular Research*, vol. 63, no. 4, pp. 593–602, 2004.

[124] H. C. Lin, M. J. Hsieh, C. H. Peng, S. F. Yang, and C. N. Huang, "Pterostilbene inhibits vascular smooth muscle cells migration and matrix metalloproteinase-2 through modulation of MAPK pathway," *Journal of Food Science*, vol. 80, no. 10, pp. H2331–H2335, 2015.

[125] M. Wicinski, B. Malinowski, M. M. Weclewicz, E. Grzesk, and G. Grzesk, "Resveratrol increases serum BDNF concentrations and reduces vascular smooth muscle cells contractility via a NOS-3-independent mechanism," *BioMed Research International*, vol. 2017, Article ID 9202954, 7 pages, 2017.

[126] H. Y. Li, M. Yang, Z. Li, and Z. Meng, "Curcumin inhibits angiotensin II-induced inflammation and proliferation of rat vascular smooth muscle cells by elevating PPAR-γ activity and reducing oxidative stress," *International Journal of Molecular Medicine*, vol. 39, no. 5, pp. 1307–1316, 2017.

[127] K. Shimada, "Immune system and atherosclerotic disease: heterogeneity of leukocyte subsets participating in the pathogenesis of atherosclerosis," *Circulation Journal*, vol. 73, no. 6, pp. 994–1001, 2009.

[128] K. J. Moore and I. Tabas, "Macrophages in the pathogenesis of atherosclerosis," *Cell*, vol. 145, no. 3, pp. 341–355, 2011.

[129] O. Rom, H. Korach-Rechtman, T. Hayek et al., "Acrolein increases macrophage atherogenicity in association with gut microbiota remodeling in atherosclerotic mice: protective role for the polyphenol-rich pomegranate juice," *Archives of Toxicology*, vol. 91, no. 4, pp. 1709–1725, 2017.

[130] S. Sarkar, A. A. Siddiqui, S. Mazumder et al., "Ellagic acid, a dietary polyphenol, inhibits tautomerase activity of human macrophage migration inhibitory factor and its pro-

inflammatory responses in human peripheral blood mononuclear cells," *Journal of Agricultural and Food Chemistry*, vol. 63, no. 20, pp. 4988–4998, 2015.

[131] E. Scoditti, A. Nestola, M. Massaro et al., "Hydroxytyrosol suppresses MMP-9 and COX-2 activity and expression in activated human monocytes via PKCα and PKCβ1 inhibition," *Atherosclerosis*, vol. 232, no. 1, pp. 17–24, 2014.

[132] L. N. Broekhuizen, D. F. van Wijk, H. Vink et al., "Reduction of monocyte chemoattractant protein 1 and macrophage migration inhibitory factor by a polyphenol-rich extract in subjects with clustered cardiometabolic risk factors," *British Journal of Nutrition*, vol. 106, no. 9, pp. 1416–1422, 2011.

[133] C. T. Ford, S. Richardson, F. McArdle et al., "Identification of (poly)phenol treatments that modulate the release of pro-inflammatory cytokines by human lymphocytes," *British Journal of Nutrition*, vol. 115, no. 10, pp. 1699–1710, 2016.

[134] C. Faggio, A. Sureda, S. Morabito et al., "Flavonoids and platelet aggregation: a brief review," *European Journal of Pharmacology*, vol. 807, pp. 91–101, 2017.

[135] G. E. Hirsch, P. R. Viecili, A. S. de Almeida et al., "Natural products with antiplatelet action," *Current Pharmaceutical Design*, vol. 23, no. 8, pp. 1228–1246, 2017.

[136] T. Mattiello, E. Trifiro, G. S. Jotti, and F. M. Pulcinelli, "Effects of pomegranate juice and extract polyphenols on platelet function," *Journal of Medicinal Food*, vol. 12, no. 2, pp. 334–339, 2009.

[137] D. A. Pearson, T. G. Paglieroni, D. Rein et al., "The effects of flavanol-rich cocoa and aspirin on ex vivo platelet function," *Thrombosis Research*, vol. 106, no. 4-5, pp. 191–197, 2002.

[138] D. Rein, T. G. Paglieroni, T. Wun et al., "Cocoa inhibits platelet activation and function," *The American Journal of Clinical Nutrition*, vol. 72, no. 1, pp. 30–35, 2000.

[139] R. R. Holt, D. D. Schramm, C. L. Keen, S. A. Lazarus, and H. H. Schmitz, "Chocolate consumption and platelet function," *JAMA*, vol. 287, no. 17, pp. 2212-2213, 2002.

[140] G. Rull, Z. N. Mohd-Zain, J. Shiel et al., "Effects of high flavanol dark chocolate on cardiovascular function and platelet aggregation," *Vascular Pharmacology*, vol. 71, pp. 70–78, 2015.

[141] R. Carnevale, L. Loffredo, P. Pignatelli et al., "Dark chocolate inhibits platelet isoprostanes via NOX2 down-regulation in smokers," *Journal of Thrombosis and Haemostasis*, vol. 10, no. 1, pp. 125–132, 2012.

[142] E. Saita, K. Kondo, and Y. Momiyama, "Anti-inflammatory diet for atherosclerosis and coronary artery disease: antioxidant foods," *Clinical Medicine Insights Cardiology*, vol. 8, Supplement 3, pp. 61–65, 2015.

[143] Y. Kokubo, H. Iso, J. Ishihara, K. Okada, M. Inoue, and S. Tsugane, "Association of dietary intake of soy, beans, and isoflavones with risk of cerebral and myocardial infarctions in Japanese populations: the Japan public health center-based (JPHC) study cohort I," *Circulation*, vol. 116, no. 22, pp. 2553–2562, 2007.

[144] H. N. Hodis, W. J. Mack, N. Kono et al., "Isoflavone soy protein supplementation and atherosclerosis progression in healthy postmenopausal women: a randomized controlled trial," *Stroke*, vol. 42, no. 11, pp. 3168–3175, 2011.

[145] D. Pala, P. O. Barbosa, C. T. Silva et al., "Acai (Euterpe oleracea Mart.) dietary intake affects plasma lipids, apolipoproteins, cholesteryl ester transfer to high-density lipoprotein and redox metabolism: a prospective study in women," *Clinical Nutrition*, 2017.

[146] T. Namekata, K. Suzuki, N. Ishizuka, and K. Shirai, "Establishing baseline criteria of cardio-ankle vascular index as a new indicator of arteriosclerosis: a cross-sectional study," *BMC Cardiovascular Disorders*, vol. 11, no. 1, p. 51, 2011.

[147] H. Imamura, T. Yamaguchi, D. Nagayama, A. Saiki, K. Shirai, and I. Tatsuno, "Resveratrol ameliorates arterial stiffness assessed by cardio-ankle vascular index in patients with type 2 diabetes mellitus," *International Heart Journal*, vol. 58, no. 4, pp. 577–583, 2017.

[148] C. Pasten, N. C. Olave, L. Zhou, E. M. Tabengwa, P. E. Wolkowicz, and H. E. Grenett, "Polyphenols downregulate PAI-1 gene expression in cultured human coronary artery endothelial cells: molecular contributor to cardiovascular protection," *Thrombosis Research*, vol. 121, no. 1, pp. 59–65, 2007.

[149] A. Sinkovic, D. Suran, L. Lokar et al., "Rosemary extracts improve flow-mediated dilatation of the brachial artery and plasma PAI-1 activity in healthy young volunteers," *Phytotherapy Research*, vol. 25, no. 3, pp. 402–407, 2011.

[150] J. Lekakis, L. S. Rallidis, I. Andreadou et al., "Polyphenols compounds from red grapes acutely improve endothelial function in patients with coronary heart disease," *European Journal of Cardiovascular Prevention & Rehabilitation*, vol. 12, no. 6, pp. 596–600, 2005.

[151] K. Magyar, R. Halmosi, A. Palfi et al., "Cardioprotection by resveratrol: a human clinical trial in patients with stable coronary artery disease," *Clinical Hemorheology and Microcirculation*, vol. 50, no. 3, pp. 179–187, 2012.

[152] M. G. Hertog, E. J. Feskens, P. C. Hollman, M. B. Katan, and D. Kromhout, "Dietary antioxidant flavonoids and risk of coronary heart disease: the Zutphen elderly study," *The Lancet*, vol. 342, no. 8878, pp. 1007–1011, 1993.

[153] P. Knekt, R. Jarvinen, A. Reunanen, and J. Maatela, "Flavonoid intake and coronary mortality in Finland: a cohort study," *BMJ*, vol. 312, no. 7029, pp. 478–481, 1996.

[154] P. J. Mink, C. G. Scrafford, L. M. Barraj et al., "Flavonoid intake and cardiovascular disease mortality: a prospective study in postmenopausal women," *The American Journal of Clinical Nutrition*, vol. 85, no. 3, pp. 895–909, 2007.

[155] S. R. Hsieh, W. C. Cheng, Y. M. Su, C. H. Chiu, and Y. M. Liou, "Molecular targets for anti-oxidative protection of green tea polyphenols against myocardial ischemic injury," *BioMedicine*, vol. 4, p. 23, 2014.

[156] H. T. Lai, D. E. Threapleton, A. J. Day, G. Williamson, J. E. Cade, and V. J. Burley, "Fruit intake and cardiovascular disease mortality in the UK Women's cohort study," *European Journal of Epidemiology*, vol. 30, no. 9, pp. 1035–1048, 2015.

[157] M. A. Martinez-Gonzalez, J. Salas-Salvado, R. Estruch, D. Corella, M. Fito, and E. Ros, "Benefits of the Mediterranean diet: insights from the PREDIMED study," *Progress in Cardiovascular Diseases*, vol. 58, no. 1, pp. 50–60, 2015.

[158] "The top 10 causes of death: WHO, fact sheet," 2017, http://who.int/mediacentre/factsheets/fs310/en/.

[159] S. M. A. A. Evers, J. N. Struijs, A. J. H. A. Ament, M. L. L. van Genugten, J. C. Jager, and G. A. M. van den Bos, "International comparison of stroke cost studies," *Stroke*, vol. 35, no. 5, pp. 1209–1215, 2004.

[160] D. Wan, Y. Zhou, K. Wang, Y. Hou, R. Hou, and X. Ye, "Resveratrol provides neuroprotection by inhibiting

phosphodiesterases and regulating the cAMP/AMPK/SIRT1 pathway after stroke in rats," *Brain Research Bulletin*, vol. 121, pp. 255–262, 2016.

[161] V. Carito, M. Ceccanti, L. Tarani, G. Ferraguti, G. N. Chaldakov, and M. Fiore, "Neurotrophins' modulation by olive polyphenols," *Current Medicinal Chemistry*, vol. 23, no. 28, pp. 3189–3197, 2016.

[162] I. L. Hung, Y. C. Hung, L. Y. Wang et al., "Chinese herbal products for ischemic stroke," *The American Journal of Chinese Medicine*, vol. 43, no. 7, pp. 1365–1379, 2015.

[163] Z. M. Wang, D. Zhao, Z. L. Nie et al., "Flavonol intake and stroke risk: a meta-analysis of cohort studies," *Nutrition*, vol. 30, no. 5, pp. 518–523, 2014.

[164] M. E. Goetz, S. E. Judd, T. J. Hartman, W. McClellan, A. Anderson, and V. Vaccarino, "Flavanone intake is inversely associated with risk of incident ischemic stroke in the REasons for geographic and racial differences in stroke (REGARDS) study," *Journal of Nutrition*, vol. 146, no. 11, pp. 2233–2243, 2016.

[165] C. C. Chang, Y. C. Chang, W. L. Hu, and Y. C. Hung, "Oxidative stress and *Salvia miltiorrhiza* in aging-associated cardiovascular diseases," *Oxidative Medicine and Cellular Longevity*, vol. 2016, Article ID 4797102, 11 pages, 2016.

Hindawi
Oxidative Medicine and Cellular Longevity
Volume 2017, Article ID 6019796, 13 pages
https://doi.org/10.1155/2017/6019796

Research Article

Effects of Aging and Tocotrienol-Rich Fraction Supplementation on Brain Arginine Metabolism in Rats

Musalmah Mazlan,[1] Hamizah Shahirah Hamezah,[2] Nursiati Mohd Taridi,[2] Yu Jing,[3] Ping Liu,[3] Hu Zhang,[4] Wan Zurinah Wan Ngah,[2] and Hanafi Ahmad Damanhuri[2]

[1]*Faculty of Medicine, Universiti Teknologi MARA, Sungai Buloh Campus, Sungai Buloh, Malaysia*
[2]*Department of Biochemistry, Faculty of Medicine, Universiti Kebangsaan Malaysia, Kuala Lumpur, Malaysia*
[3]*Department of Anatomy, University of Otago, Dunedin, New Zealand*
[4]*School of Pharmacy, University of Otago, Dunedin, New Zealand*

Correspondence should be addressed to Hanafi Ahmad Damanhuri; hanafi.damanhuri@ppukm.ukm.edu.my

Received 21 July 2017; Revised 4 October 2017; Accepted 9 October 2017; Published 19 November 2017

Academic Editor: Anna M. Giudetti

Accumulating evidence suggests that altered arginine metabolism is involved in the aging and neurodegenerative processes. This study sought to determine the effects of age and vitamin E supplementation in the form of tocotrienol-rich fraction (TRF) on brain arginine metabolism. Male Wistar rats at ages of 3 and 21 months were supplemented with TRF orally for 3 months prior to the dissection of tissue from five brain regions. The tissue concentrations of L-arginine and its nine downstream metabolites were quantified using high-performance liquid chromatography and liquid chromatography tandem mass spectrometry. We found age-related alterations in L-arginine metabolites in the chemical- and region-specific manners. Moreover, TRF supplementation reversed age-associated changes in arginine metabolites in the entorhinal cortex and cerebellum. Multiple regression analysis revealed a number of significant neurochemical-behavioral correlations, indicating the beneficial effects of TRF supplementation on memory and motor function.

1. Introduction

Declined cognitive and motor functions occur during aging even in the absence of neurodegenerative diseases. While various mechanisms, such as cellular communication, oxidative stress, and inflammation, have been suggested to be involved in age-related cognitive and motor deficits [1], a growing body of evidence indicates the role of altered arginine metabolism in the aging and neurodegenerative processes [2–4].

L-Arginine is a semiessential amino acid that can be metabolized by nitric oxide synthase (NOS) to produce nitric oxide (NO) and L-citrulline, by arginase to form L-ornithine and urea, and by arginine decarboxylase (ADC) to generate agmatine and carbon dioxide [5]. NO plays an important role in maintaining physiological function of the nervous system [6]. However, it can be neurotoxic when present in excess due to its free radical property [7]. L-Ornithine is the main precursor of the polyamines putrescine, spermidine, and spermine [5], which are required for optimal cell growth and function [8], including neurogenesis [9]. L-Ornithine can also be converted to L-glutamyl-c-semialdehyde that is further metabolized to glutamate by P5C dehydrogenase [5]. Glutamate can also be synthesized by glutaminase using glutamine as a precursor [10] and can be converted to gamma-aminobutyric acid (GABA) by glutamate decarboxylase (GAD) [5]. Agmatine, decarboxylated arginine, is a novel putative neurotransmitter and directly participates in learning and memory processing [11–13]. It also plays an important role in regulating the production of NO and polyamines [14].

Given the physiological roles of L-arginine metabolites, a considerable number of studies have investigated how brain arginine metabolism is affected by aging. Earlier research has demonstrated age-related changes in the L-arginine

metabolic profiles in the brain, particularly in the brain regions involved in learning and memory, in a region-specific manner, and the associations of neurochemical changes with animals' behavioral performance in various learning and memory tasks [2, 3, 15, 16]. It has been well documented that NO reacts with O_2^- and H_2O_2 to form $ONOO^-$, and the accumulation of these free radicals may lead to neuronal death and learning and memory impairments in the aged. To this end, pharmacological manipulations of brain L-arginine metabolism during aging may be a potential preventive or treatment strategy for age-related cognitive decline.

Neurodegeneration and cognitive decline can be modulated by dietary components rich in antioxidants such as vegetables and fruits and ascorbic acid [17–20]. Research has shown that supplementation with vitamin E is able to preserve cognitive function and general well-being in the elderly [21–23]. This is in accordance with the report that low plasma tocopherol and tocotrienol levels are associated with increased risks of mild cognitive impairment (MCI) and Alzheimer's disease (AD) [24]. Further investigation from our laboratory [25] provides additional evidence which showed 3-month daily supplementation of TRF able to reverse behavioral impairment in aged rats. In the study of Mangialasche et al. [26], elevated serum tocopherol and tocotrienol levels appear to be associated with reduced risk of cognitive impairment in older adults. Moreover, cell culture studies have demonstrated the neuroprotective effects of vitamin E, with tocotrienol being more potent than tocopherol [27–29]. The mechanisms of action of tocotrienol includes but not limited to free radical scavenging and modulation of arachidonic acid metabolism [28, 30–32], kainic acid metabolism [33], homocysteic acid metabolism [34], and mitochondrial metabolism [35].

The present study was therefore designed to further investigate how brain arginine metabolism was affected by age and to elucidate how the long-term supplementation of TRF affected brain arginine metabolism in both young and aged rats. The findings of this study demonstrated altered brain arginine metabolism in the aged rats in the chemical- and region-specific manners and the neuroprotective effect of vitamin E in the form of TRF via the modulation of brain L-arginine metabolism.

2. Materials and Methods

2.1. Animals. Thirty-six male Wistar rats were fed with standard rat chow (Gold Coin, Malaysia) and tap water ad libitum. Animals were housed one animal per cage at room temperature under a 12 h dark : light cycle. This study was approved by the Universiti Kebangsaan Malaysia Animal Ethics Committee (protocol nos. UKMAECFP/BIOK/2008/MUSALMAH/13-FEB/215-FEB-2008-OCT-2010).

2.2. Supplementation. Gold-Tri E70 (TRF) (Golden Hope Bioganic, Malaysia) consisted of approximately 149.2 mg/g α-tocopherol, 164.7 mg/g α-tocotrienol, 48.8 mg/g β-tocotrienol, 213.2 mg/g γ-tocotrienol, and 171 mg/g δ-tocotrienol. Olive oil was bought commercially (Basso, Italy). Rats were randomly divided into two groups: young and old (3 and 21 months, resp.). Rats in both groups were given either TRF (200 mg/kg body weight, oral gavage) or control (equal volume of olive oil, oral gavage) ($n = 9$ per group) daily, for 3 months. At the end of the treatment period, the rat's behavior was tested by the open-field test and Morris water maze task (see Taridi et al. [25]).

Evaluation on the locomotor activity, exploration, and anxiety of the rat in the open-field test was conducted by placing the rat into an open-field chamber ($60 \times 60 \times 20\ cm^3$). The floor of the open-field chamber was divided into 36 equal-sized square-shape cells ($10 \times 10\ cm^2$). The rat's behavior was recorded within the 5 min exploration time. Then, the number of fecal boli, the number and duration of wall-supported rearing and grooming, the number and percentage of grid squares traversed, and the number of central squares crossed were analyzed.

To investigate spatial learning and memory, the Morris water maze (MWM) task was carried out in a black circular galvanized pool (140 cm diameter), filled with 30 cm water depth. The pool was divided into four equal quadrants, and a platform (13×13 cm) was placed in a target quadrant (the center of one of the quadrants), 2 cm below the water surface. This test was conducted within 10 consecutive days: place navigation (days 1 to 6), probe test (day 7), cued navigation (day 8), and working memory task (days 9 and 10). During the place navigation test, the rat was trained to find the fixed hidden platform. The parameters measured in this place navigation test were escape latency, swim path, and swim speed. On the next day after the completion of the place navigation test, the platform was removed and the rat was tested to find the platform location. This test was repeated twice for each rat. The percentage of time the rat spent in the target quadrant and the number of platform crossings in probe 1 (the first time the rat was tested without a platform) and probe 2 (the second time the rat was tested without a platform) were measured. Meanwhile, during the cued navigation test, the platform was shifted to another quadrant and raised 2 cm above the water surface. In order to make the platform more visible, the edge of the platform was marked by a masking tape. Then, the rat was allowed to find the visible platform within 60 s. Cued navigation is a control test to ensure that the rat used in this study has an intact vision. Escape latency was measured in this test.

On the next two days of Morris water maze, the working memory test was carried out. In this test, the rat was given two trials per day (each trial consisted of a sample phase and a test phase), with the hidden platform location changed between each trial. The sample phase involved in each trial the first time that the rat was placed in the pool. The rats were rested for 1 min and 1 hour before they were retested in the test phase. The parameters measured in this test were the path length taken by the rat to reach the platform on day 1 and day 2 (sample phase) and the path length during 1 min and 1 h delay time (test phase) (see Taridi et al. [25]).

2.3. Brain Tissue Collection and Preparation. Upon the completion of the behavioral test, animals were killed by decapitation without anesthesia. The brains were rapidly removed,

wrapped in tin foil, immediately frozen on dry ice, and stored at −80°C. Before an assay, each frozen brain was sectioned at about 200 μm in the coronal plane on dry ice. The cerebellum (CE), pons and medulla (brain stem (BS)), and striatum (only the tissue anterior to the anterior commissure) were collected. The entorhinal cortex (EC) and postrhinal cortex (POR) were then dissected out based on the previous studies [36–38] (see Figure 1 of Liu et al. [39]). Brain tissues were weighed, homogenized in 10% ice-cold perchloric acid (~50 mg wet weight per ml), and centrifuged at 10,000 rpm for 10 minutes at 4°C to precipitate protein [40]. The supernatants (perchloric acid extracts) were then frozen immediately and stored at −80°C until analysis using high-performance liquid chromatography (HPLC) and liquid chromatography tandem mass spectrometry (LC/MS/MS).

2.4. Standard and Reagent Preparation. The standard and reagent preparation for amino acid and polyamine analysis was done according to the method described previously [3, 40]. Briefly, aqueous stock solutions of amino acids and polyamines were prepared in double-distilled water with an initial concentration of 10 mM, except for glutamate (50 mM) and glutamine (200 mM). These stock solutions were then diluted with water. High-purity standards were used (Sigma, USA) and all other chemicals were of analytical grade. For amino acid analysis, $KHCO_3$-KOH solution (pH 9.8), methanol, and dansyl chloride were added to the standards and samples. Dansyl chloride was prepared just before derivatization by dissolving it in acetonitrile. The mobile phase was 30 : 70 methanol/water (*v*/*v*) containing triethylamine and tetrabutylammonium hydroxide at pH 2.2. Saturated sodium carbonate, 1,7-diaminoheptane (internal standard), and dansyl chloride dissolved in acetone were added to the standards and samples for polyamine analysis. The mobile phase used for spermidine and spermine analysis was 70 : 30 acetonitrile/water and for agmatine and putrescine was 80 : 20 acetonitrile/water containing 0.1% formic acid. Samples from all groups were assayed at the same time for all brain regions and between all groups.

2.5. Amino Acid Analysis. L-Arginine, L-ornithine, glutamine, L-citrulline, glutamate, and GABA in each brain region were determined using HPLC (Shimadzu, Japan), as described previously [3]. The samples were alkalized with $KHCO_3$ solution (pH 9.8), mixed with methanol, derivatized with dansyl chloride in the dark, and incubated at 80°C for 20 minutes, and 10 μl acetic acid was added to stop the reaction. The mixture was then centrifuged at 10,000 rpm for 10 minutes, and 40 μl of the resultant supernatant was injected onto the HPLC system. The HPLC system consisted of a programmed solvent delivery system at a flow rate of 1.0 ml/min and a UV detector set at a wavelength of 218 nm. The column used was reversed-phase C_{18} (5 μm, 150 mm × 4.6 mm) (Phenomenex, USA). L-Arginine, L-ornithine, L-citrulline, glutamine, glutamate, and GABA in the brain samples were identified by comparing the retention time of the sample with the known standards. Amino acid concentrations were calculated with reference to the peak area of external standards, and values were expressed in μg/g wet tissue.

2.6. Polyamine Analysis. Agmatine and putrescine concentrations were measured by a highly sensitive LC/MS/MS method according to the method described previously [40]. The internal standard was added to the samples, alkalized with saturated sodium carbonate, derivatized with dansyl chloride in the dark, and then incubated at 70°C for 30 minutes. Agmatine, putrescine, and the internal standard were extracted with toluene and centrifuged at 10,000 rpm for 5 minutes. The toluene phase was evaporated to dryness, reconstituted with 50% acetonitrile, and injected onto the LC/MS/MS system. The column used was reversed-phase C_{18} (5 μm, 150 mm × 2.0 mm) (Phenomenex, USA). The mobile phase was 80% acetonitrile to 20% water containing 0.1% formic acid and was run at a flow rate of 0.2 ml/min. The retention time of agmatine, putrescine, and the internal standard was 1.7, 4.0, and 4.8 min, respectively, with 15 minutes of the total run time. Detection by MS/MS used an electrospray interface (ESI) in a positive ion mode. The standard curves for putrescine were linear up to 1000 ng/ml ($r^2 > 0.99$). The intra- and interassay coefficients of variance were <15%. Agmatine and putrescine concentrations in the tissues were calculated with reference to the peak area of external standards, and values were expressed as μg/g wet tissue.

Determination of spermidine and spermine was carried out according to Liu et al. [40]. Briefly, the internal standard (1,7-diaminoheptane) was added to 50 μl of samples. Samples were then alkalized with saturated sodium carbonate, derivatized with dansyl chloride in the dark, and incubated at 70°C for 30 minutes. Spermidine, spermine, and the internal standard were extracted with toluene and centrifuged at 10,000 rpm for 5 minutes. The toluene phase was then evaporated to dryness, reconstituted with 50% acetonitrile, and injected onto the HPLC system. The HPLC system had a programmed solvent delivery system at a flow rate of 1.5 ml/min, an autosampler, a reversed-phase C_{18} column, and a fluorescence detector set at excitation wavelength of 252 nm and emission wavelength of 515 nm. Identification of spermidine and spermine was by comparing the retention times of samples with known standards. The precision of the intra- and interassay coefficients of variance was <15%. Spermidine and spermine concentrations in the brain tissue were calculated with reference to the peak area of external standards, and values were expressed as μg/g wet tissue.

2.7. Statistical Analysis. Data was analyzed using two-way ANOVA, followed by the post hoc Bonferroni test to detect significant differences between groups by using GraphPad Prism 5 (GraphPad Software, USA). Data are presented as mean ± standard error mean (SEM). The significance level was set at 0.05 for all comparisons. Behavioral data (Morris water maze and open field) obtained previously [25] was analyzed for correlation with amino acids and polyamines in the different brain regions by multiple regression analysis. The significance value was set at $p < 0.025$.

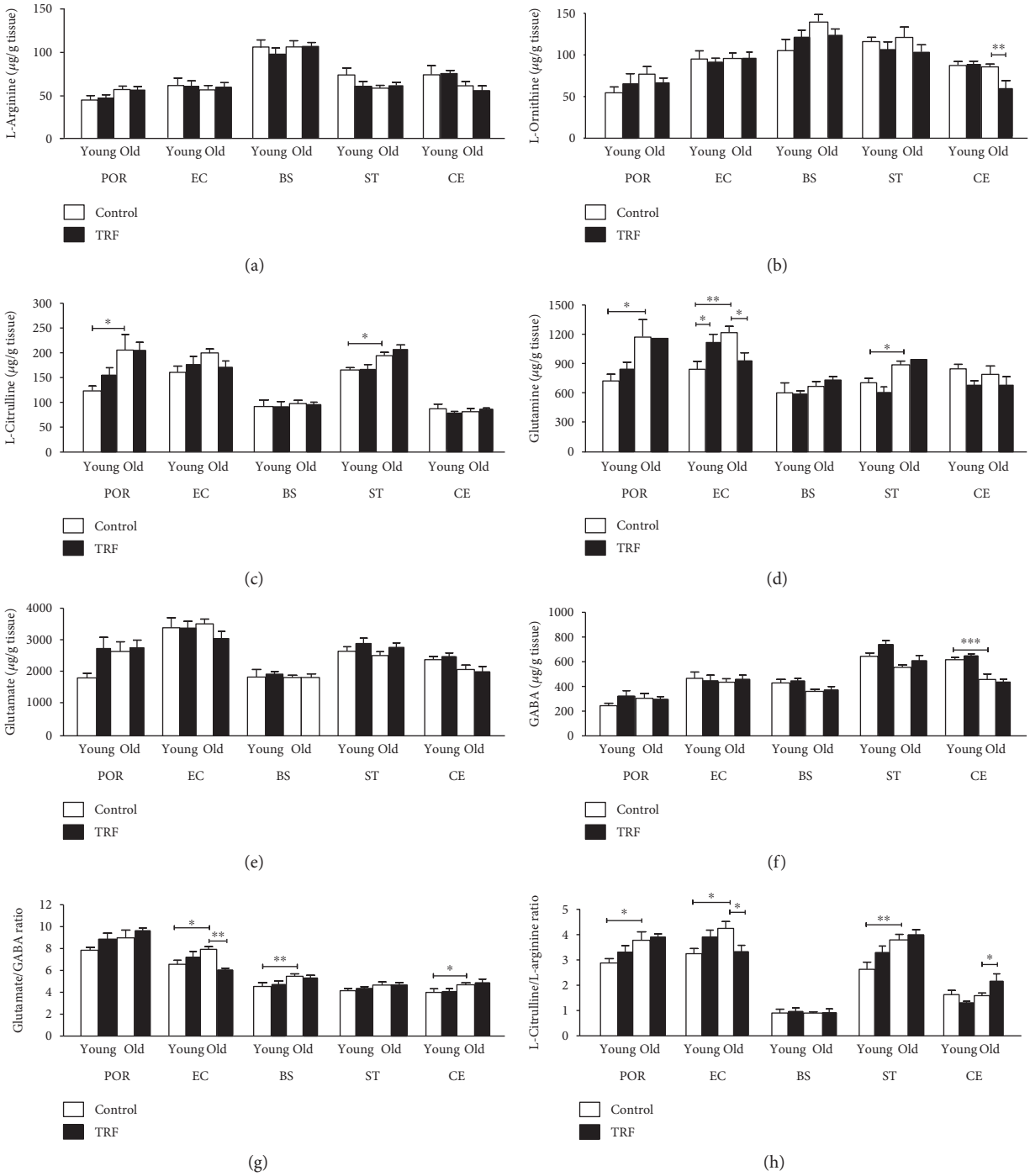

Figure 1: The levels of (a) L-arginine, (b) L-ornithine, (c) L-citrulline, (d) glutamine, (e) glutamate, (f) GABA, (g) glutamate/GABA ratio, and (h) L-citrulline/L-arginine ratio in the postrhinal cortex (POR), entorhinal cortex (EC), brain stem (BS), striatum (ST), and cerebellum (CE) in young and old rats. Data is presented as mean ± SEM. The asterisks indicate a significant difference between groups: $^{*}p < 0.05$, $^{**}p < 0.01$, and $^{***}p < 0.001$.

3. Results

3.1. Effects of Age and TRF on Amino Acid Levels. The current findings showed that the changes in the amino acid level were primarily affected by age. All amino acid levels were altered with age except L-arginine and glutamate. In addition, TRF supplementation modulates the level of L-ornithine, glutamine, glutamate/GABA ratio, and L-citrulline/L-arginine ratio in several brain regions. L-Arginine in the different brain regions across all groups are presented in Figure 1(a). There was no significant effect of age or TRF supplementation observed. Figure 1(b) represents the L-ornithine in different areas of the brain. There was no significant effect of age; however, TRF supplementation significantly decreased

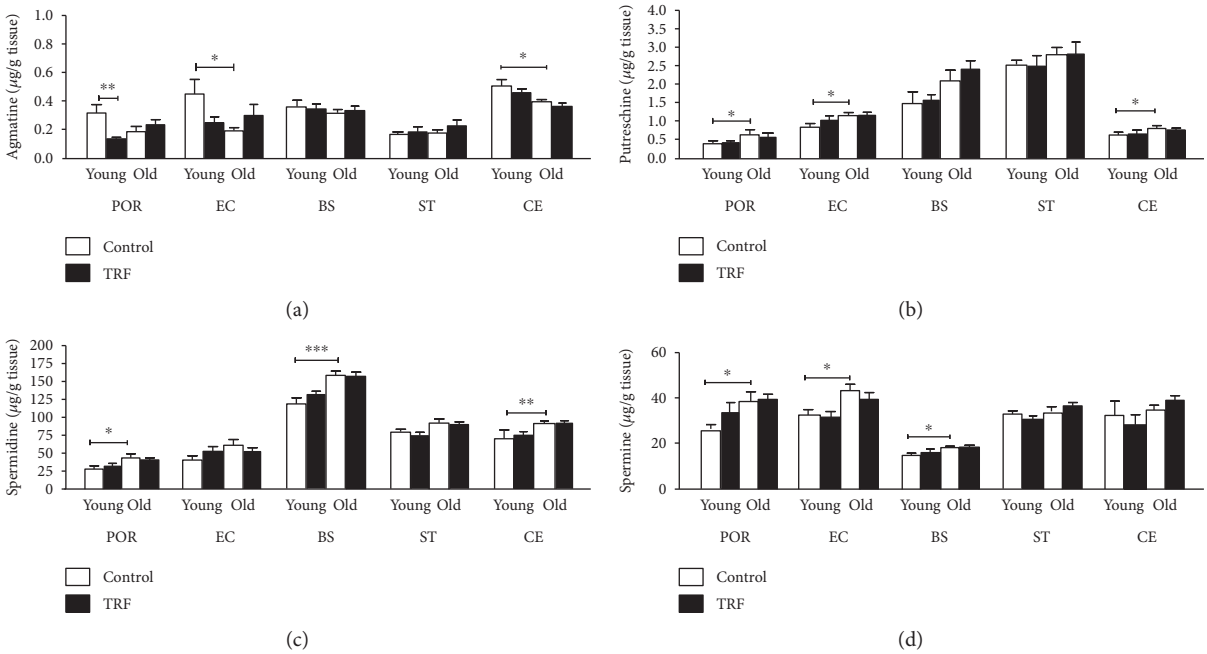

Figure 2: The levels of (a) agmatine, (b) putrescine, (c) spermidine, and (d) spermine in the postrhinal cortex (POR), entorhinal cortex (EC), brain stem (BS), striatum (ST), and cerebellum (CE) in young and old rats. Data is presented as mean ± SEM. The asterisks indicate a significant difference between groups: $^{*}p < 0.05$, $^{**}p < 0.01$, and $^{***}p < 0.001$.

the L-ornithine level in the cerebellum of old rats compared to the control (unsupplemented) ($p < 0.01$). L-Citrulline was significantly higher in the postrhinal cortex (POR) and striatum (ST) ($p < 0.05$) of old versus young rats (Figure 1(c)). L-Citrulline was unchanged with TRF supplementation in all groups. Age significantly increased glutamine in the postrhinal cortex ($p < 0.05$), entorhinal cortex ($p < 0.01$), and striatum ($p < 0.05$) (Figure 1(d)). TRF supplementation resulted in an increase in glutamine in the entorhinal cortex of young rats ($p < 0.05$) but was decreased in the old rats ($p < 0.05$). There was no significant effect of age nor TRF supplementation on glutamate (Figure 1(e)). Figure 1(f) shows that there was a significant effect of age on GABA in the cerebellum. The level of GABA was significantly lower in the old rats compared to the young rats ($p < 0.001$).

The glutamate/GABA was significantly increased in the entorhinal cortex ($p < 0.05$), brain stem ($p < 0.01$), and cerebellum ($p < 0.05$) of the old rats compared to the young rats (Figure 1(g)). TRF supplementation decreased glutamate/GABA significantly in the entorhinal cortex of the old group ($p < 0.01$). Effects of age were also observed with L-citrulline/L-arginine in the postrhinal cortex ($p < 0.05$), entorhinal cortex ($p < 0.05$), and striatum ($p < 0.01$) (Figure 1(h)). TRF supplementation significantly decreased the L-citrulline/L-arginine ratio in the entorhinal cortex ($p < 0.05$) but was increased in the cerebellum of the old rats ($p < 0.05$).

3.2. Effects of Age and TRF on Polyamines. Alterations in the polyamine levels were mainly influenced by age. Age affects all polyamines in various regions, while TRF supplementation only caused an alteration in the agmatine level only in the postrhinal cortex. Figure 2(a) shows that agmatine was significantly lower in the entorhinal cortex ($p < 0.05$) and cerebellum ($p < 0.05$) of old rats compared to young rats. TRF supplementation resulted in decreased agmatine in the postrhinal cortex ($p < 0.01$) of young rats. Putrescine was significantly increased in the postrhinal cortex ($p < 0.05$), entorhinal cortex ($p < 0.05$), and cerebellum ($p < 0.05$) of old rats compared to young rats (Figure 2(b)). Spermidine was increased in the old group compared to the young group in the postrhinal cortex ($p < 0.05$), brain stem ($p < 0.001$), and cerebellum ($p < 0.01$) (Figure 2(c)). Spermine was significantly increased in the postrhinal cortex ($p < 0.05$), entorhinal cortex ($p < 0.05$), and brain stem ($p < 0.05$) (Figure 2(d)). Figure 3 shows the summary of the effects of age and TRF supplementation on amino acids and polyamines in the different parts of the brain.

3.3. Correlations between Behavior, Amino Acids, and Polyamines. Based on the previous findings by Taridi et al. [25], TRF supplementation to the aged rats markedly improved the animals' behavioral performance in the open-field and Morris water maze tests, as shown by the increased exploratory activity and improved spatial learning and memory, respectively. Therefore, the current study further analyzed the behavioral performance data in relation to the neurochemical level in the rats' brain, to further explore the effects of age on particular behavioral parameters as well as to elucidate the potential neuroprotective effect of TRF.

The relationships between the levels of amino acids and polyamines and the animals' behavioral performance in the open-field and Morris water maze tests were analyzed using multiple regression analysis. Only those with significant correlations in each of the test group are shown in Figures 4 and

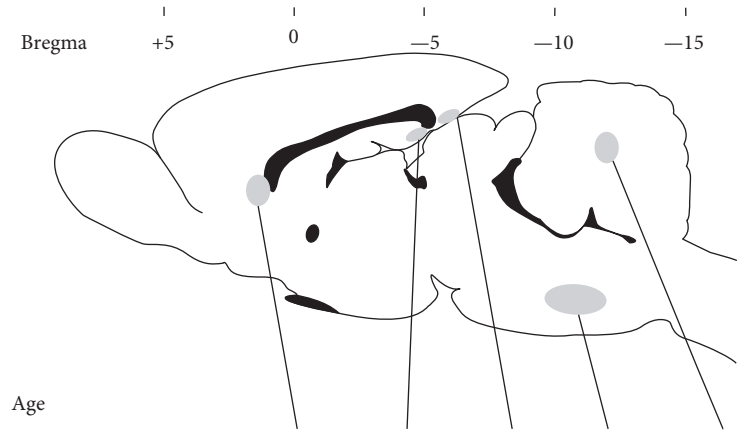

	Striatum	Entorhinal cortex	Postrhinal cortex	Brain stem	Cerebellum
L-Arginine	—	—	—	—	—
L-Ornithine	—	—	—	—	—
L-Citrulline	↑C	—	↑C	—	—
Glutamine	↑C	↑C	↑C	—	—
Glutamate	—	—	—	—	—
GABA	—	—	—	—	↑C
Glutamate/GABA ratio	—	↑C	—	↑C	↑C
L-Citrulline/L-arginine ratio	↑C	↑C	↑C	—	—
Agmatine	—	↑C	—	—	↑C
Putrescine	—	↑C	↑C	—	↑C
Spermidine	—	—	↑C	↑C	↑C
Spermine	—	↑C	↑C	↑C	—

TRF

	Striatum	Entorhinal cortex	Postrhinal cortex	Brain stem	Cerebellum
L-Arginine	—	—	—	—	—
L-Ornithine	—	—	—	—	↓O
L-Citrulline	—	—	—	—	—
Glutamine	—	↑Y↓O	—	—	—
Glutamate	—	—	—	—	—
GABA	—	—	—	—	—
Glutamate/GABA ratio	—	↓O	—	—	—
L-Citrulline/L-arginine ratio	—	↓O	—	—	↑O
Agmatine	—	—	↓Y	—	—
Putrescine	—	—	—	—	—
Spermidine	—	—	—	—	—
Spermine	—	—	—	—	—

Figure 3: Summary of the effect of age and TRF on amino acid (L-arginine, L-ornithine, L-citrulline, glutamine, glutamate, GABA, glutamate/GABA ratio, and L-citrulline/L-arginine ratio) and polyamine (agmatine, putrescine, spermidine, and spermine) levels in the striatum, postrhinal cortex, entorhinal cortex, brain stem, and cerebellum. Decreased levels are shown by downward arrows and increased levels by upward arrows. No changes are indicated by a horizontal dash. C represents the effect of age on control groups; Y represents the effect of TRF on young groups; O represents the effect of TRF on old groups. Adapted from the rat brain atlas [67].

5. In the young control group, cerebellum L-citrulline was positively correlated with the number of platform crossings during probe 2 ($r = 0.8909$, $p = 0.0172$; Figure 4(a)) indicating better memory. However, cerebellum glutamate ($r = -0.9328$, $p = 0.0066$; Figure 4(b)) and L-citrulline/L-arginine ($r = -0.9221$, $p = 0.0089$; Figure 4(c)) were negatively correlated with the percentage of cells used during the open field indicating decreased locomotor activity.

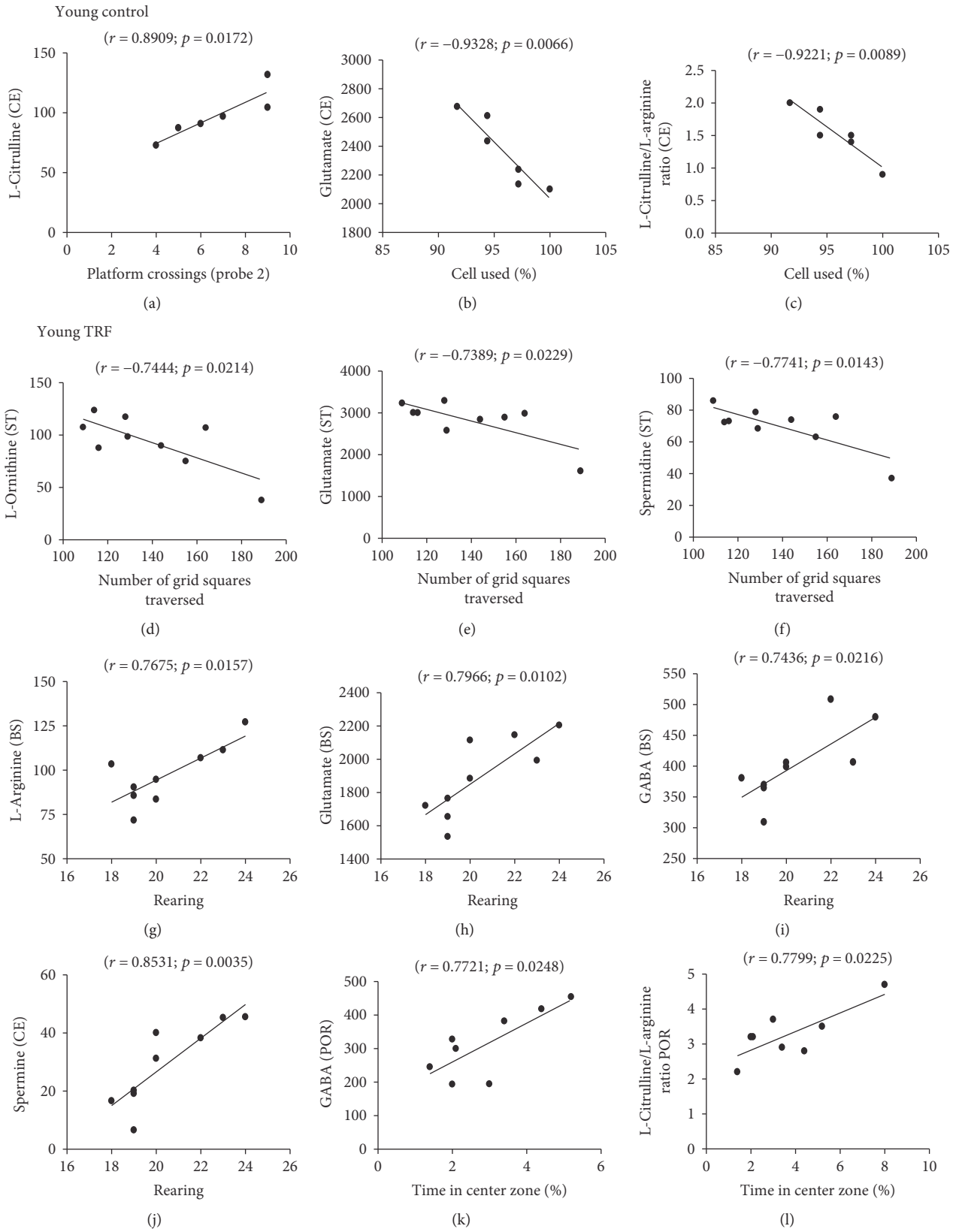

Figure 4: Scattergrams of the significant correlations between behavioral measures and neurochemical variables in the postrhinal cortex, entorhinal cortex, brain stem, striatum, and cerebellum in young rats.

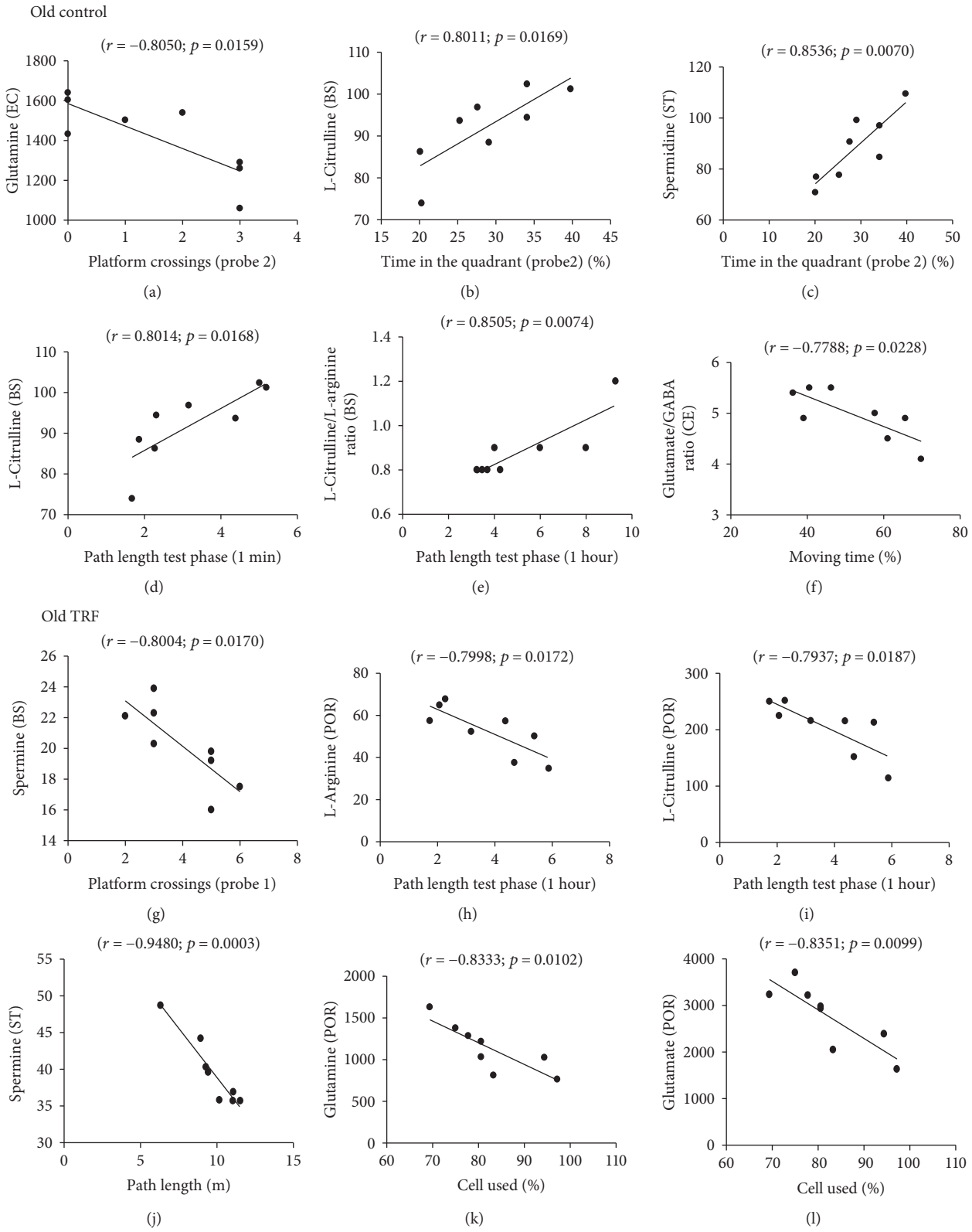

Figure 5: Scattergrams of the significant correlations between behavioral measures and neurochemical variables in the postrhinal cortex, entorhinal cortex, brain stem, striatum, and cerebellum in old rats.

In the TRF-supplemented young group, negative correlations were observed between striatum L-ornithine ($r = -0.7444$, $p = 0.0214$; Figure 4(d)), glutamate ($r = -0.7389$, $p = 0.0229$; Figure 4(e)), and spermidine ($r = -0.7741$, $p = 0.0143$; Figure 4(f)) and the number of grid squares traversed by the rats during the open field. However, positive

correlations were observed between brain stem L-arginine ($r = 0.7675$, $p = 0.0157$; Figure 4(g)), glutamate ($r = 0.7966$, $p = 0.0102$; Figure 4(h)), and GABA ($r = 0.7436$, $p = 0.0216$; Figure 4(i)) and cerebellum spermine ($r = 0.8531$, $p = 0.0035$, Figure 4(j)) and the number of rearing during the open field. Postrhinal cortex GABA ($r = 0.7721$, $p = 0.0248$; Figure 4(k)) and L-citrulline/L-arginine ($r = 0.7799$, $p = 0.0225$; Figure 4(l)) were positively correlated with the percentage of time the rats spent in the center zone during the open-field test.

In the old control group, entorhinal cortex glutamine ($r = -0.8050$, $p = 0.0159$; Figure 5(a)) was negatively correlated with the number of platform crossings during the water maze probe test. Brain stem L-citrulline ($r = 0.8011$, $p = 0.0169$; Figure 5(b)) and striatum spermidine ($r = 0.8536$; $p = 0.0070$; Figure 5(c)) were positively correlated with the percentage of time the rats spent in the target quadrant during the water maze probe test. Positive correlations were also observed between brain stem L-citrulline ($r = 0.8014$, $p = 0.0168$; Figure 5(d)) and L-citrulline/L-arginine ($r = 0.8505$, $p = 0.0074$; Figure 5(e)) and the mean path length used by the rats to reach the hidden platform during the working memory test. Cerebellum glutamate/GABA was negatively correlated with the percentage of time the rats moved during the open-field test ($r = -0.7788$, $p = 0.0228$; Figure 5(f)).

In the TRF-supplemented old group, negative correlations were observed between brain stem spermine ($r = -0.8004$, $p = 0.0170$; Figure 5(g)) and L-arginine ($r = -0.7998$, $p = 0.0172$; Figure 5(h)) and postrhinal cortex L-citrulline ($r = -0.7937$, $p = 0.0187$; Figure 5(i)) and the number of platform crossings during the probe test and the mean of path length used during the working memory test phase for 1 hour, respectively. Striatum spermine ($r = -0.9480$, $p = 0.0003$; Figure 5(j)) and glutamine ($r = -0.8333$, $p = 0.0102$; Figure 5(k)) and postrhinal cortex glutamate ($r = -0.8351$, $p = 0.0099$; Figure 5(l)) were negatively correlated with the mean of path length and the percentage of cell used, respectively. These results showed that changes in the amino acid and polyamine levels in the specific regions of the brain were associated with the rats' cognitive and locomotor functions.

4. Discussion

The present study investigated the effects of age and TRF supplementation on L-arginine and its metabolites in the postrhinal cortex, entorhinal cortex, brain stem, striatum, and cerebellum of young and old rats. The findings concurred with those of the previous reports that age-related changes in L-arginine metabolism in the brain are region specific [2, 3, 16]. Figure 3 shows that the postrhinal cortex, entorhinal cortex, and cerebellum were the regions most affected by age. The postrhinal cortex and entorhinal cortex play critical roles in memory processing. The postrhinal cortex is the area involved in spatial memory [41], while the entorhinal cortex receives spatial and nonspatial information from the postrhinal and perirhinal cortex, respectively [42]. The cerebellum is the area involved in motor control [43] as well as in emotion and cognition [44, 45]. Thus, alterations of the neurochemicals in these areas may affect memory processing, leading to cognitive impairment with age.

Age-related alterations in glutamine, L-citrulline, GABA, glutamate/GABA, and L-citrulline/L-arginine, as well as in levels of polyamines agmatine, putrescine, spermidine, and spermine were observed in the present study (Figure 3). Glutamine and L-citrulline increased with age in the postrhinal cortex and striatum while GABA decreased with age in the cerebellum. Glutamate/GABA increased with age in the entorhinal cortex, brain stem, and cerebellum. The L-citrulline/L-arginine ratio was increased in the striatum, postrhinal cortex, and entorhinal cortex.

Glutamine is the most abundant free amino acid in the human blood and regulates a variety of target genes involved in cell proliferation, differentiation, and survival [46]. Glutamine is produced by glutamine synthetase (GS), which catalyzes the formation of glutamine from glutamate and ammonia [47]. Thus, increased glutamine in aged rats may be a consequence of increased GS activity. Glutamine serves as a precursor for glutamate and hence is involved in energy production [48]. Changes in glutamine-glutamate cycle flux therefore could affect brain mitochondrial metabolism during aging [49].

In the present study, an age-related increase in L-citrulline was observed in the postrhinal cortex (Figure 1(c)) and striatum (Figure 1(c)), even though its precursors, L-arginine and L-ornithine, were largely unaffected. L-Citrulline is formed from L-ornithine by OTC as well as from L-arginine by NOS. Thus, alterations in L-citrulline level may reflect changes in the activities of NOS and/or OTC with age. Increased NOS activity with age had been reported in the postrhinal and entorhinal cortex [2, 3]. Conversion of L-citrulline to L-arginine by argininosuccinate synthase (ASS) and argininosuccinate lyase (ASL) [5] may explain why L-arginine is not affected by age. Increased L-citrulline without any changes in the L-arginine results in the increase in the L-citrulline/L-arginine observed. Increased glutamate/GABA in the entorhinal cortex, brain stem, and cerebellum (Figure 1(g)) may indicate changes in the glutamatergic and GABAergic systems which have been suggested to alter cognitive functions [50–52].

Polyamines are ubiquitous small molecules that play essential roles in learning and memory [53]. The effect of age on polyamines was also noted to be region specific (Figure 3). These changes may reflect the alterations of the activities of the enzymes involved in their synthesis. L-Arginine and L-ornithine are considered the main precursors of polyamines. Putrescine is converted to spermidine by spermidine synthase (SRM), which is then converted to spermine by spermine synthase (SMS). In this study, only agmatine was observed to decrease with age. Possible explanations may include the roles of agmatine as competitive inhibitors for NOS [54] and ODC [5, 55].

The present findings agreed with those of the earlier reports on the effect of age on amino acids [16, 56] and polyamines [16, 40]. However, there were some differences observed: glutamate and GABA in the brain stem [57] and L-arginine, L-ornithine, L-citrulline, glutamate, GABA,

putrescine, spermidine, spermine, and agmatine in the various parts of the brain [2, 3, 16]. Discrepancies in the findings on L-arginine and its metabolites in young and aged brains have also been reported previously. For example, decreased glutamate was reported in the rat entorhinal cortex [2, 3], the whole cerebral cortex [58–60], and the frontal region [61–63] while others reported increased levels [64]. Some authors have attributed these differences to differences in the animals' experience (with and without behavioral testing and treatment) [2, 3, 16].

Accumulation of polyamines can be toxic to the cells. Normally, cell protects itself against toxic accumulation of polyamines by synthesizing an antizyme, a regulatory protein that can inhibit ODC activity [65]. However, protein oxidation during aging could diminish the synthesis of an antizyme, leading to the accumulation of these polyamines to toxic level. A free radical scavenger such as vitamin E is suggested to prevent the degradation of an antizyme by quenching free radicals [66]. In the present study, TRF supplementation was observed to reduce some amino acids primarily in the entorhinal cortex and the cerebellum (Figure 3). However, TRF supplementation did not result in any changes in polyamines except for agmatine in the young rats suggesting that the neuroprotective effects of TRF could be mediated by the modulation of L-arginine metabolism rather than its antioxidant activity.

The present data shows that TRF supplementation in old rats reversed the age effect on glutamine, as well as on glutamate/GABA and L-citrulline/L-arginine in the entorhinal cortex. Glutamine is a precursor for an excitatory neurotransmitter, glutamate, while the entorhinal cortex plays a vital role in memory processing. Thus, the alteration of glutamine in the entorhinal cortex with TRF supplementation may possibly represent the involvement of TRF in modulating learning and memory. Apart from the entorhinal cortex, TRF also modulated L-ornithine and hence L-citrulline/L-arginine in the cerebellum. L-Ornithine is a precursor for putrescine and L-citrulline, catalyzed by ODC and OTC, respectively. Conversion of L-ornithine to L-glutamyl-c-semialdehyde can be further metabolized by P5C dehydrogenase for glutamate synthesis [5]. TRF modulation on L-ornithine in the cerebellum may affect cognition and locomotor activity in old rats. On the other hand, modulation of TRF on glutamate/GABA and L-citrulline/L-arginine suggested the involvement of TRF in maintaining brain glutamate, GABA, L-citrulline, and L-arginine balance.

Amino acids and polyamines were further correlated with behavioral variables observed with the same rats under the same experimental procedure, and the findings were published previously [25]. The behavioral studies were carried out using the open-field test and the Morris water maze test. The open-field tests were for the animals' locomotor activity while the Morris water maze tests for memory retention. Multiple regression analysis revealed a number of significant correlations between amino acid and polyamine levels and the rats' behavior in each group. In the young control group, higher L-citrulline in the cerebellum was correlated with better performance in the water maze (better memory). Lower glutamate and L-citrulline/L-arginine in the cerebellum were correlated with higher locomotor activity in the open field. It is interesting to note that only changes in the cerebellum amino acids influenced the cognitive behavior in the young group.

The data from this study indicate that with age, more neurochemicals from wider brain areas influenced behavior. In the old control group, poor memory was correlated with higher entorhinal cortex glutamate and glutamine; higher brain stem L-citrulline, glutamine, and L-citrulline/L-arginine; and lower brain stem L-citrulline and striatum spermidine. Higher cerebellum glutamate/GABA was correlated with the lower percentage of movement (lower locomotor activity) in the open-field test.

TRF supplementation in the young triggers the involvement of more neurochemicals from different areas of the brain to influence behavior, particularly the locomotor activity. Lower striatum L-ornithine, glutamate, and spermidine and higher brain stem L-arginine, glutamate, and GABA; cerebellum spermine; and postrhinal cortex GABA and L-citrulline/L-arginine were correlated with better performance in the open-field test (higher locomotor activity). However, TRF was able to influence both memory and locomotor activity in the old group. Lower brain stem spermine and higher postrhinal cortex L-arginine and L-citrulline were correlated with better performance in the water maze (better memory) while lower striatum spermine and postrhinal cortex glutamine and glutamate were correlated with better performance in the open-field test (higher locomotor activity). Hence, the data shows that neurotransmitters affect behavior and cognition and that this can be influenced by age and TRF supplementation.

5. Conclusion

In conclusion, the present study shows that age-related changes in L-arginine and its metabolites are region specific in the brain. TRF supplementation was able to reverse some of the age-related alterations in amino acids of the brain regions involved in both memory processing and motor control.

Abbreviations

TRF:	Tocotrienol-rich fraction
NOS:	Nitric oxide synthase
NOS:	Nitric oxide
ADC:	Arginine decarboxylase
GABA:	Gamma-aminobutyric acid
GAD:	Glutamate decarboxylase
MCI:	Mild cognitive impairment
AD:	Alzheimer's disease
HPLC:	High-performance liquid chromatography
LC/MS/MS:	Liquid chromatography tandem mass spectrometry
ESI:	Electrospray interface
GS:	Glutamine synthetase
ASS:	Argininosuccinate synthase
ASL:	Argininosuccinate lyase
SRM:	Spermidine synthase

SMS: Spermine synthase
ODC: Ornithine decarboxylase
OTC: Ornithine transcarbamylase.

Conflicts of Interest

The authors declare that they have no conflicts of interest.

Authors' Contributions

Musalmah Mazlan, Hamizah Shahirah Hamezah, Hanafi Ahmad Damanhuri, and Wan Zurinah Wan Ngah were responsible for the study design. Hamizah Shahirah Hamezah, Ping Liu, and Nursiati Mohd Taridi were responsible for the sample preparation. Hamizah Shahirah Hamezah and Yu Jing were responsible for HPLC and LC/MS/MS. Hamizah Shahirah Hamezah was responsible for the data analysis and statistics. Hamizah Shahirah Hamezah, Ping Liu, Hu Zhang, and Yu Jing were responsible for the data interpretation. Nursiati Mohd Taridi was responsible for the animal supplementation. Hamizah Shahirah Hamezah, Musalmah Mazlan, Hanafi Ahmad Damanhuri, Wan Zurinah Wan Ngah, Ping Liu, and Hu Zhang were responsible for manuscript writing and editing. Hamizah Shahirah Hamezah and Musalmah Mazlan contributed equally to this work. All authors read and approved the final manuscript.

Acknowledgments

This research was supported by Research University Grant (UKM-AP-2011-29 and GUP-2015-045) from Universiti Kebangsaan Malaysia and Long-Term Research Grant Scheme (LRGS/BU/2012/UKM-UKM/K/04) from the Ministry of Higher Education, Malaysia, and the School of Pharmacy and Department of Anatomy, University of Otago, New Zealand. The authors would like to thank all the staff at the School of Pharmacy and Department of Anatomy, University of Otago, for the chemicals, facilities, and equipment as well as for the helpful assistance.

References

[1] B. A. Yankner, T. Lu, and P. Loerch, "The aging brain," *Annual Review of Pathology: Mechanisms of Disease*, vol. 3, pp. 41–66, 2008.

[2] N. Gupta, Y. Jing, N. D. Collie, H. Zhang, and P. Liu, "Ageing alters behavioural function and brain arginine metabolism in male Sprague-Dawley rats," *Neuroscience*, vol. 226, pp. 178–196, 2012.

[3] P. Liu, Y. Jing, and H. Zhang, "Age-related changes in arginine and its metabolites in memory-associated brain structures," *Neuroscience*, vol. 164, no. 2, pp. 611–628, 2009.

[4] P. Liu, M. S. Fleete, Y. Jing et al., "Altered arginine metabolism in Alzheimer's disease brains," *Neurobiology of Aging*, vol. 35, no. 9, pp. 1992–2003, 2014.

[5] G. Wu and S. M. Morris, "Arginine metabolism: nitric oxide and beyond," *Biochemical Journal*, vol. 336, Part 1, pp. 1–17, 1998.

[6] V. Calabrese, D. Boyd-Kimball, G. Scapagnini, and D. A. Butterfield, "Nitric oxide and cellular stress response in brain aging and neurodegenerative disorders: the role of vitagenes," *In Vivo*, vol. 18, no. 3, pp. 245–267, 2004.

[7] H. Wiesinger, "Arginine metabolism and the synthesis of nitric oxide in the nervous system," *Progress in Neurobiology*, vol. 64, no. 4, pp. 365–391, 2001.

[8] H. M. Wallace, A. V. Fraser, and A. Hughes, "A perspective of polyamine metabolism," *Biochemical Journal*, vol. 376, no. 1, pp. 1–14, 2003.

[9] J. Malaterre, C. Strambi, A. Aouane, A. Strambi, G. Rougon, and M. Cayre, "A novel role for polyamines in adult neurogenesis in rodent brain," *European Journal of Neuroscience*, vol. 20, no. 2, pp. 317–330, 2004.

[10] L. G. Kaiser, N. Schuff, N. Cashdollar, and M. W. Weiner, "Age-related glutamate and glutamine concentration changes in normal human brain: ^{1}H MR spectroscopy study at 4 T," *Neurobiology of Aging*, vol. 26, no. 5, pp. 665–672, 2005.

[11] B. Leitch, O. Shevtsova, K. Reusch, D. H. Bergin, and P. Liu, "Spatial learning-induced increase in agmatine levels at hippocampal CA1 synapses," *Synapse*, vol. 65, no. 2, pp. 146–153, 2011.

[12] P. Liu, N. D. Collie, S. Chary, Y. Jing, and H. Zhang, "Spatial learning results in elevated agmatine levels in the rat brain," *Hippocampus*, vol. 18, no. 11, pp. 1094–1098, 2008.

[13] B. E. McKay, W. E. Lado, L. J. Martin, M. A. Galic, and N. M. Fournier, "Learning and memory in agmatine-treated rats," *Pharmacology Biochemistry and Behavior*, vol. 72, pp. 551–557, 2002.

[14] A. Halaris and J. Piletz, "Agmatine: metabolic pathway and spectrum of activity in brain," *CNS Drugs*, vol. 21, no. 11, pp. 885–900, 2007.

[15] J. C. Cassel, T. Schweizer, A. Lazaris et al., "Cognitive deficits in aged rats correlate with levels of L-arginine, not with nNOS expression or 3,4-DAP-evoked transmitter release in the frontoparietal cortex," *European Neuropsychopharmacology*, vol. 15, no. 2, pp. 163–175, 2005.

[16] M. Rushaidhi, Y. Jing, J. Kennard et al., "Aging affects L-arginine and its metabolites in memory-associated brain structures at the tissue and synaptoneurosome levels," *Neuroscience*, vol. 209, pp. 21–31, 2012.

[17] F. E. Harrison, G. L. Bowman, and M. C. Polidori, "Ascorbic acid and the brain: rationale for the use against cognitive decline," *Nutrients*, vol. 6, no. 4, pp. 1752–1781, 2014.

[18] J. A. Joseph, B. Shukitt-Hale, N. A. Denisova et al., "Reversals of age-related declines in neuronal signal transduction, cognitive, and motor behavioral deficits with blueberry, spinach, or strawberry dietary supplementation," *The Journal of Neuroscience*, vol. 19, no. 18, pp. 8114–8121, 1999.

[19] Z. Jovanoviv, "Antioxidative Defense Mechanisms in the Aging Brain," *Archives of Biological Sciences*, vol. 66, no. 1, pp. 245–252, 2014.

[20] L. M. Willis, B. Shukitt-Hale, and J. A. Joseph, "Modulation of cognition and behavior in aged animals: role for antioxidant- and essential fatty acid-rich plant foods," *The American Journal of Clinical Nutrition*, vol. 89, no. 5, pp. 1602–1606, 2009.

[21] M. W. Dysken, M. Sano, S. Asthana et al., "Effect of vitamin E and memantine on functional decline in Alzheimer disease: the team-AD VA cooperative randomized trial," *Journal of the American Medical Association*, vol. 311, no. 1, pp. 33–44, 2014.

[22] M. C. Morris, D. A. Evans, J. L. Bienias, C. C. Tangney, and R. S. Wilson, "Vitamin E and cognitive decline in older persons," *Archives of Neurology*, vol. 59, pp. 1125–1132, 2002.

[23] M. C. Morris, D. A. Evans, C. C. Tangney et al., "Relation of the tocopherol forms to incident Alzheimer disease and to cognitive change," *The American Journal of Clinical Nutrition*, vol. 81, no. 2, pp. 508–514, 2005.

[24] F. Mangialasche, W. Xu, M. Kivipelto et al., "Tocopherols and tocotrienols plasma levels are associated with cognitive impairment," *Neurobiology of Aging*, vol. 33, pp. 2282–2290, 2012.

[25] N. M. Taridi, N. Ab Rani, A. A. Abdul Latiff, W. Z. Wan Ngah, and M. Mazlan, "Tocotrienol rich fraction reverses age-related deficits in spatial learning and memory in aged rats," *Lipids*, vol. 49, pp. 855–869, 2014.

[26] F. Mangialasche, A. Solomon, I. Kareholt et al., "Serum levels of vitamin E forms and risk of cognitive impairment in a Finnish cohort of older adults," *Experimental Gerontology*, vol. 48, no. 12, pp. 1428–1435, 2013.

[27] M. Mazlan, S. M. Then, and W. Z. Wan Ngah, "Comparative effects of α-tocopherol and γ-tocotrienol against hydrogen peroxide induced apoptosis on primary-cultured astrocytes," *Journal of the Neurological Sciences*, vol. 243, pp. 5–12, 2006.

[28] C. K. Sen, S. Khanna, S. Roy, and L. Packer, "Molecular basis of vitamin E action: tocotrienol potently inhibits glutamate-induced pp60c-Src kinase activation and death of HT4 neuronal cells," *Journal of Biological Chemistry*, vol. 275, pp. 13049–13055, 2000.

[29] S. M. Then, W. Z. Wan Ngah, G. Mat Top, and M. Mazlan, "Comparison of the effects of α-tocopherol and γ-tocotrienol against oxidative stress in two different neuronal cultures," *Sains Malaysiana*, vol. 39, pp. 145–156, 2010.

[30] S. Khanna, S. Roy, H. Ryu et al., "Molecular basis of vitamin E action: tocotrienol modulates 12-lipoxygenase, a key mediator of glutamate-induced neurodegeneration," *Journal of Biological Chemistry*, vol. 278, no. 44, pp. 43508–43515, 2003.

[31] S. Khanna, N. L. Parinandi, S. R. Kotha et al., "Nanomolar vitamin E α-tocotrienol inhibits glutamate-induced activation of phospholipase A2 and causes neuroprotection," *Journal of Neurochemistry*, vol. 112, no. 5, pp. 1249–1260, 2010.

[32] C. Rink, S. Khanna, and C. K. Sen, "Arachidonic acid metabolism and lipid peroxidation in stroke: alpha-tocotrienol as a unique therapeutic agent," in *Studies on Experimental Models*, S. Basu and L. Wiklund, Eds., Humana Press, New York, USA, 2011.

[33] N. Y. Jung, K. H. Lee, R. Won, and B. H. Lee, "Neuroprotective effects of α-tocotrienol on kainic acid-induced neurotoxicity in organotypic hippocampal slice cultures," *International Journal of Molecular Sciences*, vol. 14, no. 9, pp. 18256–18268, 2013.

[34] S. Khanna, S. Roy, N. L. Parinandi, M. Maurer, and C. K. Sen, "Characterization of the potent neuroprotective properties of the natural vitamin E α-tocotrienol," *Journal of Neurochemistry*, vol. 98, no. 5, pp. 1474–1486, 2006.

[35] A. Navarro and A. Boveris, "Brain mitochondrial dysfunction in aging, neurodegeneration, and Parkinson's disease," *Frontiers in Aging Neuroscience*, vol. 2, no. 34, pp. 1–11, 2010.

[36] R. D. Burwell, M. P. Witter, and D. J. Amaral, "Perirhinal and postrhinal cortices of the rats: a review of the neuroanatomical literature and comparison with findings from the monkey brain," *Hippocampus*, vol. 5, pp. 390–408, 1995.

[37] R. D. Burwell, "Borders and cytoarchitecture of the perirhinal and postrhinal cortices in the rat," *The Journal of Comparative Neurology*, vol. 437, pp. 17–41, 2001.

[38] G. Paxinos and C. Watson, *The Rat Brain in Stereotaxic Coordinates*, Academic Press, San Diego, CA, 4th edition, 1998.

[39] P. Liu, P. F. Smith, I. Appleton, C. L. Darlington, and D. K. Bilkey, "Nitric oxide synthase and arginase in the rat hippocampus and the entorhinal, perirhinal, postrhinal, and temporal cortices: regional variations and age-related changes," *Hippocampus*, vol. 13, pp. 859–867, 2003.

[40] P. Liu, N. Gupta, Y. Jing, and H. Zhang, "Age-related changes in polyamines in memory-associated brain structures in rats," *Neuroscience*, vol. 155, pp. 789–796, 2008.

[41] K. L. Agster and R. D. Burwell, "Cortical efferents of the perirhinal, postrhinal, and entorhinal cortices of the rat," *Hippocampus*, vol. 19, no. 12, pp. 1159–1186, 2009.

[42] L. R. Squire, C. E. Stark, and R. E. Clark, "The medial temporal lobe," *Annual Review of Neuroscience*, vol. 27, pp. 279–306, 2004.

[43] I. Augustin, S. Korte, M. Rickmann et al., "The cerebellum-specific Munc13 isoform Munc13-3 regulates cerebellar synaptic transmission and motor learning in mice," *The Journal of Neuroscience*, vol. 21, pp. 10–17, 2001.

[44] J. D. Schmahmann and D. Caplan, "Cognition, emotion and the cerebellum," *Brain*, vol. 6129, pp. 290–292, 2006.

[45] D. J. Schutter and J. van Honk, "The cerebellum on the rise in human emotion," *Cerebellum*, vol. 4, pp. 290–294, 2005.

[46] C. Brasse-Lagnel, A. Lavoinne, and A. Husson, "Control of mammalian gene expression by amino acids, especially glutamine," *FEBS Journal*, vol. 276, pp. 1826–1844, 2009.

[47] J. Albrecht, U. Sonnewald, H. S. Waagepetersen, and A. Schousboe, "Glutamine in the central nervous system: function and dysfunction," *Frontiers in Bioscience*, vol. 12, pp. 332–343, 2007.

[48] E. Kvamme, B. Roberg, and I. A. Torgner, "Glutamine transport in brain mitochondria," *Neurochemistry International*, vol. 37, no. 2-3, pp. 131–138, 2000.

[49] F. Boumezbeur, G. F. Mason, R. A. de Graaf et al., "Altered brain mitochondrial metabolism in healthy aging as assessed by in vivo magnetic resonance spectroscopy," *Journal of Cerebral Blood Flow and Metabolism*, vol. 30, no. 1, pp. 211–221, 2009.

[50] J. Hardy, R. Adolfsson, and I. Alafuzoff, "Transmitter deficits in Alzheimer's disease," *Neurochemistry International*, vol. 7, pp. 545–563, 1985.

[51] S. L. Lowe, P. T. Francis, and A. W. Procter, "Gamma-aminobutyric acid concentration in brain tissue at two stages of Alzheimer's disease," *Brain*, vol. 111, pp. 785–799, 1988.

[52] K. J. Reinikainen, L. Paljarvi, and M. Huuskonen, "A post-mortem study of noradrenergic, serotonergic and GABAergic neurons in Alzheimer's disease," *Journal of the Neurological Sciences*, vol. 84, pp. 101–116, 1988.

[53] K. Williams, "Interactions of polyamines with ion channels," *Biochemical Journal*, vol. 325, no. 2, pp. 289–297, 1997.

[54] E. Galea, S. Regunathan, V. Eliopoulos, D. L. Feinstein, and D. J. Reis, "Inhibition of mammalian nitric oxide synthases by agmatine, an endogenous polyamine formed by decarboxylation of arginine," *Biochemical Journal*, vol. 316, pp. 247–249, 1996.

[55] J. Satriano, S. Matsufuji, Y. Murakami et al., "Agmatine suppresses proliferation by frameshift induction of antizyme and

attenuation of cellular polyamine levels," *Journal of Biological Chemistry*, vol. 273, no. 25, pp. 15313–15316, 1998.

[56] P. Liu, H. Zhang, R. Devaraj, G. S. Ganesalingam, and P. F. Smith, "A multivariate analysis of the effects of aging on glutamate, GABA and arginine metabolites in the rat vestibular nucleus," *Hearing Research*, vol. 269, no. 1-2, pp. 122–133, 2010.

[57] Y. Jing, M. S. Fleete, N. D. Collie, H. Zhang, and P. Liu, "Regional variations and age-related changes in arginine metabolism in the rat brain stem and spinal cord," *Neuroscience*, vol. 252, pp. 98–108, 2013.

[58] P. Saransaari and S. S. Oja, "Age-related changes in the uptake and release of glutamate and aspartate in the mouse brain," *Mechanisms of Ageing and Development*, vol. 81, pp. 61–71, 1995.

[59] M. Strolin-Benedetti, M. Cini, R. Fusi, P. Marrari, and P. Dostert, "The effects of aging on MAO activity and amino acid levels in rat brain," *Journal of Neural Transmission*, vol. 29, pp. 259–268, 1990.

[60] M. Strolin-Benedetti, A. Ruso, P. Marrari, and P. Dostert, "Effects of aging on the content in sulfur-containing amino acids in rat brain," *Journal of Neural Transmission*, vol. 86, pp. 191–203, 1991.

[61] R. Dawson, D. R. Wallace, and M. J. Meldrum, "Endogenous glutamate release from frontal cortex of adult and aged rats," *Neurobiology of Aging*, vol. 10, pp. 665–668, 1989.

[62] F. Fornieles, J. M. Peinado, and F. Mora, "Endogenous levels of amino acid neurotransmitters in different regions of frontal and temporal cortex of the rat during the normal process of aging," *Neuroscience Letters*, vol. 26, p. 150, 1986.

[63] D. R. Wallace and R. Dawson, "Effect of age and monosodium-L-glutamate (MSG) treatment on neurotransmitter content in brain regions from male Fischer-344 rats," *Neurochemical Research*, vol. 5, pp. 889–898, 1990.

[64] M. Messripour and A. Mesripour, "Effects of vitamin B6 on age associated changes of rat brain glutamate decarboxylase activity," *African Journal of Pharmacy and Pharmacology*, vol. 5, pp. 454–456, 2011.

[65] S. Hayashi and Y. Murakami, "Rapid and regulated degradation of ornithine decarboxylase," *Biochemical Journal*, vol. 306, no. 1, pp. 1–10, 1995.

[66] S. M. Yatin, M. Yatin, T. Aulick, K. B. Ain, and D. A. Butterfield, "Alzheimer's amyloid β-peptide associated free radicals increase rat embryonic neuronal polyamine uptake and ornithine decarboxylase activity: protective effect of vitamin E," *Neuroscience Letters*, vol. 263, no. 1, pp. 17–20, 1999.

[67] G. Paxinos and C. Watson, *The Rat Brain in Stereotaxic Coordinates*, Academic Press, San Diego, CA, 7th edition, 2014.

Hindawi
Oxidative Medicine and Cellular Longevity
Volume 2017, Article ID 7205082, 8 pages
https://doi.org/10.1155/2017/7205082

Research Article

Edible Bird's Nest Prevents Menopause-Related Memory and Cognitive Decline in Rats via Increased Hippocampal Sirtuin-1 Expression

Zhiping Hou,[1,2] Peiyuan He,[3] Mustapha Umar Imam,[2,4] Jiemen Qi,[1] Shiying Tang,[1] Chengjun Song,[1] and Maznah Ismail[2]

[1]*Department of Pathology, Chengde Medical University, Chengde, Hebei 067000, China*
[2]*Laboratory of Molecular Biomedicine, Institute of Bioscience, Universiti Putra Malaysia, 43400 Serdang, Selangor, Malaysia*
[3]*Gastroenterology Department, Affiliated Hospital of Chengde Medical University, Chengde, Hebei, China*
[4]*Precision Nutrition Innovation Center, School of Public Health, Zhengzhou University, Zhengzhou 450001, China*

Correspondence should be addressed to Zhiping Hou; zhipinghou@163.com and Mustapha Umar Imam; mustyimam@gmail.com

Received 26 June 2017; Accepted 9 August 2017; Published 20 September 2017

Academic Editor: Anna M. Giudetti

Menopause causes cognitive and memory dysfunction due to impaired neuronal plasticity in the hippocampus. Sirtuin-1 (SIRT1) downregulation in the hippocampus is implicated in the underlying molecular mechanism. Edible bird's nest (EBN) is traditionally used to improve general wellbeing, and in this study, we evaluated its effects on SIRT1 expression in the hippocampus and implications on ovariectomy-induced memory and cognitive decline in rats. Ovariectomized female Sprague-Dawley rats were fed with normal pellet alone or normal pellet + EBN (6, 3, or 1.5%), compared with estrogen therapy (0.2 mg/kg/day). After 12 weeks of intervention, Morris water maze (four-day trial and one probe trial) was conducted, and serum estrogen levels, toxicity markers (alanine transaminase, alkaline phosphatase, urea, and creatinine), and hippocampal SIRT1 immunohistochemistry were estimated after sacrifice. The results indicated that EBN and estrogen enhanced spatial learning and memory and increased serum estrogen and hippocampal SIRT1 expression. In addition, the EBN groups did not show as much toxicity to the liver as the estrogen group. The data suggested that EBN treatment for 12 weeks could improve cognition and memory in ovariectomized female rats and may be an effective alternative to estrogen therapy for menopause-induced aging-related memory loss.

1. Introduction

Estrogen regulates the development and functioning of the central nervous system [1, 2]. Decreased serum estrogen levels after menopause or ovariectomy have been shown to promote inflammatory pathology involving oxidative stress [3] and can be a risk factor for neurodegenerative diseases such as Alzheimer's disease. Recent studies have suggested the preventive effects of hormone replacement therapy (HRT) or phytoestrogen supplementation therapy on oxidative stress-mediated neurodegenerative disorders [4]. However, it has been demonstrated that HRT in postmenopausal women can lead to the development of breast, ovarian, and endometrial cancers [5–7]. Thus, an alternative phytoestrogen treatment might be of benefit compared with conventional HRT that has adverse effects.

Sirtuin-1 (SIRT1) is a member of the sirtuin family, which is known to regulate intracellular regulatory proteins with mono-ADP-ribosyl transferase activity. SIRT1 is reported to improve insulin sensitivity and affect the essential metabolic regulatory transcription factors including those of the PGC1-alpha/ERR-alpha complex [8]. Similarly, SIRT1 was demonstrated to regulate energy metabolism, stress resistance, neurodegeneration, and senescence [9–11].

Edible bird's nest (EBN) originates from the saliva of swiftlet species; they mostly come from *Collocalia fuciphaga*, *Aerodramus fuciphagus*, and *Aerodramus maximus* species, commonly found in Southeast Asia [12, 13]. EBN has been

considered a precious food tonic by Chinese people ever since the Tang dynasty (618 AD) [14], and its usage in present times is principally based on historical and observational results of its beneficial effects including antiaging and immune-enhancing properties [15]. More recent scientific evidence suggests that EBN is both nutritionally and functionally rich [16–18]. Its components include lactoferrin, sialic acid, ovotransferrin, minerals, and amino acids including essential amino acids, such as lysine, tyrosine, and serine [16, 17, 19]. There is some evidence to support its anti-inflammatory, antioxidant, and insulin-sensitizing effects [19–22]. It could also improve and attenuate age-related neurodegenerative changes [23]. However, there is no evidence suggesting that EBN could improve memory and cognition as part of its overall anti-aging properties despite its long history of medicinal use.

Thus, the present study was designed to investigate the effects of EBN on ovariectomy-induced cognitive dysfunction, especially in relation to changes in SIRT1 function.

2. Materials and Methods

2.1. Animal Treatment and Operation Procedure. Forty-two Sprague-Dawley rats (3 months old, female, 180–200 g) were housed under controlled conditions (12 h light/12 h dark cycle, 20–22°C, 40–50% humidity) with access to water and food ad libitum for two weeks prior to the experiments for acclimatization to the new environment. The use of animals was approved by the Animal Care and Use Committee (ACUC) of the Faculty of Medicine and Health Sciences, Universiti Putra Malaysia (Project approval number: UPM/IACUC/AUP-R012/2014), and animals were handled as stipulated by the guidelines for the use of animals. All ovariectomy (OVX) procedures were done as previously described [24] and were conducted under anesthesia with an injection of 10 mg/60 mg/kg xylazine/ketamine (i.p.). Briefly, bilateral OVX was performed from a dorsal approach after shaving the fur on both sides of the body, after which, the ovaries and the surrounding tissue were removed; the incisal opening was closed by stapling the muscles and suturing the skin [24]. The control group was not operated on, while the sham group underwent a sham surgery, in which, only skin and muscles were cut but the ovaries were spared. After OVX, the rats were maintained for one week and randomly assigned to seven groups ($n = 6$): OVX group, ovariectomized and received daily standard rat chow; OVX + estrogen group, ovariectomized and received 0.2 mg/kg body weight/day of estrogen orally in addition to standard rat chow; and OVX + EBN high dose, OVX + EBN medium dose, and OVX + EBN low dose groups, ovariectomized and received 1.2, 0.6, and 0.3 g/kg body weight/day of EBN, respectively, in addition to standard rat chow. Treatments lasted for 12 weeks, during which, food intake was measured daily and weight was measured weekly.

2.2. Morris Water Maze (MWM) Behavioral Test. The MWM apparatus consisted of a black circular plastic pool that measured 170 cm in diameter and 60 cm in height and a cylindrical dark colored platform with a diameter of 10 cm. It was placed in a light-controlled room, and curtains with three black distal cues were mounted around the maze. The water temperature in the pool was maintained at 22 ± 1°C, and recording was done using the ANY-maze Video Tracking System (Stoelting, Wood Dale, IL, USA), connected to a CCD camera and used to assess performance and reference memory in the water maze task. The platform was placed in the middle of the target quadrant and submerged 2 cm below water's surface and kept at the same position throughout the experiment.

The spatial acquisition phase consisted of four training days and four training trials per day per rat. The start position used distal locations for which the hidden platform is located in the northwest quadrant during the acquisition phase. The sequences of starts were designed such that the platform was to the right or left of an animal during an equal number of trials, and one trial was performed from each of the four start positions each day. Rats were released facing the pool wall at water level from the desired start position (E, S, SW, and NE tactic) and allowed to search for the platform for 60 s. If rats did not find the platform within the limited time, animals were guided to the platform and left there for 15 s. The rats were then placed in the maze after a short rest at a new start location, and the latter three trials were repeated. This was done for a total of four days. The spatial memory was evaluated by the latency (time from start to platform) and path length.

Reference memory (probe trial) version was done on the fifth day without a platform, allowing each rat to swim freely for 30 s. The rats were placed at the southeast position (opposite the target quadrant in the spatial acquisition phase). The reference memory was evaluated by the time the rat stayed in the target quadrant.

2.3. Preparation of Tissue Samples. At the end of the experiment, all animals were decapitated and exsanguinated after anesthesia with an injection of 10 mg/60 mg/kg xylazine/ketamine (i.p.). The hippocampus was removed from the brain and quickly kept in the RCL2 reagent (Alpjelys, Toulouse, France) for further analysis of molecular markers.

2.4. Serum Biochemical Analysis

2.4.1. EBN Toxicity. Blood collected after sacrifice was centrifuged at 3000 *g* for 15 mins at 4°C. The supernatant was collected and stored at −80°C. Liver enzymes (ALT, ALP, and GGT) and kidney function markers (urea and creatinine) were determined on the Dimension Xpand Plus Integrated Chemistry System (Siemens, Germany) with commercially available kits (Randox Laboratories Ltd., Antrim, UK).

2.4.2. Serum Estrogen Detection. Serum estrogen levels were determined by the commercial ELISA kit (Cusabio, Wuhan, China) in accordance with the manufacturer's instruction.

2.5. Sirtuin-1 Immunohistochemistry. For SIRT1 immunohistochemistry, paraffin sections (3 μm) were placed in an oven at 60°C for 30 min. The sections were then deparaffinized and rehydrated by xylene twice and gradient ethanol from pure to 70%. Heat-induced retrieval of antigen was done by 10 mM

Table 1: Body weights and serum estrogen levels of ovariectomized rats after 12 weeks.

	Body weight (g) before treatment	Body weight (g) end point	Total weight gain (g)	Total food intake (g)	Serum estrogen (pg/ml)
Control	221.5 ± 33.5	227.5 ± 6.0	6.0	1109.3 ± 40.6	151.1 ± 8
Sham	217.8 ± 44.0	224.6 ± 6.8	6.8	1065.4 ± 23.8	156.7 ± 13
OVX	230 ± 29.7	283.1 ± 23.1[b]	53.1[b]	1276.2 ± 56.9[b]	35.6 ± 0.9[b]
Estrogen	236 ± 33.3	239 ± 3.0[a]	3.0[a]	976.8 ± 47.5[a,b]	169.8 ± 11.4[a]
EBN (high)	213.1 ± 41.8	214.5 ± 1.4[a]	1.4[a]	1023.5 ± 23.3[a]	150.4 ± 7.4[a]
EBN (middle)	228.1 ± 53.9	242.8 ± 14.6[a]	14.6[a]	1088.6 ± 40.4[a]	147.8 ± 8.7[a]
EBN (low)	216 ± 31.5	242.6 ± 26.7	26.7[a]	1111.5 ± 37.6[a]	143.3 ± 13.4[a]

Control: standard rat chow; sham: surgically opened but not ovariectomized and fed with standard rat chow; OVX: ovariectomized with semipurified pellet; estrogen: ovariectomized and fed with standard rat chow and 0.2 mg/kg body weight of estrogen; EBN high, medium, and low: ovariectomized and fed with standard rat chow and 1.2, 0.6, and 0.3 g/kg body weight of edible bird's nest/day, respectively. Values are mean ± SD, $n = 5 - 6$. [a]Mean value was significantly different from that of the OVX group ($P < 0.05$); [b]mean value was significantly different from that of the sham group ($P < 0.05$).

sodium citrate (pH 6.0), 3% hydrogen peroxide for 10 mins to suppress the endogenous peroxidase activity, and 1% bovine serum albumin (all from Sigma, St. Louis, MO, USA) for 15 mins to block nonspecific binding. After this, the sections were incubated in rabbit polyclonal anti-SIRT1 (Abnova-PAB0004, Abnova Corporation, Taipei, Taiwan) antiserum at a dilution of 1 : 225 overnight at 4°C. After washing in TBS-T, the sections were incubated with a HRP-conjugated secondary antibody (1 : 400) at room temperature for 1 hr, followed by the DAB staining for 10 min at room temperature. Water was then used to rinse for 5 min followed by counterstaining with hematoxylin. Finally, the sections were dehydrated and mounted to evaluate SIRT1 immunohistochemistry in the hippocampus. All the sections were captured by the confocal laser scanning microscope (LSM 5 Pa) equipped with the acquisition software ZEN 2007 (both from Carl Zeiss MicroImaging GmbH, Jena, Germany). Hippocampal neurons with 10 random circles in each image were recorded, and their densitometric readings were combined together and averaged to get the total optical density (TOD) [25]. In order to avoid bias, the background staining (BOD) of each image was measured as TOD. The expected OD of each image was the gap between TOD and BOD. For the minus control of immunohistochemistry, PBS instead of primary antibody was used (data not shown).

2.6. Statistics. All statistical analyses were done using SPSS software (version 20.0). The parameters that were evaluated in the MWM special acquisition and reference memory were analyzed by repeated measure analysis of variance and one-way or two-way ANOVA, respectively. Statistical data were expressed as means ± SEM. The criteria for statistical significance was defined as $P < 0.05$.

3. Results

3.1. Food Intake, Body Weight, and Estrogen Levels. Body weights were similar at the beginning of the experiment, but at the end of the intervention, the OVX group had significantly higher body weight than the sham group (Table 1). After 12 weeks of EBN supplementation, the OVX + EBN groups had significantly lower body weights in comparison with the OVX group. Similarly, after 12 weeks of treatment, the OVX group had higher food intake compared to the sham group, while the group with EBN and estrogen supplementation significantly had reduced food intake compared to the OVX group. Specifically, the OVX + EBN high-dose group had similar food intake to the OVX + estrogen group. Serum estradiol levels were found to be significantly lower in the OVX group and higher in the EBN groups compared with the sham group. The reduced serum estradiol levels and increased food intake and weight gain in the OVX group suggested that the OVX model was successful, since EBN could regulate food intake, weight gain, and estrogen levels especially at higher doses.

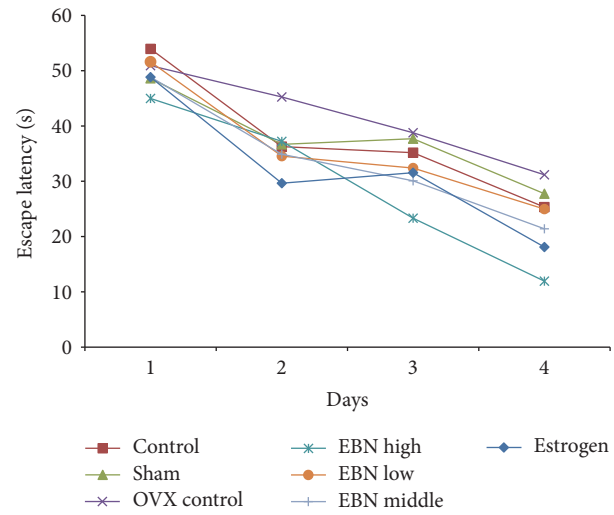

Figure 1: Effect of EBN on MWM performance in the spatial memory acquisition phase. All values are expressed as mean ± SEM for 6 animals in each group. Sham: surgically opened but not ovariectomized and fed with standard rat chow for 12 weeks. OVX: ovariectomized and fed with standard rat chow for 12 weeks; estrogen: ovariectomized and fed with standard rat chow and 0.2 mg/kg body weight of estrogen for 12 weeks; EBN high, medium, and low: ovariectomized and fed with standard rat chow and 1.2, 0.6, and 0.3 g/kg body weight of EBN/day, respectively, for 12 weeks.

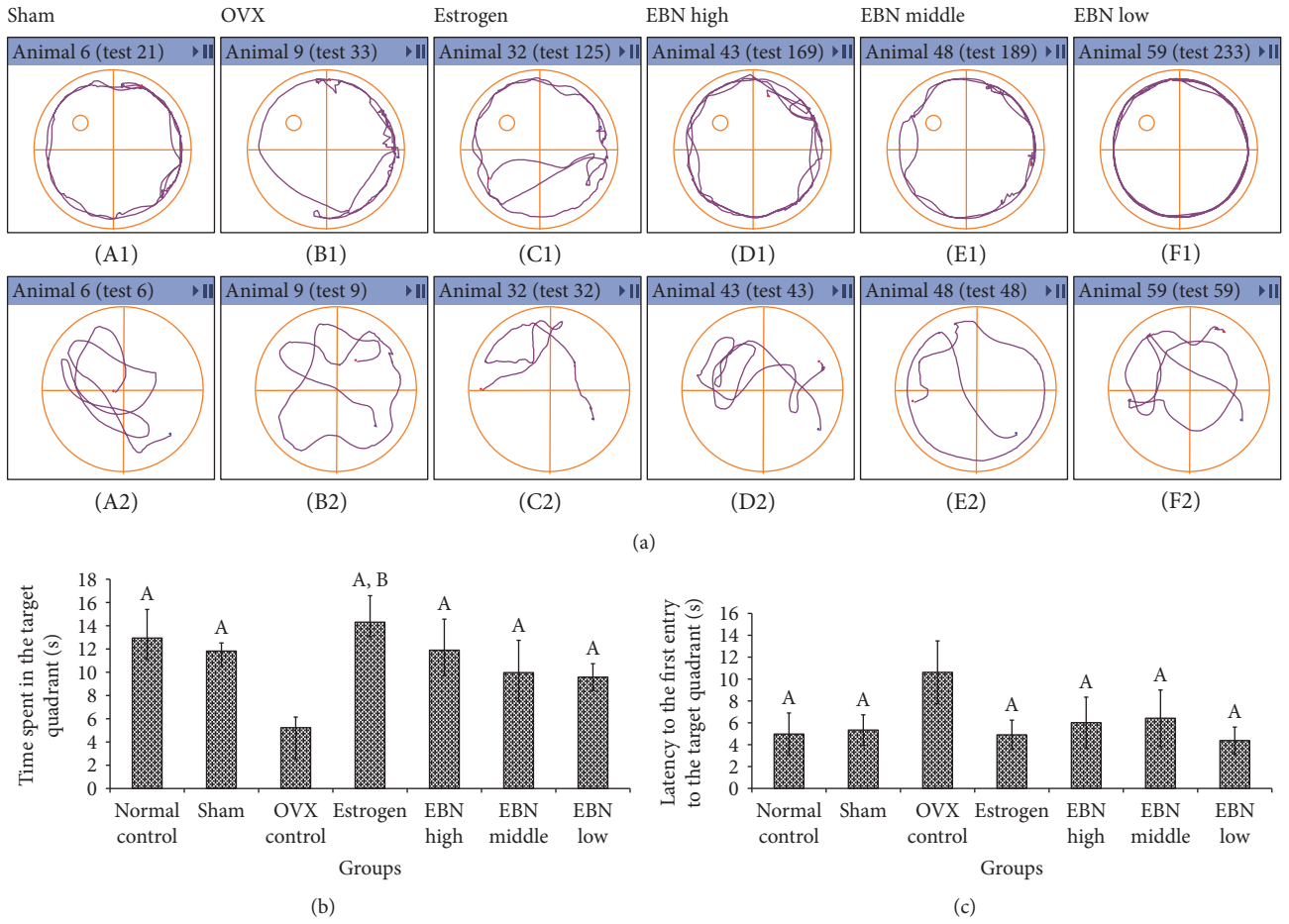

Figure 2: (a) Representative path tracings of the Morris water maze. A: sham group (A1, first day first trial; A2, probe trial); B: OVX group (B1, first day first trial; B2, probe trial); C: estrogen group (C1, first day first trial; C2, probe trial); D: EBNH group (D1, first day first trial; D2, probe trial); E: EBNM group (E1, first day first trial; E2, probe trial); F: EBNL group (F1, first day first trial; F2, probe trial). (b) Time in the target quadrant in the probe trial; (c) latency to the first entry to the target quadrant. $^{A}P < 0.05$ compared with OVX group; $^{B}P < 0.05$ compared with sham group for spending time in the target quadrant and latency to the first entry to the target quadrant (ANOVA). OVX: ovariectomized. Groups are the same as in Figure 1.

3.2. Morris Water Maze. To determine the dose efficiency of EBN supplementation on learning and memory in ovariectomized rats, behavioral performances were compared among all the groups which received the MWM test before sacrifice. Figure 1 shows that rats from all groups learned the task well and displayed a gradual decrease in escape latencies over the 4-day training acquisition ($F(3, 140) = 352.1$; $P < 0.001$). The control and sham groups had no changes in escape latencies ($F(1, 40) = 6.575e-005$; $P = 0.9936$). Furthermore, the rats in the EBN high-dose group were faster than those in the estrogen group on escape latencies. The MWM revealed that the escape latency (the average time to find the hidden platform) in EBN treatment groups was considerably decreased from low dose to high dose.

Figure 2(a) shows the representative path tracings of the MWM. There was general preference for the target quadrant in the spatial version (lower panel) and the preference of circling for the same animals in the spatial version (upper panel). Two-way ANOVA revealed that the OVX group showed lower ability to learn and find the target platform compared to the sham group ($F(1, 40) = 12.01$; $P = 0.0013$). In contrast, the group with estrogen and EBN supplementation (0.6 and 1.2 g/kg/day) showed strong ability to find the target platform compared to the sham group ($F(3, 80) = 24.59$; $P < 0.0001$).

In the probe test, swimming time (min) in the target quadrant for each group was as follows: estrogen (14.63 ± 2.23) > EBN high dose (12.73 ± 2.02) > control (12.5 ± 2.19) > EBN middle dose (10.58 ± 2.37) > sham (10.50 ± 0.62) > EBN low dose (10.23 ± 2.47) > OVX (4.65 ± 0.81). There were no significant differences for the time in the target quadrant (Figure 2(b)) between the control and sham groups ($P > 0.05$). However, rats in the OVX group spent less time in the target quadrant compared with those in the sham group ($P < 0.01$). Similarly, the estrogen and EBN groups' data showed more time spending on the target quadrant compared to those of the OVX group. The latency to the first entry to the target quadrant (Figure2(c)) of each group was determined as follows: estrogen (4.90 ± 1.33) < control (4.97 ± 1.93) < EBNL (4.38 ± 1.22) < sham (5.33 ± 1.40) < EBNH (6.02 ± 2.33) < EBNM (6.42 ± 2.59) < OVX (10.62 ± 2.87).

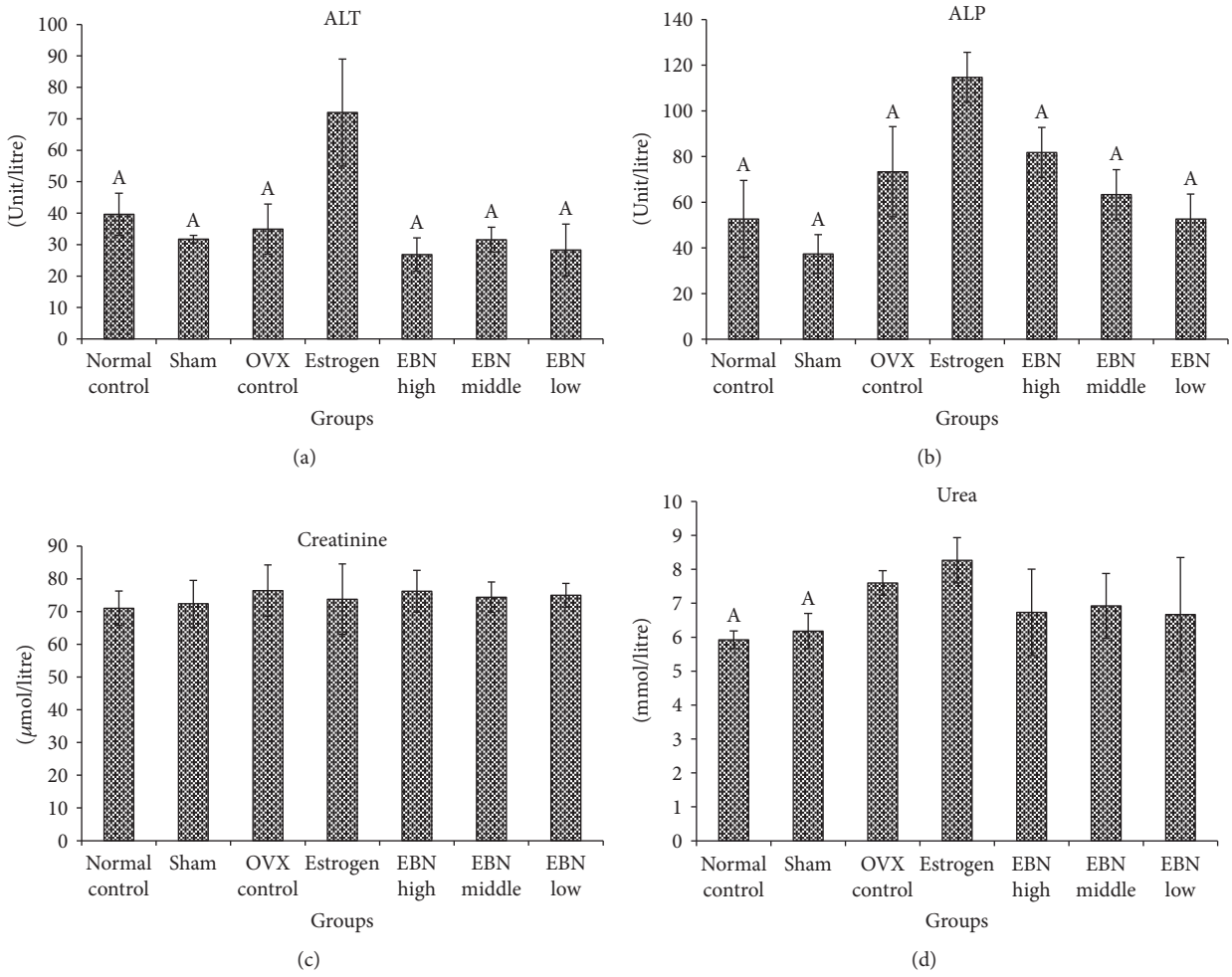

Figure 3: Liver enzymes and kidney function. (a) Serum ALT activity; (b) serum ALP activity; (c) serum creatinine activity; (d) serum urea activity. Data are expressed as mean ± SEM of six animals. $^{A}P < 0.01$ compared with estrogen group. Groups are the same as in Figure 1.

3.3. Toxicity Evaluation. Rats treated (p.o.) with estrogen demonstrated increases in ALT and ALP enzyme activities by 128% and 207%, respectively, compared to the sham group (Figures 3(a) and 3(b)). Conversely, the EBN treatment did not increase the levels of these enzymes as much as estrogen did. The serum creatinine levels (Figure 3(c)) were similar for all groups, while serum urea (Figure 3(d)) was marginally elevated in the treatment groups compared to the control and sham groups.

3.4. SIRT1 Expression in the Hippocampus. The SIRT1-immunoreactive neurons were observed and analyzed in the pyramidal layer of the hippocampus (Figure 4) and the dentate gyrus (Figure 5). In the sham-operated group, numerous neurons in the hippocampal formation were darkly stained with SIRT1 immunohistochemistry. However, for the OVX group, the SIRT1 immunoreactivity was drastically decreased. Similarly, the immunoreactivity in the estrogen and EBN groups was moderate to strong in the dentate gyrus and pyramidal neuron in the CA2 area. Quantitative analysis (Figure 6) revealed that the optical density of hippocampal SIRT1 staining was significantly reduced from 1.31 ± 0.13 (pyramidal neuron) and 1.25 ± 0.05 (dentate gyrus) in the sham-operated group to 0.44 ± 0.03 (pyramidal neuron) and 0.46 ± 0.09 (dentate gyrus) in OVX rats (Figure 4).

4. Discussion

The present study provides evidence that cognitive function could be affected by EBN treatment through improving SIRT1 expression in the hippocampus of ovariectomized female rats. We observed that the preservative effect of EBN was dose-dependent on cognition and hippocampal neuronal SIRT1. Moreover, EBN treatment was less toxic compared to estrogen therapy, which is commonly used in HRT for menopausal symptoms.

The MWM is primarily a test of spatial learning and reference memory [26, 27]. During the navigation test, there was a decrease in escape latencies across successive four days in all the groups. This indicated that under normal physiological or neurodegenerative conditions, four trainings per day can establish the effective reference memory, subsequently improving the next day's navigation performance [27]. However, at the fourth day training, the OVX group had the longest escape latency compared with the sham and

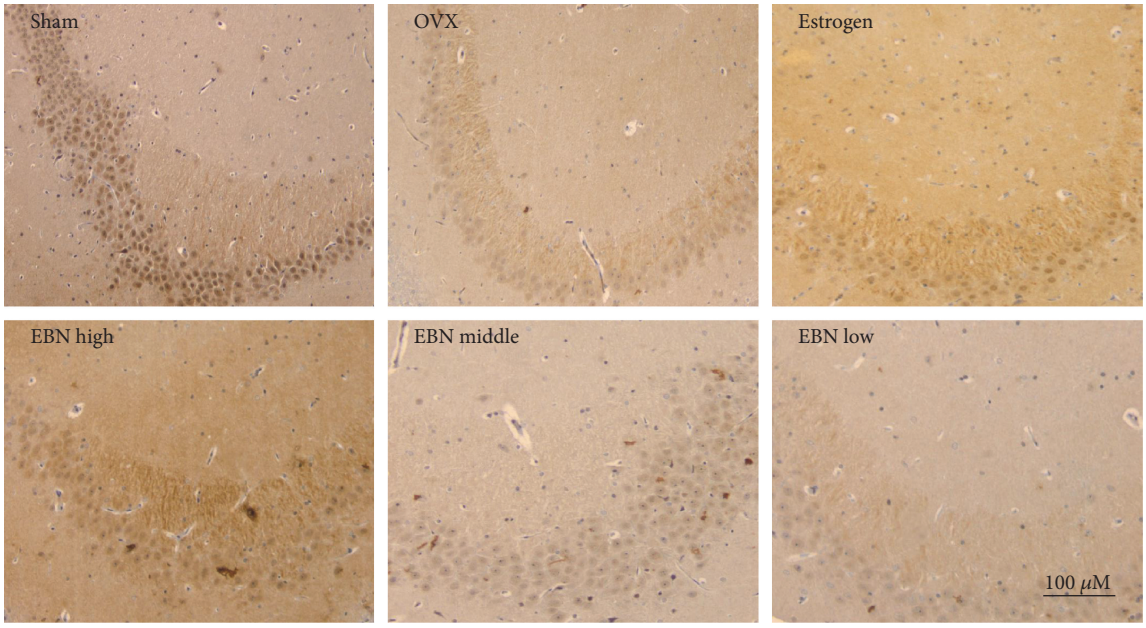

Figure 4: SIRT1 immunoreactivity in the pyramidal layer of the hippocampus (100x). Representative micrographs of SIRT1 ($n = 6$) show the pyramidal layer of the hippocampus. The age-associated reduction in SIRT1 immunoreactivity is attenuated by OVX and ameliorated by EBN treatment. Groups are the same as in Figure 1.

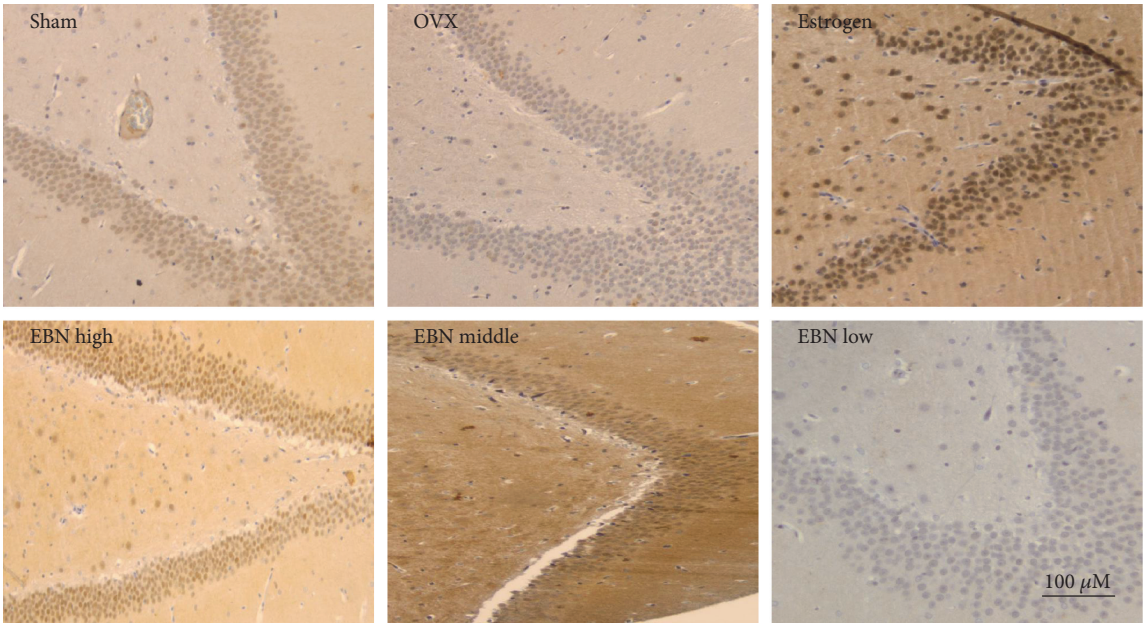

Figure 5: SIRT1 immunoreactivity in the dentate gyrus (100x). Representative micrographs of SIRT1 ($n = 6$) in the dentate gyrus demonstrate that the age-associated reduction in SIRT1 immunoreactivity is attenuated by OVX and ameliorated by EBN treatment. Groups are the same as in Figure 1.

EBN treatment groups, suggesting that the spatial learning ability was impaired in these rats. The effect of EBN treatment was very similar to that of the estrogen treatment suggesting that EBN was as effective as estrogen in improving menopause-related cognitive decline.

Spatial learning and memory in rodents are mainly associated with hippocampal function and morphology [28]. Thus, the present findings suggest that the ability of EBN to improve memory and learning in ovariectomized rats may be tied to its effects on SIRT1 expression in the pyramidal layer and dentate gyrus of the hippocampus. SIRT1 is an enzyme that may increase lifespan through mediation of neuronal plasticity [29–31]. Furthermore, estrogen is able to enhance hippocampal SIRT1 expression as the basis for its ability to improve neuronal plasticity critical for modulating learning and memory [2, 3]. However, because estrogen is

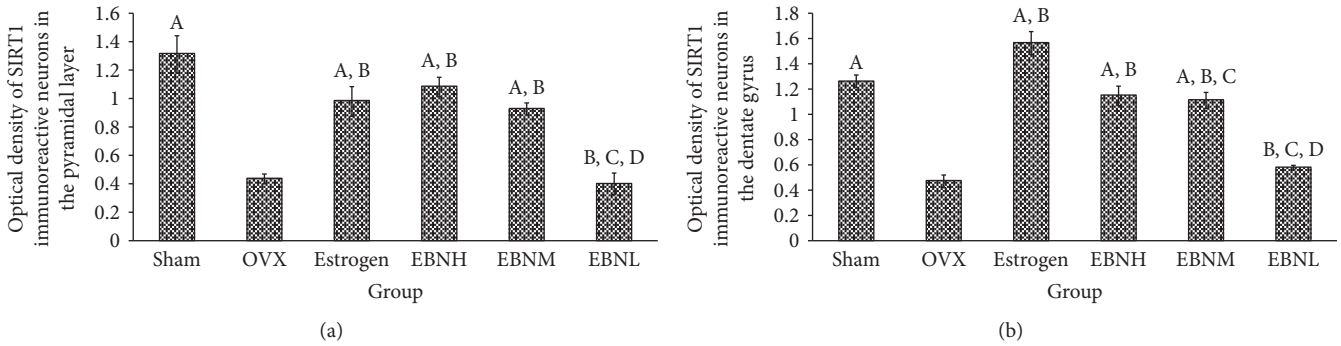

Figure 6: Bar graphs showing the optical density (OD) of SIRT1 immunoreactivity in the pyramidal layer (a) and dentate gyrus (b). $^{A}P < 0.05$ compared with OVX; $^{B}P < 0.05$ compared with sham operation group; $^{C}P < 0.05$ compared with estrogen; $^{D}P < 0.05$ compared with EBN group. Groups are the same as in Figure 1.

associated with adverse effects [5–7], the search for safer alternatives is ongoing. Moreover, the toxicity results in the present study showed that ALT, ALP, and urea in the estrogen group were significantly higher than those in other groups. Taken together, the present toxicity data corroborates the adverse effects of estrogen supplementation. Therefore, although estrogen can improve learning and memory deficits of OVX rats, its effects on liver enzymes and kidney function are unwanted.

Furthermore, EBN is known to possess multiple bioactive compounds that synergistically contribute to its bioactivity [16–18]. Moreover, we have demonstrated previously that the two major components of EBN (lactoferrin and ovotransferrin) could not account for the entire antioxidant effects of EBN [19] suggesting that the presence of other compounds may enhance the overall effects of EBN. This is in line with the concepts of food synergy [32] and bioactive rich fraction [33], which propose that interactions between multiple food nutrients or plant phytochemicals and their relationship with the food matrix may play a more significant role in producing the beneficial effects of foods or plant phytochemicals over any single nutrient present in the food or plant.

5. Conclusions

This study has shown for the first time that EBN treatment preserved hippocampal SIRT1 activity in adult female rats subjected to OVX-related aging, which may have been the basis for the cognitive-enhancing properties of EBN. The positive function of EBN is probably mediated by enhancing the SIRT1-mediated neuronal plasticity that contributes to normal cognitive activity. Although the detailed cellular and molecular mechanisms related to OVX-induced cognitive impairment still remain unclear, the potent neuroprotective effects of EBN suggest that EBN could be an attractive candidate and novel strategy for the management of cognitive dysfunction associated with menopause.

Abbreviations

EBN: Edible bird's nest
OVX: Ovariectomy
MWM: Morris water maze
SIRT1: Sirtuin-1
ALP: Alanine transaminase
ALT: Alkaline phosphatase.

Conflicts of Interest

The authors declare that they have no competing interests.

Authors' Contributions

Zhiping Hou and Peiyuan He designed the study and, together with Mustapha Umar Imam, conducted the experiments. Jiemen Qi, Shiying Tang, and Chengjun Song contributed to the data analysis. Zhiping Hou and Mustapha Umar Imam wrote the manuscript.

Acknowledgments

The present work was supported by grants from the Ministry of Science, Technology and Innovation, e-sciencefund (Vote no. 5450666), Malaysia; the Scientific Research Foundation for the Returned Overseas Chinese Scholars, Hebei Provincial Department of Human Resources and Social Security (Grant no.: 201703); the Health and Family Planning Commission of Hebei (Grant no.: 20160315); the Administration of Traditional Chinese Medicine of Hebei (Grant no.: 2017196); and the Key Discipline Construction Project of Hebei Provincial Universities (Grant no.: JiJiaoGao-2013-(4)-2012-37). The authors thank the staff of the Laboratory of Molecular Biomedicine for their assistance during the study.

References

[1] A. Jayaraman and C. J. Pike, "Differential effects of synthetic progestagens on neuron survival and estrogen neuroprotection in cultured neurons," *Molecular and Cellular Endocrinology*, vol. 384, no. 1-2, pp. 52–60, 2014.

[2] B. S. McEwen, "Estrogens effects on the brain: multiple sites and molecular mechanisms," *Journal of Applied Physiology*, vol. 91, pp. 2785–2801, 2001.

[3] S. Pozzi, V. Benedusi, A. Maggi, and E. Vegeto, "Estrogen action in neuroprotection and brain inflammation," *Annals*

of the New York Academy of Sciences, vol. 1089, pp. 302–323, 2006.

[4] J. Xu, J. Zhu, C. Shi, K. Guo, and D. T. Yew, "Effects of genistein on hippocampal neurodegeneration of ovariectomized rats," *Journal of Molecular Neuroscience*, vol. 31, pp. 101–112, 2007.

[5] M. Clemons and P. Goss, "Estrogen and the risk of breast cancer," *New England Journal of Medicine*, vol. 344, no. 4, pp. 276–285, 2001.

[6] J. V. Lacey Jr., P. J. Mink, J. H. Lubin et al., "Menopausal hormone replacement therapy and risk of ovarian cancer," *The Journal of the American Medical Association*, vol. 288, no. 3, pp. 334–341, 2002.

[7] D. Grady, T. Gebretsadik, K. Kerlikowske, V. Ernster, and D. Petitti, "Hormone replacement therapy and endometrial cancer risk: a meta-analysis," *Obstetrics & Gynecology*, vol. 85, no. 2, pp. 304–313, 1995.

[8] C. Sun, F. Zhang, X. Ge et al., "SIRT1 improves insulin sensitivity under insulin-resistant conditions by repressing PTP1B," *Cell Metabolism*, vol. 6, no. 4, pp. 307–319, 2007.

[9] A. Quintas, A. J. de Solís, F. Javier Díez-Guerra, J. M. Carrascosa, and E. Bogónez, "Age-associated decrease of SIRT1 expression in rat hippocampus prevention by late onset caloric restriction," *Experimental Gerontology*, vol. 47, pp. 198–201, 2012.

[10] L. Bordone and L. Guarente, "Caloric restriction, SIRT1 and metabolism: understanding longevity," *Nature Reviews Molecular Cell Biology*, vol. 6, pp. 298–305, 2005.

[11] J. T. Rodgers, C. Lerin, Z. Gerhart-Hines, and P. Puigserver, "Metabolic adaptations through the PGC-1α and SIRT1 pathways," *FEBS Letters*, vol. 582, pp. 46–53, 2008.

[12] L. C. Koon, "Features–bird's nest soup–market demand for this expensive gastronomic delicacy threatens the aptly named edible-nest swiftlets with extinction in the east," *Wildlife Conservation*, vol. 103, no. 1, pp. 30–35, 2000.

[13] L. C. Koon and Cranbrook, *Swiftlets of Borneo: Builders of Edible Nests*, Natural History Publication (Borneo) Sdn. Bhd, Sabah, 2002.

[14] Y. C. Kong, W. M. Keung, T. T. Yip, K. M. Ko, S. W. Tsao, and M. H. Ng, "Evidence that epidermal growth factor is present in swiftlet's (*Collocalia*) nest," *Comparative Biochemistry & Physiology B*, vol. 87, no. 2, pp. 221–226, 1987.

[15] L. Zhang, *Ben Jing Feng Yuan [Encountering the Sources of the Classic of Material Medica]*, Shang Hai Science Technology Press, Shang Hai, 1959.

[16] M. K. Norhayati, O. Azman, and W. M. Nazaimoon, "Preliminary study of the nutritional content of Malaysian edible bird's nest," *Malaysian Journal of Nutrition*, vol. 16, no. 3, pp. 389–396, 2010.

[17] M. F. Marcone, "Characterization of the edible bird's nest the "caviar of the east"," *Food Research International*, vol. 38, no. 10, pp. 1125–1134, 2005.

[18] R. S. Wong, "Edible bird's nest: food or medicine?," *Chinese Journal of Integrative Medicine*, vol. 19, no. 9, pp. 643–649, 2013.

[19] Z. P. Hou, M. U. Imam, M. Ismail et al., "Lactoferrin and ovotransferrin contribute toward antioxidative effects of edible bird's nest against hydrogen peroxide-induced oxidative stress in human SH-SY5Y cells," *Bioscience, Biotechnology, and Biochemistry*, vol. 79, no. 10, pp. 1570–1578, 2015.

[20] Z. Yida, M. U. Imam, M. Ismail et al., "Edible bird's nest attenuates high fat diet-induced oxidative stress and inflammation via regulation of hepatic antioxidant and inflammatory genes," *BMC Complementary and Alternative Medicine*, vol. 15, no. 1, p. 310, 2015.

[21] Z. Yida, M. U. Imam, M. Ismail et al., "Edible bird's nest prevents high fat diet-induced insulin resistance in rats," *Journal of Diabetes Research*, vol. 2015, Article ID 760535, 11 pages, 2015.

[22] H. Zhiping, M. U. Imam, M. Ismail, D. J. Ooi, A. Ideris, and R. Mahmud, "Nutrigenomics effects of edible bird's nest on insulin signaling in ovariectomised rats," *Drug Design, Development and Therapy*, vol. 9, pp. 4115–4125, 2015.

[23] H. Zhiping, M. U. Imam, M. Ismail et al., "Effects of edible bird's nest on hippocampal and cortical neurodegeneration in ovariectomized rats," *Food and Function*, vol. 6, no. 5, pp. 1701–1711, 2015.

[24] S. I. Muhammad, I. Ismail, R. Mahmud, M. D. Z. Abu Bakar, and M. U. Imam, "Up-regulation of genes related to bone formation by γ-amino butyric acid and γ-oryzanol in pregerminated brown rice is via the activation of GABAB-receptors and reduction in serum IL-6 in rats," *Clinical Interventions in Aging*, vol. 8, pp. 1259–1271, 2013.

[25] H. M. Chang, Y. L. Huang, C. T. Lan, U. I. Wu, M. E. Hu, and S. C. Youn, "Melatonin preserves superoxide dismutase activity in hypoglossal motoneurons of adult rats following peripheral nerve injury," *Journal of Pineal Research*, vol. 44, pp. 172–180, 2008.

[26] M. Inostroza, E. Cid, J. Brotons-Mas et al., "Hippocampal-dependent spatial memory in the water maze is preserved in an experimental model of temporal lobe epilepsy in rats," *PLoS One*, vol. 6, no. 7, article e22372, 2011.

[27] C. V. Vorhees and M. T. Williams, "Morris water maze: procedures for assessing spatial and related forms of learning and memory," *Nature Protocols*, vol. 1, pp. 848–858, 2006.

[28] M. Gallagher and M. M. Nicolle, "Animal models of normal aging: relationship between cognitive decline and markers in hippocampal circuitry," *Behavioural Brain Research*, vol. 57, pp. 155–162, 1993.

[29] S. Imai, C. M. Amstrong, M. Kaeberlein, and L. Guarente, "Transcriptional silencing and longevity protein Sir2 is an NAD-dependent histone deacetylase," *Nature*, vol. 403, pp. 795–800, 2000.

[30] W. Qin, W. Zhao, L. Ho et al., "Regulation of forkhead transcription factor FoxO3a contributes to calorie restriction-induced prevention of Alzheimer's disease-type amyloid neuropathology and spatial memory deterioration," *Annals of the New York Academy of Sciences*, vol. 1147, pp. 335–347, 2008.

[31] G. Ramadori, C. E. Lee, A. L. Bookout et al., "Brain SIRT1: anatomical distribution and regulation by energy availability," *The Journal of Neuroscience*, vol. 28, pp. 9989–9996, 2008.

[32] D. R. Jacobs Jr., M. D. Gross, and L. C. Tapsell, "Food synergy: an operational concept for understanding nutrition," *The American Journal of Clinical Nutrition*, vol. 89, pp. 1543S–1548S, 2009.

[33] M. U. Imam, M. Ismail, D. J. Ooi et al., "Are bioactive-rich fractions functionally richer?," *Critical Reviews in Biotechnology*, vol. 36, pp. 585–593, 2016.

Hindawi
Oxidative Medicine and Cellular Longevity
Volume 2017, Article ID 2198243, 22 pages
https://doi.org/10.1155/2017/2198243

Research Article

Resveratrol Modulation of Protein Expression in *parkin*-Mutant Human Skin Fibroblasts: A Proteomic Approach

Daniele Vergara,[1,2] Antonio Gaballo,[3] Anna Signorile,[4] Anna Ferretta,[4] Paola Tanzarella,[4] Consiglia Pacelli,[5] Marco Di Paola,[6] Tiziana Cocco,[4] and Michele Maffia[1,2]

[1]*Department of Biological and Environmental Sciences and Technologies, University of Salento, Lecce, Italy*
[2]*Laboratory of Clinical Proteomic, "Giovanni Paolo II" Hospital, ASL-Lecce, Lecce, Italy*
[3]*CNR NANOTEC-Istituto di Nanotecnologia, Polo di Nanotecnologia, Campus Ecotekne, Lecce, Italy*
[4]*Department of Basic Medical Sciences, Neurosciences and Sense Organs, University 'A. Moro', Bari, Italy*
[5]*Department of Clinical and Experimental Medicine, University of Foggia, Foggia, Italy*
[6]*Institute of Clinical Physiology, National Research Council, Campus Ecotekne, Lecce, Italy*

Correspondence should be addressed to Tiziana Cocco; tizianamaria.cocco@uniba.it and Michele Maffia; michele.maffia@unisalento.it

Received 11 May 2017; Accepted 19 July 2017; Published 12 September 2017

Academic Editor: Giuseppe Cirillo

In this study, we investigated by two-dimensional gel electrophoresis (2-DE) and mass spectrometry (MS) analysis the effects of resveratrol treatment on skin primary fibroblasts from a healthy subject and from a *parkin*-mutant early onset Parkinson's disease patient. Parkin, an E3 ubiquitin ligase, is the most frequently mutated gene in hereditary Parkinson's disease. Functional alteration of parkin leads to impairment of the ubiquitin-proteasome system, resulting in the accumulation of misfolded or aggregated proteins accountable for the neurodegenerative process. The identification of proteins differentially expressed revealed that resveratrol treatment can act on deregulated specific biological process and molecular function such as cellular redox balance and protein homeostasis. In particular, resveratrol was highly effective at restoring the heat-shock protein network and the protein degradation systems. Moreover, resveratrol treatment led to a significant increase in GSH level, reduction of GSSG/GSH ratio, and decrease of reduced free thiol content in patient cells compared to normal fibroblasts. Thus, our findings provide an experimental evidence of the beneficial effects by which resveratrol could contribute to preserve the cellular homeostasis in *parkin*-mutant fibroblasts.

1. Introduction

Parkinson's disease (PD) is a multifactorial neurodegenerative disorder that predominantly affects the population over 65 years of age [1]. From a clinical point of view, the disease is characterized by the presence of motor deficit associated with abnormal intracellular protein deposits called Lewy bodies (LBs) and loss of dopaminergic neurons, primarily, within the *substantia nigra pars compacta* (SNpc) [2]. Several risk factors were identified including disease-causing mutations in a specific set of genes that mediate the autosomal-dominant or autosomal-recessive forms of PD [3], among which mutations in *alpha synuclein* (SNCA) and in *leucine-rich repeat kinase 2* (LRRK2) are responsible for autosomal-dominant PD forms whereas mutations in *parkin*, *PTEN-induced putative kinase 1* (PINK1), *DJ-1*, and *ATP13A2* are accountable for PD that displays an autosomal recessive mode of inheritance [3].

The most common mutant gene implicated in familial PD is *parkin*, and various loss-of-function mutations occurring in both alleles produce an aggressive, generally early form of PD [4–6]. Parkin is a cytosolic protein with E3 ubiquitin ligase activity, for ubiquitin-proteasome-dependent protein turnover, with a central role in mitochondrial maintenance and turnover. In response to mitochondrial damage, PINK1 induces the activation of parkin by phosphorylation.

Once activated, parkin conjugates ubiquitin onto proteins on the outer mitochondrial membrane (OMM), leading to mitochondrial engulfment by the autophagosome via the endosomal sorting complexes required for transport (ESCRT) machinery [7–9]. Pathogenic mutations of *parkin* lead to the accumulation of damaged mitochondria and are associated with several cellular dysfunctions including impaired energy metabolism, deregulated reactive oxygen species (ROS) production, failure of ubiquitin-proteasome pathway, and protein misfolding [10–13].

Mass spectrometry- (MS-) based studies made possible to shed lights on the cellular pathways modified after parkin loss [14–16]. Proteomic analysis of human primary fibroblasts isolated from patients with a genetic deficit of *parkin* revealed that parkin is implicated in the modulation of multiple cellular functions including cytoskeleton structure dynamics, calcium homeostasis, oxidative stress response, and protein and RNA processing [17]. In this cellular model, the absence of parkin has also been associated with a specific phospholipid and glycosphingolipid lipidomic profile likely related to dysfunction of autophagy and mitochondrial turnover [18].

Current pharmacological treatments of PD remain largely symptomatic, and the development of new therapeutic strategies may provide effective alternative treatment options. In recent years, resveratrol has emerged as a compound conferring protective effects against metabolic and other stresses in age-related diseases, including neurodegeneration [19]. Resveratrol (*trans*-3,5,4′-trihydroxystilbene) a dietary polyphenol present in several medical plants [20] demonstrated multiple biological activities, including anti-inflammatory properties [21], antioxidant effects [22], and neuroprotection in both cerebral ischemia and neurodegenerative diseases, such as Alzheimer's disease and Parkinson's disease [23, 24]. Studies performed on animal models of PD have shown that resveratrol protects dopaminergic neurons from 6-hydroxydopamine- (6-OHDA-) and 1-methyl-4-phenyl-1,2,3,6-tetrahydropyridine- (MPTP-) induced degeneration, possibly via modulation of autophagy and proinflammatory pathways [25–27]. Ex vivo models of PD also gained interest for the preclinical assessment of the biological and medical properties of resveratrol. Previous studies of our group have shown that resveratrol treatment of *parkin*-null cellular model induced a partial rescue of mitochondrial functions and oxidative stress through the activation of the AMP-activated protein kinase (AMPK)/sirtuin 1 (SIRT1)/peroxisome proliferator-activated receptor gamma coactivator 1-alpha (PGC-1α) pathway [28].

In this work, we investigated by two-dimensional gel electrophoresis (2-DE) and mass spectrometry (MS) analysis the effects of resveratrol in *parkin*-mutant human skin fibroblasts. The analysis of proteins differentially expressed revealed that resveratrol treatment acts on deregulated specific biological process and molecular function such as cellular redox balance and protein homeostasis. In particular, resveratrol was highly effective at restoring the heat-shock protein network and the protein degradation systems as well as the GSH/GSSG ratio, together responsible for the maintaining of the normal protein homeostasis which is essential to proper cellular function.

2. Materials and Methods

2.1. Cell Culture Conditions. Primary skin fibroblasts from one subject affected by an early onset PD with *parkin* compound heterozygous mutations (P1 with del exon2-3/del exon3) and from the parental healthy subject (CTR) [13, 28] were obtained by explants from skin punch biopsy, after informed consent. Cells were grown in high-glucose Dulbecco's modified Eagle's medium (DMEM) supplemented with 10% (*v*/*v*) fetal bovine serum (FBS), 1% (*v*/*v*) L-glutamine, and 1% (*v*/*v*) penicillin/streptomycin, at 37°C in a humidified atmosphere of 5% CO_2.

In cell culture experiments, resveratrol (Sigma, R5010) was dissolved in dimethyl sulfoxide (DMSO) and used at the concentration of 25 μM; control cells were treated with an equivalent volume of DMSO (vehicle, 0.02%).

2.2. Sample Preparation and Protein Separation by 2-DE. Cell pellets were dissolved in a lysis solution that contained 7 M urea, 2 M thiourea, 4% CHAPS, and a cocktail of protease and phosphatase inhibitors (Biotool). Samples were then sonicated on ice for three rounds of 10 s and processed according to the methods described before [29–31] with minor modification. Briefly, total proteins (80 μg) were diluted up to 250 μL with a rehydration buffer (7 M urea, 2 thiourea, 4% CHAPS, 65 mM DTT, and 0.5% *v*/*v* IPG buffer) and applied to IPG strips (13 cm, pH 3–10 NL). IEF and second dimension were carried out using an IPGphor IEF and a Hoefer SE 600 Ruby electrophoresis system (GE Healthcare). The IPG strips were loaded and run on a 12% SDS-PAGE gel and stained according to the protocol of Chevallet et al. [32]. Gels were scanned by Image Master scanner and analyzed by Image Master software 5.0 (GE Healthcare) using TIF format images at 300 dpi. Spot detection and matching were carried out by the software tools and corrected manually when necessary. The parameter that we used to compare gels was the volume % (vol %) of each spot, expressed as percentage of the spot volume over the total volume of all spots in the gel. Student's *t*-test with a set value of $p < 0.05$ was used to determine significant differences in protein expression levels. Each experiment was performed three times independently.

2.3. Mass Spectrometry Identification and Data Analysis

2.3.1. Protein Identification by nHPLC ESI-Trap Analysis. Protein spots were manually excised from 2D gels, destained with H_2O_2, and subjected to trypsin digestion followed by identification using an nLC-MS/MS as described [29–31]. The nano-HPLC separation of peptides was performed using a Proxeon Easy-nLC (Thermo Fisher Scientific, Waltham, MA, USA) equipped with a NS-AC-10 analytical column, 5 μM, C18, 375 μM OD × 75 μM ID × 10 cm length, protected by an NS-MP-10 guard column, 5 μM, C18, 375 μM OD × 100 μM ID × 2 cm length (Nano Separations, Nieuwkoop, The Netherlands).

2.3.2. Protein Identification by MALDI-TOF/TOF. Spots of interest were dehydrated with 50 μL of acetonitrile and trypsin digested overnight as described [29]. Resulting peptides

were then concentrated by using C18 Zip-Tips (Millipore) and eluted with 2 μL of CHCA matrix (66 μL TFA, 0.1%; 33 μL ACN) directly on an MTP AnchorChipTM 384 BC plate (Bruker Daltonics). Peptides were analyzed by peptide mass fingerprinting (PMF) and MS/MS analysis with a MALDI-TOF/TOF Ultraflextreme (Bruker Daltonics) in positive ion reflector mode (m/z range 500–4000), operating at 1 kHz frequency and controlled by the FlexControl 3.4 software. External calibration was performed using the Peptide Standard Calibration II (Bruker Daltonics). Spectra were processed using the software FlexAnalysis (version 3.4, Bruker Daltonics) and precursor ions with a signal to noise ratio greater than 10 selected for subsequent MS/MS analysis.

Compound lists were submitted to Mascot using the software BioTools (version 3.2, Bruker Daltonics). Peptide masses were compared with those present in the Swiss-Prot human protein database. Database search was performed using the following parameters: peptide tolerance, 0.05 Da; fragment mass tolerance, 0.25 Da; enzyme, trypsin; missed cleavage, one; and instrument, MALDI-TOF/TOF. Peptide tolerance was set to ±1.2 Da, the MS/MS tolerance was set to 0.6 Da, and searching peptide charges were of 1+, 2+, and 3+ for ESI-Trap data. Moreover, carbamidomethyl (C) and oxidation (M) were chosen as fixed and variable modifications, respectively. Identified proteins were subjected to Gene Ontology (GO) analysis and protein-protein interaction (PPI) analysis by STRING software (version 10.0, http://string-db.org/).

2.4. GSH and GSSG Determination. For GSH and GSSG assay, fibroblasts were collected by trypsinization and centrifuged at 500 ×g and then resuspended in cold 5% (*w*/*v*) metaphosphoric acid. The sample was exposed to ultrasound energy for 15 s at 0°C and centrifuged at 12,000 ×g for 5 minutes. The supernatant was used to determine GSH and GSSG concentration using an enzymatic/colorimetric assay kit (Enzo Life Sciences) according to the manufacturer's instructions. The measurements were performed on a Victor 2030 Explorer (PerkinElmer). Total protein concentration was determined by Bio-Rad protein assay. GSH and GSSG levels were normalized to protein concentration and expressed as nmol/mg protein.

2.5. P-SH Measurement. Cells were collected by trypsinization and centrifugation at 500 ×g and then resuspended in phosphate-buffered saline (PBS), pH 7.4, in the presence of the protease inhibitor phenylmethanesulfonyl fluoride (PMSF). The content of P-SH in total cellular lysate was measured with a modification of the Ellman's procedure [33]. The protein pellet was obtained by precipitation with 4% SSA and centrifugation. Next, the pellet was resuspended in 6 M guanidine, pH 6.0. Optical density was read spectrophotometrically at 412 and 530 nm before and after 30 min of incubation with 10 mM 5,5-dithiobis (2-nitrobenzoic acid). P-SH concentrations were calculated using a standard curve generated with reduced glutathione.

2.6. Analysis of Glutathionylated Proteins. Glutathionylated proteins were detected by Western blot analysis of cellular lysates after nonreducing SDS-PAGE. Cells were collected by trypsinization and centrifugation at 500 ×g and then resuspended in PBS, pH 7.4, containing the protease inhibitor PMSF and supplemented with 5 mM *N*-ethylmaleimide (NEM) to block unreacted thiol group. Total cellular proteins (50 μg per lane) were separated on 12% (*w*/*v*) SDS-PAGE and transferred to nitrocellulose membranes. Glutathionylated proteins were visualized with anti-GSH antibody (1 : 1000, Thermo Fisher Scientific number MA1-7620). Glyceraldehyde-3-phosphate dehydrogenase (GAPDH) (Sigma) was used as loading control. After several washes in Tween/Tris-buffered saline solution (TTBS), the membrane was incubated for 60 minutes with an anti-rabbit or anti-mouse IgG peroxidase-conjugate antibody (diluted 1 : 5000). Immunodetection was then performed with the enhanced chemiluminescence (ECL) (Bio-Rad, Milan, Italy). The VersaDoc imaging system was used to perform densitometric analysis (Bio-Rad, Milan, Italy).

2.7. Western Blot Analysis. Whole proteins were extracted with RIPA buffer (Cell Signaling) and quantified by the Bradford protein assay (Bio-Rad). Samples were separated by 10% SDS-PAGE and transferred to the Hybond ECL nitrocellulose membrane. The membranes were blocked overnight in Blotto A (Santa Cruz) at 4°C and subsequently probed by the appropriately diluted primary antibodies for 2 h at room temperature. Protein bands were visualized by incubating with a horseradish peroxidase-conjugated secondary antibody (Amersham, ECL Western blotting detection reagents).

3. Results and Discussion

3.1. Proteomic Profile Alteration in PD Fibroblasts. In our previous work, we analyzed, by 2-DE and MALDI-MS, proteins isolated from fibroblast cultures of healthy subjects and patients affected by PD [17]. This comparative proteomic approach led to the identification of several differentially expressed proteins. Here, we modified some of the experimental parameters used previously to separate proteins from fibroblast cultures, including 2-DE buffer composition and isoelectric focusing conditions, in order to increase the number of proteins separated by 2-DE and the potential number of differentially expressed proteins identified after comparative analysis. We focused on control (CTR) and PD patient (P1) fibroblasts that we recently characterized for a variety of cellular alterations associated with the modulation of metabolic and cytoskeletal proteins [13, 34]. With these technical improvements, we identified 15 additional differentially expressed proteins which are not yet identified in the previous work [17]. The identity of these proteins was determined by MALDI-TOF MS/MS and listed in Table 1. By combining these new results with the precedent group of identified proteins, we obtained a dataset of 44 distinct and well-annotated differentially expressed proteins that were subjected to bioinformatics analysis. GO classification and protein-protein interaction network (PPI) of this dataset are shown in Tables 2, 3, and 4 and Figure 1(b). Data showed a significant decrease, in P1 compared to CTR cells, of the expression of

Table 1: List of differentially expressed proteins identified by MS/MS in CTR and P1 samples.

Spot number	Swiss-Prot accession number	Protein name	Gene name	Mascot score		Sequence coverage MS	Sequence coverage MS/MS	Peptides	Fold change P1/CTR	p value	Instrument
Spot 1	Q9Y4L1	Hypoxia-upregulated protein (HYOU1)	*HYOU1*	181	106	25%	2%	K.LCQGLFFR.V K.QADNPHVALYQAR.F	2.2	***	MALDI-TOF/TOF
Spot 2	Q06830	Peroxiredoxin-1 (PRDX1)	*PRDX1*	/	47	/	29%	R.TIAQDYGVLK.A K.ATAVMPDGQFK.D + oxidation (M) R.LVQAFQFTDK.H R.QITVNDLPVGR.S	1.6	***	ESI-Trap
Spot 3	P09936	Ubiquitin carboxyl-terminal hydrolase isozyme L1 (UCHL1)	*UCHL1*	86	220	49%	19%	R.LGVAGQWR.F R.MPFPVNHGASSEDTLLK.D + oxidation (M) K.NEAIQAAHDAVAQEGQCR.V	3.8	***	MALDI-TOF/TOF
Spot 4	P63244	Guanine nucleotide-binding protein subunit beta-2-like 1 (GBLP)	*GNB2L1*	97	84	38%	6%	R.VWQVTIGTR.- R.DETNYGIPQR.A	2.3	**	MALDI-TOF/TOF
Spot 5	Q8WUM4	Programmed cell death 6 interacting protein (PDC6I)	*PDCD6IP*	175	167	29%	4%	R.TPSNELYKPLR.A R.YYDQICSSIEPK.F K.MVPVSVQQSLAAYNQR.K	1.6	*	MALDI-TOF/TOF
Spot 6	P15311	Ezrin (EZRI)	*EZR*	111	134	25%	4%	K.IGFPWSEIR.N R.IQVWHAEHR.G K.KAPDFVFYAPR.L	−5.5	***	MALDI-TOF/TOF
Spot 7	P17987	T-complex protein 1 subunit alpha (TCPA)	*TCP1*	96	214	22%	6%	K.YFVEAGAMAVR.R K.IHPTSVISGYR.L R.YINENLIVNTDELGR.D	−1.6	***	MALDI-TOF/TOF
Spot 8	P34897	Serine hydroxymethyltransferase mitochondrial (GLYM)	*SHMT2*	61	142	27%	9%	R.LIIAGTSAYAR.L K.TGLIDYNQLALTAR.L R.GYSLVSGGTDNHLVLVDLRPK.G	1.8	***	MALDI-TOF/TOF
Spot 9	Q16658	Fascin (FSCN1)	*FSCN1*	150	171	42%	6%	R.FLIVAHDDGR.W K.LINRPIIVFR.G K.NASCYFDIEWR.D	−1.7	**	MALDI-TOF/TOF
Spot 10	P49368	T-complex protein 1 subunit gamma (TCPG)	*CCT3*	87	145	12%	6%	R.NLQDAMQVCR.N R.TLIQNCGASTIR.L K.AMTGVEQWPYR.A + oxidation (M)	−1.8	**	MALDI-TOF/TOF
Spot 11	P07741	Adenine phosphoribosyltransferase (APT)	*APRT*	60	147	28%	21%	R.IDYIAGLDSR.G R.SFPDFPTPGVVFR.D K.AELEIQKDALEPGQR.V	1.6	**	MALDI-TOF/TOF

Table 1: Continued.

Spot number	Swiss-Prot accession number	Protein name	Gene name	Mascot score		Sequence coverage MS	Sequence coverage MS/MS	Peptides	Fold change P1/CTR	p value	Instrument
Spot 12	P07195	L-lactate dehydrogenase B chain (LDH-B)	*LDHB*	125	127	33%	11%	K.IVVVTAGVR.G R.VIGSGCNLDSAR.F K.GEMMDLQHGSLFLQTPK.I + oxidation (M)	1.9	***	MALDI-TOF/TOF
Spot 13	P35998	26S proteasome regulatory subunit 7 (PRS7)	*PSMC2*	61	67	20%	9%	R.KIEFSLPDLEGR.T K.QTLQSEQPLVAR.C K.ACLIFFDEIDAIGGAR.F	1.8	**	MALDI-TOF/TOF
Spot 14	P07355	Annexin A2 (ANXA2)	*ANXA2*	67	82	21%	7%	K.WISIMTER.S + oxidation (M) K.AYTNFDAER.D R.QDIAFAYQR.R	2	***	MALDI-TOF/TOF
Spot 15	P00338	L-lactate dehydrogenase A chain (LDHA)	*LDHA*	96	83	26%	7%	K.LVIITAGAR.Q K.DQLIYNLLKEEQTPQNK.I	2	***	MALDI-TOF/TOF

Spot numbers match those reported in the representative 2-DE images shown in Figure 1. Accession number in Swiss-Prot/UniprotKB (http://www.uniprot.org/). Fold change (P1 versus CTR cells) was calculated dividing the average of %V P1 cells by the average of %V CTR cells of three independent experiments. *t*-test was performed by GraphPad v4.0 software to determine if the relative change was statistically significant ($p < 0.05$); $^{*}p < 0.05$; $^{**}p < 0.01$; $^{***}p < 0.001$.

Table 2: List of significantly enriched biological processes in CTR versus P1 protein dataset identified by STRING software.

Biological process (GO) Pathway ID	Pathway description	Count in gene set	False discovery rate
GO:0006928	Movement of a cell or subcellular component	16	1.1*e*−05
GO:0006457	Protein folding	8	4.08*e*−05
GO:0030049	Muscle filament sliding	5	4.08*e*−05
GO:0006986	Response to unfolded protein	7	5.67*e*−05
GO:0022607	Cellular component assembly	16	9.99*e*−05

Table 3: List of significantly enriched molecular functions in CTR versus P1 protein dataset identified by STRING software.

Molecular function (GO) Pathway ID	Pathway description	Count in gene set	False discovery rate
GO:0005515	Protein binding	30	1.16*e*−08
GO:0005509	Calcium ion binding	12	7.71*e*−06
GO:0051082	Unfolded protein binding	6	7.71*e*−06
GO:0003723	RNA binding	16	1.33*e*−05
GO:0044822	Poly(A) RNA binding	13	0.000172

Table 4: List of significantly enriched molecular functions in CTR versus P1 protein dataset identified by STRING software.

KEGG pathways (GO) Pathway ID	Pathway description	Count in gene set	False discovery rate
04141	Protein processing in endoplasmic reticulum	7	1.25*e*−05

protein related to several biological processes like those involved in cell movement or subcellular components as well as those involved in regulating, assembly and protein folding, calcium ion binding, and unfolded protein binding. Kyoto Encyclopedia of Genes and Genomes (KEGG) pathway enrichment analysis identified protein processing in the endoplasmic reticulum (ER) as significantly modified (Table 4). This includes a list of 7 well-connected proteins HYOU1, GANAB, CALR, HSPA5, HSP90B1, VCP, and HSPA8 as determined by PPI analysis (Figure 1(c)). Most of these proteins belong to the heat-shock protein (HSP) family, and all of them participate in protein folding. HSPs have become a research focus in PD because the pathogenesis of this disease is highlighted by the intracellular protein misfolding and inclusion body formation. HSPs are mainly involved, by interaction with different cochaperones, in folding nascent polypeptides to their appropriate conformation and refolding mild denatured/damaged proteins. Moreover, working together with the ubiquitin-proteasome system (UPS), they are involved in the decomposition of aberrant proteins. In addition, HSPs may possess antiapoptotic effects and keep the cellular homeostasis against stress conditions [35–38]. Evidence involving a direct role for UPS in PD results from the association between genetic mutations in *parkin* with familial parkinsonism [4].

It is noteworthy to highlight the high level of the ubiquitin carboxyl-terminal hydrolase isozyme L1 (UCHL1), a protein component of UPS, observed in PD fibroblasts (3.8-fold increase with respect to CTR cells) (Table 1). In addition to its major function related to protein degradation as a component of UPS [39], UCHL1 possesses an ubiquitin ligase-like enzymatic activity [40], placing it in a pathway potentially related to parkin. It is reported that interaction with parkin promotes UCHL1 lysosomal degradation [41] and consequently the lack of parkin could lead to the abnormal UCHL1 accumulation in PD patient cells. P1 cells are also characterized by a deregulation of redox state, and, according to previous work showing a different expression level of protein involved in oxidative stress response [17], 2-DE data revealed a significant increase of peroxiredoxin-1 (PRDX1) in P1 with respect to CTR cells (Table 1).

A differential expression level of energy metabolism-associated proteins was also observed. L-lactate dehydrogenase A chain (LDH-A) and B chain (LDH-B) resulted both overexpressed in P1 fibroblasts. This is consistent with the finding that P1 cells, characterized by mitochondrial dysfunctions, showed a high glycolytic ATP production, lactate level, and intracellular LDH activity [13].

Perturbation of protein folding homeostasis is a common pathologic feature of many neurodegenerative diseases,

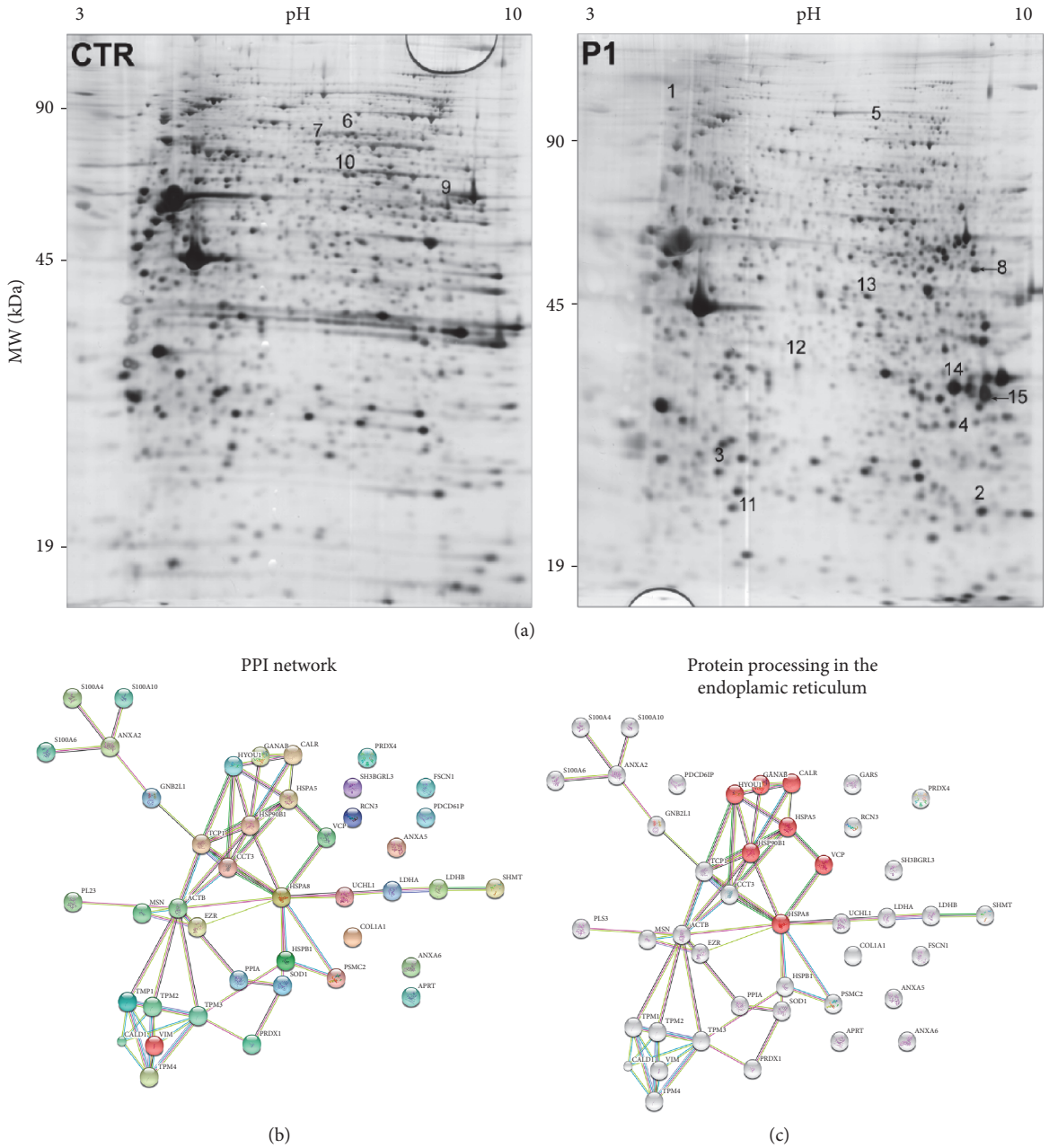

Figure 1: Representative 2-DE gel map of proteins isolated from human CTR and P1 fibroblasts. (a) A total of 80 μg of proteins were separated by 2-DE using a 13 cm IPG strip pH 3–10 NL and 12% SDS-PAGE. Proteins were visualized by silver staining. Spot numbers indicate proteins that were differentially regulated between CTR and P1 samples. (b, c) Bioinformatics analysis of differentially expressed proteins. (b) A high confidence protein-protein interaction network generated with STRING using our protein dataset is shown. The network nodes are input proteins. The edges represent the predicted functional associations. An edge may be drawn with up to 7 differently colored lines—these lines represent the existence of the seven types of evidence used in predicting the associations. A red line indicates the presence of fusion evidence; a green line, neighborhood evidence; a blue line, coocurrence evidence; a purple line, experimental evidence; a yellow line, textmining evidence; a light blue line, database evidence; and a black line, coexpression evidence. (c) Proteins involved in protein processing in the endoplasmic reticulum proteins are highlighted in red (HYOU1, GANAB, CALR, HSPA5, HSP90B1, VCP, and HSPA8) in the main PPI network.

including Alzheimer's disease and PD [42, 43]. Protein folding in the ER is finely regulated by various conditions including redox state and calcium concentrations. In the list of the molecular functions (Table 3), we observed that the calcium ion binding and unfolded protein binding pathways were significantly enriched in CTR versus P1 cells suggesting that the defect of these functions in P1 cells could be responsible for the altered cellular homeostasis. Furthermore, according to our previous work [17, 34], we detected in PD samples with respect to CTR a significantly lower level of the protein

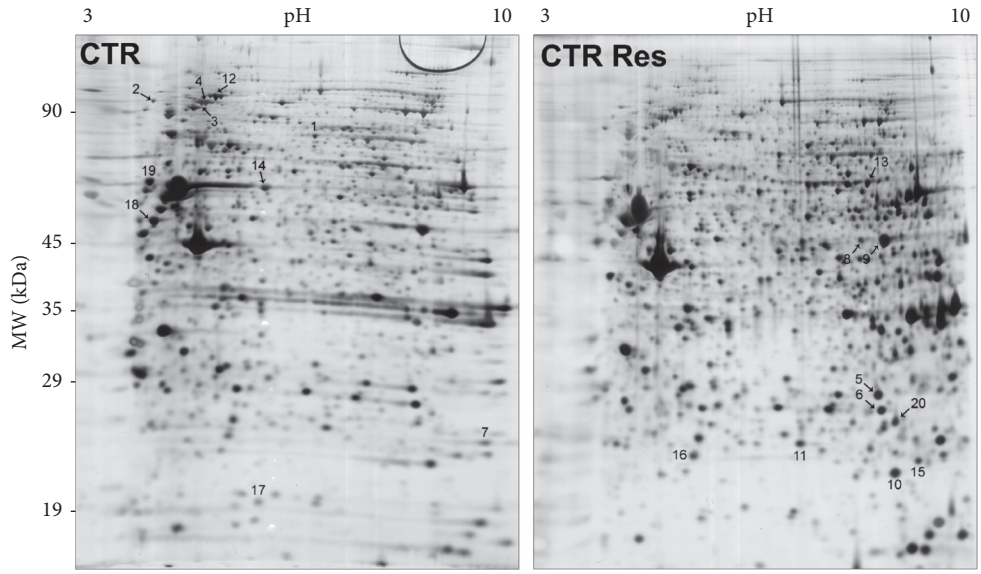

Figure 2: Representative 2-DE gel map of CTR and CTR-Res-treated cell proteins. A total of 80 μg of proteins were separated by 2-DE using a 13 cm IPG strip pH 3–10 NL and 12% SDS-PAGE. Proteins were visualized by silver staining. Spot numbers indicate differentially expressed proteins.

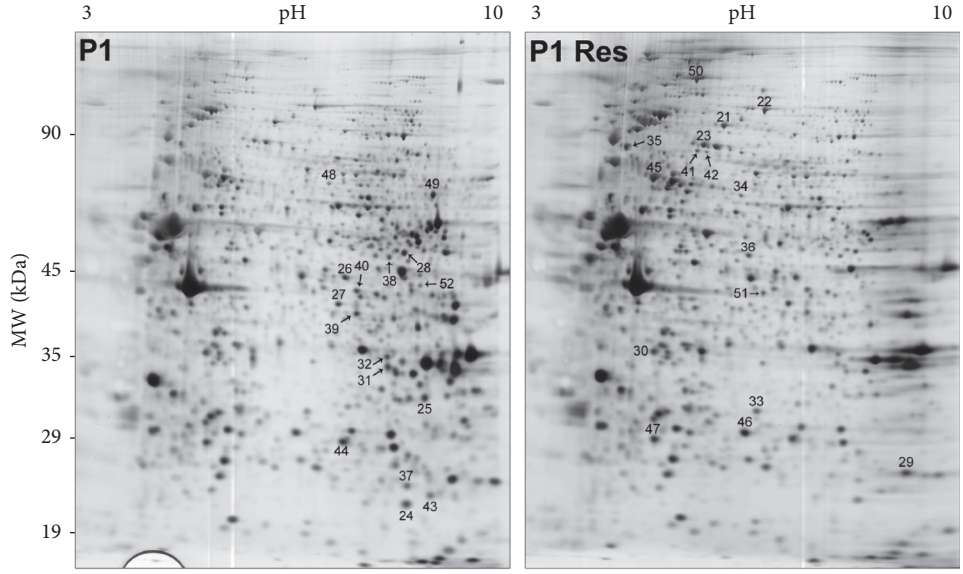

Figure 3: Representative 2-DE gel map of P1 and P1-Res-treated cell proteins. A total of 80 μg of proteins were separated by 2-DE using a 13 cm IPG strip pH 3–10 NL and 12% SDS-PAGE. Proteins were visualized by silver staining. Spot numbers indicate differentially expressed proteins.

ezrin, a member of the ERM (ezrin, radixin, and moesin) protein family, involved in the connection of major cytoskeletal structures to the plasma membrane [44].

Overall these new data, together with the previously obtained results, point to the involvement of parkin in the regulation of a complex network of processes related to cytoskeletal rearrangements and protein folding organization in the ER [17, 34].

3.2. Establishing a Proteomic Expression Signature Associated with Resveratrol Treatment in Control and PD Fibroblasts. Since *in vitro* and *in vivo* studies demonstrated the promising effects of resveratrol on neuronal diseases, with a well-described effect in retarding or even reversing the accelerated rate of neuronal degeneration [25–27, 45, 46], we went through the study of protein expression profile in a cellular PD model to gain further insights into the molecular effects induced by resveratrol treatment.

Protein expression was investigated by 2-DE and MALDI-MS/MS analysis after 24 h of treatment with resveratrol at the concentration of 25 μM or with vehicle (DMSO) (Figures 2 and 3). A specific dataset of proteins resulted

Table 5: List of differentially expressed proteins identified by MS/MS in CTR and CTR-Res-treated samples.

Spot number	Swiss-Prot accession number	Protein name	Gene name	Mascot score		Sequence coverage MS	Sequence coverage MS/MS	Peptides	Fold change CTR-Res/CTR	p value	Instrument
				PMF	MS/MS						
Spot 1	P41250	Glicine-tRNA ligase (SYG)	*GARS*	91	144	21%	6%	K.NNIIQTWR.Q R.SCYDLSCHAR.A K.LPFAAAQIGNSFR.N K.TSYGWIEIVGCCADR.S	−1.6	**	MALDI-TOF/TOF
Spot 2	Q9Y4L1	Hypoxia upregulated protein (HYOU1)	*HYOU1*	181	106	25%	2%	K.LCQGLFFR.V K.QADNPHVALYQAR.F	−2.3	***	MALDI-TOF/TOF
Spot 3	O43707	Alpha-actinin 4 (ACTN4)	*ACTN4*	130	111	26%	3%	K.GYEEWLLNEIR.R R.ASFNHFDKDHGGALGPEEFK.A	−1.9	***	MALDI-TOF/TOF
Spot 4	P55072	Transitional endoplasmic reticulum ATPase (TERA)	*VCP*	/	97	/	24%	R.GILLYGPPGTGK.T R.EVDIGIPDATGR.L R.WALSQSNPSALR.E R.IVSQLLTLMDGLK.Q R.LGDVISIQPCPDVK.Y R.LDQLIYIPLPDEK.S K.MTNGFSGADLTEICQR.A K.NAPAIIFIDELDAIAPK.R K.MTNGFSGADLTEICQR.A + oxidation (M) R.QAAPCVLFFDELDSIAK.A R.EDEEESLNEVGYDDIGGCR.K R.ETVVEVPQVTWEDIGGLEDVKR.E	−2.5	**	ESI-Trap
Spot 5	P18669	Phosphoglycerate mutase 1(PGAM1)	*PGAM1*	73	149	27%	8%	R.VLIAAHGNSLR.G R.HGESSAWNLENR.F	1.7	*	**MALDI-TOF/TOF**
Spot 6	P60174	Triosephosphate isomerase (TPIS)	*TPI1*	112	175	42%	9%	R.HVFGESDELIGQK.V K.DCGATWVVLGHSER.R	1.6	**	MALDI-TOF/TOF
Spot 7	Q06830	Peroxiredoxin-1 (PRDX1)	*PRDX1*	/	47	/	29%	R.TIAQDYGVLK.A K.ATAVMPDGQFK.D + oxidation (M) R.LVQAFQFTDK.H R.QITVNDLPVGR.S	−1.9	***	ESI-Trap
Spot 8	P06733	Alpha enolase (ENOA)	*ENO1*	145	162	51%	14%	R.YISPDQLADLYK,S K.LAQANGWGVMVSHR.S + oxidation (M) R.AAVPSGASTGIYEALELR.D K.LAMQEFMILPVGAANFR.E + 2 oxidation (M)	2.2	**	MALDI-TOF/TOF

Table 5: Continued.

Spot number	Swiss-Prot accession number	Protein name	Gene name	Mascot score		Sequence coverage MS	Sequence coverage MS/MS	Peptides	Fold change CTR-Res/CTR	p value	Instrument
				PMF	MS/MS						
Spot 9	P06733	Alpha enolase (ENOA)	*ENO1*	145	96	51%	8%	R.AAVPSGASTGIYEALELR.D K.LAMQEFMILPVGAANFR.E + 2 oxidation (M)	2.4	***	MALDI-TOF/TOF
Spot 10	P02511	Alpha-crystallin B chain (CRYAB)	*CRYAB*	103	79	12%	11%	R.QDEHGFISR.E R.RPFFPFHSPSR.L	1.6	*	MALDI-TOF/TOF
Spot 11	Q99497	DJ-1 (PARK7)	*PARK7*	88	44	50%	19%	K.DGLILTSR.G K.MMNGGHYTYSENR.V + oxidation (M) K.GAEEMETVIPVDVMR.R	1.7	*	MALDI-TOF/TOF
Spot 12	Q14764	Major vault protein (MVP)	MVP	160	117	31%	3%	R.GAVASVTFDDFHK.N R.IPPYHYIHVLDGNSNVSR.V	−1.6	**	MALDI-TOF/TOF
Spot 13	P02545	Prelamin A/C (LMNA)	*LMNA*	130	185	29%	5%	R.LADALQELR.A R.TLEGELHDLR.G R.NSNLVGAAHEELQQSR.I	1.8	**	MALDI-TOF/TOF
Spot 14	P30101	Protein disulfide-isomerase A3 (PDIA3)	*PDIA3*	107	59	23%	1%	K.QAGPASVPLR.T	−2.1	***	MALDI-TOF/TOF
Spot 15	P30086	Phosphatidylethanolamine-binding protein 1 (PEBP1)	*PEBP1*	187	238	67%	22%	K.LYTLVLTDPDAPSR.K K.NRPTSISWDGLDSGK.L R.YVWLVYEQDRPLK.C	2.2	***	MALDI-TOF/TOF
Spot 16	P32119	Peroxiredoxin-2 (PRDX2)	*PRDX2*	93	324	47%	14%	R.QITVNDLPVGR.S K.EGGLGPLNIPLLADVTR.R R.KEGGLGPLNIPLLADVTR.R	1.8	**	MALDI-TOF/TOF
Spot 18	P08670	Vimentin (VIME)	*VIM*	62	124	15%	13%	K.FADLSEAANRNNDALR.Q R.QVQSLTCEVDALKGTNESLER.Q	−1.6	***	MALDI-TOF/TOF
Spot 19	P07237	Protein disulfide-isomerase (PDIA1)	*P4HB*	130	142	27%	7%	K.FFPASADR.T K.VDATEESDLAQQYGVR.G K.ILFIFIDSDHTDNQR.I	−2	***	MALDI-TOF/TOF
Spot 20	P62826	GTP-binding nuclear protein Ran	*RAN*	74	99	25%	8%	K.YVATLGVEVHPLVFHTNR.G K.KYVATLGVEVHPLVFHTNR.G	1.8	**	MALDI-TOF/TOF

Spot numbers match those reported in the representative 2-DE images shown in Figure 2. Accession number in Swiss-Prot/UniprotKB (http://www.uniprot.org/). Fold change (resveratrol-treated cells versus control cells) was calculated dividing the average of %V resveratrol-treated cells by the average of %V control cells of three independent experiments. *t*-test was performed by GraphPad v4.0 software to determine if the relative change was statistically significant ($p < 0.05$); $^{*}p < 0.05$; $^{**}p < 0.01$; $^{***}p < 0.001$.

Table 6: List of differentially expressed proteins identified by MS/MS in P1 and P1-Res-treated samples.

Spot number	Swiss-Prot accession number	Protein name	Gene name	Mascot score		Sequence coverage MS	Sequence coverage MS/MS	Peptides	Fold change P1 Res/P1	p value	Instrument
				PMF	MS/MS						
Spot 21	Q14697	Neutral alpha-glucosidase AB (GANAB)	*GANAB*	265	137	37%	3%	K.AEKDEPGAWEETFK.T K.MMDYLQGSGETPQTDVR.W + oxidation (M)	1.9	**	MALDI-TOF/TOF
Spot 22	P18206	Vinculin (VINC)	*VCL*	/	105	/	10%	R.WIDNPTVDDR.G R.VMLVNSMNTVK.E + oxidation (M) K.MTGLVDEAIDTK.S + oxidation (M) K.QVATALQNLQTK.T K.AQQVSQGLDVLTAK.V R.DPSASPGDAGEQAIR.Q R.GILSGTSDLLLTFDEAEVR.K R.GILSGTSDLLLTFDEAEVR.K K.LLAVAATAPPDAPNREEVFDER.A	1.6	*	Esi-Trap
Spot 23	P42224	STAT1 (STAT1)	*STAT1*	86	85	24%	4%	K.YLYPNIDKDHAFGK.Y K.QDWEHAANDVSFATIR.F	2.2	***	MALDI-TOF/TOF
Spot 24	P02511	Alpha-crystallin B chain (CRYAB)	*CRYAB*	103	79	12%	11%	R.QDEHGFISR.E R.RPFFPFHSPSR.L	−2.3	***	MALDI-TOF/TOF
Spot 25	P63244	Guanine nucleotide-binding protein subunit beta-2-like 1 (GBLP)	*GNB2L1*	97	84	38%	6%	R.VWQVTIGTR.-R.DETNYGIPQR.A	−1.9	**	MALDI-TOF/TOF
Spot 26	P61163	Alpha-centractin (ACTZ)	*ACTR1A*	78	87	23%	4%	K.AQYYLPDGSTIEIGPSR.F	−1.6	*	MALDI-TOF/TOF
Spot 27	P61160	Actin-related protein 2 (ARP2)	*ACTR2*	61	151	20%	10%	K.HLWDYTFGPEK.L R.GYAFNHSADFETVR.M K.HIVLSGGSTMYPGLPSR.L + oxidation (M)	−1.7	**	MALDI-TOF/TOF
Spot 28	P00367/ Q15654	Glutamate dehydrogenase 1, mitochondrial (DHE3)/ thyroid receptor-interacting protein 6 (TRIP6)	*GLUD1/ TRIP6*	84/123	91/73	29%/39%	3%/8%	K.MVEGFFDR.G R.DDGSWEVIEGYR.A / R.GTPGPPPAHGAALQPHPR.V R.VNFCPLPSEQCYQAPGGPEDR.G	−2.1	**	MALDI-TOF/TOF
Spot 29	Q06830	Peroxiredoxin-1 (PRDX1)	*PRDX1*	/	47	/	29%	R.TIAQDYGVLK.A K.ATAVMPDGQFK.D + oxidation (M) R.LVQAFQFTDK.H R.QITVNDLPVGR.S	2	***	ESI-Trap
Spot 30	P52907	F-actin-capping protein subunit alpha-1 (CAZA1)	*CAPZA1*	59	109	34%	9%	R.LLLNNDNLLR.E K.FITHAPPGEFNEVFNDVR.L	1.8	**	MALDI-TOF/TOF

Table 6: Continued.

Spot number	Swiss-Prot accession number	Protein name	Gene name	Mascot score		Sequence coverage MS	Sequence coverage MS/MS	Peptides	Fold change P1 Res/P1	p value	Instrument
				PMF	MS/MS						
Spot 31	P40925	Malate dehydrogenase, cytoplasmic (MDHC)	*MDH1*	58	173	18%	6%	K.GEFVTTVQQR.G K.FVEGLPINDFSR.E	1.7	**	MALDI-TOF/TOF
Spot 33	P78417	Glutathione S-transferase omega I (GSTO1)	*GSTO1*	102	137	36%	17%	R.FCPFAER.T R.HEVININLK.N K.GSAPPGPVPEGSIR.I K.EDYAGLKEEFR.K	−1.6	***	MALDI-TOF/TOF
Spot 34	P09960	Leukotriene A-4 hydrolase (LKHA4)	*LTA4H*	66	42	17%	5%	R.TLTGTAALTVQSQEDNLR.S R.MQEVYNFAINNSEIR.F + oxidation (M)	−1.6	*	MALDI-TOF/TOF
Spot 35	P07900	Heat-shock protein HSP 90-alpha (HS90A)	*HSP90AA1*	/	70	/	12%	K.DQVANSAFVER.L K.ADLINNLGTIAK.S R.ELISNSSDALDK.I K.EDQTEYLEER.R K.EGLELPEDEEEK.K R.GVVDSEDLPLNISR.E R.NPDDITNEEYGEFYK.S K.TKPIWTRNPDDITNEEYGEFYK.S	−1.5	*	Esi-Trap
Spot 37	P30086	Phosphatidylethanolamine-binding protein 1 (PEBP1)	*PEBP1*	61	177	28%	22%	K.LYTLVLTDPDAPSR.K K.NRPTSISWDGLDSGK.L R.YVWLVYEQDRPLK.C	2	***	MALDI-TOF/TOF
Spot 39	P61160	Actin-related protein 2 (ARP2)	*ACTR2*	61	151	20%	10%	K.HLWDYTFGPEK.L R.GYAFNHSADFETVR.M K.HIVLSGGSTMYPGLPSR.L + oxidation (M)	1.7	**	MALDI-TOF/TOF
Spot 41	P30086	Phosphatidylethanolamine-binding protein 1 (PEBP1)	*PEBP1*	187	238	67%	22%	K.LYTLVLTDPDAPSR.K K.NRPTSISWDGLDSGK.L R.YVWLVYEQDRPLK.C	−1.6	**	MALDI-TOF/TOF
Spot 42	P13010	X-ray repair cross-complementing protein 5 (XRCC5)	*XRCC5*	89	110	12%	4%	R.LFQCLLHR.A R.HIEIFTDLSSR.F R.ANPQVAFPHIK.H	1.8	***	MALDI-TOF/TOF

Table 6: Continued.

Spot number	Swiss-Prot accession number	Protein name	Gene name	Mascot score		Sequence coverage MS	Sequence coverage MS/MS	Peptides	Fold change P1 Res/P1	p value	Instrument
				PMF	MS/MS						
Spot 44	P30041	Peroxiredoxin-6 (PRDX6)	*PRDX6*	122	244	61%	16.5%	R.NFDEILR.V K.LPFPIIDDR.N M.PGGLLLGDVAPNFEANTTVGR.I	−1.6	**	MALDI-TOF/TOF
Spot 45	P11142	Heat-shock cognate 71 kDa protein (HSP7C)	*HSPA8*	/	178	/	28%	K.VEIIANDQGNR.T R.FEELNADLFR.G R.FDDAVVQSDMK.H K.NSLESYAFNMK.A K.CNEIINWLDK.N K.NSLESYAFNMK.A + oxidation (M) K.SQIHDIVLVGGSTR.I R.TTPSYVAFTDTER.L K.SFYPEEVSSMVLTK.M K.NQVAMNPTNTVFDAK.R R.IINEPTAAAIAYGLDK.K K.STAGDTHLGGEDFDNR.M K.TVTNAVVTVPAYFNDSQR.Q K.TVTNAVVTVPAYFNDSQR.Q K.SINPDEAVAYGAAVQAAILSGDK.S	2.1	***	MALDI-TOF/TOF
Spot 46	P04792	Heat-shock protein beta 1 (HSPB1)	*HSPB1*	127	171	51%	13%	R.LFDQAFGLPR.L K.LATQSNEITIPVTFESR.A	1.6	**	MALDI-TOF/TOF
Spot 47	P09936	Ubiquitin carboxyl-terminal hydrolase isozyme L1 (UCHL1)	*UCHL1*	86	220	49%	19%	R.LGVAGQWR.F R.MPFPVNHGASSEDTLLK.D + oxidation (M) K.NEAIQAAHDAVAQEGQCR.V	1.7	**	MALDI-TOF/TOF
Spot 48	P15311	Ezrin (EZRI)	*EZR*	111	134	25%	4%	K.IGFPWSEIR.N R.IQVWHAEHR.G K.KAPDFVFYAPR.L	−1.7	**	MALDI-TOF/TOF
Spot 49	P29401	Transketolase (TKT)	*TKT*	139	222	25%	7%	R.VLDPFTIKPLDR.K R.TVPFCSTFAAFFTR.A R.FIECYIAEQNMVSIAVGCATR.N	−1.5	**	MALDI-TOF/TOF
Spot 50	P42704	Leucine-rich PPR motif-containing protein, mitochondrial (LPPRC)	*LRPPRC*	109	37	15%	1%	K.SNTLPISLQSIR.S K.VIEPQYFGLAYLFR.K	−2.1	***	MALDI-TOF/TOF

Table 6: Continued.

Spot number	Swiss-Prot accession number	Protein name	Gene name	Mascot score		Sequence coverage MS	Sequence coverage MS/MS	Peptides	Fold change P1 Res/P1	p value	Instrument
				PMF	MS/MS						
Spot 51	P23526	Adenosylhomocysteinase (SAHH)	*AHCY*	/	84	/	10%	K.VPAINVNDSVTK.S K.ALDIAENEMPGLMR.M + oxidation (M) K.ALDIAENEMPGLMR.M + 2 oxidation (M) R.ATDVMIAGKVAVVAGYGDVGK.G + oxidation (M)	−1.7	**	Esi-Trap
Spot 52	P07954	Fumaratehydratase, mitochondrial (FUMH)	*FH*	66	158	18%	5%	R.IEYDTFGELK.V R.IYELAAGGTAVGTGLNTR.I	−1.9	***	MALDI-TOF/TOF

Spot numbers match those reported in the representative 2-DE images shown in Figure 3. Accession number in Swiss-Prot/UniprotKB (http://www.uniprot.org/). Fold change (P1 resveratrol-treated cells versus P1 cells) was calculated dividing the average of %V P1 resveratrol-treated cells by the average of %V P1 cells of three independent experiments. *t*-test was performed by GraphPad v4.0 software to determine if the relative change was statistically significant ($p < 0.05$); $^{*}p < 0.05$; $^{**}p < 0.01$; $^{***}p < 0.001$.

Table 7: List of significantly enriched biological processes in CTR versus CTR-Res protein dataset identified by STRING software.

Biological process (GO) Pathway ID	Pathway description	Count in gene set	False discovery rate
GO:0001666	Response to hypoxia	5	0.00305
GO:0034976	Response to endoplasmic reticulum stress	5	0.00305
GO:0042743	Hydrogen peroxide metabolic process	3	0.00305
GO:0061621	Canonical glycolysis	3	0.00305
GO:2000152	Regulation of ubiquitin-specific protease activity	2	0.00305

Table 8: List of significantly enriched molecular functions in CTR versus CTR-Res protein dataset identified by STRING software.

Molecular function (GO) Pathway ID	Pathway description	Count in gene set	False discovery rate
GO:0051920	Peroxiredoxin activity	3	8.22e–05
GO:0003723	RNA binding	10	0.000179
GO:0044822	Poly(A) RNA binding	9	0.000179
GO:0005515	Protein binding	13	0.00361
GO:0008379	Thioredoxin peroxidase activity	2	0.00361

Table 9: List of significantly enriched molecular functions in P1 versus P1-Res protein dataset identified by STRING software.

Molecular function (GO) Pathway ID	Pathway description	Count in gene set	False discovery rate
GO:0019899	Enzyme binding	11	0.000172
GO:0031625	Ubiquitin protein ligase binding	6	0.000172
GO:0044822	Poly(A) RNA binding	10	0.000228
GO:0005515	Protein binding	15	0.00801
GO:0051920	Peroxiredoxin activity	2	0.0162

differentially expressed in CTR and P1 fibroblasts and listed in Tables 5 and 6. These datasets were functionally annotated using the software STRING. The most enriched GO terms of molecular functions and biological processes are depicted in Tables 7, 8, and 9. After resveratrol treatment, CTR fibroblasts showed changes in the protein level associated with peroxiredoxin activity (Table 8). This is in line with previous observations that linked resveratrol action with the modulation of enzymes involved in the ROS metabolism [28, 47]. The effect of resveratrol treatment on proteins with peroxiredoxin activity was also observed, to a lesser extent, in P1 fibroblasts (Table 9). These results were validated by Western blotting analysis (Figure 4). Consistent with MS data, P1 resveratrol-treated cells expressed higher levels of PXR1 and lower levels of PXR6 compared to untreated cells. By contrast, CTR cells showed a trend towards a lower PXR1 and higher PXR6 expression in resveratrol-treated cells compared to untreated cells.

3.3. Modulation of Redox Status of Sulfhydryl Groups upon Treatment with Resveratrol. Mammalian cells have a well-defined set of antioxidant enzymes, which includes superoxide dismutase, catalase, glutathione peroxidases, and peroxiredoxins, ubiquitous enzymes that have emerged as an important and widespread peroxide and peroxynitrite scavenging system [48]. PD is characterized by changes in oxidative balance, and the loss of glutathione (GSH) level is one of the earliest biochemical changes detectable in PD [49]. GSH is a major component of cellular antioxidant system, whose reduced and oxidized forms (GSH and GSSG) act in concert with other redox-active compounds (e.g., NAD(P)H) to regulate and maintain cellular redox status [50]. Glutathione depletion may occur as a defect of its synthesis, as well as its metabolism, when the redox state of the cells is altered. In these conditions, the GSSG produced can be reduced back to GSH, but the formation and export of GSH conjugates could lead to GSH depletion. As shown in Figure 5, total GSH level was significantly lower in P1 fibroblasts as compared to CTR cells (Figure 5(a)). However, treatment of P1 cells with 25 μM Res for 24 h resulted in a significant increase of GSH content (Figure 5(c)), whereas the treatment had no effect on the GSH level in CTR cells (Figure 5(b)). The analysis of oxidized glutathione (GSSG) revealed an increase of GSSG/GSH ratio in P1 cells (Figure 5(d)), which was partially reversed after resveratrol treatment, though the value

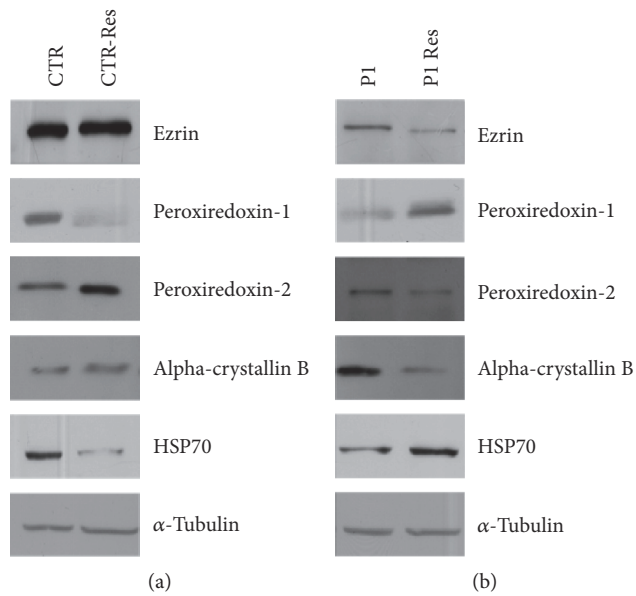

Figure 4: Western blot analysis of CTR and P1 fibroblasts treated with resveratrol. CTR and P1 cells were treated with resveratrol at the concentration of 25 μM for 24 h. Proteins were separated by SDS-PAGE and probed with the following antibodies: ezrin (1 : 2000, Santa Cruz, sc-20773), alpha B crystallin (1 : 1000, Proteintech, 15808-1-AP), peroredoxin-1 (1 : 2000, Santa Cruz, sc-7381), peroredoxin-2 (1 : 2000, Santa Cruz, sc-33572), peroredoxin-6 (1 : 2000, Santa Cruz, sc-393024), and heat-shock protein (HSP70) (1 : 2000, Sigma, H51747). α-Tubulin was used as loading control (1 : 4000, Santa Cruz, sc-23948). This image is representative of three independent experiments.

did not reach a statistical significance ($p = 0.06$) (Figure 5(f)). These data are consistent with the observation that resveratrol could act positively on glutathione homeostasis by increasing the activity and the expression, through NRF2, of glutamate cysteine ligase (GCL), the rate-limiting enzyme for de novo GSH synthesis that catalyzes the formation of γ-glutamylcysteine [51, 52].

Changes in GSH metabolism prompted us to investigate the redox state of thiol groups of protein (P-SH). The thiol groups of the protein are characterized by a reversible formation of a mixed disulfide bond between two cysteines and with glutathione (glutathionylation), which controls correct protein folding and represents an emergent mechanism of posttranslational modification to regulate signal transduction [53]. Quantitative analysis of free sulfhydryl groups of protein (P-SH) in total cellular lysate reveals higher levels of P-SH in P1 cells respect to CTR cells (Figure 6(a)), and this result could reflect the high steady-state cellular redox state ($NADH/NAD^+$) measured in these cells [28]. As expected, resveratrol treatment of CTR cells results in a significant increase of P-SH (Figure 6(b)), reflecting the antioxidant capacity of the employed polyphenol [54]. The P-SH increase could be potentially related to the decreased level of two disulfide isomerases, PDIA3 and P4HB, as detected by the proteomic analysis (Table 6). These proteins check the oxidation (formation), reduction (break down), and isomerization (rearrangement) of protein disulfide bonds via disulfide interchange activity. PDIs also have a chaperone activity by binding to misfolded proteins to prevent them from aggregating and targeting misfolded proteins for degradation [55].

Interestingly, treatment of P1 cells with resveratrol resulted in the decrease of P-SH content reflecting the resveratrol enhancement, in an AMPK-dependent manner, of the $NAD^+/NADH$ ratio [28], capable of restoring the basal level of CTR fibroblasts (Figure 6(c)).

Therefore, while the antioxidant effects of resveratrol are predominant in the CTR cells [22, 26] the capacity of this natural compound to modulate additional pathways is more evident in P1 cells [28, 51], including those regulating the glutathionylation status of proteins.

The redox state of thiol groups is related to glutathionylation of proteins which occurs in unstressed cells under physiological conditions as well as during cellular redox defense [56]. The glutathionylation is either a spontaneous or enzymatically driven finely controlled reversible process, which can involve both the GSH and GSSG [57]. To investigate the modifications in protein glutathionylated residues (PSSG), whole proteins were separated under nonreducing conditions. Western blotting analysis with an antibody against glutathionylated residues revealed, as expected, many protein bands (Figure 6(d)). Densitometric analysis showed a lower level of proteins detected by anti-GSH antibody in P1 cells compared to CTR cells (Figure 6(e)). Furthermore, resveratrol treatment resulted in a decrease of bands detected in control cells and, on the contrary, in an increase of bands detected in P1 cells (Figure 6(e)). These results (Figures 6(d) and 6(e)) are in agreement with the specific changes in P-SH levels (Figures 6(a), 6(b), and 6(c)), considering that a P-SH increase corresponds to a P-SSG decrease. Many enzymes are involved in the balance of the redox state of the SH groups, among which glutathione transferases (GST) catalyze protein glutathionylation [58]. Proteomic analysis reveals that resveratrol treatment of P1 cells leads to an increase of the glutathione S-transferase omega I (GSTO1) expression (Table 6), a protein possibly responsible for reversing the deregulation of GSH system and the redox state

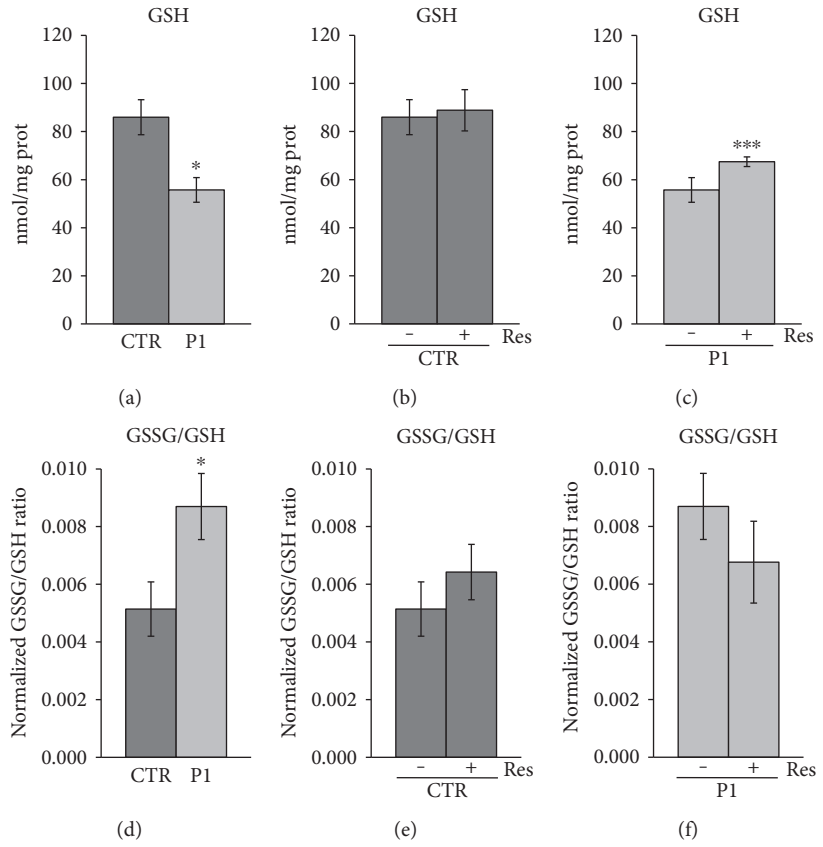

Figure 5: Effect of resveratrol treatment on GSH and GSSG content in patient and control cells. Primary fibroblasts from patient (P1) and control fibroblasts (CTR) were grown as specified in *Materials and Methods*. As indicated, cells were incubated with 25 μM resveratrol for 24 hours (Res). GSH and GSSG content were determined in total cellular lysate. (a) The histogram represents the mean values of GSH basal level ± SEM of different experiments ($n = 3$). (b, c) Effect of Res treatment on GSH content in CTR and P1 cells. The values are means ± SEM of different experiments ($n = 3$). (d) The histogram represents the mean values of normalized GSSG/GSH ratio ± SEM of different experiments ($n = 3$). (e, f) Effect of Res treatment on GSSG/GSH ratio in CTR and P1 cells. The values are means ± SEM of different experiments ($n = 3$). p value was determined by Student's t-test, $^{*}p < 0.05$, $^{***}p < 0.001$.

of protein sulfhydryl groups. In a *Drosophila* model of PD, upregulation of *Drosophila melanogaster* GST Sigma 1 (DmGSTO1) suppressed phenotypes caused by parkin loss of function, including the degeneration of DA neurons and muscle [59].

Deglutathionylation is catalyzed by thiol-disulfide oxidoreductase enzymes, such as glutaredoxin (GRX), thioredoxin (Trx), and protein disulfide isomerase (PDI). PRXs are also involved in the control of protein glutathionylation. Their primary role is associated to H_2O_2 detoxification, a process in which the active cysteines of PRX are oxidized. The recycling step of PRX involves the reduction of the disulfide bridge by the thioredoxin system, utilizing NADPH as a source of reducing power [60].

Overall, these data suggest that in P1 cells, there is a deregulation of GSH homeostasis and consequently of the redox state of sulfhydryl groups. The low availability of GSH and deregulation of protein folding processes in the ER, the first intracellular compartment for protein processing such as disulfide bond formation [61], could explain the high level of P-SH and the low level of glutathionylated protein observed P1 cells. In our previous study, proteomic analysis revealed a low level of PRDX4 [17], an ER-resident protein, in P1 compared to CTR cells. In the present study, a higher level of PRDX1, a cytosolic protein with antioxidant properties [62], was detected in P1 compared to CTR cells. Both peroxidases use thioredoxin as physiological reductant [48]. Resveratrol treatment restored GSH level and induced normal homeostasis of protein thiol groups in P1 cells. Moreover, in P1 cells, resveratrol treatment induced an upregulation of PRX1 and a downregulation of PRDX6, which uses glutathione as the physiological reductant, saving the amount of the glutathione for other activities.

3.4. Modulation of Chaperone Proteins upon Treatment with Resveratrol. Resveratrol, apart from being an effective scavenger of free radicals, may directly stimulate the cell defense against stress response through cellular chaperone in early time treatment [63]. Some members of the HSPs are differentially expressed in CTR and P1 samples after resveratrol treatment (Tables 5 and 6). Recently, many studies provided evidence that AMPK is a key mediator of the metabolic benefits produced by resveratrol, upstream of SIRT1 activation [64–67]. In the PD cellular model used in our previous study, we have shown that resveratrol regulates energy homeostasis through activation of AMPK and SIRT1 and raises mRNA

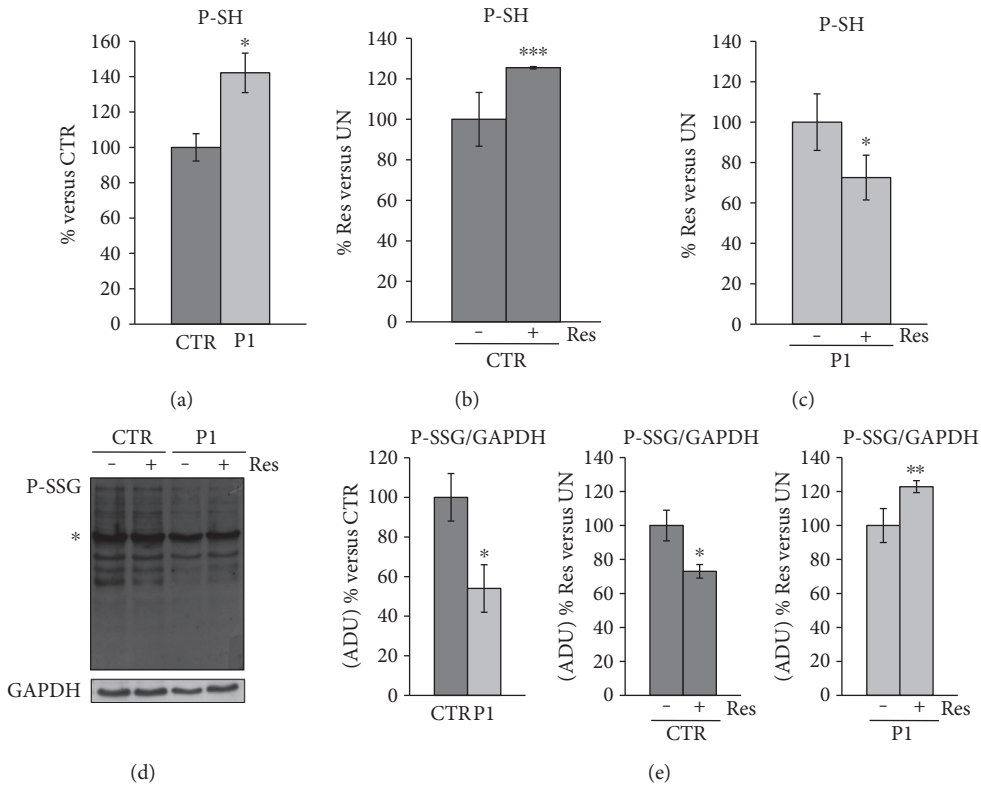

Figure 6: Effect of resveratrol treatment on free thiol groups (P-SH) of protein and glutathionylation in patient and control cells. Primary fibroblasts from patient (P1) and control fibroblasts (CTR) were grown as specified in *Materials and Methods*. As indicated, cells were incubated with 25 μM resveratrol for 24 hours (Res). The P-SH levels were measured in total cellular lysate. (a) The histogram represents the percentage changes with respect to P-SH content of CTR. (b, c) The histograms represent the percentage changes with respect to P-SH content of CTR and P1 untreated cells (UN). (a, b, c) The values are means ± SEM of different experiments ($n = 3$). (d) A representative image of glutathionylated proteins. Proteins of cellular lysate were loaded on 12% SDS-PAGE, under nonreducing conditions, transferred to nitrocellulose membranes, and immunoblotted with the antibody against GSH (P-SSG). Protein loading was assessed with the GAPDH antibody. (e) Densitometric analysis of PSSG proteins, normalized to GAPDH, was performed considering all bands immune-revealed by the GSH antibody, excluding the protein band marked with an asterisk. This band is not specific; it also appears in SDS-PAGE under reducing conditions (data not shown). The histograms represent the percentage changes of ADU express as P-SSG/GAPDH ratio. The values are means ± SEM of different experiments ($n = 3$). p value determined by Student's t-test, $^{*}p < 0.05$, $^{**}p < 0.01$, $^{***}p < 0.001$.

expression of a number of PGC-1α's target genes resulting in enhanced mitochondrial oxidative function, likely related to a decrease of oxidative stress and to an increase of mitochondrial biogenesis [28]. SIRT1 can deacetylate and activate heat-shock factor 1 (HSF1), which affects transcription of molecular chaperones [68].

In addition to protein refolding or degradation, HSPs also support a specialized autophagy mechanism called chaperone-mediated autophagy (CMA). This is a highly selective and constitutive subtype of autophagy that utilizes chaperone proteins and lysosomal receptors to directly target proteins into the lysosomal lumen for their degradation, under both physiological and pathological conditions to maintain cellular homeostasis [69–73]. There are multiple lines of evidence for the impairment of CMA activity in both familial and sporadic PD [74, 75]. In the CMA process, which is activated after macroautophagy and activation persists for days [76], the heat-shock cognate 70 (Hsc70/HSPA8), a constitutive chaperone, binds target proteins and transports them to the surface of endoplasmic reticulum where it specifically binds to lysosomal receptor protein LAMP-2A and HSP90, an inducible chaperone. Resveratrol treatment of P1 cells induces increased expression of both HSPA8 and HSP90, possibly leading to CMA. Interestingly, we have shown in our previous study that resveratrol treatment caused an enhanced macroautophagic flux through activation of an LC3-independent pathway [28].

Furthermore, concerning the behaviour of alpha-crystallin B chain (CRYAB), which belongs to the chaperone family whose main role is to bind improperly folded proteins to prevent protein aggregation [77], we have found that the treatment with resveratrol increased the expression of CRYAB in CRT cells and, on the contrary, induced a decreased expression in P1 cells, reestablishing the levels of control cells (Tables 5 and 7) (Figure 4).

HSPs are proving to be a therapeutic target in neurodegenerative disorders because the pathogenesis of these diseases is thought to be related to an abnormal increase of unfolded protein response (UPR), failure of UPS, and protein misfolding and/or aggregation [78] and their regulation could be mediated by polyphenols as resveratrol [79, 80].

3.5. Modulation of Metabolic Proteins upon Treatment with Resveratrol. As already described, resveratrol can carry out its functions by activating AMPK, a crucial cellular energy sensor. Once activated, it promotes ATP production by increasing the activity or expression of proteins involved in catabolism while conserving ATP by switching off biosynthetic pathways [81]. A significant number of proteins differentially expressed after resveratrol treatment are involved in energy metabolism pathways. We observed an upregulation of several proteins related to glycolysis in resveratrol-treated CTR cells. These include phosphoglycerate mutase 1 (PGAM1), triose phosphate isomerase (TPIS), and alpha enolase (ENOA). A changed rate of glycolysis may affect substrate levels for the tricarboxylic acid cycle and subsequent oxidative phosphorylation, in turn influencing ATP levels. Furthermore, we observed an upregulation of the cytoplasmic isoform of malate dehydrogenase (MDHc) in resveratrol-treated P1 cells. MDHc is a metabolic isoform involved in the malate-aspartate shuttle that aids in the transfer of reducing equivalents of NADH into the mitochondria. This is in line with the low steady-state cellular ratio NADH/NAD^+ present in resveratrol-treated P1 cells, which indicates the enhancement of oxidative capacity attested by the increase in mitochondrial ATP production [28].

All these data confirm and extend our previous observations on the metabolic dysfunction of P1 fibroblasts, which show a deregulation of pathways involved in key cellular processes such as protein folding, protein degradation, and cellular redox balance. The analysis of differentially expressed proteins identified after resveratrol treatment of CTR and P1 cells reveals the great ability of resveratrol to act on protein expression modifying pathway and reversing the molecular defects in P1 fibroblast cells.

4. Conclusions

P1 fibroblasts are characterized by a dysregulated expression of proteins linked to biological processes regarding cell movement or subcellular component, assembly and protein folding, calcium ion binding, unfolded protein binding, and redox homeostasis. In this study, we show the biological effects of resveratrol acting through the modulation of the expression of proteins involved in protecting cells from the damaging effects of ROS, in protein refolding or degradation, and, specifically, in chaperone-mediated autophagy.

Overall, the complex proteome alterations shown in this ex vivo model of PD could provide further insights into the pathogenic processes involved in the disease. Importantly, the elucidation of the biomarkers might provide new therapeutic targets for the treatment and prevention of PD. Evidences are emerging to support the potential of small bioactive molecules, as resveratrol, against neurodegenerative disorders, to control and modulate ROS and abnormal protein.

Conflicts of Interest

The authors declare that they have no conflicts of interest.

Acknowledgments

This work was supported by local grants of the University of Bari to Tiziana Cocco, by FIR 2015-2018 H6SH8W9 from Apulia Region to Consiglia Pacelli, by FIRB-MERIT 2008 no. RBNE08HWLZ012 to Marco Di Paola, and by the National Operational Programme for Research and Competitiveness (PONREC) 'RINOVATIS' (PON02_00563_3448479) to Michele Maffia. The authors gratefully acknowledge funding from the Apulia Regional Cluster project "SISTEMA" project code T7WGSJ3.

References

[1] L. Hirsch, N. Jette, A. Frolkis, T. Steeves, and T. Pringsheim, "The incidence of Parkinson's disease: a systematic review and meta-analysis," *Neuroepidemiology*, vol. 46, no. 4, pp. 292–300, 2016.

[2] L. V. Kalia and A. E. Lang, "Parkinson's disease," *Lancet (London England)*, vol. 386, no. 9996, pp. 896–912, 2015.

[3] C. Klein and M. G. Schlossmacher, "The genetics of Parkinson disease: implications for neurological care," *Nature Clinical Practice. Neurology*, vol. 2, no. 3, pp. 136–146, 2006.

[4] T. Kitada, S. Asakawa, N. Hattori et al., "Mutations in the parkin gene cause autosomal recessive juvenile parkinsonism," *Nature*, vol. 392, no. 6676, pp. 605–608, 1998.

[5] S. Biskup, M. Gerlach, A. Kupsch et al., "Genes associated with Parkinson syndrome," *Journal of Neurology*, vol. 255, Supplement 5, pp. 8–17, 2008.

[6] S. Lesage and A. Brice, "Parkinson's disease: from monogenic forms to genetic susceptibility factors," *Human Molecular Genetics*, vol. 18, no. R1, pp. R48–R59, 2009.

[7] D. Narendra, A. Tanaka, D.-F. Suen, and R. J. Youle, "Parkin is recruited selectively to impaired mitochondria and promotes their autophagy," *The Journal of Cell Biology*, vol. 183, no. 5, pp. 795–803, 2008.

[8] C. Vives-Bauza, C. Zhou, Y. Huang et al., "PINK1-dependent recruitment of Parkin to mitochondria in mitophagy," *Proceedings of the National Academy of Sciences of the United States of America*, vol. 107, no. 1, pp. 378–383, 2010.

[9] B. C. Hammerling, R. H. Najor, M. Q. Cortez et al., "A Rab5 endosomal pathway mediates Parkin-dependent mitochondrial clearance," *Nature Communications*, vol. 8, article 14050, 2017.

[10] J. J. Palacino, D. Sagi, M. S. Goldberg et al., "Mitochondrial dysfunction and oxidative damage in *parkin*-deficient mice," *The Journal of Biological Chemistry*, vol. 279, no. 18, pp. 18614–18622, 2004.

[11] N. C. Chan, A. M. Salazar, A. H. Pham et al., "Broad activation of the ubiquitin-proteasome system by Parkin is critical for mitophagy," *Human Molecular Genetics*, vol. 20, no. 9, pp. 1726–1737, 2011.

[12] N. C. Chan and D. C. Chan, "Parkin uses the UPS to ship off dysfunctional mitochondria," *Autophagy*, vol. 7, no. 7, pp. 771-772, 2011.

[13] C. Pacelli, D. De Rasmo, A. Signorile et al., "Mitochondrial defect and PGC-1α dysfunction in *parkin*-associated familial Parkinson's disease," *Biochimica et Biophysica Acta (BBA) - Molecular Basis of Disease*, vol. 1812, no. 8, pp. 1041–1053, 2011.

[14] M. Periquet, O. Corti, S. Jacquier, and A. Brice, "Proteomic analysis of parkin knockout mice: alterations in energy metabolism, protein handling and synaptic function," *Journal of Neurochemistry*, vol. 95, no. 5, pp. 1259–1276, 2005.

[15] P. G. Unschuld, J. Dächsel, F. Darios et al., "Parkin modulates gene expression in control and ceramide-treated PC12 cells," *Molecular Biology Reports*, vol. 33, no. 1, pp. 13–32, 2006.

[16] E. J. Davison, K. Pennington, C. C. Hung et al., "Proteomic analysis of increased Parkin expression and its interactants provides evidence for a role in modulation of mitochondrial function," *Proteomics*, vol. 9, no. 18, pp. 4284–4297, 2009.

[17] R. Lippolis, R. A. Siciliano, C. Pacelli et al., "Altered protein expression pattern in skin fibroblasts from *parkin*-mutant early-onset Parkinson's disease patients," *Biochimica et Biophysica Acta (BBA) - Molecular Basis of Disease*, vol. 1852, no. 9, pp. 1960–1970, 2015.

[18] S. Lobasso, P. Tanzarella, D. Vergara, M. Maffia, T. Cocco, and A. Corcelli, "Lipid profiling of *parkin*-mutant human skin fibroblasts," *Journal of Cellular Physiology*, vol. 232, no. 12, pp. 3540–3551, 2017.

[19] M. Pallàs, D. Porquet, A. Vicente, and C. Sanfeliu, "Resveratrol: new avenues for a natural compound in neuroprotection," *Current Pharmaceutical Design*, vol. 19, no. 38, pp. 6726–6731, 2013.

[20] J. Burns, T. Yokota, H. Ashihara, M. E. J. Lean, and A. Crozier, "Plant foods and herbal sources of resveratrol," *Journal of Agricultural and Food Chemistry*, vol. 50, no. 11, pp. 3337–3340, 2002.

[21] S. Das and D. K. Das, "Anti-inflammatory responses of resveratrol," *Inflammation & Allergy Drug Targets*, vol. 6, no. 3, pp. 168–173, 2007.

[22] M. Kairisalo, A. Bonomo, A. Hyrskyluoto et al., "Resveratrol reduces oxidative stress and cell death and increases mitochondrial antioxidants and XIAP in PC6.3-cells," *Neuroscience Letters*, vol. 488, no. 3, pp. 263–266, 2011.

[23] J. A. Baur and D. A. Sinclair, "Therapeutic potential of resveratrol: the in vivo evidence," *Nature Reviews Drug Discovery*, vol. 5, no. 6, pp. 493–506, 2006.

[24] A. Y. Sun, Q. Wang, A. Simonyi, and G. Y. Sun, "Resveratrol as a therapeutic agent for neurodegenerative diseases," *Molecular Neurobiology*, vol. 41, no. 2-3, pp. 375–383, 2010.

[25] F. Jin, Q. Wu, Y.-F. Lu, Q.-H. Gong, and J.-S. Shi, "Neuroprotective effect of resveratrol on 6-OHDA-induced Parkinson's disease in rats," *European Journal of Pharmacology*, vol. 600, no. 1–3, pp. 78–82, 2008.

[26] M. M. Khan, A. Ahmad, T. Ishrat et al., "Resveratrol attenuates 6-hydroxydopamine-induced oxidative damage and dopamine depletion in rat model of Parkinson's disease," *Brain Research*, vol. 1328, pp. 139–151, 2010.

[27] D. D. Lofrumento, G. Nicolardi, A. Cianciulli et al., "Neuroprotective effects of resveratrol in an MPTP mouse model of Parkinson's-like disease: possible role of SOCS-1 in reducing pro-inflammatory responses," *Innate Immunity*, vol. 20, no. 3, pp. 249–260, 2014.

[28] A. Ferretta, A. Gaballo, P. Tanzarella et al., "Effect of resveratrol on mitochondrial function: implications in parkin-associated familiar Parkinson's disease," *Biochimica et Biophysica Acta (BBA) - Molecular Basis of Disease*, vol. 1842, no. 7, pp. 902–915, 2014.

[29] D. Vergara, P. Simeone, P. del Boccio et al., "Comparative proteome profiling of breast tumor cell lines by gel electrophoresis and mass spectrometry reveals an epithelial mesenchymal transition associated protein signature," *Molecular BioSystems*, vol. 9, no. 6, pp. 1127–1138, 2013.

[30] D. Vergara, P. Simeone, D. Latorre et al., "Proteomics analysis of E-cadherin knockdown in epithelial breast cancer cells," *Journal of Biotechnology*, vol. 202, pp. 3–11, 2015.

[31] D. Vergara, P. Simeone, S. De Matteis et al., "Comparative proteomic profiling of Hodgkin lymphoma cell lines," *Molecular BioSystems*, vol. 12, no. 1, pp. 219–232, 2016.

[32] M. Chevallet, H. Diemer, S. Luche, A. van Dorsselaer, T. Rabilloud, and E. Leize-Wagner, "Improved mass spectrometry compatibility is afforded by ammoniacal silver staining," *Proteomics*, vol. 6, no. 8, pp. 2350–2354, 2006.

[33] G. L. Ellman, "Tissue sulfhydryl groups," *Archives of Biochemistry and Biophysics*, vol. 82, no. 1, pp. 70–77, 1959.

[34] D. Vergara, M. M. Ferraro, M. Cascione et al., "Cytoskeletal alterations and biomechanical properties of *parkin*-mutant human primary fibroblasts," *Cell Biochemistry and Biophysics*, vol. 71, no. 3, pp. 1395–1404, 2015.

[35] R. J. Ellis, "Molecular chaperones: assisting assembly in addition to folding," *Trends in Biochemical Sciences*, vol. 31, no. 7, pp. 395–401, 2006.

[36] J. Becker and E. A. Craig, "Heat-shock proteins as molecular chaperones," *European Journal of Biochemistry*, vol. 219, no. 1-2, pp. 11–23, 1994.

[37] K. Richter, M. Haslbeck, and J. Buchner, "The heat shock response: life on the verge of death," *Molecular Cell*, vol. 40, no. 2, pp. 253–266, 2010.

[38] J. H. Hoffmann, K. Linke, P. C. F. Graf, H. Lilie, and U. Jakob, "Identification of a redox-regulated chaperone network," *The EMBO Journal*, vol. 23, no. 1, pp. 160–168, 2004.

[39] P. Bishop, D. Rocca, and J. M. Henley, "Ubiquitin C-terminal hydrolase L1 (UCH-L1): structure, distribution and roles in brain function and dysfunction," *The Biochemical Journal*, vol. 473, no. 16, pp. 2453–2462, 2016.

[40] Z. Liu, S. Hamamichi, B. D. Lee et al., "Inhibitors of LRRK2 kinase attenuate neurodegeneration and Parkinson-like phenotypes in *Caenorhabditis elegans* and *Drosophila* Parkinson's disease models," *Human Molecular Genetics*, vol. 20, no. 20, pp. 3933–3942, 2011.

[41] J. E. McKeon, D. Sha, L. Li, and L.-S. Chin, "Parkin-mediated K63-polyubiquitination targets ubiquitin C-terminal hydrolase L1 for degradation by the autophagy-lysosome system," *Cellular and Molecular Life Sciences*, vol. 72, no. 9, pp. 1811–1824, 2015.

[42] S. Matus, L. H. Glimcher, and C. Hetz, "Protein folding stress in neurodegenerative diseases: a glimpse into the ER," *Current Opinion in Cell Biology*, vol. 23, no. 2, pp. 239–252, 2011.

[43] C. Hetz and B. Mollereau, "Disturbance of endoplasmic reticulum proteostasis in neurodegenerative diseases," *Nature Reviews Neuroscience*, vol. 15, no. 4, pp. 233–249, 2014.

[44] R. G. Fehon, A. I. McClatchey, and A. Bretscher, "Organizing the cell cortex: the role of ERM proteins," *Nature Reviews Molecular Cell Biology*, vol. 11, no. 4, pp. 276–287, 2010.

[45] C. Ramassamy, "Emerging role of polyphenolic compounds in the treatment of neurodegenerative diseases: a review of their intracellular targets," *European Journal of Pharmacology*, vol. 545, no. 1, pp. 51–64, 2006.

[46] A. Rajeswari and M. Sabesan, "Inhibition of monoamine oxidase-B by the polyphenolic compound, curcumin and its metabolite tetrahydrocurcumin, in a model of Parkinson's disease induced by MPTP neurodegeneration in mice," *Inflammopharmacology*, vol. 16, no. 2, pp. 96–99, 2008.

[47] S. S. Leonard, C. Xia, B. H. Jiang et al., "Resveratrol scavenges reactive oxygen species and effects radical-induced cellular responses," *Biochemical and Biophysical Research Communications*, vol. 309, no. 4, pp. 1017–1026, 2003.

[48] P. A. Karplus, "A primer on peroxiredoxin biochemistry," *Free Radical Biology & Medicine*, vol. 80, pp. 183–190, 2015.

[49] H. L. Martin and P. Teismann, "Glutathione–a review on its role and significance in Parkinson's disease," *The FASEB journal*, vol. 23, no. 10, pp. 3263–3272, 2009.

[50] F. Q. Schafer and G. R. Buettner, "Redox environment of the cell as viewed through the redox state of the glutathione disulfide/glutathione couple," *Free Radical Biology & Medicine*, vol. 30, no. 11, pp. 1191–1212, 2001.

[51] H. Zhang, A. Shih, A. Rinna, and H. J. Forman, "Resveratrol and 4-hydroxynonenal act in concert to increase glutamate cysteine ligase expression and glutathione in human bronchial epithelial cells," *Archives of Biochemistry and Biophysics*, vol. 481, no. 1, pp. 110–115, 2009.

[52] C. Chen, X. Jiang, Y. Lai, Y. Liu, and Z. Zhang, "Resveratrol protects against arsenic trioxide-induced oxidative damage through maintenance of glutathione homeostasis and inhibition of apoptotic progression," *Environmental and Molecular Mutagenesis*, vol. 56, no. 3, pp. 333–346, 2015.

[53] B. G. Hill and A. Bhatnagar, "Protein S-glutathiolation: redox-sensitive regulation of protein function," *Journal of Molecular and Cellular Cardiology*, vol. 52, no. 3, pp. 559–567, 2012.

[54] J. A. Santos, G. S. G. de Carvaho, V. Oliveira, N. R. B. Raposo, and A. D. da Silva, "Resveratrol and analogues: a review of antioxidant activity and applications to human health," *Recent Patents on Food, Nutrition & Agriculture*, vol. 5, no. 2, pp. 144–153, 2013.

[55] A. M. Benham, "The protein disulfide isomerase family: key players in health and disease," *Antioxidants & Redox Signaling*, vol. 16, no. 8, pp. 781–789, 2012.

[56] I. Dalle-Donne, G. Colombo, N. Gagliano et al., "S-glutathiolation in life and death decisions of the cell," *Free Radical Research*, vol. 45, no. 1, pp. 3–15, 2011.

[57] D. Popov, "Protein S-glutathionylation: from current basics to targeted modifications," *Archives of Physiology and Biochemistry*, vol. 120, no. 4, pp. 123–130, 2014.

[58] D. M. Townsend, Y. Manevich, L. He, S. Hutchens, C. J. Pazoles, and K. D. Tew, "Novel role for glutathione S-transferase pi. Regulator of protein S-glutathionylation following oxidative and nitrosative stress," *The Journal of Biological Chemistry*, vol. 284, no. 1, pp. 436–445, 2009.

[59] K. Kim, S.-H. Kim, J. Kim, H. Kim, and J. Yim, "Glutathione s-transferase omega 1 activity is sufficient to suppress neurodegeneration in a Drosophila model of Parkinson disease," *The Journal of Biological Chemistry*, vol. 287, no. 9, pp. 6628–6641, 2012.

[60] N. P. Hoyle and J. S. O'Neill, "Oxidation-reduction cycles of peroxiredoxin proteins and nontranscriptional aspects of timekeeping," *Biochemistry (Mosc)*, vol. 54, no. 2, pp. 184–193, 2015.

[61] D. M. Townsend, "S-glutathionylation: indicator of cell stress and regulator of the unfolded protein response," *Molecular Interventions*, vol. 7, no. 6, pp. 313–324, 2007.

[62] E.-M. Hanschmann, J. R. Godoy, C. Berndt, C. Hudemann, and C. H. Lillig, "Thioredoxins, glutaredoxins, and peroxiredoxins–molecular mechanisms and health significance: from cofactors to antioxidants to redox signaling," *Antioxidants & Redox Signaling*, vol. 19, no. 13, pp. 1539–1605, 2013.

[63] A. Putics, E. M. Végh, P. Csermely, and C. Soti, "Resveratrol induces the heat-shock response and protects human cells from severe heat stress," *Antioxidants & Redox Signaling*, vol. 10, no. 1, pp. 65–75, 2008.

[64] J. A. Baur, K. J. Pearson, N. L. Price et al., "Resveratrol improves health and survival of mice on a high-calorie diet," *Nature*, vol. 444, no. 7117, pp. 337–342, 2006.

[65] C. Cantó and J. Auwerx, "AMP-activated protein kinase and its downstream transcriptional pathways," *Cellular and Molecular Life Sciences*, vol. 67, no. 20, pp. 3407–3423, 2010.

[66] B. Dasgupta and J. Milbrandt, "Resveratrol stimulates AMP kinase activity in neurons," *Proceedings of the National Academy of Sciences of the United States of America*, vol. 104, no. 17, pp. 7217–7222, 2007.

[67] C. E. Park, M. J. Kim, J. H. Lee et al., "Resveratrol stimulates glucose transport in C2C12 myotubes by activating AMP-activated protein kinase," *Experimental & Molecular Medicine*, vol. 39, no. 2, pp. 222–229, 2007.

[68] S. D. Westerheide, J. Anckar, S. M. Stevens, L. Sistonen, and R. I. Morimoto, "Stress-inducible regulation of heat shock factor 1 by the deacetylase SIRT1," *Science*, vol. 323, no. 5917, pp. 1063–1066, 2009.

[69] S. Kaushik and A. M. Cuervo, "Chaperone-mediated autophagy," *Methods in Molecular Biology (Clifton, N.J.)*, vol. 445, pp. 227–244, 2008.

[70] U. Bandyopadhyay, S. Kaushik, L. Varticovski, and A. M. Cuervo, "The chaperone-mediated autophagy receptor organizes in dynamic protein complexes at the lysosomal membrane," *Molecular and Cellular Biology*, vol. 28, no. 18, pp. 5747–5763, 2008.

[71] A. K. Rout, M.-P. Strub, G. Piszczek, and N. Tjandra, "Structure of transmembrane domain of lysosome-associated membrane protein type 2a (LAMP-2A) reveals key features for substrate specificity in chaperone-mediated autophagy," *The Journal of Biological Chemistry*, vol. 289, no. 51, pp. 35111–35123, 2014.

[72] R. Kiffin, C. Christian, E. Knecht, and A. M. Cuervo, "Activation of chaperone-mediated autophagy during oxidative stress," *Molecular Biology of the Cell*, vol. 15, no. 11, pp. 4829–4840, 2004.

[73] A. C. Massey, S. Kaushik, G. Sovak, R. Kiffin, and A. M. Cuervo, "Consequences of the selective blockage of chaperone-mediated autophagy," *Proceedings of the National Academy of Sciences of the United States of America*, vol. 103, no. 15, pp. 5805–5810, 2006.

[74] L. Alvarez-Erviti, M. C. Rodriguez-Oroz, J. M. Cooper et al., "Chaperone-mediated autophagy markers in Parkinson disease brains," *Archives of Neurology*, vol. 67, no. 12, pp. 1464–1472, 2010.

[75] K. E. Murphy, A. M. Gysbers, S. K. Abbott et al., "Lysosomal-associated membrane protein 2 isoforms are differentially affected in early Parkinson's disease," *Movement Disorders: Official Journal of the Movement Disorder Society*, vol. 30, no. 12, pp. 1639–1647, 2015.

[76] A. M. Cuervo, E. Knecht, S. R. Terlecky, and J. F. Dice, "Activation of a selective pathway of lysosomal proteolysis in rat liver by prolonged starvation," *The American Journal of Physiology*, vol. 269, no. 5, Part 1, pp. C1200–C1208, 1995.

[77] S. Yamamoto, A. Yamashita, N. Arakaki, H. Nemoto, and T. Yamazaki, "Prevention of aberrant protein aggregation by anchoring the molecular chaperone αB-crystallin to the endoplasmic reticulum," *Biochemical and Biophysical Research Communications*, vol. 455, no. 3-4, pp. 241–245, 2014.

[78] C. Sõti, E. Nagy, Z. Giricz, L. Vígh, P. Csermely, and P. Ferdinandy, "Heat shock proteins as emerging therapeutic targets," *British Journal of Pharmacology*, vol. 146, no. 6, pp. 769–780, 2005.

[79] S. Han, J.-R. Choi, K. Soon Shin, and S. J. Kang, "Resveratrol upregulated heat shock proteins and extended the survival of G93A-SOD1 mice," *Brain Research*, vol. 1483, pp. 112–117, 2012.

[80] M. Currò, A. Trovato-Salinaro, A. Gugliandolo et al., "Resveratrol protects against homocysteine-induced cell damage via cell stress response in neuroblastoma cells," *Journal of Neuroscience Research*, vol. 93, no. 1, pp. 149–156, 2015.

[81] D. G. Hardie, F. A. Ross, and S. A. Hawley, "AMPK: a nutrient and energy sensor that maintains energy homeostasis," *Nature Reviews Molecular Cell Biology*, vol. 13, no. 4, pp. 251–262, 2012.

Hindawi
Oxidative Medicine and Cellular Longevity
Volume 2017, Article ID 4184562, 11 pages
https://doi.org/10.1155/2017/4184562

Research Article

Pharmacological Basis for Use of *Armillaria mellea* Polysaccharides in Alzheimer's Disease: Antiapoptosis and Antioxidation

Shengshu An,[1] Wenqian Lu,[1] Yongfeng Zhang,[1] Qingxia Yuan,[1] and Di Wang[1,2]

[1]*School of Life Sciences, Jilin University, Changchun 130012, China*
[2]*Zhuhai College, Jilin University, Zhuhai 519041, China*

Correspondence should be addressed to Di Wang; jluwangdi@outlook.com

Received 23 March 2017; Revised 19 July 2017; Accepted 27 July 2017; Published 10 September 2017

Academic Editor: Anna M. Giudetti

Armillaria mellea, an edible fungus, exhibits various pharmacological activities, including antioxidant and antiapoptotic properties. However, the effects of *A. mellea* on Alzheimer's disease (AD) have not been systemically reported. The present study aimed to explore the protective effects of mycelium polysaccharides (AMPS) obtained from *A. mellea*, especially AMPSc via 70% ethanol precipitation in a L-glutamic acid- (L-Glu-) induced HT22 cell apoptosis model and an $AlCl_3$ plus D-galactose- (D-gal-) induced AD mouse model. AMPSc significantly enhanced cell viability, suppressed nuclear apoptosis, inhibited intracellular reactive oxygen species accumulation, prevented caspase-3 activation, and restored mitochondrial membrane potential (MMP). In AD mice, AMPSc enhanced horizontal movements in an autonomic activity test, improved endurance times in a rotarod test, and decreased escape latency time in a water maze test. Furthermore, AMPSc reduced the apoptosis rate, amyloid beta (Aβ) deposition, oxidative damage, and p-Tau aggregations in the AD mouse hippocampus. The central cholinergic system functions in AD mice improved after a 4-week course of AMPSc administration, as indicated by enhanced acetylcholine (Ach) and choline acetyltransferase (ChAT) concentrations, and reduced acetylcholine esterase (AchE) levels in serum and hypothalamus. Our findings provide experimental evidence suggesting *A. mellea* as a neuroprotective candidate for treating or preventing neurodegenerative diseases.

1. Introduction

Devastating neurodegenerative disorders, such as Alzheimer's disease (AD), are caused by neuronal loss and synapse degeneration. These disorders are clinically characterized by learning and memory decline, as well as cognitive deficits, and no cure is currently available [1]. The neuronal losses observed in neurodegenerative diseases are attributable to the oxidative death of these oxidative stress-sensitive cells [2]. Oxidative stress promotes neurotoxicity by increasing amyloid beta (Aβ) aggregation concomitantly with inflammatory events such as reactive oxygen species (ROS) production [3]. Additionally, excess extracellular glutamate levels have been found to correlate with the development of neurodegenerative disorders by triggering oxidative glutamate damage, preventing the intracellular antioxidant synthesis, and ultimately leading to ROS accumulation [4]. The overproduction of ROS and Aβ causes a feedback loop that results in synaptic dysfunction, as well as mitochondria-mediated apoptosis [5]. Therefore, antioxidant therapies are being considered as new options for protecting neurons from the oxidative damage associated with AD. These antioxidants not only can scavenge free radicals but may also reduce damage due to oxidative stress and thus maintain the cellular redox balance [6].

Several types of fungus are currently used as functional foods. In addition, many exhibit pharmacological activities with few side effects and are used as medicinal agents. Encouragingly, many fungal species have been reported to display neuroprotective properties in the context of

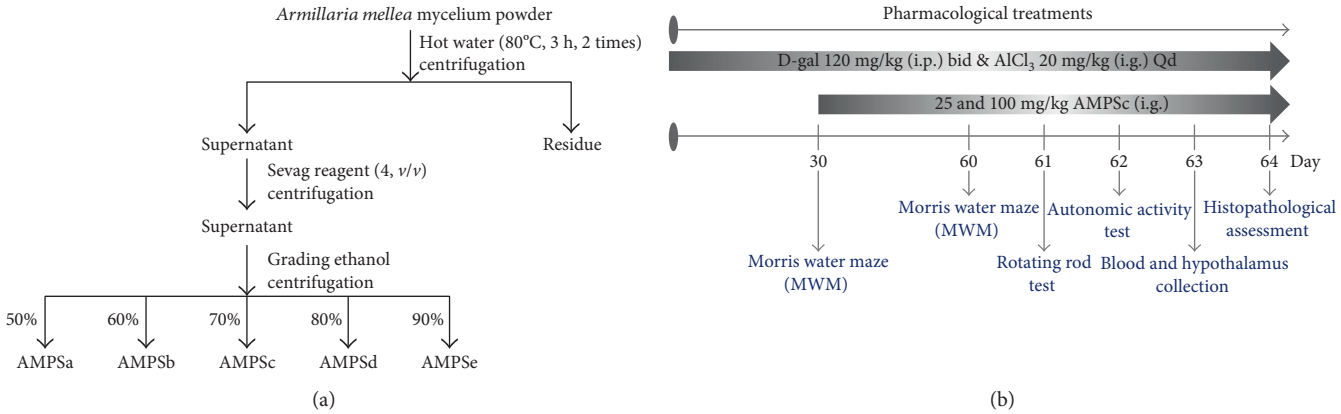

Figure 1: (a) The preparation of polysaccharides isolated from *A. mellea* mycelium obtained via submerged fermentation. (b) The process of $AlCl_3$ combined with D-gal-induced Alzheimer's disease mouse model establishment and drug administration.

neurodegenerative diseases [7]. Our group found that a polysaccharide isolated from *Sparassis crispa* protected PC12 cells against L-glutamic acid- (L-Glu-) induced apoptosis via the mitochondrial apoptotic pathway [8]. Furthermore, aqueous extracts of *Hericium erinaceus* yielded therapeutic effects that were attributed to both mitochondria-mediated apoptosis and neurotransmitter modulation in apoptotic cells and in an $AlCl_3$ plus D-galactose- (D-gal-) induced mouse model of AD [9]. *Armillaria mellea*, an edible and medicinal fungus, has been used for hundreds of years in East Asia. Polysaccharides isolated from *A. mellea* have been reported to exhibit antioxidant activities by superoxide radical scavenging [10] and significant antitumor activities via the mitochondrial apoptotic pathway and caspase cascade activation [11]. All previous data have indicated that *A. mellea* may exert protective effects against neurodegenerative diseases, especially AD.

The neurotoxin-induced mouse hippocampal neuronal cell (i.e., HT22 cell) apoptosis model is a well-recognized *in vitro* model for screening the neuroprotective effects of various agents [12]. Additionally, an aging model induced by D-gal is used in animal studies. This model involves the blocking of natural physiological features of aging and exhibits cellular AD phenomena, including a wide range of astrocytic and neuronal vacuolization, neuronal degeneration or death, and Aβ production and deposition, followed by cerebral cortex atrophy and cognitive and memory dysfunction [13]. The use of a combination of $AlCl_3$ and D-gal in a mouse model induces AD-like behavior and more readily generates pathological alterations than either $AlCl_3$- or D-gal-only treatment [14].

In the present study, we used L-Glu-induced HT22 apoptotic cells and D-gal plus $AlCl_3$-induced AD mice to investigate the neuroprotective effects of *A. mellea* mycelium polysaccharides (AMPS). We found that in HT22 cells, AMPS improved cell viability, restored mitochondrial membrane potential (MMP), and reduced cell apoptosis and excess caspase-3 activity. Moreover, AMPS treatment regulated the behavior and physiological and biochemical indexes of AD mice. Taken together, our data suggest the usefulness of *A. mellea* as a therapeutic agent or functional food for the treatment of AD.

Table 1: Effect of different ratios of ethanol on the polysaccharides yield from *A. mellea* mycelium.

Ethanol concentration	Name	Yield (%)
50%	AMPSa	0.93
60%	AMPSb	1.30
70%	AMPSc	1.93
80%	AMPSd	1.60
90%	AMPSe	1.00

2. Materials and Methods

2.1. Preparation of A. mellea Polysaccharides. *A. mellea* (CICC 14066; China Center of Industrial Culture Collection, Beijing, China) mycelium was obtained through submerged fermentation with the medium consisted of 20 g/L of sucrose, 10 g/L of glucose, 10 g/L yeast extract powder, 10 g/L of peptone, 1.5 g/L of KH_2PO_4, 0.75 g/L of $MgSO_4$, and 0.01 g/L of vitamin B1. *A. mellea* was extracted by hot water at 80°C for 3 h twice, removed proteins using Sevag reagent (n-butanol and chloroform in 1 : 4 ratio), and then collected after precipitation using 50%, 60%, 70%, 80%, and 90% ethanol at 4°C overnight and named AMPSa–e (Figure 1(a)). The yield of polysaccharides within *A. mellea* mycelium was shown in Table 1.

2.2. Cell Culture. The mouse hippocampal neuronal cell line (HT22; BNCC; 337709) was cultured in Dulbecco's modified Eagle's medium (DMEM; Invitrogen, USA) supplemented with 10% fetal bovine serum (FBS, Invitrogen, USA), 100 μg/mL streptomycin, and 100 units/mL penicillin (Invitrogen, USA) in a 5% CO2 and 95% air incubator supplying a humidified atmosphere at 37°C. Before treatment, HT22 cells were differentiated in Neurobasal medium (Invitrogen) containing 2 mmol/L glutamine and 1× N_2 supplement (Invitrogen) for 24 hours [15].

2.3. Cell Viability Assay. HT22 cells were pretreated with AMPSa–e at a dose of 40 μg/mL or AMPSc at doses of 10, 20, 40, and 80 μg/mL for 3 h and then incubated with 25 mM of L-GLu for 24 h. 3-(4,5-Dimethyl-2-thiazolyl)-

2,5-diphenyl-2H-tetrazolium bromide assay (MTT, Sigma-Aldrich, USA) was applied for cell viability assessment similarly as previous research [8].

2.4. Cell Apoptosis Assay. HT22 cells were pretreated with AMPSc at doses of 40 and 80 μg/mL for 3 h and then incubated with 25 mM of L-Glu for another 24 h. Cells were then incubated with propidium iodide (PI) and annexin V (AV) for 20 min at room temperature in darkness. The intensity of fluorescence was measured utilizing Muse™ Cell Analyzer from Millipore (Billerica, MA) following manufacturer's instructions.

2.5. MMP Assay. Cells were pretreated with AMPSc (40 and 80 μg/mL) for 3 h and then exposed to 25 mM of L-Glu for another 12 h and then incubated with JC-1 (5,5′,6,6′-tetrachloro-1,1′,3,3′tetraethylbenzimidazol-ylcarbocyanine iodide) at 37°C for 20 min in darkness. The ratio of green/red fluorescence analyzed using Muse Cell Analyzer (Millipore; USA) indicated the value of mitochondrial membrane potential.

2.6. Intracellular ROS Generation Assessment. HT22 cells were pretreated with AMPSc (40 and 80 μg/mL) for 3 h and then exposed to 25 mM of L-Glu for another 12 h. Treated cells were incubated with 10 μmol/L of 2′,7′-dichlorofluorescein diacetate (DCFH-DA) at 37°C for 20 minutes. Green fluorescence intensity detected with a fluorescent microscope (40x; CCD camera, IX73, Olympus) represented the level of intracellular ROS.

2.7. Assessment of Caspase Activities. HT22 cells were pretreated with AMPSc (40 and 80 μg/mL) for 3 h and then exposed to 25 mM of L-Glu for another 24 h. The activities of caspase-3 were analyzed via commercial kits (Nanjing Jiancheng Bioengineering Institute, Nanjing, China).

2.8. Experiments Applied on Alzheimer's Disease Mouse Model. The experiments were carried out under the approval of Institution Animal Ethics Committee of Jilin University. 50 Balb/c male mice (20–22 g; 10 weeks) were housed in cages in an air-conditioned room under temperature (23 ± 1°C) and humidity (40–60%) with sufficient water and food and randomly divided into five groups ($n = 10$). 30 mice were subcutaneously injected with 120 mg/kg of D-gal and orally treated with 20 mg/kg of $AlCl_3$ once a day for 8 weeks. Starting from the fifth week, mice were intragastrically treated with normal saline (model group) and AMPSc at doses of 25 and 100 mg/kg/day for four weeks. 10 mice serving as control group were treated with normal saline for 8 weeks. Another 10 mice were treated with normal saline for 4 weeks, following with 100 mg/kg of AMPSc administration for another 4 weeks (Figure 1(b)).

At the end of behavioral tests as follows, blood was collected from the rats' tails under anesthesia with 10% chloral hydrate, and the brains were removed and homogenized (1 : 9 *w*/*v*) in NaCl buffer. The whole hemisphere was immersed in 4% formaldehyde for pathologic analysis.

2.9. Behavioral Tests

2.9.1. Morris Water Maze Test. Memory ability and spatial learning were analyzed by Morris water maze (MT-200, Chengdu, China). After 5-day training, on the 60th day, mice were put into a circular pool filled with opacified water containing titanium dioxide (23 ± 2°C, 10 cm in depth). The escape latency of mice to find the platform was recorded within 120 s.

2.9.2. Fatigue Rotarod Test. On the 61st day, after 3 times training, mice were placed on the turning device (ZB-200, Chengdu Techman Software Co. Ltd., Chengdu, China) with 15 rpm speed, and the time when mice under induced muscle fatigue fell off was recorded.

2.9.3. Autonomic Activity Test. On the 62nd day, mice were placed in the chamber covered with the light-blocking plate to detect their autonomic activities. The number of mouse activities including the horizontal movements and the vertical movements was recorded for 5 min.

2.10. Determination of the Levels of Ach, AchE, and ChAT in Serum and Hypothalamus. The levels of acetylcholine (Ach), acetylcholine esterase (AchE), and choline acetyltransferase (ChAT) in serum and hypothalamus were measured by enzyme-linked immunosorbent assay (ELISA) according to the procedures provided by the related assay kits (Nanjing Jiancheng Bioengineering Institute, Nanjing, China).

2.11. Determination of Oxidation Status in Serum or Hypothalamus. The levels of superoxide dismutase (SOD), glutathione peroxidase (GSH-Px), and ROS in serum and/or hypothalamus were detected by ELISA kit according to related procedures (Nanjing Jiancheng Bioengineering Institute, Nanjing, China).

2.12. TUNEL Assay. Apoptosis in the hippocampus was detected using the terminal deoxynucleotidyl transferase-mediated dUTP nick end labeling (TUNEL). After deparaffinization, hippocampus tissue sections were washed twice in phosphate-buffered saline (PBS) for 5 minutes and completely covered by the permeabilization reagent (Proteinase K) for 15 min at room temperature. After washing with PBS, sections were incubated with 50 μL of the prepared TdT reaction mixture at 37°C for 60 min in the dark. The reactions were subsequently terminated, and the tissue sections were analyzed under a Nikon Eclipse TE 2000-S fluorescence microscope (20x; CCD camera, IX73, Olympus).

2.13. Determination of Levels of Aβ in Serum and Hippocampus. The levels of Aβ1-42 in serum were detected by ELISA kit according to related procedures (Nanjing Jiancheng Bioengineering Institute, Nanjing, China).

Brain coronal sections were deparaffinized, placed in thioflavin-S solution for 5 min, and then differentiated in 70% fresh alcohol for 10 min. After washing, images were captured using a confocal microscope (40x; CCD camera, IX73, Olympus).

2.14. Immunohistochemistry. The protein expressions of Aβ1-40, phospho- (p-) Tau (ser404), and 4-hydroxynonenal (4-HNE) in the hippocampus of mice were detected via immunohistochemistry to visualize Aβ deposition, tau aggregations, and oxidative stress-associated damage. The paraffin sections were deparaffinized in xylene and rehydrated in different graded alcohol. Then, sections were heated in antigen repair solution (citrate buffer) in a microwave for 20 min to retrieve antigens. After extensive washing with PBS for 5 min, sections were incubated with 3% hydrogen peroxide for 10 min at room temperature to block endogenous peroxidase followed by blocking with 2% goat serum dissolved in PBS. The slides were incubated with polyclonal anti-Aβ1-40 (1 : 200, Bioss bs-0877R); anti-p-Tau (ser404) (1 : 200, Bioss bs-2392R); and anti-4-HNE (1 : 800, Abcam: ab46545) antibodies individually overnight at 4°C. Subsequently, slides were washed with PBS and incubated with secondary antibody conjugated horseradish peroxidase (HRP) at room temperature for 1 h. And then, the sections were washed in PBS and visualized with DAB (3,3′-diaminobenzidine) (Solarbio, Beijing, China) followed by incubating with Mayer's hematoxylin for 3 min. Finally, the sections were dehydrated with dilutions of ethanol and xylene and digitized using an Olympus IX73 microscope (Olympus, Tokyo, Japan).

2.15. Statistical Analysis. Data were expressed as mean ± S.E.M. A one-way analysis of variance (ANOVA) was used to detect statistical significance followed by post hoc multiple comparisons (Dunn's test). Statistical significance was accepted for $P < 0.05$.

3. Results

3.1. AMPS Improved Cell Viability and Apoptosis and Reduced Caspase-3 Activity. Compared with L-Glu-treated cells, cells pretreated with 40 μg/mL of AMPSb and AMPSc for 3 h improved HT22 cell viability by 10% and 11%, respectively ($P < 0.05$; Figure 2(a)), whereas treatment with AMPSa, d, and e had no effect. Additionally, pretreatment with 40 or 80 μg/mL of AMPSc for 3 h before a 24 h incubation with 25 mM of L-Glu improved HT22 cell viability by 6.9% and 13.7%, respectively ($P < 0.05$; Figure 2(b)). AV-PI staining revealed that whereas exposure to 25 mM L-Glu led to an apoptosis rate of 25% in HT22 cells, a 3 h preincubation with AMPSc led to a reduction in apoptosis of >14% (Figure 2(c)). When compared to L-Glu-damaged HT22 cells, a 3 h AMPSc pretreatment reduced caspase-3 activity by >24% during a 24 h incubation (Figure 2(d)).

3.2. AMPSc Restored the Dissipation of MMP and Reduced ROS Accumulation. Altered mitochondrial apoptosis, which is characterized by disruption of the MMP, is a common feature of cell apoptosis [8]. Compared with L-Glu-damaged HT22 cells, AMPSc improved MMP depolarization by nearly 10% after a 12 h incubation (Figure 3(a)). Furthermore, a 3-h AMPSc pretreatment strongly suppressed L-Glu-induced ROS accumulation, as indicated by reduced green fluorescence (Figure 3(b)).

3.3. AMPSc Affected the Behavior of AD Mice. We next subjected D-gal plus $AlCl_3$-induced AD model mice for behavioral testing to further confirm the beneficial activities of AMPSc against AD. In an autonomic activity test, AMPSc enhanced the horizontal movements of AD mice relative to controls ($P < 0.05$; Figure 4(a)), but failed to influence vertical movements ($P > 0.05$; Figure 4(b)). In a fatigue rotarod test, AMPSc enhanced the endurance times of AD mice by >25% ($P < 0.01$; Figure 4(c)) but had no significant effects on control mice (Figure 4(c)).

The water maze test is commonly used to evaluate learning and memory in animals [16]. Here, we applied this test to evaluate the effects of AMPS on the cognitive abilities of AD mice. We initially observed a >15% enhancement in the escape latency times of AD mice ($P < 0.01$; Figure 4(d)). A 4-week course of AMPSc administration led to a nearly 20% decrease in the escape latency times ($P < 0.05$; Figure 4(d)). AMPSc failed to influence the escape latency times of control mice ($P > 0.05$; Figure 4(d)).

TUNEL staining was used to analyze the apoptotic statuses of hippocampal neurons. In both control and AMPSc-treated mice, we observed few TUNEL-positive cells, suggesting that a minority of neurons were apoptotic. Larger amounts of TUNEL-positive apoptotic neurons were noted in AD mice, whereas a 4-week course of AMPSc administration strongly reduced apoptosis in this population, as demonstrated by the reduction in green fluorescence intensity (Figure 4(e)).

3.4. AMPSc Regulated Ach, AchE, and ChAT Concentrations in Serum and Hypothalamus. We noted significant reductions in the serum and hypothalamic Ach and ChAT concentrations, which were accompanied by increased AchE concentrations, in $AlCl_3$ and D-gal-induced AD mice relative to control mice ($P < 0.05$; Figure 5), suggesting disruption of the central cholinergic function. Compared to AD mice, AMPSc increased both the Ach and ChAT levels and reduced the AchE levels in the serum and hypothalamus in a dose-dependent manner ($P < 0.05$; Figure 5).

3.5. AMPSc Regulated Oxidative Status in the Serum and Hypothalamus. Oxidative stress is the basis for an important hypothesis regarding the pathophysiology of neurodegenerative disorders. Compared with control mice, AMPSc alone significantly enhanced the serum and/or hypothalamic levels of SOD and GSH-Px and reduced the levels of ROS in AD mice ($P < 0.05$; Table 2). Compared with AD mice, a 4-week course of AMPSc administration yielded in >50% and 20% increases in SOD and GSH-Px activities, resp., and a >45% reduction in ROS levels in the serum and/or hypothalamus ($P < 0.01$; Table 2).

3.6. AMPSc Regulated Aβ Levels in the Serum and Hippocampus. Aβ, which exhibits strong aggregating properties, is considered the core component of amyloid plaques. Compared with control mice, we observed no significant changes in the serum Aβ1-42 levels in AD mice, whereas a 4-week course of AMPSc led to a >20% increase in serum

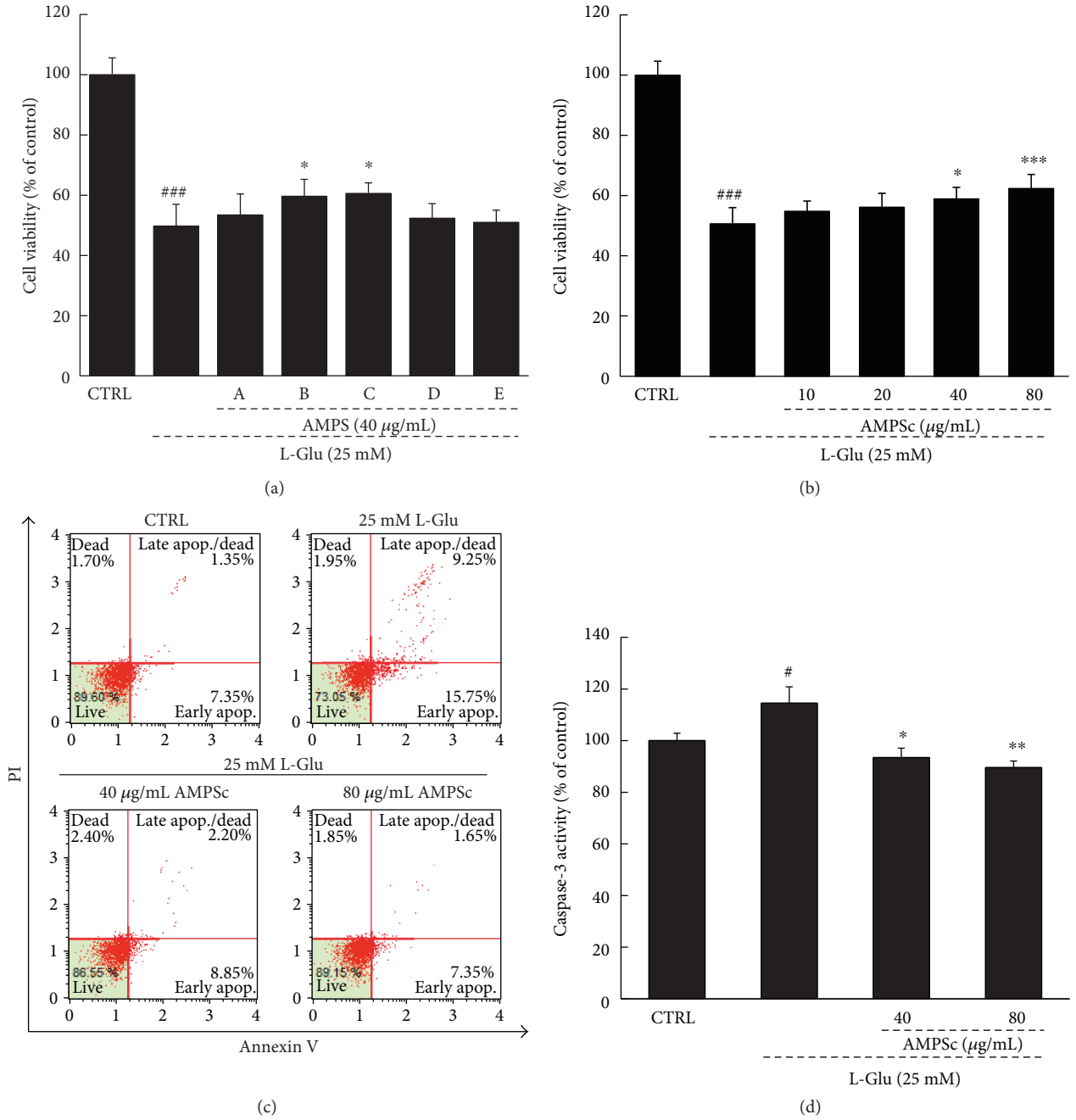

Figure 2: The neuroprotective effects of AMPS against L-Glu-induced cell damage in HT22 cells. (a) 3 h AMPSb and c preincubation improved cell viability in L-Glu-exposed HT22 cells. (b) 3 h AMPSc (40 and 80 μg/mL) pretreatment improved cell viability in HT22 cells after 24 h incubation with 25 mM of L-Glu. (c) 3 h AMPSc preincubation strongly reduced the apoptotic rate of HT22 cells exposed to L-Glu for 24 h. (d) 3 h AMPSc pretreatment weakened caspase-3 activations in HT22 cells exposed to 25 mM of L-Glu for 24 h. Data were expressed as a percentage of corresponding control cells and means ± S.E.M. ($n = 6$). $^{\#}P < 0.05$ and $^{\#\#\#}P < 0.001$ versus CTRL; $^{*}P < 0.05$, $^{**}P < 0.01$, and $^{***}P < 0.001$ versus L-Glu-exposed cells. AMPS: *A. mellea* polysaccharides.

Aβ1-42 concentrations ($P < 0.05$; Figure 6(a)). Furthermore, AMPSc also increased the serum Aβ1-42 levels in control mice ($P < 0.05$; Figure 6(a)). In the hippocampus, AMPSc suppressed the strong expression of Aβ in AD mice, as indicated by the reduction in green fluorescence intensity (Figure 6(b)). The suppressive effects of AMPSc on Aβ1-40 deposition were also confirmed by immunohistochemistry (Figure 6(c)).

3.7. AMPSc Regulated Oxidative Damage and p-Tau Aggregations in Hippocampus. Compared to control mice, high expression levels of 4-NHE (Figure 7, a) and excessive aggregations of p-Tau (Figure 7, b) in the hippocampus were noted in AD mice. In contrast, four-week AMPSc treatment strongly reduced the expression levels of 4-NHE (Figure 7, a) and attenuated the aggregations of p-Tau in AD mice (Figure 7, b).

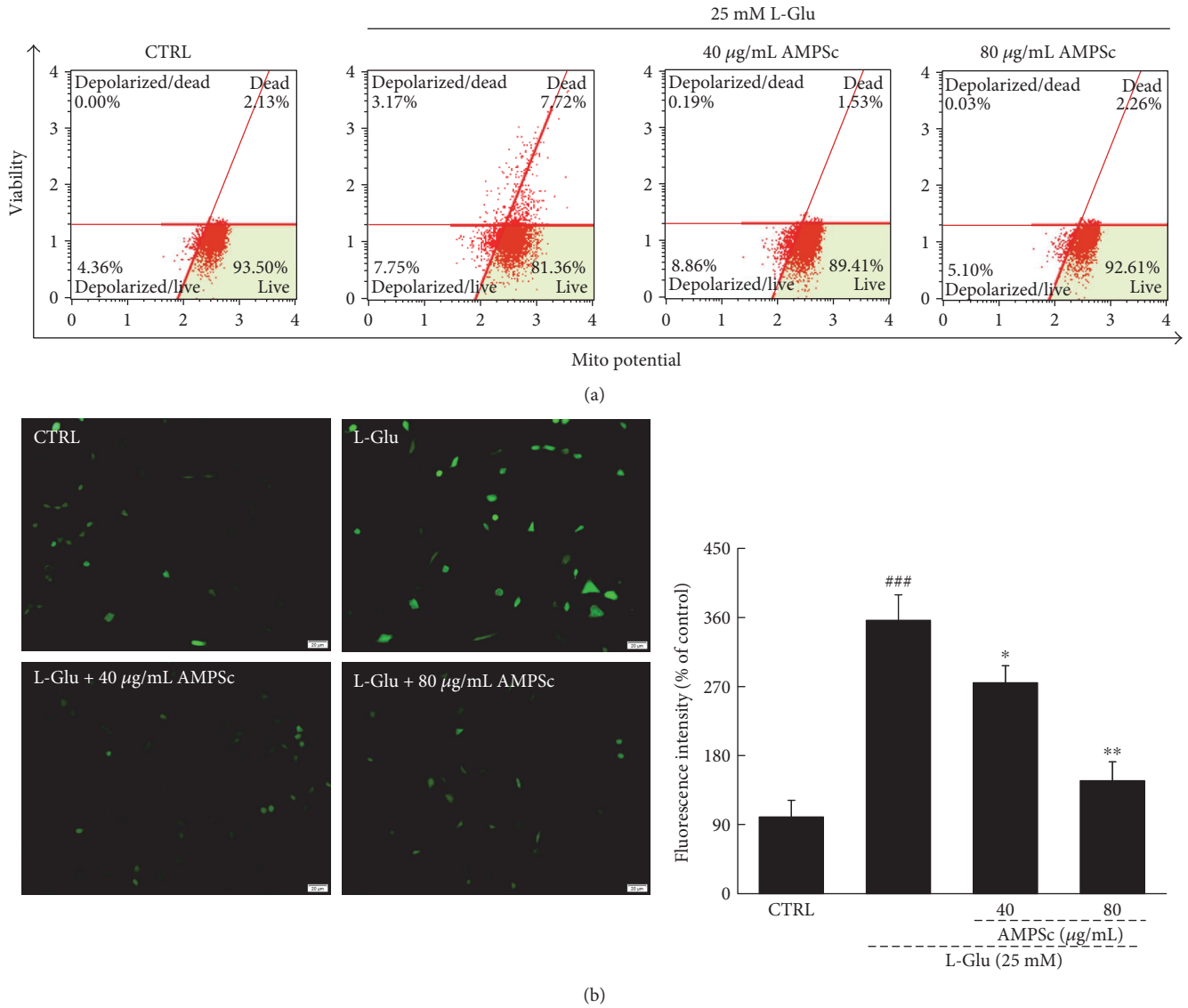

Figure 3: (a) The dissipation of MMP caused by 12 h L-Glu incubation was strongly restored by 3 h AMPSc pretreatment analyzing via JC-1 staining ($n = 6$). (b) The overproduction of ROS induced by 12 h L-Glu exposure was significantly decreased by 3 h AMPSc pretreatment analyzed by DCFH-DA staining ($n = 6$). Scale bar: 20 μm. Qualification data were expressed as the percentage of green fluorescent intensity compared to control cells. Data are expressed as means ± S.E.M. ($n = 6$). $^{###}P < 0.001$ versus CTRL; $^{*}P < 0.05$ and $^{**}P < 0.01$ versus L-Glu-exposed cells. AMPS: *A. mellea* polysaccharides.

4. Discussion

By 2050, the number of patients suffering with dementia is expected to reach 115.4 million [17]. Our present study successfully confirmed the neuroprotective effects of AMPS in L-Glu-induced HT22 apoptotic cells and a chemically induced AD mouse model, as evidenced by the significant amelioration of nuclear and mitochondrial apoptosis. Furthermore, a clinical decline in short-term memory is considered a symptom of AD, and AMPS was shown to affect the behavior of AD mice. In contrast to other agents used to treat AD, AMPS contains multiple polysaccharides that affect systemic targets and exert various functions, such as antioxidative and antiapoptotic effects, to eliminate the symptoms of AD in a much more natural manner.

In our *in vitro* study, the robust protection provided by AMPS against apoptosis was associated with the inhibition of ROS overproduction and the reversal of MMP depolarization. ROS accumulation causes oxidative stress and thus leads to cellular dysfunction and apoptosis [18], which are associated with the opening of the mitochondrial permeability transition pore [19]. Within a feedback loop, MMP dissipation leads to further ROS release from the mitochondria to the cytoplasm [20], while activating other proapoptotic molecules such as caspase-3 [21]. Caspase-3 is an active component of proteolytic cleavage, which directs the execution of the apoptotic program [22]. Our data obtained from L-Glu-induced HT22 apoptotic cells suggest an association between AMPS-mediated neuroprotection and oxidative stress-mediated mitochondrial apoptotic signaling.

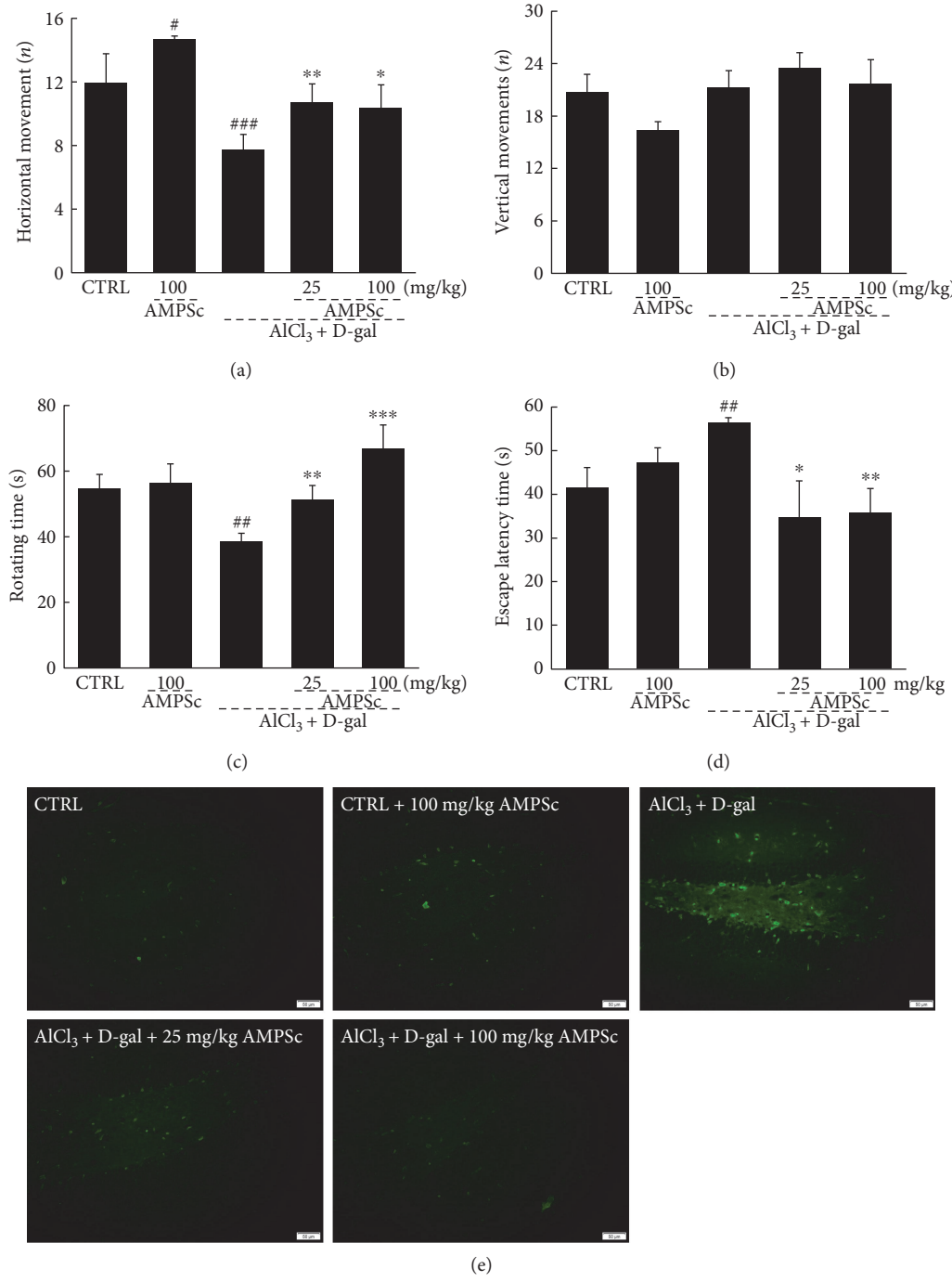

Figure 4: AMPSc improved AD-like behaviors in $AlCl_3$ and D-gal induced AD mice. AMPSc enhanced (a) horizontal movements, but not (b) vertical movements in autonomous activity test, (c) prolonged endurance time in rotarod test, and (d) decreased escape latency time in water maze test in AD mice. Data are expressed as mean ± S.E.M. ($n = 10$). $^{\#}P < 0.05$, $^{\#\#}P < 0.01$, and $^{\#\#\#}P < 0.001$ versus normal mice (CTRL); $^{*}P < 0.05$, $^{**}P < 0.01$, and $^{***}P < 0.001$ versus AD mice. (e) AMPSc reduced apoptotic cell rate in the hippocampus of AD mice determined by TUNEL assay ($n = 6$). Scale bar: 50 μm. AMPS: *A. mellea* polysaccharides.

In the present study, our $AlCl_3$ and D-gal-induced AD mice exhibited signs of enhanced oxidative stress. As a biomarker of oxidative damage, 4-HNE is a cytotoxic end product of lipid peroxidation, which is essential for cell survival signaling [23]. The increase of 4-HNE triggers inflammatory responses and elevates ROS [24]. Comparatively, AMPS induced significant antioxidative effects, as shown by the suppression on 4-HNE expressions, the reductions in ROS levels, and increases in the activities of the endogenous antioxidants SOD and GSH-Px, which play an important role in removing oxygen-free radicals. $AlCl_3$ has been reported to induce the generation of free radicals and neurotoxicity in the brain,

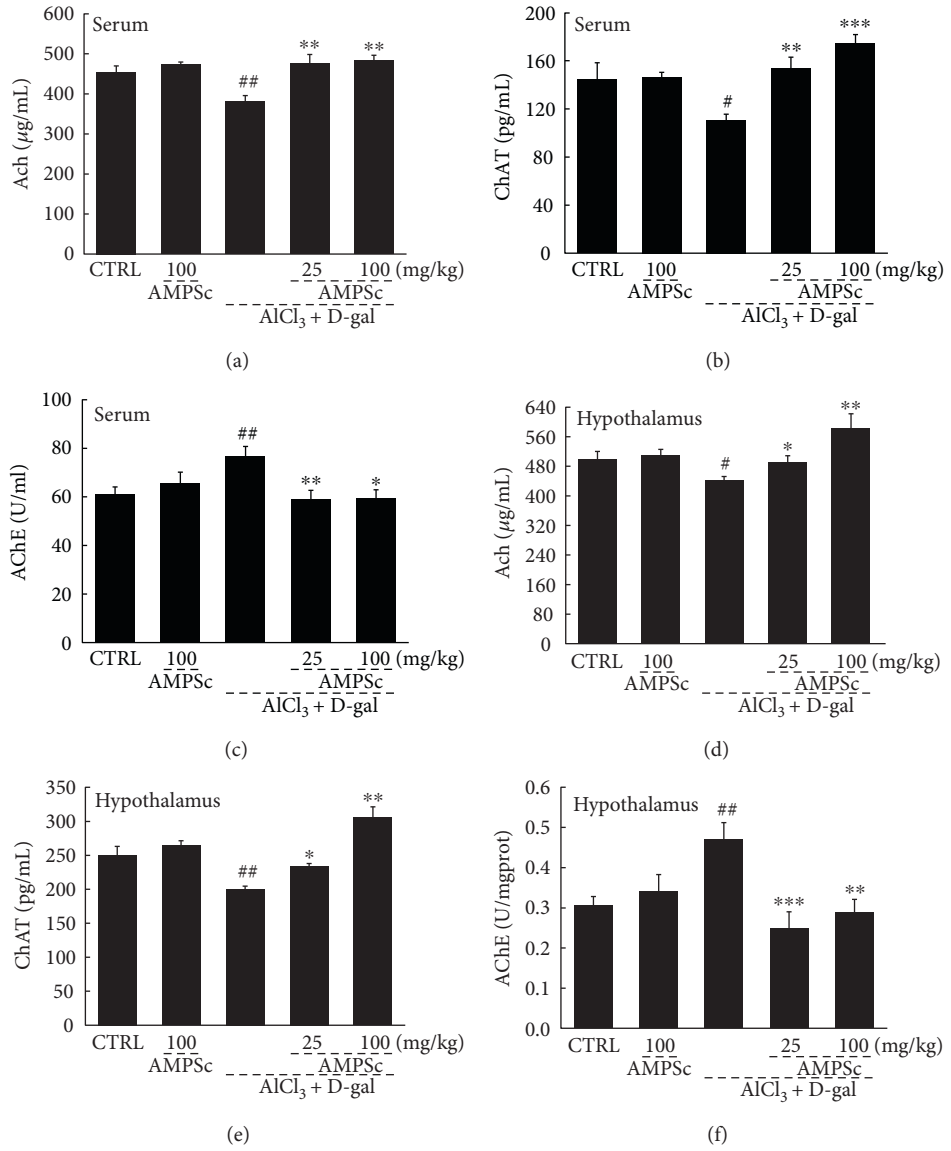

Figure 5: AMPSc enhanced the levels of (a and d) Ach and (b and e) ChAT and reduced the levels of (c and f) AchE in serum and hypothalamus of AD mice detecting via ELISA method. Data are expressed as mean ± S.E.M. ($n = 10$). $^{\#}P < 0.05$ and $^{\#\#}P < 0.01$ versus normal mice (CTRL); $^{*}P < 0.05$, $^{**}P < 0.01$, and $^{***}P < 0.001$ versus AD mice.

Table 2: The effects of AMPSc on oxidative statues in serum or hypothalamus in AD mice.

		CTRL	CTRL + AMPSc (mg/kg) 100	$AlCl_3$ + D-gal	$AlCl_3$ + D-gal + AMPSc (mg/kg) 25	100
Serum	SOD (U/mL)	98.6 ± 7.4	117.0 ± 5.7$^{\#}$	75.9 ± 3.9$^{\#}$	110.3 ± 5.3**	111.5 ± 9.0**
	GSH-Px (U/mL)	249.8 ± 13.1	251.3 ± 5.7	213.4 ± 10.5$^{\#\#}$	254.4 ± 9.0**	290.9 ± 16.0***
Hypothalamus	SOD (U/mgprot)	44.4 ± 2.1	55.9 ± 4.6$^{\#}$	30.1 ± 2.6$^{\#\#}$	47.0 ± 4.8**	66.1 ± 6.4***
	GSH-Px (U/mL)	326.1 ± 13.9	385.0 ± 27.2$^{\#}$	282.3 ± 16.4$^{\#}$	405.7 ± 31.1**	501.4 ± 15.2***
	ROS (FI/mgprot)	23087.4 ± 1905.5	15564.8 ± 3030.9$^{\#}$	34418.8 ± 3986.2$^{\#}$	14104.1 ± 1260.5**	17877.6 ± 2713.4***

Treatment with AMPSc and the levels of SOD, GSH-Px, and ROS in serum and/or hypothalamus were detected via ELISA method. Data are expressed as mean ± S.E.M. ($n = 10$). $^{\#}P < 0.05$ and $^{\#\#}P < 0.01$ versus normal mice (CTRL); $^{**}P < 0.01$ and $^{***}P < 0.001$ versus AD mice.

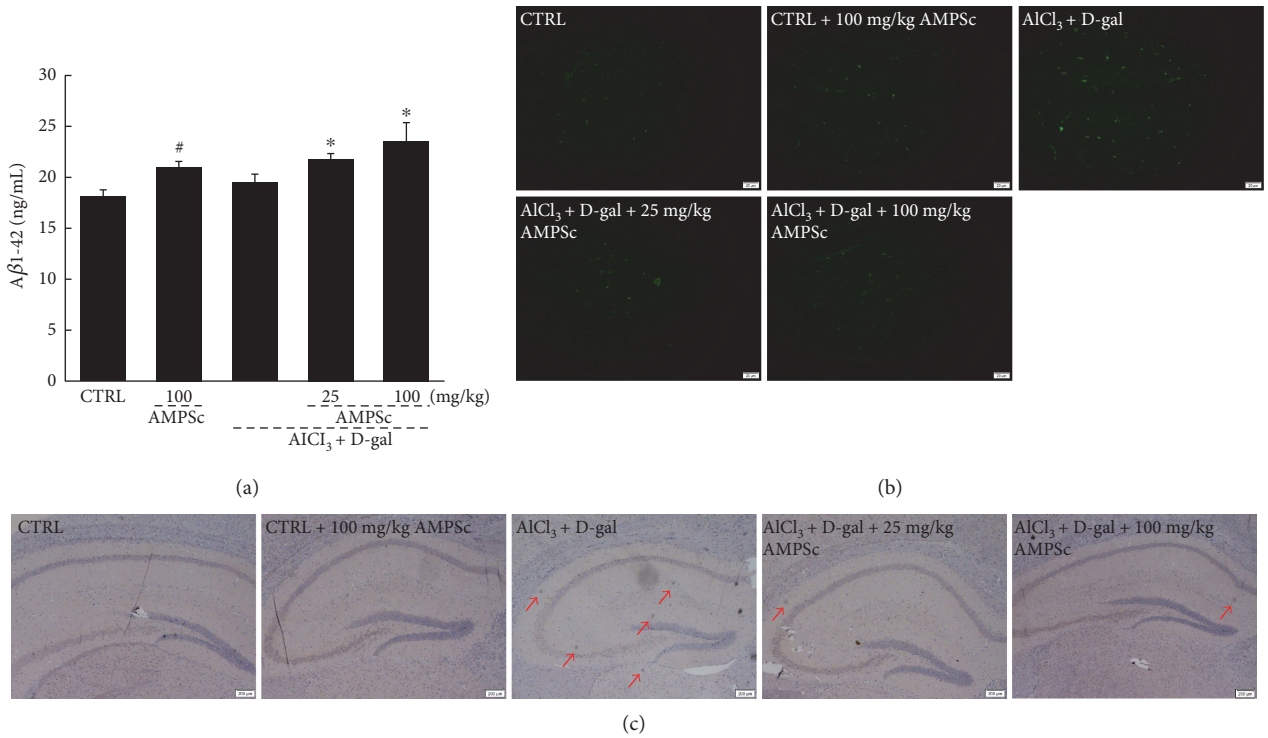

Figure 6: Effect of AMPSc on Aβ clearance in the blood and hippocampus. (a) The levels of Aβ in serum were significantly enhanced by AMPS. Data are expressed as mean ± S.E.M. ($n = 10$). $^{\#}P < 0.05$ versus normal mice (CTRL), $^{*}P < 0.05$ versus AD mice. AMPS significantly reduced Aβ aggregates in hippocampus of AD mice analyzed via (b) thioflavin-S fluorescence staining ($n = 6$; scale bar: 20 μm) and (c) immunohistochemistry staining ($n = 6$; scale bar: 200 μm). AMPS: *A. mellea* polysaccharides.

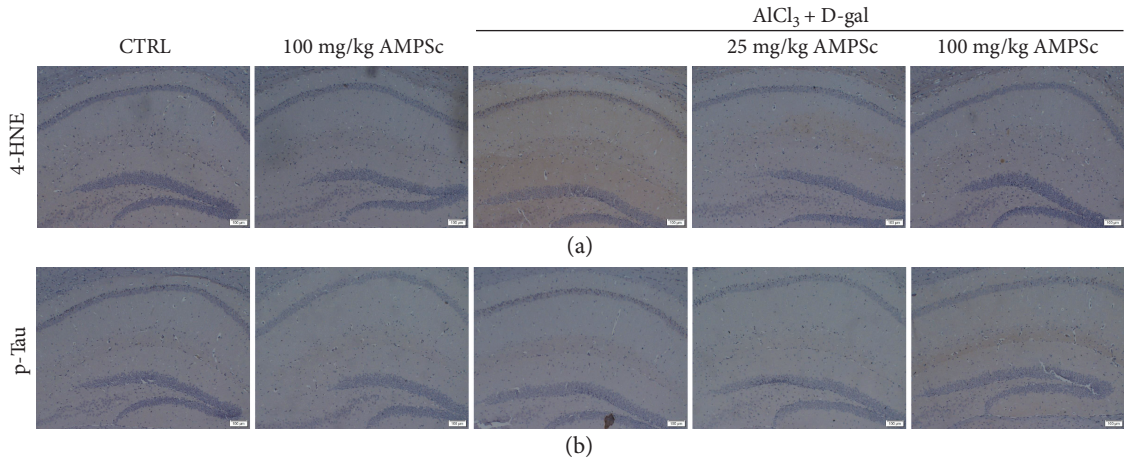

Figure 7: The effects of AMPSc on (a) 4-HNE expression levels and (b) p-Tau aggregations in hippocampus of AD mouse via immunohistochemistry staining ($n = 6$) (scale bar: 100 μm). AMPS: *A. mellea* polysaccharides.

which might lead to degenerative disorders [25]. Over the long term, D-gal injections not only induce impairments in learning and memory but also cause mitochondrial dysfunction and ROS accumulation in the brain [26]. The brain contains large amounts of polyunsaturated fatty acids, and its structure, which can be damaged by oxidation of proteins and lipids, is very sensitive to oxidative stress [27]. In AD, oxidative stress damage causes neuronal cell apoptosis by destroying the balance between ROS generation and mitochondrial removal [28]. D-gal induced the dissipation of MMP, and neurodegeneration is promoted by caspase-mediated apoptosis, which mainly occurs in the dentate gyrus (DG) region of the hippocampus [29]. Using TUNEL staining, we confirmed that AMPS successfully suppressed neuronal apoptosis in the hippocampus, compared to non-treated AD mice. Together with our *in vitro* data, these results demonstrate that the AMPS-induced improvements in the cognitive performances of AD mice may be related

to its antioxidant activities, which led to further suppression of apoptosis.

AMPS also enhanced the serum levels of Aβ while reducing the hippocampal expression of Aβ. The overproduction of Aβ protein and resulting formation of intracellular neurofibrillary tangles lead to the generation of extracellular senile plaques, which serve as the pathological index in the brain of a rodent with AD [30]. Aβ aggregation induces oxidative stress and mitochondrial dysfunction and leads to the production of ROS, which are involved in the pathogenesis of AD [31]. In a normal physiological state, Aβ can be detected in the blood and cerebrospinal fluid as it is slowly removed from the brain into the periphery via the transport mechanism and enzyme degradation. In AD patients, the clearance of Aβ accumulated in the brain may cause the increased levels of Aβ in the peripheral blood [32]. As reported, the fruit of *Cornus officinalis*, a traditional medicinal agent, exerts neuroprotective activity and significantly increases the plasma levels of Aβ [33]. On the other hand, the deposits of Aβ trigger the deficits of memory and synaptic degeneration, which further result in the neuronal signaling downstream of p-Tau pathology. The deposition of tau protein due to abnormal phosphorylation and glycosylation modification eventually leads to the formation of neurofibrillary tangles, which is related to the existence of excessive Aβ and plaques, proving the tau pathology in AD. We found that the ability of AMPS to reduce the hippocampal deposition of Aβ in mice played a central role in its ability to improve AD-like behaviors in mice.

The cholinergic system, which involves neurotransmitters such as Ach, is essential for the establishment, storage, and recovery of long-term memory. As reported, the decreases in Ach and ChAT release and enhancement of AchE activity caused by an impaired cholinergic system are key alterations affecting the cognitive deficit characteristic of AD pathogenesis [34]. Ach, ChAT, and AchE are among the neurotransmitters with crucial roles in synaptic transmission, which is related to memory and learning deficits [35]. *H. erinaceus* extracts were previously found to improve the $AlCl_3$ and D-gal-induced impairment of learning and memory in mice by regulating Ach and ChAT levels [9]. Similarly, the modulatory effects of AMPS on neurotransmitters might define an important protective role of cholinergic function in AD mice.

Our present study had some limitations. First, although we isolated polysaccharides from *A. mellea* mycelia, we could not obtain sufficient purity for a structural analysis. Further investigation is required. Second, the relationships among oxidative stress, neurotransmitter levels, and Aβ deposition should be investigated in greater detail.

In conclusion, our results demonstrate that AMPS protects against L-Glu-induced neurotoxicity in HT22 cells and mitigates AD-like behaviors in an $AlCl_3$ and D-gal-induced mouse model of AD. These effects might be largely attributable to the ability of AMPS to modulate oxidative stress. Our findings provide experimental evidence that *A. mellea* might be a useful neuroprotective agent for the treatment or prevention of neurodegenerative disease.

Abbreviations

ANOVA: One-way analysis of variance
Ach: Acetylcholine
AchE: Acetylcholine esterase
AD: Alzheimer's disease
AMPS: *A. mellea* mycelium polysaccharides
Aβ: Amyloid beta
ChAT: Choline acetyltransferase
DG: Dentate gyrus
D-gal: D-Galactose
ELISA: Enzyme-linked immunosorbent assay
GSH-Px: Glutathione peroxidase
L-Glu: L-Glutamic acid
MMP: Mitochondrial membrane potential
ROS: Reactive oxygen species
SOD: Superoxide dismutase
4-HNE: 4-Hydroxynonenal.

Conflicts of Interest

The authors have declared that there is no conflict of interest.

Acknowledgments

This work was supported by the Science and Technology Key Project in Jilin Province of China (Grant nos. 20150203002NY, 20160520036JH, and 20160204029YY).

References

[1] M. Z. Khan, N. Atlas, and W. Nawaz, "Neuroprotective effects of Caralluma tuberculata on ameliorating cognitive impairment in a d-galactose-induced mouse model," *Biomedicine & Pharmacotherapy*, vol. 84, pp. 387–394, 2016.

[2] E. Tonnies and E. Trushina, "Oxidative stress, synaptic dysfunction, and Alzheimer's disease," *Journal of Alzheimer's Disease*, vol. 57, no. 4, pp. 1105–1121, 2017.

[3] M. A. Daulatzai, "Cerebral hypoperfusion and glucose hypometabolism: key pathophysiological modulators promote neurodegeneration, cognitive impairment, and Alzheimer's disease," *Journal of Neuroscience Research*, vol. 95, no. 4, pp. 943–972, 2017.

[4] K. Pathakoti, L. Goodla, M. Manubolu, and T. Tencomnao, "Metabolic alterations and the protective effect of punicalagin against glutamate-induced oxidative toxicity in HT22 cells," *Neurotoxicity Research*, vol. 31, no. 4, pp. 521–531, 2017.

[5] J. F. Hu, S. F. Chu, N. Ning et al., "Protective effect of (−)clausenamide against Abeta-induced neurotoxicity in differentiated PC12 cells," *Neuroscience Letters*, vol. 483, no. 1, pp. 78–82, 2010.

[6] F. U. Amin, S. A. Shah, and M. O. Kim, "Vanillic acid attenuates Abeta1-42-induced oxidative stress and cognitive impairment in mice," *Scientific Reports*, vol. 7, article 40753, 2017.

[7] L. Janjusevic, M. Karaman, F. Sibul et al., "The lignicolous fungus Trametes versicolor (L.) Lloyd (1920): a promising natural source of antiradical and AChE inhibitory agents," *Journal of Enzyme Inhibition and Medicinal Chemistry*, vol. 32, no. 1, pp. 355–362, 2017.

[8] S. Hu, D. Wang, J. Zhang et al., "Mitochondria related pathway is essential for polysaccharides purified from Sparassis crispa

mediated neuro-protection against glutamate-induced toxicity in differentiated PC12 cells," *International Journal of Molecular Sciences*, vol. 17, no. 2, 2016.

[9] J. Zhang, S. An, W. Hu et al., "The neuroprotective properties of Hericium erinaceus in glutamate-damaged differentiated PC12 cells and an Alzheimer's disease mouse model," *International Journal of Molecular Sciences*, vol. 17, no. 11, 2016.

[10] K. C. Siu, L. Xu, X. Chen, and J. Y. Wu, "Molecular properties and antioxidant activities of polysaccharides isolated from alkaline extract of wild Armillaria ostoyae mushrooms," *Carbohydrate Polymers*, vol. 137, pp. 739–746, 2016.

[11] J. Wu, J. Zhou, Y. Lang et al., "A polysaccharide from Armillaria mellea exhibits strong in vitro anticancer activity via apoptosis-involved mechanisms," *International Journal of Biological Macromolecules*, vol. 51, no. 4, pp. 663–667, 2012.

[12] T. Liu, M. Lee, J. J. Ban, W. Im, I. Mook-Jung, and M. Kim, "Cytosolic extract of human adipose stem cells reverses the amyloid beta-induced mitochondrial apoptosis via P53/Foxo3a pathway," *PLoS One*, vol. 12, no. 1, article e0168859, 2017.

[13] H. Chu, A. Zhang, Y. Han et al., "Metabolomics approach to explore the effects of Kai-Xin-San on Alzheimer's disease using UPLC/ESI-Q-TOF mass spectrometry," *Journal of Chromatography B, Analytical Technologies in the Biomedical and Life Sciences*, vol. 1015-1016, pp. 50–61, 2016.

[14] Y. Luo, F. Niu, Z. Sun et al., "Altered expression of Aβ metabolism-associated molecules from d-galactose/AlCl3 induced mouse brain," *Mechanisms of Ageing and Development*, vol. 130, no. 4, pp. 248–252, 2009.

[15] M. He, J. Liu, S. Cheng, Y. Xing, and W. Z. Suo, "Differentiation renders susceptibility to excitotoxicity in HT22 neurons," *Neural Regeneration Research*, vol. 8, no. 14, pp. 1297–1306, 2013.

[16] S. Athari Nik Azm, M. Vafa, M. Sharifzadeh, M. Safa, A. Barati, and A. Mirshafiey, "Effects of M2000 (D-mannuronic acid) on learning, memory retrieval, and associated determinants in a rat model of Alzheimer's disease," *American Journal of Alzheimer's Disease and Other Dementias*, vol. 32, no. 1, pp. 12–21, 2017.

[17] P. H. Reddy, S. Tonk, S. Kumar et al., "A critical evaluation of neuroprotective and neurodegenerative microRNAs in Alzheimer's disease," *Biochemical and Biophysical Research Communications*, vol. 483, no. 4, pp. 1156–1165, 2017.

[18] D. I. Brown and K. K. Griendling, "Regulation of signal transduction by reactive oxygen species in the cardiovascular system," *Circulation Research*, vol. 116, no. 3, pp. 531–549, 2015.

[19] M. L. Circu and T. Y. Aw, "Reactive oxygen species, cellular redox systems, and apoptosis," *Free Radical Biology & Medicine*, vol. 48, no. 6, pp. 749–762, 2010.

[20] X.-Q. Tang, J.-Q. Feng, J. Chen et al., "Protection of oxidative preconditioning against apoptosis induced by H2O2 in PC12 cells: mechanisms via MMP, ROS, and Bcl-2," *Brain Research*, vol. 1057, no. 1-2, pp. 57–64, 2005.

[21] F. Bensassi, C. Gallerne, O. S. el Dein, M. R. Hajlaoui, H. Bacha, and C. Lemaire, "Mechanism of Alternariol monomethyl ether-induced mitochondrial apoptosis in human colon carcinoma cells," *Toxicology*, vol. 290, no. 2-3, pp. 230–240, 2011.

[22] D. Hippe, A. Gais, U. Gross, and C. G. Luder, "Modulation of caspase activation by Toxoplasma gondii," *Methods in Molecular Biology*, vol. 470, pp. 275–288, 2009.

[23] A. Fragoulis, S. Siegl, M. Fendt et al., "Oral administration of methysticin improves cognitive deficits in a mouse model of Alzheimer's disease," *Redox Biology*, vol. 12, pp. 843–853, 2017.

[24] P. Cisternas, C. B. Lindsay, P. Salazar et al., "The increased potassium intake improves cognitive performance and attenuates histopathological markers in a model of Alzheimer's disease," *Biochimica et Biophysica Acta (BBA) - Molecular Basis of Disease*, vol. 1852, no. 12, pp. 2630–2644, 2015.

[25] A. Justin Thenmozhi, M. Dhivyabharathi, T. Manivasagam, and M. M. Essa, "Tannoid principles of Emblica officinalis attenuated aluminum chloride induced apoptosis by suppressing oxidative stress and tau pathology via Akt/GSK-3βsignaling pathway," *Journal of Ethnopharmacology*, vol. 194, pp. 20–29, 2016.

[26] Z. Qu, J. Zhang, H. Yang et al., "Protective effect of tetrahydropalmatine against d-galactose induced memory impairment in rat," *Physiology & Behavior*, vol. 154, pp. 114–125, 2016.

[27] T. Jiang, Q. Sun, and S. Chen, "Oxidative stress: a major pathogenesis and potential therapeutic target of antioxidative agents in Parkinson's disease and Alzheimer's disease," *Progress in Neurobiology*, vol. 147, pp. 1–19, 2016.

[28] M. Paul, R. M. Thushara, S. Jagadish et al., "Novel sila-amide derivatives of N-acetylcysteine protects platelets from oxidative stress-induced apoptosis," *Journal of Thrombosis and Thrombolysis*, vol. 43, no. 2, pp. 209–216, 2017.

[29] S. U. Rehman, S. A. Shah, T. Ali, J. I. Chung, and M. O. Kim, "Anthocyanins reversed D-galactose-induced oxidative stress and neuroinflammation mediated cognitive impairment in adult rats," *Molecular Neurobiology*, vol. 54, no. 1, pp. 255–271, 2017.

[30] X. Y. Song, Y. Y. Wang, S. F. Chu et al., "A new coumarin derivative, IMM-H004, attenuates okadaic acid-induced spatial memory impairment in rats," *Acta Pharmacologica Sinica*, vol. 37, no. 4, pp. 444–452, 2016.

[31] D. I. Kim, K. H. Lee, A. A. Gabr et al., "Abeta-induced Drp1 phosphorylation through Akt activation promotes excessive mitochondrial fission leading to neuronal apoptosis," *Biochimica et Biophysica Acta (BBA) - Molecular Cell Research*, vol. 1863, no. 11, pp. 2820–2834, 2016.

[32] M. Fei, W. Jianghua, M. Rujuan, Z. Wei, and W. Qian, "The relationship of plasma Abeta levels to dementia in aging individuals with mild cognitive impairment," *Journal of the Neurological Sciences*, vol. 305, no. 1-2, pp. 92–96, 2011.

[33] J. W. Lee, "Fructus corni officinalis water extract ameliorates memory impairment and beta amyloid (Aβ) clearance by LRP-1 expression in the hippocampus of a rat model of Alzheimer's disease," *Journal of Physiology & Pathology in Korean Medicine*, vol. 30, no. 5, p. 347, 2016.

[34] G. A. Elmegeed, H. H. Ahmed, M. A. Hashash, M. M. Abd-Elhalim, and D. S. El-kady, "Synthesis of novel steroidal curcumin derivatives as anti-Alzheimer's disease candidates: evidences-based on in vivo study," *Steroids*, vol. 101, pp. 78–89, 2015.

[35] K. Biswas, A. K. Azad, T. Sultana et al., "Assessment of in-vitro cholinesterase inhibitory and thrombolytic potential of bark and seed extracts of Tamarindus indica (L.) relevant to the treatment of Alzheimer's disease and clotting disorders," *Journal of Intercultural Ethnopharmacology*, vol. 6, no. 1, pp. 115–120, 2017.

Hindawi
Oxidative Medicine and Cellular Longevity
Volume 2017, Article ID 6405278, 9 pages
https://doi.org/10.1155/2017/6405278

Research Article

Role of Diet and Nutritional Supplements in Parkinson's Disease Progression

Laurie K. Mischley,[1] Richard C. Lau,[2] and Rachel D. Bennett[1]

[1]*Bastyr University Research Institute, 14500 Juanita Dr. NE, Kenmore, WA 98028, USA*
[2]*Oregon State University, 101 Milam Hall, Corvallis, OR 97331, USA*

Correspondence should be addressed to Laurie K. Mischley; lmischley@bastyr.edu

Received 11 April 2017; Revised 19 July 2017; Accepted 30 July 2017; Published 10 September 2017

Academic Editor: Anna M. Giudetti

Objectives. The goal of this study is to describe modifiable lifestyle variables associated with reduced rate of Parkinson's disease (PD) progression. *Methods*. The patient-reported outcomes in PD (PRO-PD) were used as the primary outcome measure, and a food frequency questionnaire (FFQ) was used to assess dietary intake. In this cross-sectional analysis, regression analysis was performed on baseline data to identify the nutritional and pharmacological interventions associated with the rate of PD progression. All analyses were adjusted for age, gender, and years since diagnosis. *Results*. 1053 individuals with self-reported idiopathic PD were available for analysis. Foods associated with the reduced rate of PD progression included fresh vegetables, fresh fruit, nuts and seeds, nonfried fish, olive oil, wine, coconut oil, fresh herbs, and spices ($P < 0.05$). Foods associated with more rapid PD progression include canned fruits and vegetables, diet and nondiet soda, fried foods, beef, ice cream, yogurt, and cheese ($P < 0.05$). Nutritional supplements coenzyme Q10 and fish oil were associated with reduced PD progression ($P = 0.026$ and $P = 0.019$, resp.), and iron supplementation was associated with faster progression ($P = 0.022$). *Discussion*. These are the first data to provide evidence that targeted nutrition is associated with the rate of PD progression.

1. Introduction

Epidemiological studies have shown that consumption of green tea, coffee, and blueberries and dairy avoidance are associated with reduced likelihood of being diagnosed with Parkinson's disease (PD) [1–4]. Food which protects does not necessarily treat and patients already diagnosed want to know "Does my diet and/or lifestyle affect the course of my disease?"

PD is a slowly progressing disease, so disease-modification trials require long follow-up periods. The heterogeneity of the disease requires enrollment of large populations, both of which increase the expense of clinical trials. Motor symptoms are now known to occur late in the disease and thus may not be an ideal outcome measure for protection, although biomarkers of early disease are lacking. Further complicating matters, results of efficacy (or lack thereof) seen in the controlled, ideal environment of a randomized controlled trial, may or may not translate to effectiveness in a real-life setting. To circumvent these issues, a study was designed to ask patients directly about their food choices and use of supplements. The positive deviance approach uses disease heterogeneity to our advantage, permitting the identification of individuals progressing at a substantially slower or faster rate of PD progression [5]. The goal of this study was to describe whether modifiable aspects of lifestyle are associated with PD symptom severity and progression.

2. Materials and Methods

"Complementary and alternative medicine in PD (CAM Care in PD)" is a pragmatic, prospective observational study that was designed to accomplish the task. The questionnaire was designed by the PI (LKM) based on her experience as a nutritional neuroepidemiologist, clinical trialist, and physician specializing in PD. A study webpage, hosted by Bastyr University, provided automated access to participation. In

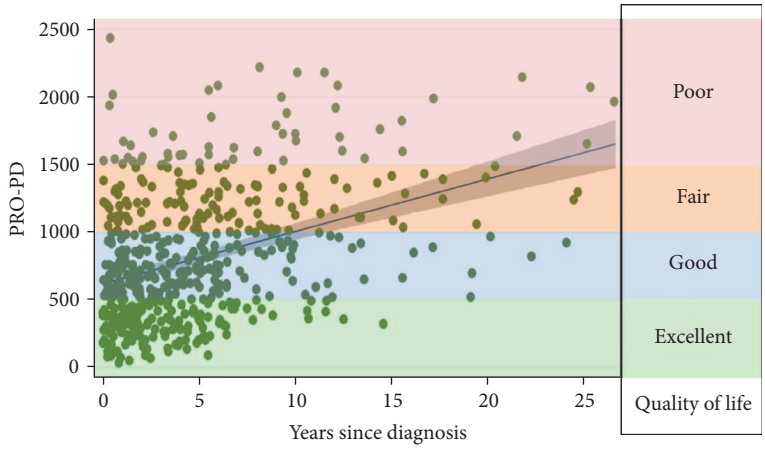

Figure 1: The PRO-PD score is the sum of 33 motor, mood, and other nonmotor symptoms common in PD. Higher scores represent either more symptoms or greater symptom severity of a few symptoms. Lower PRO-PD scores correlate with better social, emotional, and physical quality of life [7].

addition to recruitment via social media, IRB-approved recruitment cards were distributed at PD support groups and to colleagues at neurology conferences.

The primary outcome measure was an assessment tool, patient-reported outcomes in PD (PRO-PD), designed to assess PD severity. The PRO-PD consists of 33 common PD symptoms, and the participant is asked to move the tab on a slider bar according to symptom severity. The left side of the bar always represents optimal health (lack of symptom), and the right side of the bar always represents maximum symptom severity. The PRO-PD score is the cumulative score of each of the symptoms, each of which is assigned a value 0–100, resulting in a continuous outcome measure that increases over time. In a cross-sectional analysis, PRO-PD scores correlated with disease duration ($r = 0.388$, $P < 0.000$), total UPDRS ($r = 0.446$, $P = 0.008$), patient-assessed Hoehn and Yahr (HY) ($r = 0.636$, $P < 0.000$), PDQ-39 ($r = 0.763$, $P < 0.000$), PROMIS Global quality of life question ($r = -0.744$, $P < 0.000$) (Figure 1), and the Timed Up and Go (TUG) ($r = 0.457$, $P < 0.006$). The PRO-PD nonmotor subscore correlated with Nonmotor Symptom Scores (NMSS) ($r = 0.911$, $P < 0.000$) [6].

Individuals with all forms of parkinsonism were invited to participate in the CAM Care in PD study. While the CAM Care in PD study is designed to be longitudinal, this initial analysis is cross-sectional, as more time is needed before there will be adequate sample size for a robust longitudinal analysis. In the meantime, a cross-sectional study adjusted for years since diagnosis can still offer insights into the association between PD severity and diet and lifestyle factors. For this cross-sectional analysis, only baseline data from individuals with a self-reported diagnosis of idiopathic PD were used. PD severity is defined by the cumulative PRO-PD score, and PD progression is defined by the PRO-PD score adjusted for years since diagnosis.

A food frequency questionnaire (FFQ) was developed to quantify dietary intake. The FFQ used in this study was created to be pragmatic and meet the needs of this study by drawing on limitations and successes of other nutritional intake questionnaires. Participants were asked to estimate their intake of foods, on average, over the prior six months. For all dietary variables, participants were given 10 options for rating consumption frequency, ranging from "never" to "5-6 times daily." Other variables chosen were based on incidence data as well as on biological and clinical relevance. Participants were directed to "Please mark the box if you have taken any of the following consistently over the past 6 months" as well as to identify lifestyle choices that they had been engaged in consistently for the last 6 months. All supplement and behavior variables were recorded as binary variables as people either reported using specific supplements/lifestyles or did not.

Multiple linear and logistic regression models were used to examine the association between diet, lifestyle factors, and PD severity, with PRO-PD scores used as the outcome variable. Food frequency questionnaire data is ordinal; due to the relatively large number (10) of consumption frequencies that were offered as options, it was analyzed as a continuous variable. All models controlled for factors known to heavily influence PD severity including age, years since diagnosis, and gender. Additionally, a second model was created that also incorporated income, which may be associated with lifestyle and access factors that may affect PD severity. All statistical work was done using Stata Version 11 (College Station, TX) with alpha set to 0.05. No adjustments were made for multiple comparisons to avoid increasing the risk of type II errors, and the failure to detect an association that is present was a priority for this observational study [8].

3. Results and Discussion

Of the 1307 participants with parkinsonism, 1053 were identified as having a diagnosis of idiopathic PD and were thus available for analysis. The average age of participants was 63 years, with an average 5.2 years since diagnosis. Accordingly, the majority of the study participants were in HY stages 1–3 (93.5%). While gender and income were

Table 1: Demographics of the study participants.

	$N = 1053$
Age, years (SD)	63.1 (9.2)
Years since diagnosis (SD)	5.2 (5.5)
Gender	
Male	463 (44%)
Female	556 (53%)
Ethnicity	
Caucasian	978 (92.9%)
Black	7 (0.7%)
Hispanic	14 (1.3%)
Native American	2 (0.2%)
Asian/Pacific Islander	9 (0.9%)
Other	12 (1.1%)
Income	
Less than $20,000	56 (5.3%)
Between $20 and 40,000	148 (14.1%)
Between $40 and 60,000	139 (13.2%)
Between $60 and 80,000	145 (13.8%)
Between $80 and 100,000	137 (13%)
Between $100 and 150,000	193 (18.3%)
More than $150,000	155 (14.7%)
Hoehn & Yahr stage	
(1) 1-sided symptoms, minimal disability	
(2) Both sides affected, balance is stable	522 (49.6%)
(3) Mild-to-moderate disability, balance affected	171 (16.2%)
	292 (27.7%)
(4) Severe disability, able to walk and stand without help	34 (3.2%)
	2 (0.2%)
(5) Confinement to bed or wheelchair unless aided	9 (0.9%)
Do not know	

evenly distributed across the study population, there was very little ethnic diversity (Table 1).

3.1. Dietary Variables. Using the food frequency questionnaire, the results of this analysis suggest that a plant- and fish-based diet is associated with the lowest PD severity score (Table 2). Fresh vegetables, fresh fruit, nuts and seeds, fish, olive oil, wine, coconut oil, fresh herbs, and the use of spices were all associated with statistically significant lower rates of disease progression.

These foods largely comprise the Mediterranean diet, which has been associated with reduced PD incidence and later age of diagnosis [9]. Likewise, there is evidence that this diet decreases risk and progression of Alzheimer's disease, a related neurodegenerative disorder [10–12]. Only fresh herbs lost statistical significance after adjusting for income, suggesting that fresh herbs may be a luxury item afforded to those in the higher-income brackets.

Ice cream, cheese, and yogurt intakes were associated with higher rates of PD progression (Table 2). Dairy has been repeatedly associated with PD incidence [13–16], and this is the first study to demonstrate an association between dairy consumption and an increased rate of PD progression. In this cohort, neither milk nor butter are associated with PD progression. Previous studies suggested the association was strongest for milk, ice cream, and cream [16], which was replicated with the Greek study [17]; the latter study suggesting yogurt was not associated with increased risk of PD incidence. These data contradict the findings on yogurt from the Greek study but do support the associations with cream. Self-reported dietary intake is notoriously difficult to assess [18], and it may be that the study participants are underestimating milk and butter consumption. For example, it is difficult to estimate how much milk and butter contribute to foods like mashed potatoes and baked goods.

There may be several mechanisms responsible to explain the association between PD progression and dairy consumption:

(1) Dairy intake lowers uric acid [19]. Uric acid quenches peroxynitrite in the CNS, and low uric acid levels are associated with greater PD incidence and faster PD progression [20].

(2) Diary consumption is associated with insulin resistance [21]. There is a growing body of evidence that PD and other neurodegenerative diseases are a form of "type III diabetes" [22].

(3) Lactose intolerance, occurring when the enzyme, lactase, that digests the milk sugar decreases with age, is especially common in individuals of African, Asian, Hispanic, and Native American decent [23]. Consuming dairy in the absence of sufficient lactase may contribute to intestinal inflammation and intestinal permeability.

(4) Presence of a neurotoxic component or contaminant, for example, pesticides, may be present in dairy [23].

(5) Introduction of bovine microbiota, facilitating seeding of methanogenic organisms, leads to the development of methane-dominant small intestinal bacterial overgrowth (SIBO) and other forms of abnormal intestinal flora [24–26].

Consumption of canned fruits and vegetables was a strong predictor of PD progression. Initially thought to be associated with socioeconomic status, the association remained after adjusting for income. Bisphenol A (BPA) is used extensively worldwide in the inner coating of food cans, and there is evidence that BPA contaminates foods stored in the cans. BPA is a well-established endocrine conductor associated with obesity, and more recent evidence suggests that it is an energy balance disruptor [27]. Additionally, aluminum is an established neurotoxicant, and the aluminum content of the cans may be contributing to the association [28].

The association with fried foods may be related to lipid peroxidation resulting from the well-established increase in reactive oxygen species (ROS) observed in PD. Lipid peroxidation results in the production of aldehydes, such as acrolein, that bind covalently with thiol groups of proteins, leading to protein aggregation and dysfunction [29]. In the PD substantia nigra, acrolein accumulates in dopaminergic neurons, modifies alpha-synuclein, and inhibits proteasome

Table 2: Multiple linear regression model of dietary intake and PD progression. Predicted PD severity score, as measured by the PRO-PD, per unit increase in food intake frequency, intake measured on a 10-point scale: never, <1/month, 1/month, 2-3×/month, 1/week, 2–4×/week, 5-6×/week, 1/day, 2–4×/day, 5-6×/day. *Adjusted for years since diagnosis, age, and gender. **Adjusted for years since diagnosis, age, gender, and income.

Association between dietary practices and Parkinson's disease progression				
Food item (serving size)	Mean change in PRO-PD score (SE)*	*P* value (95% CI)*	Mean change in PRO-PD score (SE)**	*P* value (95% CI)**
Fresh vegetables (1/2 cup)	−53.2 (7.9)	<0.000 (−68.7 to −37.6)	−48.9 (8.3)	<0.000 (−64.7 to −33.1)
Fresh fruit (1/2 cup)	−44.1 (8.5)	<0.000 (−60.7 to −27.5)	−40.7 (8.6)	<0.000 (−57.5 to −23.9)
Nuts (1/4 cup or 2 tbsp spread)	−38.5 (7.5)	<0.000 (−53.2 to −23.7)	−33.2 (7.6)	<0.000 (−48.1 to −18.4)
Fish (4 oz)	−37.1 (8.9)	<0.000 (−54.6 to −19.5)	−29.5 (9.1)	0.001 (−47.3 to −11.6)
Olive oil (1 tsp)	−34.1 (6.8)	<0.000 (−47.4 to −20.8)	−31.4 (6.8)	<0.000 (−44.7 to −18.1)
Wine (6 oz)	−23.6 (5.3)	<0.000 (−34.1 to −13.1)	−14.6 (5.6)	0.009 (−25.5 to −3.7)
Turkey (4 oz)	−20.2 (18.7)	0.281 (−57.1 to 16.7)	−10.8 (19.2)	0.573 (−48.7 to 27)
Coconut oil (1 tsp)	−18.6 (5.5)	0.001 (−29.3 to −7.8)	−20.2 (5.5)	<0.000 (−31 to −9.4)
Fresh herbs (1 tsp)	−14.9 (6.4)	0.02 (−27.4 to −2.4)	−8.9 (6.5)	0.169 (−21.7 to 3.8)
Spices (1/4 tsp)	−14.2 (6.4)	0.027 (−26.7 to −1.6)	−13.4 (6.4)	0.037 (−26 to −0.8)
Eggs (1 egg)	−9.5 (8.2)	0.251 (−25.6 to 6.7)	−9.7 (8.3)	0.241 (−26 to 6.5)
Bread (1 slice)	−7.7 (6.8)	0.26 (−21.2 to 5.7)	−6.9 (6.9)	0.314 (−20.4 to 6.6)
Beans (1/2 cup)	−6.3 (8.6)	0.466 (−23.3 to 10.7)	−5.4 (8.8)	0.54 (−22.6 to 11.8)
Butter (1 tsp)	−4 (5.9)	0.494 (−15.6 to 7.5)	−3.8 (6)	0.522 (−15.5 to 7.9)
Oatmeal (1 cup)	−3.2 (6.5)	0.624 (−15.9 to 9.5)	−4.4 (6.6)	0.501 (−17.3 to 8.5)
Liquor (1 oz)	−2.8 (7.7)	0.717 (−17.8 to 12.3)	3.6 (7.7)	0.47 (−11.5 to 18.7)
Green tea (1 cup)	−2.3 (5.7)	0.68 (−13.5 to 8.8)	1.6 (5.7)	0.779 (−9.6 to 12.7)
Juice (8 oz)	−2.3 (5.8)	0.687 (−13.8 to 9.1)	−1.4 (5.9)	0.811 (−12.9 to 10.1)
Frozen fruit (1/2 cup)	−1.9 (6.1)	0.757 (−13.8 to 10)	−2.2 (6.1)	0.714 (−14.1 to 9.7)
Cream (1/4 cup)	−0.5 (7.4)	0.942 (−15.2 to 14.1)	−0.3 (7.4)	0.971 (−14.7 to 14.2)
Coffee (8 oz)	−0.1 (4.4)	0.983 (−8.8 to 8.6)	4.3 (4.5)	0.342 (−4.5 to 13.1)
Soy (3 oz)	0.4 (7.9)	0.962 (−15.2 to 16)	2.3 (8)	0.77 (−13.4 to 18.1)
Safflower oil (1 tsp)	0.7 (6.9)	0.922 (−12.8 to 14.2)	6.8 (6.9)	0.325 (−6.8 to 20.5)
Beer (12 oz)	1.1 (7.6)	0.88 (−13.7 to 16)	2 (7.5)	0.789 (−12.8 to 16.8)
Chicken (4 oz)	3.3 (9.7)	0.34 (−15.6 to 22.3)	13.4 (9.8)	0.171 (−5.8 to 32.5)
Milk (1 cup) (mammalian, for example, cow)	5.8 (4.8)	0.226 (−3.6 to 15.2)	5.1 (4.8)	0.291 (−4.4 to 14.5)
Pork (4 oz)	6.1 (8.6)	0.482 (−10.8 to 22.9)	7 (8.7)	0.42 (−10 to 24)
Black tea (1 cup)	8.6 (5.6)	0.121 (−2.3 to 19.5)	8.4 (5.6)	0.131 (−2.5 to 19.3)
Eat food from a can	9.6 (8.1)	0.234 (−6.2 to 25.4)	6.1 (8.1)	0.449 (−9.7 to 22)
Pasta (1 cup)	10.1 (9.3)	0.28 (−8.2 to 28.4)	9.2 (9.4)	0.326 (−9.2 to 27.6)
Frozen vegetables (1/2 cup)	11 (6.9)	0.11 (−2.5 to 24.4)	10.3 (6.9)	0.137 (−3.3 to 23.9)
Cheese (1 slice, 1/2 oz, 1 tbsp)	11.7 (6.9)	0.091 (−1.9 to 25.3)	15.5 (6.9)	0.026 (1.9 to 29.1)
Yogurt (3/4 cup)	13.5 (7.5)	0.073 (−1.3 to 28.3)	15.2 (7.6)	0.046 (0.2 to 30.1)
Ice cream (1/2 cup)	13.8 (7.4)	0.064 (−0.8 to 28.3)	18.3 (7.5)	0.015 (3.6 to 32.9)
Soda (12 oz)	15.4 (7.8)	0.049 (0.03 to 30.7)	15.2 (7.9)	0.054 (−0.3 to 30.6)
Beef (4 oz)	16.2 (8.3)	0.051 (−0.1 to 32.4)	21.8 (8.3)	0.009 (5.5 to 38.1)
Fried food (4 oz)	19.5 (8.8)	0.027 (2.2 to 36.8)	23 (8.9)	0.009 (5.6 to 40.4)
Canned vegetables (1/2 cup)	19.9 (7)	0.005 (6.1 to 33.6)	18.3 (7)	0.009 (4.5 to 32.1)
Diet soda (12 oz)	20.7 (6.1)	0.001 (8.7 to 32.8)	23.6 (6.1)	<0.000 (11.6 to 35.6)
Canned fruit (1/2 cup)	36.1 (7.9)	<0.000 (20.5 to 51.6)	32 (7.9)	<0.000 (16.5 to 47.6)

activity [30]. Accordingly, in recent years, there has been a call to develop new PD treatments that target lipid peroxidation [31].

Soda, specifically diet soda, was also associated with a faster rate of PD progression. Soda is a sugar-sweetened beverage associated with additional caloric intake and obesity

Table 3: Logistic regression model of nutritional supplements and PD progression. Predicted PD severity score, as measured by the PRO-PD, based on the positive report of consistently using of supplements over the previous 6 months. *Adjusted for years since diagnosis, age, and gender. **Adjusted for years since diagnosis, age, gender, and income.

Association between dietary supplements & risk of Parkinson's disease progression					
Nutritional supplement	*n*	Mean change in PRO-PD score (SE)*	*P* value (95% CI)*	Mean change in PRO-PD score (SE)**	*P* value (95% CI)**
Inosine	13	−181.1 (125.6)	0.15 (−427.5 to 65.3)	−107.1 (122.9)	0.384 (−348.4 to 134.2)
Glutathione, oral	43	−126.1 (69)	0.068 (−261.6 to 9.3)	−126.7 (70)	0.07 (−263.9 to 10.5)
DHEA	47	−87.6 (70.8)	0.216 (−226.6 to 51.4)	−72.2 (70.9)	0.309 (−211.3 to 67)
Lithium, low dose	21	−84.9 (100.2)	0.397 (−281.6 to 111.8)	−118.9 (100.4)	0.237 (−315.9 to 78.1)
Low-dose naltrexone	14	−76.1 (120.9)	0.529 (−313.4 to 161.2)	−87.8 (118)	0.457 (−319.3 to 143.8)
CoQ10	286	−70.4 (31.5)	0.026 (−132.2 to −8.6)	−46.6 (31.6)	0.141 (−108.7 to 15.4)
Fish oil	376	−69.5 (29.5)	0.019 (−127.4 to −11.6)	−57.7 (29.6)	0.052 (−115.7 to 0.4)
Quercetin	21	−50.7 (105.9)	0.632 (−258.5 to 157.1)	−60.5 (106.4)	0.569 (−269.3 to 148.2)
Turmeric/curcumin	197	−47.3 (35.6)	0.186 (−117.3 to 22.8)	−49.5 (35.9)	0.168 (−120 to 20.9)
Gingko biloba	30	−47.2 (83.2)	0.57 (−210.5 to 116)	−61.1 (81.2)	0452 (−220.5 to 98.2)
Coconut oil	190	−35.8 (36.4)	0.324 (−107.2 to 35.5)	−52.7 (36.4)	0.147 (−124.1 to 18.6)
Resveratrol	43	−28.5 (70.7)	0.687 (−167.3 to 110.3)	−18.7 (72.7)	0.797 (−161.4 to 124)
Vitamin D	623	−26.1 (29)	0.368 (−83 to 30.8)	−3.6 (29.2)	0.902 (−60.9 to 53.7)
Alpha-lipoic acid	79	−19.1 (53.4)	0.72 (−123.9 to 85.7)	0.05 (54.4)	0.999 (−106.7 to 106.7)
5-Methyltetrahydrofolate (5-MTHF)	27	−17.1 (91.4)	0.852 (−196.4 to 162.2)	−25.1 (95.6)	0.793 (−212.7 to 162.5)
Probiotics	249	−12.3 (32.7)	0.708 (−76.5 to 52)	−12.4 (32.9)	0.706 (−77 to 52)
NADH	14	−9.7 (120.8)	0.936 (−246.7 to 227.3)	−25.2 (122.6)	0.837 (−265.7 to 215.4)
Multivitamin/mineral	342	−7.8 (30.2)	0.795 (−67.1 to 51.4)	9.9 (30.3)	0.744 (−49.6 to 69.5)
Calcium	324	−6.2 (32.2)	0.847 (−69.4 to 57)	12.5 (32.6)	0.701 (−51.4 to 76.4)
B6, B12, folic acid, betaine combination	88	3.4 (49.7)	0.946 (−94.2 to 101)	11.1 (48.9)	0.82 (−84.9 to 107.1)
Vitamin C	327	4.2 (30.6)	0.891 (−55.9 to 64.3)	−3.8 (31)	0.902 (−64.6 to 56.9)
N-Acetyl cysteine (NAC)	59	12.8 (60.1)	0.831 (−105 to 130.7)	26.9 (60.8)	0.658 (−92.4 to 146.1)
Vitamin B12 (methyl-B12/cyano-B12)	353	26.7 (29.8)	0.37 (−31.8 to 85.3)	43 (29.8)	0.15 (−15.6 to 101.6)
Rubidium	2	34.2 (306)	0.911 (−566.4 to 634.7)	93.1 (298.5)	0.755 (−492.7 to 678.8)
Estrogen	51	40 (67.4)	0.553 (−92.2 to 172.3)	15.2 (69.6)	0.827 (−121.4 to 151.8)
Glutathione, intranasal	24	62.9 (95.5)	0.51 (−124.5 to 250.4)	55.6 (93.2)	0.551 (−127.3 to 238.5)
Mucuna	33	67 (81.7)	0.412 (−93.3 to 227.2)	21.8 (80)	0.785 (−135.1 to 178.6)
Fava beans	17	122 (109)	0.263 (−92 to 336)	87.8 (110.1)	0.425 (−128.2 to 303.8)
Melatonin	148	139.3 (40.5)	0.001 (59.8 to 218.8)	134.8 (40.2)	0.001 (56 to 213.6)
Iron (Fe)	57	146.4 (63.9)	0.022 (21 to 271.9)	179.7 (64.3)	0.005 (53.6 to 305.9)

[32], which was also associated with PD progression in this study (Table 3). As was discussed in the section on dairy, there is growing evidence that PD might be considered type 3 diabetes. The association with PD progression was higher for diet soda than regular soda. Following consumption, aspartame is metabolized to phenylalanine, aspartic acid, and methanol. The increase in phenylalanine and aspartic acid interferes with the transport of serotonin and dopamine to the brain, increases neuronal hyperexcitability, and leads to degeneration in astrocytes and neurons [33, 34].

The association between beef and PD progression is congruent with traditional epidemiologic research demonstrating an association between beef consumption and PD incidence [2]. Beef and pork, the most frequently consumed mammals in the Western diet, have several things in common, including a high-fat content and slow intestinal transit time. That intake of pork which was not statistically significantly associated with worse prognosis suggests that future research should be directed toward variables unique to beef, such as the higher iron content. Recent research suggests that alpha-synuclein in the enteric nervous system is associated with immune cell activation [35]; as both milk and meat from bovine sources have been linked to incidence and progression of PD, cross-reactivity between common antigens in the enteric nervous system should also be considered [36]. It is well known that dietary protein competes with levodopa for intestinal absorption and it is possible the high protein content of beef and dairy may not be affecting the disease, but making the medication less effective.

3.2. Nutritional Supplements. Of all the nutritional supplements studied, only coenzyme Q10 and fish oil were

associated with statistically significant reduced rates of PD progression (Table 3). The association between coenzyme Q10 and PD progression disappeared after adjusting for income, which was not unexpected given the high cost of the supplement and lack of third-party reimbursement. In a clinical case series, patients with PD had significantly greater odds of deficiency in coenzyme Q10 status compared to controls (OR: 4.7–5.4; 95% CI: 1.5–17.7; $P = 0.003$–0.009). The proportion of PD cases with coenzyme Q10 deficiency was also significantly greater in cases than in controls (32–36% versus 8-9%; $P = 0.0012$–0.006) [37]. Coenzyme Q10 has been very successful in preclinical models and early human studies [38], although failed in a large multicenter, double-blind, placebo-controlled, randomized clinical trial [39]. A recent meta-analysis of randomized controlled trials failed to demonstrate any improvement in PD motor symptoms following coenzyme Q10 supplementation [40]. The improvement in PD progression in this pragmatic survey that lost statistical significance when income was considered suggests that either individual in higher-income brackets is wasting their money on the ineffective coenzyme Q10 supplement or that higher income provides access to more neuroprotective nutrients and therapies. If the latter is true, the study design of controlled trials should be re-evaluated, as the artificial environment of controlled trials, for example, dopamine restriction, or the outcome measure, for example, UPDRS, may not be well suited to evaluating the effectiveness of coenzyme Q10 in a real-life setting.

Fish oil is a rich source of the omega-3 fatty acids eicosapentaenoic acid (EPA) and docosahexaenoic acid (DHA). There has been a tremendous amount of research conducted on the role of EPA and DHA in neuronal health. The neuroprotective effects of DHA, in particular, have been attributed to multiple mechanisms. In addition to acting as an antioxidant, DHA reduces inflammation by reducing arachidonic acid and its metabolites. As a precursor to neuroprotectin D1, it exerts antiapoptotic activity, enhances the synthesis of the neurotrophic factor, brain-derived neurotrophic factor (BDNF), and promotes neurogenesis via enhanced synaptogenesis and neurite outgrowth [41–43]. Only one randomized clinical trial has been conducted in which fish oil supplements were given to individuals with PD thus far, specifically targeting depression. In this pilot study, 31 individuals were randomized to fish oil capsules or mineral oil capsules for 12 weeks. At the end of the intervention period, those randomized to the fish oil capsules had statistically significant improvements in depression over the group randomized to mineral oil, as measured by the Montgomery-Asberg Rating Scale and Clinical Global Impression-Depression score, although this benefit was not apparent using the Beck Depression Inventory [44].

There is conflicting evidence regarding the use of melatonin, a hormone produced by the pineal gland, in PD. Melatonin regulates the body's circadian rhythm: levels increase at night in response to the absence of light. The presence of this hormone induces the neurophysiological changes that occur during the brain restoration taking place during sleep. Sleep disorders are common in PD [45], and a substantial body of literature exists related to the neuroprotective role of melatonin, as well as to its putative role in treating PD motor and nonmotor impairments, including insomnia, anxiety, depression, and cognitive impairment [46]. A recent meta-analysis of randomized controlled clinical trials of exogenous melatonin for sleep disorders in neurodegenerative diseases found that melatonin improved rapid eye movement (REM) sleep behavior disorder (RBD) and Pittsburgh Sleep Quality Index (PSQI), although there was no evidence of improvement in objective sleep outcomes [47]. Thus, these data suggesting that melatonin use was associated with PD progression were at odds with the hypothesis that melatonin may stave off PD progression (Table 3). Because insomnia is also associated with PD progression and individuals with impaired sleep are more likely to take melatonin than those without sleep disorders, we observed whether the association remained after adjusting for impaired sleep (Figure 2). Insomnia and PRO-PD scores were correlated, and after adjusting for self-reported insomnia, the association between melatonin and PD progression was no longer significant ($P = 0.001$ and $P = 0.406$, resp.). These data suggest that insomnia, not the use of melatonin, is associated with PD progression.

Iron, prone to oxidation, has long been implicated in PD, and these results suggest that iron supplementation is associated with PD progression (Table 3). It is thought that the high iron content of the substantia nigra, required for dopamine synthesis, contributes to the selective vulnerability of the region. As already discussed, red meat consumption is associated with PD progression, while other high-fat meats, for example, pork, were not; it is possible that the high iron content of red meat may explain this correlation.

3.3. Nutritional Behaviors. After adjusting for age, gender, years since diagnosis, and income, individuals who prepare their own meals, and meals for others, were afforded protection against PD progression (Table 4). Individuals who report purchasing food from a local farmer's markets and going out of their way to eat organically grown food were also more likely to have lower PRO-PD scores (Table 4). This line of questions was designed to be a surrogate for mindfulness and attention to ingredients.

Individuals who find it difficult to afford food, especially healthy food, were associated with a faster rate of PD progression. While type 2 diabetes increases risk of PD [48], the association between the body weight index and risk of PD has been less clear [49].

4. Conclusions

This pragmatic, natural history study offers the first evidence-base for prescribing lifestyle modification (beyond exercise) to patients with PD. The foods shown here to be associated with slower PD progression are common to the Mediterranean diet and support an existing body of literature. Whether iron, beef, dairy, fried foods, diet soda, or canned goods provide environmental insults that accelerate disease progression warrants immediate attention; until

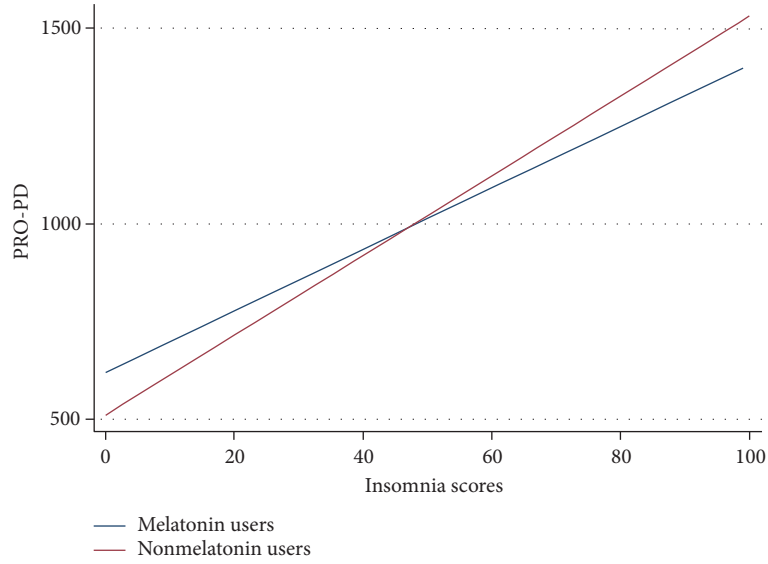

Figure 2: Correlation between insomnia and PD severity among individuals who do, and do not, report consistent use of melatonin over the previous six months.

Table 4: Logistic regression model of dietary behaviors and PD progression. Predicted PD severity score, as measured by the PRO-PD. Participants were asked to select all of the statements that were true over the prior 6 months; plastic bottle utilization was evaluated on a 10-point scale, also over the prior 6 months. *Adjusted for years since diagnosis, age, and gender. **Adjusted for years since diagnosis, age, gender, and income.

Dietary behaviors associated with Parkinson's disease progression				
Dietary behaviors	Mean change in PRO-PD score (SE)*	*P* value (95% CI)*	Mean change in PRO-PD score (SE)**	*P* value (95% CI)**
I routinely prepare meals for others.	−141.1 (29.3)	<0.000 (−198.7 to −83.6)	−112.8 (29.7)	<0.000 (−171.2 to −4.4)
I cook most of my meals.	−115.1 (30.2)	<0.000 (−174.4 to −55.7)	−135.4 (30.3)	<0.000 (−194.9 to −5.8)
I buy food from a local farmers (co-op, farmer's markets)	−98 (28.3)	0.001 (−153.5 to −42.5)	−97.2 (28.4)	0.001 (−153 to −41.5)
I try to eat organically grown foods when possible.	−61.3 (28.1)	0.029 (−116.5 to −6.2)	−74.9 (28.1)	0.008 (−130 to −19.8)
I drink from a plastic bottle.	11.2 (5.4)	0.039 (0.6 to 21.8)	11.9 (5.4)	0.029 (1.2 to 22.6)
I am overweight.	169.4 (28.5)	<0.000 (113.5 to 225.3)	165.8 (28.5)	<0.000 (109.8 to 221.8)
It is difficult to afford groceries.	443.5 (51.2)	<0.000 (343.1 to 543.9)	348.7 (55.4)	<0.000 (240 to 457.3)
I find it difficult to afford healthy food.	473.6 (46.1)	<0.000 (383 to 564.1)	389.3 (49.5)	<0.000 (292.2 to 486.5)

further research is conducted, minimizing exposure to these foods is justified.

Because weight loss commonly occurs as the disease progresses, any suggestion that patients avoid foods increases the risk of restricting calories and contributing to malnutrition. Patients should be counseled on alternative sources of protein (e.g., beans, nuts, and seeds) and calcium (e.g., almonds, green leafy vegetables, and tofu).

Fish oil supplementation is warranted in individuals with a diagnosis of PD and justified based on biological plausibility and the clinical epidemiological data. As fish oil supplements are sold over the counter, there is a tremendous amount of diversity in both content of EPA and DHA, as well as in quality (e.g., presence of contaminants), whereas providers should familiarize themselves with available products and recommend buying from companies that perform analysis on stability, purity, and potency. Consumption of nonfried oily fish, such as herring, sardines, mackerel, and salmon should be encouraged. Because the association between coenzyme Q10 and PD progression was no longer significant after adjusting for income, more research needs to be done before recommending patients to start supplementing coenzyme Q10.

Health care providers should routinely review patients' supplement lists and ensure that the only patients taking iron are those with iron-deficiency anemia being treated under medical supervision. Because iron is commonly added to multivitamins, men and nonmenstruating women should not take a multivitamin containing iron, unless recommended by their physician.

The risk of bias should be considered in interpreting these data. Dietary intake is difficult to estimate (e.g., ingredients in casserole) and susceptible to recall bias (e.g., tasting food while cooking, food samples at the store, and other snacking are often under-reported). This is offset in this study because the questionnaire only asked about recent intake, the prior six months, and that all subjects in the study are affected equally by this limitation in recall. There is likely to be selection bias in this sample, as individuals using integrative medicine are expected to be more likely to enroll in a study called "Complementary and Alternative Medicine (CAM) in PD". In an attempt to minimize this bias, the study home page explains that all individuals are invited to participate, regardless of disease duration, severity, or CAM use. Still, the degree to which these data are generalizable to the larger PD population has yet to be determined.

These data would be substantially improved with associated biomarkers of nutrient intake and physical examination of participants, both to screen for evidence of nutritional deficiencies and to confirm the diagnosis. This study is also limited by the homogeneity of the population, which was largely Caucasian and from the United States. Despite these limitations, these data suggest that the survey study design and PRO-PD are useful tools for deriving information about food, nutrition, and PD progression. As this is a longitudinal study that is still enrolling participants, it is likely that the foods and supplements associated with PD progression will change over time, as more people enroll, with evaluation of the longitudinal data. Clinicians now have data on which to base their recommendation for healthy eating in PD, and patients are likely to be empowered to know that their day-to-day choices may influence progression.

Conflicts of Interest

Dr. Laurie K. Mischley owns the PRO-PD rating scale. There are no other conflicts to disclose.

Acknowledgments

This work was supported by the NCCIH, National Institutes of Health/Bernard Osher K01 Career Transition Award (NIH K01 AT004404) and a donation from Sondra and Bill Fondren.

References

[1] X. Gao, A. Cassidy, M. A. Schwarzschild, E. B. Rimm, and A. Ascherio, "Habitual intake of dietary flavonoids and risk of Parkinson disease," *Neurology*, vol. 78, pp. 1138–1145, 2012.

[2] X. Gao, H. Chen, T. T. Fung et al., "Prospective study of dietary pattern and risk of Parkinson disease," *The American Journal of Clinical Nutrition*, vol. 86, pp. 1486–1494, 2007.

[3] A. Ueki and M. Otsuka, "Life style risks of Parkinson's disease: association between decreased water intake and constipation," *Journal of Neurology*, vol. 251, Supplement 7, pp. vII18–vII23, 2004.

[4] G. Hu, S. Bidel, P. Jousilahti, R. Antikainen, and J. Tuomilehto, "Coffee and tea consumption and the risk of Parkinson's disease," *Movement disorders*, vol. 22, pp. 2242–2248, 2007.

[5] D. R. Marsh, D. G. Schroeder, K. A. Dearden, J. Sternin, and M. Sternin, "The power of positive deviance," *British Medical Journal*, vol. 329, pp. 1177–1179, 2004.

[6] L. K. Mischley, R. C. Lau, and N. S. Weiss, "Use of a self-rating scale of the nature and severity of symptoms in Parkinson's disease (PRO-PD): correlation with quality of life and existing scales of disease severity," *NPJ Parkinson's Disease*, vol. 3, p. 20, 2017.

[7] L. K. Mischley, "Patient reported outcomes in Parkinson's disease (PRO-PD) rating scale validation: 1566," *Movement Disorders*, vol. 31, article S514, 2016.

[8] K. J. Rothman, "No adjustments are needed for multiple comparisons," *Epidemiology*, vol. 1, pp. 43–46, 1990.

[9] R. N. Alcalay, Y. Gu, H. Mejia-Santana, L. Cote, K. S. Marder, and N. Scarmeas, "The association between Mediterranean diet adherence and Parkinson's disease," *Movement Disorders*, vol. 27, pp. 771–774, 2012.

[10] B. Singh, A. K. Parsaik, M. M. Mielke et al., "Association of Mediterranean diet with mild cognitive impairment and Alzheimer's disease: a systematic review and meta-analysis," *Journal of Alzheimer's Disease*, vol. 39, pp. 271–282, 2014.

[11] J. E. Morley, "New horizons in the management of Alzheimer disease," *Journal of the American Medical Directors Association*, vol. 16, pp. 1–5, 2015.

[12] D. E. Bredesen, E. C. Amos, J. Canick et al., "Reversal of cognitive decline in Alzheimer's disease," *Aging (Albany NY)*, vol. 8, pp. 1250–1258, 2016.

[13] W. Jiang, C. Ju, H. Jiang, and D. Zhang, "Dairy foods intake and risk of Parkinson's disease: a dose-response meta-analysis of prospective cohort studies," *European Journal of Epidemiology*, vol. 29, pp. 613–619, 2014.

[14] H. Chen, E. O'Reilly, M. L. McCullough et al., "Consumption of dairy products and risk of Parkinson's disease," *American Journal of Epidemiology*, vol. 165, pp. 998–1006, 2007.

[15] H. Chen, S. M. Zhang, M. A. Hernan, W. C. Willett, and A. Ascherio, "Diet and Parkinson's disease: a potential role of dairy products in men," *Annals of Neurology*, vol. 52, pp. 793–801, 2002.

[16] M. Park, G. W. Ross, H. Petrovitch et al., "Consumption of milk and calcium in midlife and the future risk of Parkinson disease," *Neurology*, vol. 64, pp. 1047–1051, 2005.

[17] A. Kyrozis, A. Ghika, P. Stathopoulos, D. Vassilopoulos, D. Trichopoulos, and A. Trichopoulou, "Dietary and lifestyle variables in relation to incidence of Parkinson's disease in Greece," *European Journal of Epidemiology*, vol. 28, no. 1, 2013.

[18] A. K. Illner, H. Freisling, H. Boeing, I. Huybrechts, S. P. Crispim, and N. Slimani, "Review and evaluation of innovative technologies for measuring diet in nutritional epidemiology," *International Journal of Epidemiology*, vol. 41, pp. 1187–1203, 2012.

[19] N. Dalbeth, R. Ames, G. D. Gamble et al., "Effects of skim milk powder enriched with glycomacropeptide and G600 milk fat extract on frequency of gout flares: a proof-of-concept randomised controlled trial," *Annals of the Rheumatic Diseases*, vol. 71, pp. 929–934, 2012.

[20] E. Vieru, A. Koksal, B. Mutluay, A. C. Dirican, Y. Altunkaynak, and S. Baybas, "The relation of serum uric acid levels with L-dopa treatment and progression in patients with Parkinson's disease," *Neurological Sciences*, vol. 37, pp. 743–747, 2016.

[21] L. A. Tucker, A. Erickson, J. D. LeCheminant, and B. W. Bailey, "Dairy consumption and insulin resistance: the role of body fat, physical activity, and energy intake," *Journal of Diabetes Research*, vol. 2015, Article ID 206959, 11 pages, 2015.

[22] A. I. Duarte, E. Candeias, S. C. Correia et al., "Crosstalk between diabetes and brain: glucagon-like peptide-1 mimetics as a promising therapy against neurodegeneration," *Biochimica et Biophysica Acta (BBA) - Molecular Basis of Disease*, vol. 1832, pp. 527–541, 2013.

[23] P. Bertron, N. D. Barnard, and M. Mills, "Racial bias in federal nutrition policy, part I: the public health implications of variations in lactase persistence," *Journal of the National Medical Association*, vol. 91, pp. 151–157, 1999.

[24] A. H. Tan, S. Mahadeva, A. M. Thalha et al., "Small intestinal bacterial overgrowth in Parkinson's disease," *Parkinsonism & Related Disorders*, vol. 20, pp. 535–540, 2014.

[25] R. Sandyk and M. A. Gillman, "Motor dysfunction following chronic exposure to a fluoroalkane solvent mixture containing nitromethane," *European Neurology*, vol. 23, pp. 479–481, 1984.

[26] M. Makhani, J. Yang, J. Mirocha, K. Low, and M. Pimentel, "Factor analysis demonstrates a symptom cluster related to methane and non-methane production in irritable bowel syndrome," *Journal of Clinical Gastroenterology*, vol. 45, pp. 40–44, 2011.

[27] L. Le Corre, P. Besnard, and M. C. Chagnon, "BPA, an energy balance disruptor," *Critical Reviews in Food Science and Nutrition*, vol. 55, pp. 769–777, 2015.

[28] J. Campdelacreu, "Parkinson disease and Alzheimer disease: environmental risk factors," *Neurología*, vol. 29, pp. 541–549, 2014.

[29] N. Plotegher and L. Bubacco, "Lysines, Achilles' heel in alpha-synuclein conversion to a deadly neuronal endotoxin," *Ageing Research Reviews*, vol. 26, pp. 62–71, 2016.

[30] M. Shamoto-Nagai, W. Maruyama, Y. Hashizume et al., "In parkinsonian substantia nigra, alpha-synuclein is modified by acrolein, a lipid-peroxidation product, and accumulates in the dopamine neurons with inhibition of proteasome activity," *Journal of Neural Transmission*, vol. 114, pp. 1559–1567, 2007.

[31] C. C. de Farias, M. Maes, K. L. Bonifacio et al., "Highly specific changes in antioxidant levels and lipid peroxidation in Parkinson's disease and its progression: disease and staging biomarkers and new drug targets," *Neuroscience Letters*, vol. 617, pp. 66–71, 2016.

[32] V. S. Malik, M. B. Schulze, and F. B. Hu, "Intake of sugar-sweetened beverages and weight gain: a systematic review," *The American Journal of Clinical Nutrition*, vol. 84, pp. 274–288, 2006.

[33] T. J. Maher and R. J. Wurtman, "Possible neurologic effects of aspartame, a widely used food additive," *Environmental Health Perspectives*, vol. 75, pp. 53–57, 1987.

[34] K. Rycerz and J. E. Jaworska-Adamu, "Effects of aspartame metabolites on astrocytes and neurons," *Folia Neuropathologica*, vol. 51, pp. 10–17, 2013.

[35] E. Stolzenberg, D. Berry, D. Yang et al., "A role for neuronal alpha-synuclein in gastrointestinal immunity," *Journal of Innate Immunity*, 2017.

[36] P. Restani, C. Ballabio, S. Tripodi, and A. Fiocchi, "Meat allergy," *Current Opinion in Allergy and Clinical Immunology*, vol. 9, pp. 265–269, 2009.

[37] L. K. Mischley, J. Allen, and R. Bradley, "Coenzyme Q10 deficiency in patients with Parkinson's disease," *Journal of the Neurological Sciences*, vol. 318, pp. 72–75, 2012.

[38] R. C. Seet, E. C. Lim, J. J. Tan et al., "Does high-dose coenzyme Q10 improve oxidative damage and clinical outcomes in Parkinson's disease?," *Antioxidants & Redox Signaling*, vol. 21, pp. 211–217, 2014.

[39] M. F. Beal, D. Oakes, I. Shoulson et al., "A randomized clinical trial of high-dosage coenzyme Q10 in early Parkinson disease: no evidence of benefit," *JAMA Neurology*, vol. 71, pp. 543–552, 2014.

[40] Z. G. Zhu, M. X. Sun, W. L. Zhang, W. W. Wang, Y. M. Jin, and C. L. Xie, "The efficacy and safety of coenzyme Q10 in Parkinson's disease: a meta-analysis of randomized controlled trials," *Neurological Sciences*, vol. 38, pp. 215–224, 2017.

[41] F. Calon and G. Cole, "Neuroprotective action of omega-3 polyunsaturated fatty acids against neurodegenerative diseases: evidence from animal studies," *Prostaglandins, Leukotrienes, and Essential Fatty Acids*, vol. 77, pp. 287–293, 2007.

[42] G. M. Cole and S. A. Frautschy, "DHA may prevent age-related dementia," *The Journal of Nutrition*, vol. 140, pp. 869–874, 2010.

[43] H. M. Su, "Mechanisms of n-3 fatty acid-mediated development and maintenance of learning memory performance," *The Journal of Nutritional Biochemistry*, vol. 21, pp. 364–373, 2010.

[44] T. M. Silvada, R. P. Munhoz, C. Alvarez et al., "Depression in Parkinson's disease: a double-blind, randomized, placebo-controlled pilot study of omega-3 fatty-acid supplementation," *Journal of Affective Disorders*, vol. 111, pp. 351–359, 2008.

[45] K. Suzuki, M. Miyamoto, T. Miyamoto, M. Iwanami, and K. Hirata, "Sleep disturbances associated with Parkinson's disease," *Parkinson's Disease*, vol. 2011, Article ID 219056, 10 pages, 2011.

[46] J. M. Mack, M. G. Schamne, T. B. Sampaio et al., "Melatoninergic system in Parkinson's disease: from neuroprotection to the management of motor and nonmotor symptoms," *Oxidative Medicine and Cellular Longevity*, vol. 2016, Article ID 3472032, 31 pages, 2016.

[47] W. Zhang, X. Y. Chen, S. W. Su et al., "Exogenous melatonin for sleep disorders in neurodegenerative diseases: a meta-analysis of randomized clinical trials," *Neurological Sciences*, vol. 37, pp. 57–65, 2016.

[48] Y. W. Yang, T. F. Hsieh, C. I. Li et al., "Increased risk of Parkinson disease with diabetes mellitus in a population-based study," *Medicine*, vol. 96, article e5921, 2017.

[49] Y. L. Wang, Y. T. Wang, J. F. Li, Y. Z. Zhang, H. L. Yin, and B. Han, "Body mass index and risk of Parkinson's disease: a dose-response meta-analysis of prospective studies," *PLoS One*, vol. 10, article e0131778, 2015.

Hindawi
Oxidative Medicine and Cellular Longevity
Volume 2017, Article ID 3103272, 15 pages
https://doi.org/10.1155/2017/3103272

Research Article

A Cystine-Rich Whey Supplement (Immunocal®) Provides Neuroprotection from Diverse Oxidative Stress-Inducing Agents *In Vitro* by Preserving Cellular Glutathione

Aimee N. Winter,[1] Erika K. Ross,[1] Vamsi Daliparthi,[1] Whitney A. Sumner,[1] Danielle M. Kirchhof,[1] Evan Manning,[1] Heather M. Wilkins,[1] and Daniel A. Linseman[1,2]

[1]*Department of Biological Sciences, University of Denver, 2199 S. University Blvd., Denver, CO 80208, USA*
[2]*Knoebel Institute for Healthy Aging, University of Denver, 2155 E. Wesley Ave., Denver, CO 80208, USA*

Correspondence should be addressed to Daniel A. Linseman; daniel.linseman@du.edu

Received 15 February 2017; Accepted 13 July 2017; Published 15 August 2017

Academic Editor: Tommaso Cassano

Oxidative stress is a principal mechanism underlying the pathophysiology of neurodegeneration. Therefore, nutritional enhancement of endogenous antioxidant defenses may represent a viable treatment option. We investigated the neuroprotective properties of a unique whey protein supplement (Immunocal®) that provides an essential precursor (cystine) for synthesis of the endogenous antioxidant, glutathione (GSH). Primary cultures of rat cerebellar granule neurons (CGNs), NSC34 motor neuronal cells, or HT22 hippocampal cells were preincubated in medium containing Immunocal and then subsequently treated with agents known to induce oxidative stress. Immunocal protected CGNs against neurotoxicity induced by the Bcl-2 inhibitor, HA14-1, the nitric oxide donor, sodium nitroprusside, $CuCl_2$, and $AlCl_3$. Immunocal also significantly reduced NSC34 cell death due to either H_2O_2 or glutamate and mitigated toxicity in HT22 cells overexpressing β-amyloid$_{1\text{-}42}$. The neuroprotective effects of Immunocal were blocked by inhibition of γ-glutamyl-cysteine ligase, demonstrating dependence on de novo GSH synthesis. These findings indicate that sustaining GSH with Immunocal significantly protects neurons against diverse inducers of oxidative stress. Thus, Immunocal is a nutritional supplement worthy of testing in preclinical animal models of neurodegeneration and in future clinical trials of patients afflicted by these diseases.

1. Introduction

Oxidative stress and mitochondrial dysfunction are major factors underlying the pathophysiology of several neurodegenerative disorders including Parkinson's disease, Alzheimer's disease, and amyotrophic lateral sclerosis (ALS) [1–4]. For instance, complex I deficiency and the consequent increase in mitochondrial reactive oxygen species (ROS) play a critical role in the death of dopaminergic neurons in Parkinson's disease [5, 6]. In models of Alzheimer's disease, evidence of mitochondrial dysfunction and oxidative stress precedes the deposition of characteristic amyloid beta-plaques during disease progression [7, 8]. In the case of ALS, mutant forms of copper-zinc superoxide dismutase (SOD1), which are collectively responsible for approximately 20% of cases of familial ALS, accumulate at mitochondria and trigger a shift in the redox state of these organelles [9]. The above findings strongly indicate that oxidative stress, particularly at the level of the mitochondria, plays a central role in the neuronal death that underlies a diverse group of neurodegenerative diseases.

Glutathione (GSH) is an endogenous tripeptide antioxidant that plays a key role in preventing oxidative stress, thereby preserving mitochondrial function and averting cellular apoptosis [10]. In many neurodegenerative disorders, GSH levels have been shown to be significantly depleted in patients suffering from these diseases, resulting in a diminished capacity to cope with increases in cellular ROS [11–13]. Indeed, decreases in GSH are often observed to precede other hallmarks of disease pathology, such as

complex I deficiency and loss of dopaminergic neurons in Parkinson's disease [14]. Intriguingly, *in vitro* studies on GSH depletion have demonstrated that decreases in total cellular GSH levels can recapitulate disease pathology. For instance, in a dopaminergic PC12 cell line, deficiencies in GSH synthesis that led to an overall decrease in cellular GSH resulted in complex I inhibition, increased indices of oxidative stress, and deficits in mitochondrial respiration, as seen in cases of Parkinsonism [15]. Similarly, NSC34 motor neuron-like cells stably expressing the human G93A mutant form of SOD1 displayed a significant and selective depletion of mitochondrial GSH content in comparison to parental cells, reminiscent of some forms of familial ALS [16]. GSH depletion *in vitro* has also been shown to sensitize neurons to oxidative stress and mitochondrial dysfunction, leading to subsequent increases in ROS and apoptotic cell death. This was clearly demonstrated by a study in which primary cortical neurons treated with subtoxic levels of the GSH-depleting agent, buthionine sulfoximine (BSO), underwent apoptosis in the presence of trace amounts of extracellular copper [17]. Similarly, TAR DNA-binding protein-43 (TDP-43) forms cytoplasmic inclusions, which are a hallmark pathology observed in sporadic ALS patients, in cultured neurons subjected to GSH depletion [18]. Collectively, these studies demonstrate a critical role for GSH depletion in disease progression and pathology in multiple neurodegenerative disease states.

Given the prominent relationship between GSH depletion and neurodegeneration, it is not surprising that many studies have been undertaken to determine the neuroprotective effects of bolstering GSH levels through various treatment paradigms. Such treatments include administration of the GSH precursor, N-acetylcysteine (NAC), and GSH-monoethylester (GSH-MEE), a cell permeable form of GSH, and induction of the transcription factor, nuclear factor erythroid 2-related factor-2 (Nrf2), which is involved in transcriptional regulation of γ-glutamyl-cysteine ligase, the rate-limiting enzyme necessary for GSH synthesis [19]. Studies with NAC are extensive and indicate that NAC treatment offers a number of benefits across numerous disease models. For example, NAC demonstrated a significant protective capacity in a rotenone (complex I inhibition) rat model of Parkinson's disease by decreasing ROS generation, sustaining normal GSH levels, and ultimately preventing dopaminergic cell death [20]. In the G93A mutant SOD1 mouse model of familial ALS, NAC delayed the onset of disease-associated motor deficits and significantly extended survival, possibly due to its ability to elevate GSH levels in these animals [21]. Lastly, SAMP8 senescence-accelerated mice, which display many of the pathological features of Alzheimer's disease, demonstrated an increased cognitive performance with NAC treatment as compared to vehicle-treated controls [22]. Another study utilizing GSH-MEE in an MPTP rat model of Parkinson's disease demonstrated that GSH-MEE supplementation is capable of raising GSH levels in the brain when centrally delivered, and this increase in GSH corresponded to partial preservation of striatal dopamine levels [23]. Studies such as this have led to recent clinical trials testing the safety and tolerability of intranasal delivery of GSH to patients with PD [24]. Finally, Nrf2 induction or overexpression has shown similar promise in animal models of Parkinson's, ALS, and Alzheimer's disease. In the MPTP mouse model of Parkinson's disease, overexpression of Nrf2 in astrocytes attenuated the development of a Parkinsonian phenotype [25]. Likewise, astrocytic overexpression of Nrf2 in a mouse model of ALS both delayed onset and increased survival, as did treatment with chemical Nrf2 inducers [26, 27]. Comparatively, lentiviral Nrf2 overexpression caused significant improvements in observed learning deficits in a mouse model of Alzheimer's disease, accompanied by decreased amyloid plaque burden [28]. Cumulatively, these data indicate that treatments aimed at increasing GSH levels in the brain may be a viable option for treatment and prevention of neurodegenerative disease.

However, while existing treatment strategies have shown some promise in this capacity, the efficacy of such treatments is significantly limited by the relatively low stability and bioavailability of compounds such as GSH-MEE and NAC [23, 29]. Moreover, GSH-MEE requires direct injection into the brain for significant effects to be observed, further limiting its efficacy for treatment in human patients [23]. In the current study, we investigated the neuroprotective potential of a nondenatured whey protein supplement, Immunocal, *in vitro* in several models of oxidative stress. Immunocal has previously been shown to substantially increase blood or lymphocyte GSH levels in patients with HIV infection or cystic fibrosis, respectively, owing to its high concentration of nondenatured whey proteins containing the cysteine precursor, cystine (see Table 1 for composition) [30–32]. Cystine is resistant to trypsin proteolysis and able to travel through the bloodstream to the target cell where it is then readily reduced to two cysteine molecules which can serve as essential precursors for de novo GSH synthesis. In this manner, the stability of Immunocal lends itself to increased bioavailability, such that it can act as a cysteine delivery system. This is significant, as cysteine is spontaneously catabolized in the GI tract and bloodstream, and its supplementation alone can produce toxicity [33]. Additionally, because of its superior stability, the effects of Immunocal are not dependent upon an invasive administration system as is needed for GSH-MEE and have been observed with standard oral dosing regimens. These unique characteristics spurred us to examine the neuroprotective potential of Immunocal.

2. Materials and Methods

2.1. Materials. Immunocal was provided by Immunotec Inc. (Quebec, Canada; Table 1). 2-Amino-6-bromo-α-cyano-3-(ethoxycarbonyl)-4H-1-benzopyran-4-acetic acid ethyl ester (HA14-1) and sodium nitroprusside (SNP) were obtained from Calbiochem (San Diego, CA). DL-buthionine-sulfoximine (BSO), 4, 6-diamidino-2-phenylindole (DAPI), Hoechst dye 33258, and a monoclonal antibody against β-tubulin (clone AA2; used at a dilution of 1 : 250) were from Sigma Aldrich Co. LLC (St Louis, MO). FITC-conjugated secondary antibodies were from Jackson Immunoresearch Laboratories (West Grove, PA).

Table 1: Immunocal constituents by mass per one packet of supplement (one packet of Immunocal contains approximately 10 g of protein supplement (one serving) in fine powder form and 40 calories per serving).

Component	Supplement content	Percent of total supplement
Whey proteins (β-lactoglobulin, immunoglobulin, serum albumin, α-lactalbumin, and lactoferrin)	8.8–9.2 g	88–92%
Fat	~0.05 g	<0.5%
Lactose	~0.15 g	<1.5%
Minerals (Ca, Na)	~0.30 g	<3.0%
Moisture	0.5 g	~5%

2.2. Cell Culture and Treatment. Rat cerebellar granule neurons (CGNs) were isolated as previously described from 7-day-old Sprague-Dawley rat pups of both sexes [34]. CGNs were seeded on 35 mm diameter plastic dishes coated with poly-L-lysine at an average density of 2.0×10^6 cells/mL in basal modified Eagle's medium containing 10% fetal bovine serum, 25 mM KCl, 2 mM L-glutamine, and penicillin (100 units/mL)/streptomycin (100 μg/mL). Cytosine arabinoside (10 μM) was added to the culture medium 24 h after plating. Experiments were performed after 6 days in culture. In general, cells were pretreated with Immunocal at a concentration of 3.3%, *w*/*v* (unless otherwise noted) in serum-free medium for 24 h prior to treatment with the specified insult (i.e., SNP, HA14-1, etc.) for an additional 24 h.

NSC34 cells were maintained in DMEM with high glucose containing 10% fetal bovine serum, 2 mM L-glutamine, and penicillin (100 units/mL)/streptomycin (100 μg/mL). NSC34 cells were preincubated with Immunocal for 24 h prior to exposure to H_2O_2 or glutamate. For glutamate experiments, NSC34 cells were differentiated by withdrawing serum for 7 days prior to experimentation.

For transient transfection, HT22 mouse hippocampal cells were seeded in 6-well plates at an approximate confluency of 1.0×10^6 cells/mL and then cultured for 24 h in DMEM with low glucose containing 10% fetal bovine serum, 2 mM L-glutamine, and penicillin (100 units/mL)/streptomycin (100 μg/mL). Cells were transfected using lipofection (5 μg DNA/mL, 5 μL lipofectamine/mL) in OptiMEM medium for 4 h with either empty pIRES 2DsRed-Express2 bicistronic vector (Clontech, Mountain View, CA) or vector containing the sequence for amyloid-beta 1-42 ($A\beta_{1\text{-}42}$). Following transfection, OptiMEM medium was replaced with DMEM culture medium, and cells were treated with Immunocal for 24 h. Percent apoptosis was then determined for only transfected (DSRed-positive) cells based on nuclear morphology.

2.3. Cell Viability, Lipid Peroxidation, and Cellular GSH Assay. All assays were performed according to commercially available manufacturer's instructions. GSH/GSSG assay kit was purchased from Oxford Biomedical Research (Oxford, MI). MTT cell viability assay was from BioAssay Systems (Hayward, CA). Malondialdehyde (MDA) lipid peroxidation assay was obtained from OXIS Research Inc. (Foster City, CA).

2.4. Immunofluorescence Microscopy. After treatment, cells were fixed in 4% paraformaldehyde for 1 h, washed once in PBS, and then permeabilized and blocked in 0.2% Triton X-100 and 5% bovine serum albumin (BSA) in PBS. Primary antibody (monoclonal antibody against β-tubulin; clone AA2; used at a dilution of 1 : 250; Sigma Aldrich Co. LLC, St Louis, MO) was diluted in 2% BSA and 0.2% Triton X-100 in PBS, and cells were incubated with primary antibodies for 24 h at 4°C. They were then washed 5 times in PBS and then incubated for 1 h in FITC-conjugated secondary antibody diluted in 2% BSA and 0.2% Triton-X 100 in PBS with DAPI. The cells were washed 5 times with PBS before the addition of antiquench (0.1% *p*-phenylenediamine in PBS). Images were captured using a Zeiss Axiovert 200 M epifluorescence microscope equipped with Zeiss Axiovision software.

2.5. Statistical Analysis. Each experiment was done in duplicate and repeated a minimum of three times; data are reported as mean ± SEM. Statistical significance was analyzed with a one-way analysis of variance (ANOVA) followed by post hoc Tukey's test.

3. Results

3.1. Immunocal Preserves Cellular GSH and Prevents Apoptosis in CGNs Exposed to the Bcl-2 Inhibitor, HA14-1. Initially, primary CGNs were incubated with 3.3% (*w*/*v*) Immunocal for 24 h to assess any potential toxicity that this supplement might induce. Immunocal is composed of five primary cystine- and glutamylcysteine-containing proteins, β-lactoglobulin, immunoglobulin, α-lactalbumin, serum albumin, and lactoferrin (Table 2) [35, 36]. Based upon the relative percentages for each of these four proteins within the whey protein fraction and the number of cystine or glutamylcysteine residues contained within each protein, we calculated the approximate concentration of each of these GSH precursors with which CGNs were treated (Table 3). In general, a 3.3% solution of Immunocal in culture medium contains 85.3 mM cystine and 30 mM glutamylcysteine, both of which have the potential to act as GSH precursors; however, it should be noted that since both precursors are contained within much larger proteins it is unlikely that all cystine and glutamylcysteine molecules are freely available to be utilized in GSH synthesis. Thus, the values calculated in Table 3 for these precursors should be considered as concentrations that could potentially be achieved rather than absolute concentrations.

Following Immunocal treatment, cells were fixed and stained with DAPI to analyze nuclear morphology. Cells treated with Immunocal alone displayed nuclear morphology comparable to that of untreated control cells (Figure 1). Moreover, observation under brightfield demonstrated that cells treated with Immunocal maintained a healthy neuronal morphology with intact processes and large somas,

Table 2: Cystine [$(Cys)_2$] and glutamylcysteine [Glu-$(Cys)_2$] content of Immunocal whey proteins.

Whey protein	Molecular mass (kDa)	Percent of protein fraction	Cystine $(Cys)_2$ per molecule	Glu-$(Cys)_2$ per molecule
β-Lactoglobulin	18,400	56.3%	2	0
Immunoglobulin	166,000	9.2%	4	0
α-Lactalbumin	14,200	22.8%	4	0
Serum albumin	66,000	11.1%	17	6
Lactoferrin	77,000	0.7%	17	4

Table 3: Cystine [$(Cys)_2$] and glutamylcysteine [Glu-$(Cys)_2$] content of Immunocal in preincubation culture medium (3.3%, *w/v* final concentration).

Whey protein	Total molecules per mL	Total number of $(Cys)_2$ per mL	Total number of Glu-$(Cys)_2$ per mL
β-Lactoglobulin	5.44×10^{14}	1.09×10^{15}	0
Immunoglobulin	9.91×10^{12}	3.96×10^{13}	0
α-Lactalbumin	2.91×10^{14}	1.17×10^{15}	0
Serum albumin	3.01×10^{18}	5.11×10^{19}	1.80×10^{19}
Lactoferrin	1.63×10^{16}	2.76×10^{17}	6.50×10^{16}
Final concentration	—	85.3 mM	30.0 mM

comparable to cells that were not supplemented with Immunocal (Figure 1).

Having established that Immunocal displayed no overt toxicity to CGNs, cells were next treated with Immunocal and then exposed to the Bcl-2 homology-3 domain (BH3) mimetic, HA14-1. We have previously shown this Bcl-2 inhibitor to induce GSH-sensitive mitochondrial oxidative stress and intrinsic apoptosis in CGNs [37, 38]. HA14-1 induced marked nuclear condensation and microtubule disruption (Figure 2(a)) indicative of apoptosis (Figure 2(b)), while also causing significant depletion of GSH (Figure 2(c)). Immunocal significantly protected CGNs from apoptosis induced by HA14-1 and significantly preserved GSH levels. To confirm that the mechanism of protection was dependent, at least in part, on enhanced GSH synthesis, CGNs were cotreated with Immunocal and the γ-glutamyl-cysteine ligase inhibitor, BSO, which prevents GSH synthesis [39]. Coincubation with Immunocal and BSO for 24 h before HA14-1 treatment completely prevented any protective effect that Immunocal alone displayed against the Bcl-2 inhibitor (Figure 2(b)). Moreover, the capacity of Immunocal to preserve cellular GSH levels upon HA14-1 exposure was eliminated by BSO cotreatment (Figure 2(c)).

3.2. Immunocal Protects CGNs from $CuCl_2$-Induced Oxidative Damage and Decreases Cellular Lipid Peroxidation. To further investigate the neuroprotective potential of Immunocal in primary neurons, we used copper chloride ($CuCl_2$) as a model of oxidative stress. Copper overload is associated with free radical-induced lipid peroxidation and disruption of mitochondrial complex activity [40, 41]. Immunofluorescence analysis of the microtubule network revealed robust

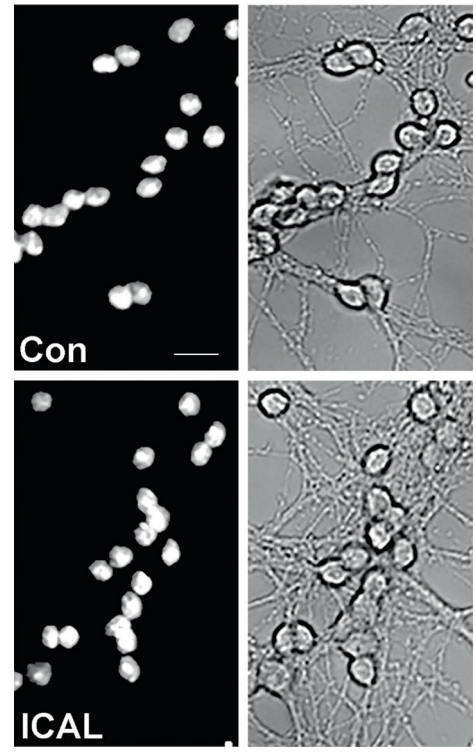

Figure 1: Cells treated with Immunocal display healthy neuronal morphology. Cells were left untreated (a) or treated with Immunocal alone (b) and assessed for overall health and appearance. Left-hand panels are representative images of cell nuclei stained with DAPI. Right-hand panels depict the same fields as viewed under brightfield to assess the state of neuronal processes and soma. Con: control; ICAL: Immunocal. Scale bar, 10 μm.

protection from this transition metal in CGNs pretreated with Immunocal (Figure 3(a)). Quantification of apoptotic cells revealed that there was a significant reduction in CGN apoptosis with Immunocal pretreatment compared to CGNs treated with $CuCl_2$ alone (Figure 3(b)). The antioxidant effect of Immunocal was confirmed with a lipid peroxidation assay which revealed a significant decrease in malondialdehyde content in CGNs pretreated with Immunocal (Figure 3(c)).

3.3. Immunocal Protects CGNs Exposed to Sodium Nitroprusside- (SNP-) Generated Nitric Oxide Species and from $AlCl_3$-Induced Neurotoxicity. SNP is a nitric oxide donor that causes dissipation of the mitochondrial

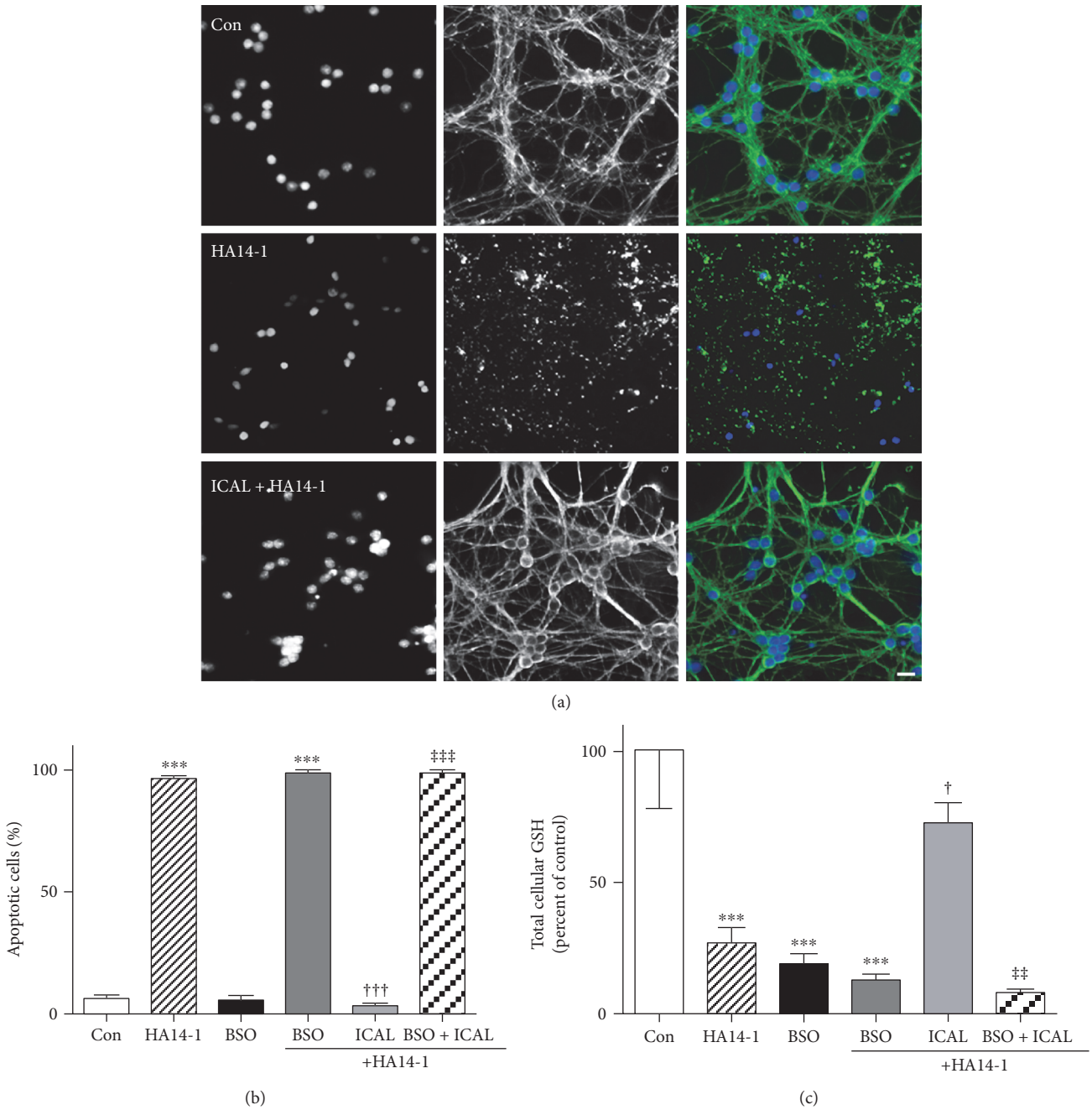

Figure 2: Immunocal preserves cellular GSH and prevents apoptosis in CGNs exposed to the Bcl-2 inhibitor, HA14-1. (a) Representative images of CGNs left untreated (control), treated with HA14-1 (15 μM), or preincubated for 24 h with Immunocal before HA14-1 treatment for further 24 h. Panels from left to right, DAPI (nuclei), β-tubulin, merged images showing β-tubulin (green), and DAPI (blue). Scale bar, 10 μm. (b) Quantification of apoptosis for 4 independent experiments performed as in (a) except some cultures were preincubated with 200 μM BSO as well. Apoptotic cells were those with condensed or fragmented nuclei. Results are shown as mean ± SEM, $n = 4$. *** indicates $p < 0.001$ compared to control, ††† indicates $p < 0.001$ compared to HA14-1, ‡‡‡ indicates $p < 0.001$ compared to ICAL + HA14-1. (c) CGNs were treated exactly as described in (b). Total cellular GSH was measured as described in Materials and Methods. Data shown represent the percent of control cellular GSH concentration, mean ± SEM, $n = 4$. *** indicates $p < 0.001$ compared to control, † indicates $p < 0.05$ compared to HA14-1, and ‡‡ indicates $p < 0.01$ compared to ICAL + HA14-1. Significant differences were determined by one-way ANOVA with a post hoc Tukey's test. Con: control; ICAL: Immunocal; BSO: buthionine sulfoximine.

membrane potential and enhanced generation of mitochondrial ROS in cortical neurons and CGNs [42, 43]. As expected, nitric oxide species generated by SNP caused overt apoptotic cell death in CGNs which was significantly mitigated by pretreatment with Immunocal (Figure 4(a)). Apoptotic cell counts confirmed that there was significant neuroprotection in CGNs pretreated with Immunocal, decreasing apoptosis by approximately 80% (Figure 4(b)).

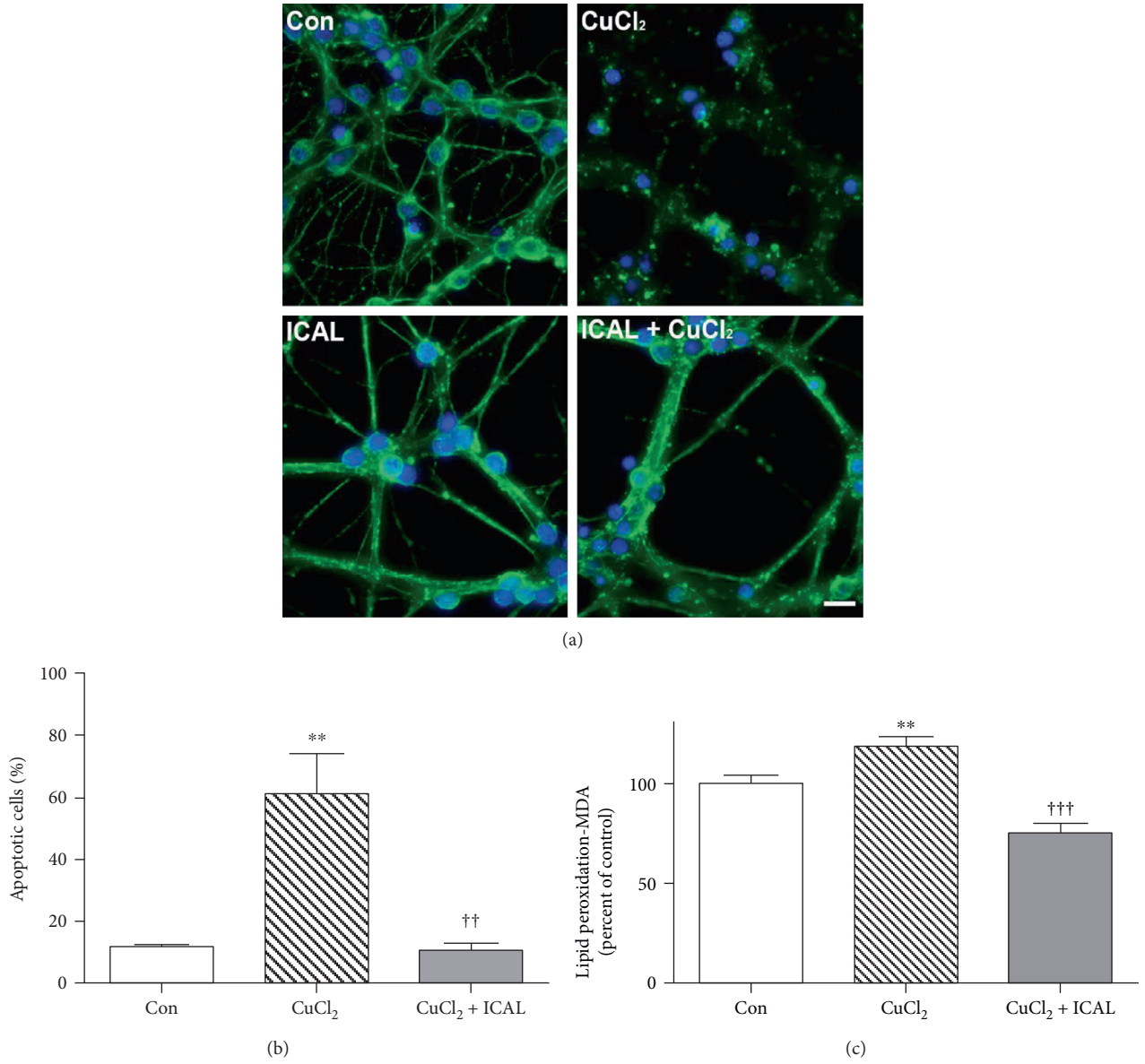

Figure 3: Immunocal decreases $CuCl_2$-induced apoptosis and lipid peroxidation in CGNs. (a) Representative images of CGNs left untreated (control), treated with $CuCl_2$ (50 μM), or preincubated with Immunocal for 24 h before $CuCl_2$ treatment for further 24 h. Immunofluorescence shows β-tubulin (green) and DAPI (blue). Scale bar, 10 μm. (b) Quantification of apoptosis for 4 independent experiments performed as in (a). Results are shown as mean ± SEM, $n = 4$. ** indicates $p < 0.01$ compared to control and †† indicates $p < 0.01$ compared to $CuCl_2$. (c) Cellular lipid peroxidation (malondialdehyde (MDA)) was measured as described in Materials and Methods. Results are shown as mean ± SEM, $n = 5$. ** indicates $p < 0.01$ compared to control, ††† indicates $p < 0.001$ compared to $CuCl_2$. Con: control; ICAL: Immunocal.

An MTT cell viability assay demonstrated similar results and showed that mitochondrial viability was also significantly preserved in Immunocal-pretreated cells, compared to CGNs treated with SNP alone (Figure 4(c)).

Aluminum is a neurotoxic metal that impairs mitochondrial structure and function in neural cells exposed *in vitro* and *in vivo* [44, 45]. Aluminum chloride- ($AlCl_3$-) induced toxicity in CGNs was characterized by nuclear condensation and marked disruption of the microtubule network; these effects were markedly decreased in CGNs pretreated with Immunocal (Figure 5(a)). To confirm that this protection was due to cysteine supplementation, and not metal chelation, we removed the Immunocal after the pretreatment period and washed the CGNs with serum-free media before treating with $AlCl_3$. Under these conditions, we still observed a significant reduction in apoptosis compared to CGNs treated with $AlCl_3$ alone (Figure 5(b)).

3.4. Immunocal Protects NSC34 Motor Neuron-Like Cells from H_2O_2 and Glutamate/Glycine-Induced Excitotoxicity. H_2O_2-mediated cell death is a classic model of ROS toxicity in neuronal systems, as it generates free radicals that are

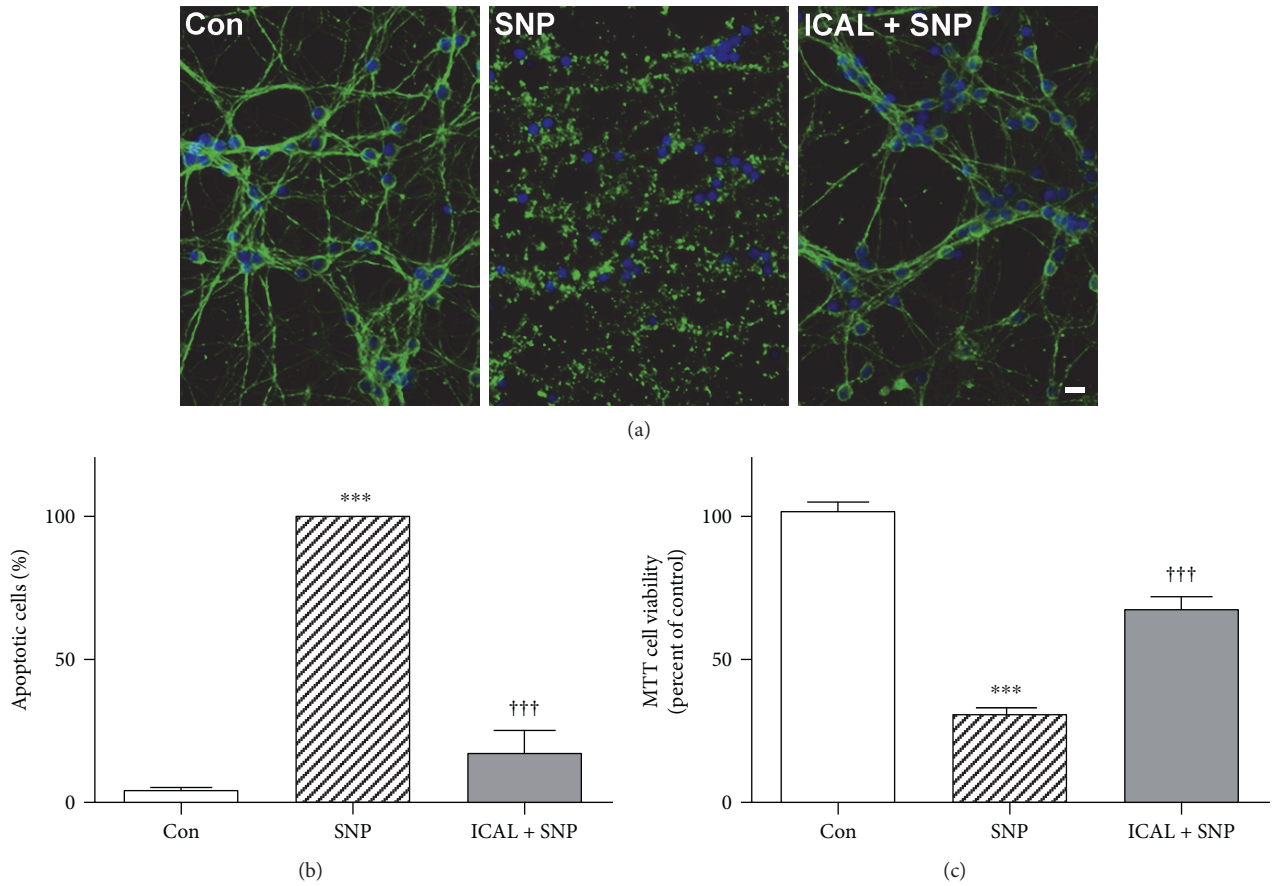

Figure 4: Immunocal preserves CGN viability and protects from apoptosis after exposure to SNP. (a) Representative images of CGNs left untreated (control), treated with SNP (100 μM), or preincubated with Immunocal for 24 h before SNP treatment for further 24 h. Immunofluorescence shows β-tubulin (green) and DAPI (blue). Scale bar, 10 μm. (b) Quantification of apoptosis for 5 independent experiments performed as in (a). Results are shown as mean ± SEM, $n = 5$. (c) MTT cell viability was measured as described in Materials and Methods. Results are shown as mean ± SEM, $n = 3$. For (b) and (c), $***$ indicates $p < 0.001$ compared to control, and ††† indicates $p < 0.001$ compared to SNP. Con: control; ICAL: Immunocal.

implicated in neurodegeneration [46]. As expected, ROS generated by H_2O_2 caused an overt loss of viability in NSC34 cells, which was significantly mitigated by pretreatment with Immunocal. An MTT cell viability assay demonstrated that mitochondrial viability was preserved in Immunocal-pretreated cells in a dose-dependent manner, compared to NSC34 cells treated with H_2O_2 alone (Figure 6(a)). Incubation with Immunocal alone had no significant adverse effect on NSC34 cell viability assessed by MTT assay (data not shown).

Glutamate excitotoxicity is thought to play a significant role in several forms of neurodegenerative disease, leading to neuronal damage and cell death through both apoptotic and nonapoptotic mechanisms. NSC34 motor neuron-like cells do not typically express functional glutamate receptors, which are the primary mediators of excitotoxicity. However, if they are exposed to serum withdrawal for 7 days, then they attain a semi-differentiated state and express functional N-methyl-D-aspartate (NMDA) receptors (Figure 6(b)). After this, point cells become sensitive to glutamate excitotoxicity [47]. We observed that exposure to glutamate/glycine caused a significant loss of viability in NSC34 cells differentiated by serum withdrawal. An MTT cell viability assay demonstrated that mitochondrial viability was significantly preserved in Immunocal-pretreated cells in a dose-dependent manner, compared to NSC34 cells treated with glutamate/glycine alone (Figure 6(c)).

3.5. Immunocal Protects HT22 Mouse Hippocampal Cells from Toxicity Induced by Overexpression of Amyloid-Beta Peptide ($A\beta_{1\text{-}42}$). $A\beta_{1\text{-}42}$ is the major constituent of senile plaques, which form in the brains of Alzheimer's patients, leading to the hypothesis that increased production of this protein from aberrant processing of amyloid precursor protein is a major contributor to neuronal death and disease pathogenesis [48]. HT22 mouse hippocampal cells transfected with $A\beta_{1\text{-}42}$ displayed a marked increase in apoptosis compared to controls transfected with empty vector, indicated by the presence of condensed and fragmented nuclei (Figure 7(a)). Strikingly, this effect was entirely mitigated by treatment with Immunocal, which preserved neuronal viability to an extent similar to that of empty vector controls (Figure 7(b)).

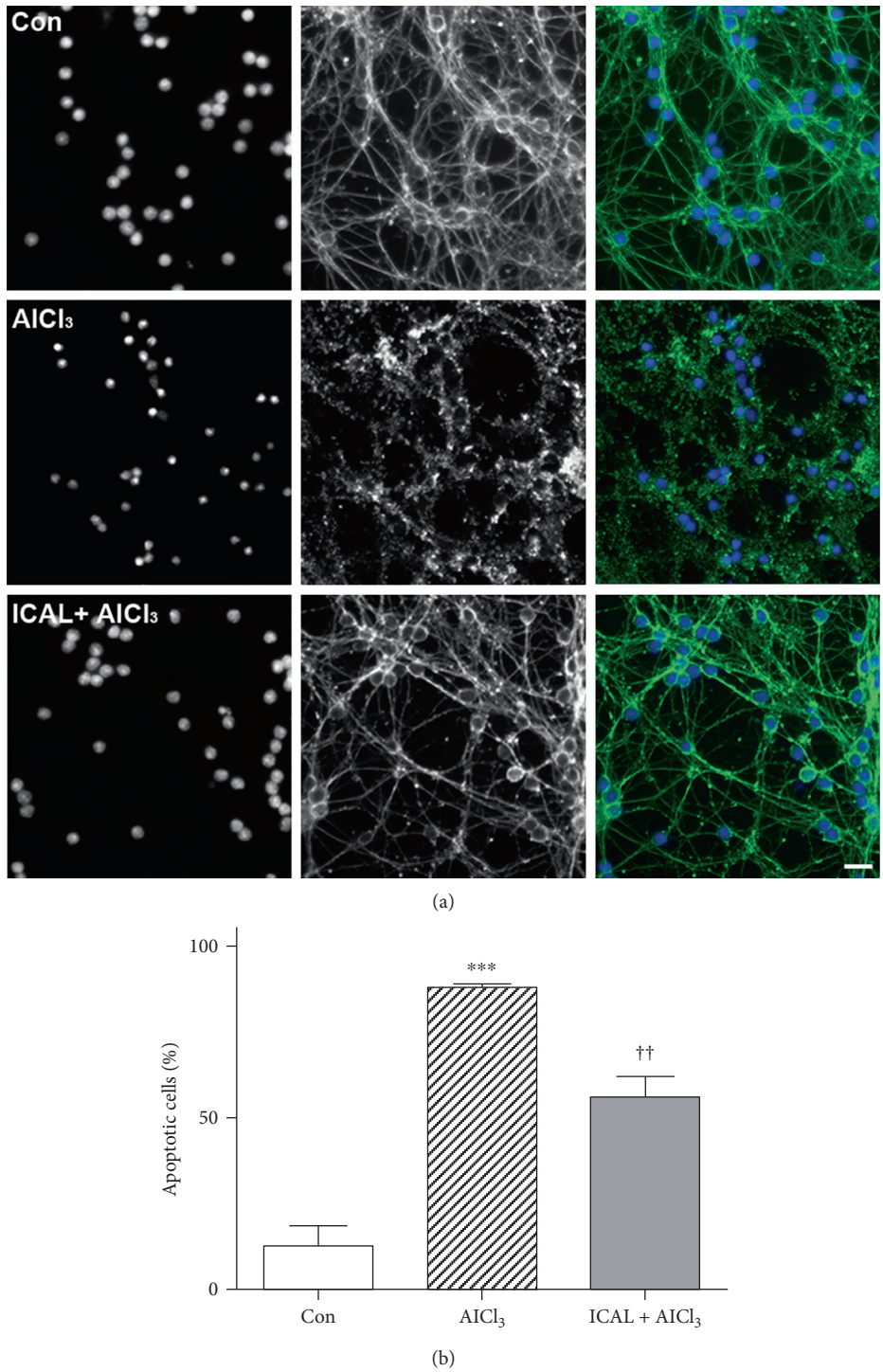

Figure 5: Immunocal protects CGNs from $AlCl_3$-induced toxicity. (a) Representative images of CGNs left untreated (control), treated with $AlCl_3$ (10 μM), or preincubated with Immunocal for 24 h before $AlCl_3$ treatment for further 48 h. Panels from left to right, DAPI (nuclei), β-tubulin, and merged image showing β-tubulin (green), and DAPI (blue). Scale bar, 10 μm. (b) CGN apoptosis was quantified for 4 independent experiments as described in (a). Results are shown as mean ± SEM, $n = 4$. *** indicates $p < 0.001$ compared to control, and †† indicates $p < 0.01$ compared to $AlCl_3$. Con: control; ICAL: Immunocal.

4. Discussion

Strategies aimed at scavenging ROS, including those that enhance the capacity of endogenous antioxidant defenses like GSH, are actively being investigated as therapeutic approaches for neurodegenerative diseases. In the present study, we assessed the neuroprotective potential of Immunocal, a cystine-rich whey protein supplement, against oxidative stress *in vitro*. This supplement contains high concentrations of proteins such as serum albumin,

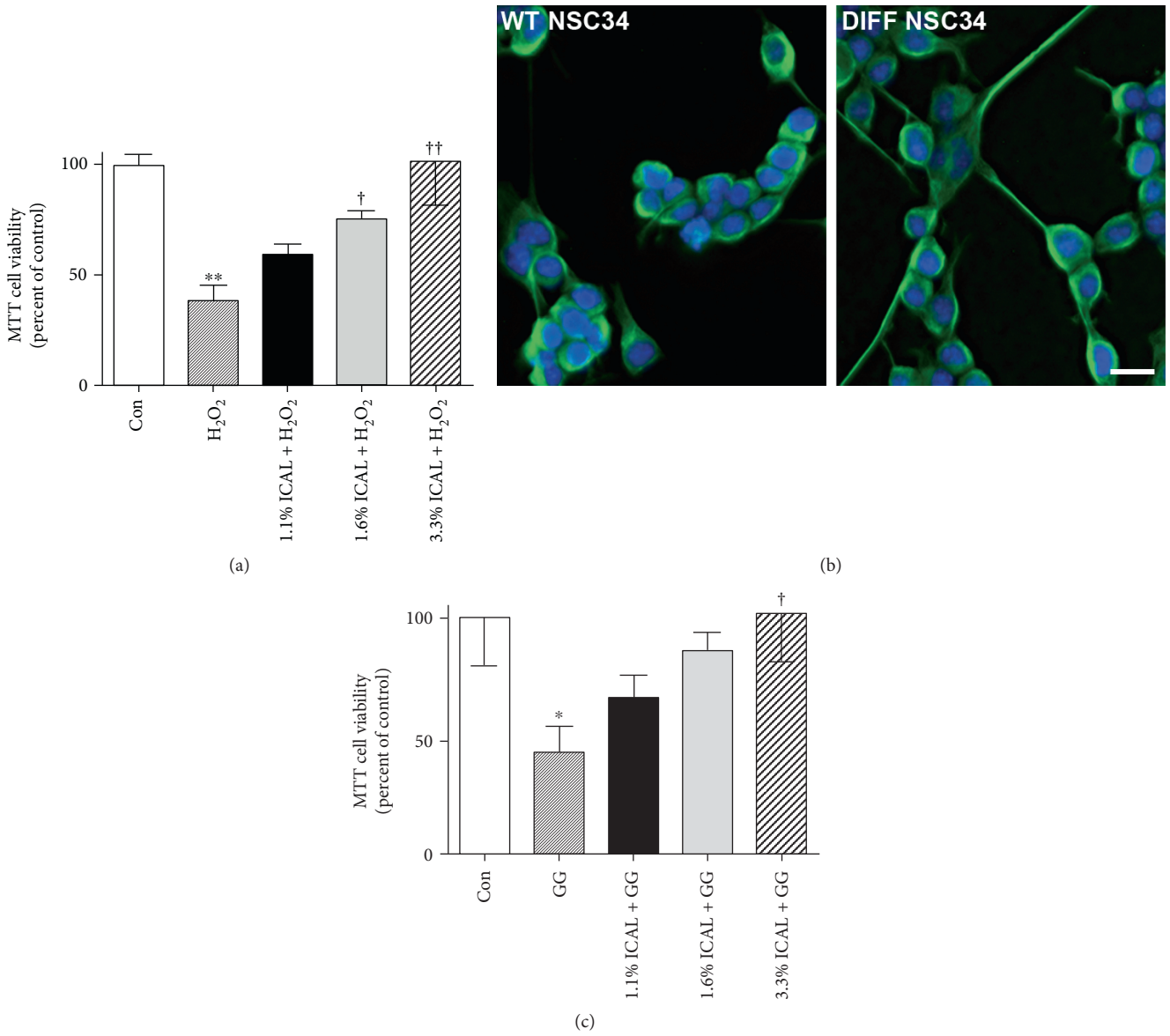

Figure 6: Immunocal protects NSC34 cells from H_2O_2 and glutamate/glycine-induced excitotoxicity. (a) Cell survival was quantified with MTT cell viability assay for 5 independent experiments in undifferentiated NSC34 left untreated (control), treated with H_2O_2 (250 μM), or preincubated with Immunocal for 24 h before H_2O_2 treatment for further 24 h. Results are shown as mean ± SEM, $n = 5$. ** indicates $p < 0.01$ compared to control, † indicates $p < 0.05$ compared to H_2O_2, and †† indicates $p < 0.01$ compared to H_2O_2. (b) Representative images showing morphological differences between undifferentiated (wildtype (WT)) and differentiated (DIFF) NSC34 cells, β-tubulin (green), and DAPI (blue). Scale bar, 10 μm. (c) Cell survival was quantified for 5 independent experiments with an MTT cell viability assay in differentiated NSC34 cells left untreated (control), treated with glutamate/glycine (1 mM/100 μM), or preincubated with Immunocal for 24 h before glutamate/glycine treatment for further 24 h. * indicates $p < 0.05$ compared to control, and † indicates $p < 0.05$ compared to glutamate/glycine. Con: control; ICAL: Immunocal; GG: glutamate/glycine.

alpha-lactalbumin, and lactoferrin, which possess a substantial number of cystine residues in the unique nondenatured preparation. In addition, the direct GSH precursor, glutamylcysteine, is also present in the serum albumin fraction of this supplement. Due to these unique features, Immunocal has been used as a cysteine delivery system to boost GSH levels in individuals diagnosed with diseases for which oxidative stress is a prominent underlying factor [31, 32, 49]. Therefore, Immunocal may be an effective approach to elevate GSH in cases of neurodegeneration for which oxidative stress plays a significant role. To this end, we studied the potential of Immunocal to protect neurons *in vitro* from a diverse array of oxidative insults, which are not only known to cause oxidative damage and mitochondrial dysfunction but also to imitate some pathogenic factors in neurodegeneration such as diminished Bcl-2 function, increased levels of nitric oxide, or metal ion toxicity (Figure 8).

GSH depletion is a widely studied phenomenon in cases of neurodegeneration. Although there are multiple mechanisms by which GSH may be depleted, one involves the

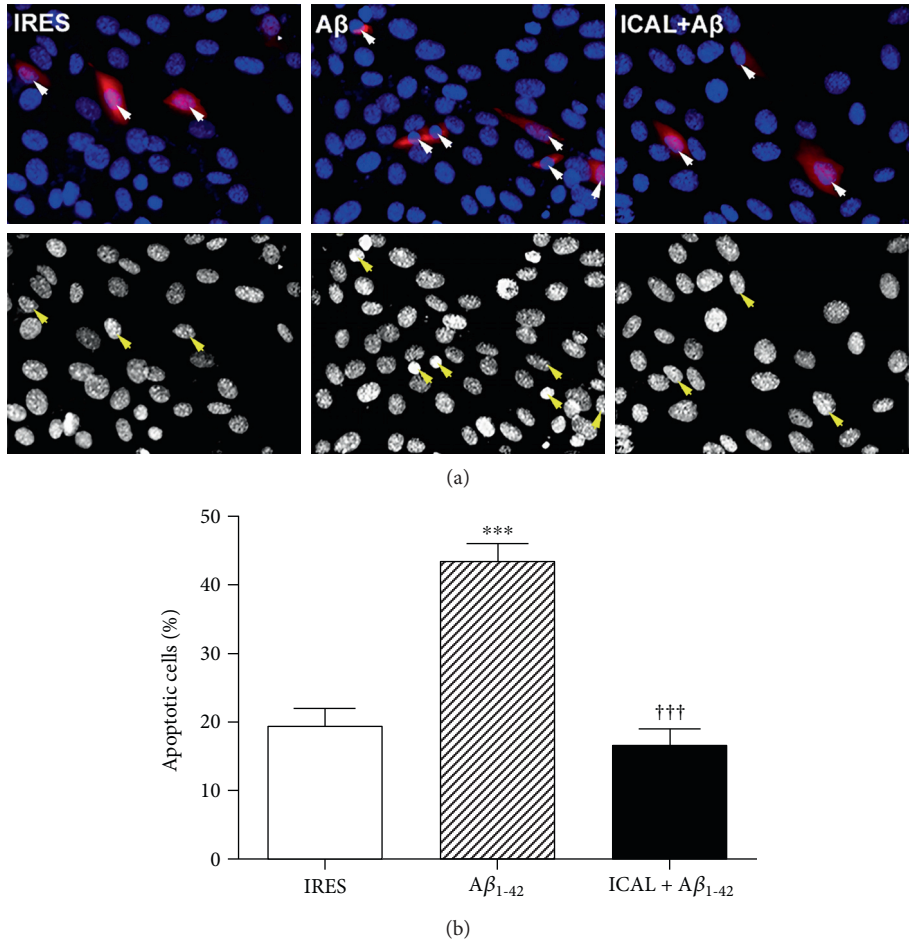

Figure 7: Immunocal protects HT22 cells from toxicity induced by overexpression of $A\beta_{1\text{-}42}$. (a) Representative images of HT22 cells transfected with either empty vector (IRES) or $A\beta_{1\text{-}42}$. Top panels display colored images showing successful transfection of the cells, and bottom panels display decolorized images of cell nuclei to visualize nuclear condensation. Arrows indicate transfected cells. (b) Quantification of apoptosis for 4 independent experiments performed as in (a). Results are shown as mean ± SEM, $n = 4$. *** indicates $p < 0.001$ compared to control, and ††† indicates $p < 0.001$ compared to cells transfected with $A\beta_{1\text{-}42}$ without Immunocal preincubation. $A\beta$: amyloid-beta; ICAL: Immunocal.

downregulation of Bcl-2 expression or function. Increased expression of Bcl-2 leads to enhanced GSH synthesis and decreased GSH efflux from the cell [50, 51]. On the other hand, Bcl-2 knockdown leads to decreased levels of tissue GSH [52]. In the current study, we utilized the Bcl-2 inhibitor, HA14-1, to mimic loss of Bcl-2 function and assess the neuroprotective potential of Immunocal. We have previously shown HA14-1 to decrease the cellular GSH pool with a propensity to affect the mitochondrial GSH pool first and induce mitochondrial oxidative stress and intrinsic apoptosis in CGNs [37, 38]. Under these conditions, Immunocal displayed robust neuroprotection, indicating a capacity to counter the effects of mitochondrial GSH depletion and oxidative stress induced by loss of Bcl-2 function. Moreover, the protective effect of Immunocal against Bcl-2 inhibition is dependent upon de novo GSH synthesis as coincubation of Immunocal with BSO blocked neuroprotection.

Another factor implicated in the pathogenesis of several neurodegenerative diseases is copper toxicity. GSH is known to play a significant role in mitigating copper toxicity by facilitating the transport of copper to proteins that can safely store this toxic metal in the intracellular environment [53]. Depletion of GSH disrupts this important process and sensitizes neuronal cells to copper toxicity through copper-associated ROS generation, even when exposed to only trace amounts of copper [17, 54, 55]. Thus, copper toxicity may be a process that is dependent on GSH depletion, and indeed, increased concentrations of copper and dysregulation of copper homeostasis are observed in several neurodegenerative diseases in which GSH status is reduced, including Alzheimer's disease and models of ALS [54, 56]. In our study, elevation of GSH levels in cultured primary neurons with Immunocal proved to be an effective way to ameliorate the toxic effects of copper treatment by attenuating copper-induced lipid peroxidation, resulting in reduced cell death.

Neuroinflammation, in which microglia and astrocytes take on an inflammatory phenotype and secrete toxic factors such as cytokines and nitric oxide, is another major

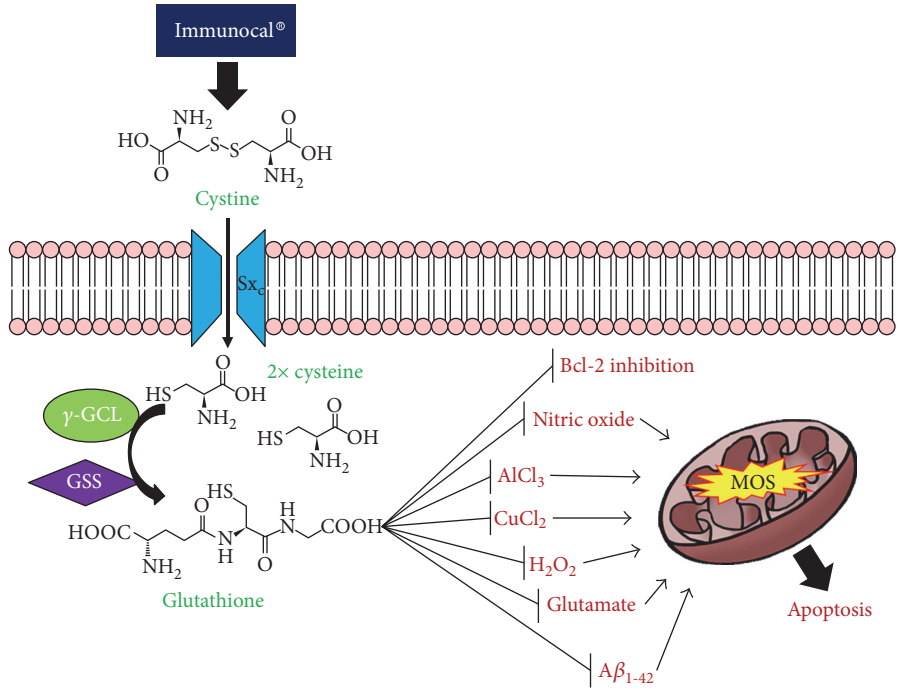

Figure 8: Proposed neuroprotective mechanism of Immunocal. Immunocal provides the essential GSH precursor, cystine, which is transported into cerebellar granule neurons via the system x_c^- antiporter (Sx_c^-). Upon entry into the cell, cystine is rapidly hydrolyzed to form two cysteine molecules, which are then utilized in the de novo synthesis of GSH by γ-glutamylcysteine ligase (γ-GCL) and glutathione synthase (GSS). Newly synthesized glutathione inhibits oxidation caused by a variety of insults, thereby preventing mitochondrial oxidative stress (MOS) and subsequent induction of apoptosis.

component of neurodegenerative disease [57, 58]. Induction of nitric oxide synthase (NOS) and subsequent production of nitric oxide is a well-established mechanism by which inflammatory cells trigger neuronal cell death [57]. Markers of nitrosative stress are prevalent in tissues from both Parkinson's and Alzheimer's disease patients, indicating a significant role for nitric oxide in disease pathogenesis [59, 60]. Reactive nitrogen species (RNS) such as nitric oxide promote damage to mitochondrial components, leading to dissipation of mitochondrial membrane potential and further increases in ROS and RNS production [42, 43]. This feed forward cycle ultimately exacerbates inflammatory responses and eventually results in neuronal death. GSH is known to detoxify both ROS and RNS, making it an essential antioxidant and key neuroprotective molecule. Consistent with this, preincubation with Immunocal significantly protected CGNs from toxicity induced by the nitric oxide donor SNP.

The neurotoxic effects of aluminum exposure are well documented, and recently, environmental aluminum and aluminum-containing vaccines have garnered attention as potential causes of neurodegeneration. In general, *in vitro* exposure of neural cells to aluminum has been shown to result in pronounced alterations in mitochondrial structure and function, leading to marked increases in ROS, reduction of mitochondrial enzyme activity, and cell death [45]. Aluminum also interferes with the activity of NADP-isocitrate at the mitochondria, decreasing the pool of NADPH that is available and necessary for the regeneration of GSH, and thereby decreasing GSH levels [61]. *In vivo* examination of aluminum neurotoxicity has demonstrated that healthy mice treated with aluminum hydroxide display significant motor deficits and develop pathological features similar to those observed in ALS [62]. These results are notable in that Veterans of the 1990-1991 Gulf War who received vaccines containing aluminum hydroxide adjuvant demonstrate a significant increase in the incidence of ALS, implicating aluminum toxicity as one potential environmental factor in some forms of sporadic ALS [62, 63]. Our experiments clearly demonstrate that Immunocal pretreatment is capable of significantly reducing the degree of neurotoxicity observed with aluminum in CGN cultures. We further confirmed that the protective effects of Immunocal were not due to metal chelation by removing Immunocal-containing media prior to the addition of $AlCl_3$.

To determine if the protective action of Immunocal observed in CGNs was reproducible in other neuronal cell types bearing relevance to neurodegenerative disease, we examined the capacity of this supplement to protect NSC34 motor neuron-like cells from oxidative stress and excitotoxicity. NSC34 cells are a hybrid cell line consisting of spinal cord motor neurons fused with mouse neuroblastoma cells [64]. We first analyzed the ability of Immunocal to protect NSC34 cells from H_2O_2-induced oxidative stress. Immunocal pretreatment of NSC34 cells dose-dependently attenuated H_2O_2-induced cell death. We next examined the potential of Immunocal to ameliorate damage induced by excitotoxic insult in NSC34 cells,

which were differentiated by prolonged serum withdrawal to induce the expression of NMDA receptors [47]. Excitotoxicity is known to play a prevalent role in the pathogenesis of multiple neurodegenerative diseases, including ALS, and is intimately linked with both oxidative and nitrosative stress [65]. Immunocal pretreatment of differentiated NSC34 motor neuron-like cells significantly reduced the injurious effects of glutamate excitotoxicity in a dose-dependent manner.

Lastly, we evaluated the ability of Immunocal to defend HT22 mouse hippocampal cells from toxicity induced by the overexpression of $A\beta_{1\text{-}42}$. As previously discussed, $A\beta_{1\text{-}42}$ is the primary constituent of senile plaques, one of the hallmarks of Alzheimer's disease pathology. In addition, this protein is also known to accumulate with amyloid precursor protein at mitochondria, leading to significant mitochondrial dysfunction [48]. Indeed, $A\beta_{1\text{-}42}$ accumulation at the mitochondria has been shown to occur both in transgenic mouse models of the disease and in the brains of Alzheimer's patients [66–68]. Our data indicate that pretreatment with Immunocal was able to preserve HT22 hippocampal cell viability to a significant degree, indicating that GSH supplementation may be an effective way to mitigate cell death caused by $A\beta_{1\text{-}42}$-induced toxicity.

5. Conclusions

Immunocal was initially studied for application to clinical disorders of immune system deficiency and cancer as an approach to augment the available GSH pool and increase cellular antioxidant and immune system defenses. More recently, Immunocal has been investigated as a potential treatment for disorders involving the CNS. Oral administration of Immunocal for 45 days has been shown to elevate GSH levels in the brains of healthy, nontransgenic mice by up to 300% compared to casein-treated controls, demonstrating that this supplement is able to directly affect the antioxidant status of tissues in the CNS [69]. Furthermore, we recently demonstrated that oral administration of Immunocal in the G93A mutant SOD1 mouse model of ALS delayed disease onset and preserved grip strength to a significant degree, in comparison to untreated transgenic mice [70]. These therapeutic effects correlated with preservation of both blood and spinal cord GSH levels in comparison to untreated transgenic controls, indicating that Immunocal is able to act directly on the CNS to preserve GSH status in the context of neurodegenerative disease. Based on the above studies and the data shown here, we suggest that Immunocal might hold significant potential as a novel therapeutic approach to bolster GSH levels in neurodegenerative disorders for which the underlying pathology involves significant oxidative stress. In the future, it will be of interest to further assess the therapeutic benefit of GSH precursor supplementation with Immunocal in additional preclinical animal models of neurodegeneration and ultimately in clinical trials of patients afflicted with neurodegenerative disorders.

Abbreviations

$A\beta$:	Amyloid beta
ALS:	Amyotrophic lateral sclerosis
BH3:	Bcl-2 homology domain-3
BSA:	Bovine serum albumin
BSO:	Buthionine sulfoximine
CGN:	Cerebellar granule neuron
DAPI:	4,6-Diamidino-2-phenylindole
γ-GCL:	γ-Glutamyl-cysteine ligase
GSH:	Glutathione
GSH-MEE:	Glutathione monoethylester
GSS:	Glutathione synthase
HA14-1:	2-Amino-6-bromo-α-cyano-3-(ethoxycarbonyl)-4H-1-benzopyran-4-acetic acid ethyl ester
ICAL:	Immunocal
NAC:	N-Acetyl cysteine
NMDA:	N-Methyl-D-aspartate
Nrf2:	Nuclear factor erythroid 2-related factor-2
ROS:	Reactive oxygen species
RNS:	Reactive nitrogen species
SOD1:	Copper-zinc superoxide dismutase
SNP:	Sodium nitroprusside
Sx_c^-:	System x_c^-
TDP-43:	TAR DNA binding protein-43.

Disclosure

Significant portions of this work have previously been published as part of one of the coauthor's master's thesis (Erika K. Ross, "Nutraceutical Antioxidants and Their Therapeutic Potential in Neurodegeneration" (2012). Electronic Theses and Dissertations. Paper 563). This work has previously been presented in poster form at the Society for Neuroscience Annual Meeting.

Conflicts of Interest

The authors have received funding from Immunotec Inc. (Quebec, Canada) to support the research on the neuroprotective effects of Immunocal.

Authors' Contributions

Erika K. Ross, Vamsi Daliparthi, Aimee N. Winter, Whitney A. Sumner, Danielle M. Kirchhof, Evan Manning, and Heather M. Wilkins had substantial contributions to the conception and design, acquisition, and analysis or interpretation of data. Aimee N. Winter, Erika K. Ross, and Daniel A. Linseman are involved in drafting the article or revising it critically for important intellectual content. Daniel A. Linseman is responsible for the final approval of the version to be published.

Acknowledgments

This study was supported in part by funding from Immunotec Inc. (Quebec, Canada).

References

[1] M. T. Lin and M. F. Beal, "Mitochondrial dysfunction and oxidative stress in neurodegenerative diseases," *Nature*, vol. 443, pp. 787–795, 2006.

[2] E. F. Smith, P. J. Shaw, and K. J. De Vos, "The role of mitochondria in amyotrophic lateral sclerosis," *Neuroscience Letters*, 2017.

[3] T. Cassano, L. Pace, G. Bedse et al., "Glutamate and mitochondria: two prominent players in the oxidative stress-induced neurodegeneration," *Current Alzheimer Research*, vol. 13, pp. 185–197, 2016.

[4] T. Jiang, Q. Sun, and S. Chen, "Oxidative stress: a major pathogenesis and potential therapeutic target of antioxidative agents in Parkinson's disease and Alzheimer's disease," *Progress in Neurobiology*, vol. 147, pp. 1–19, 2016.

[5] T. M. Dawson and V. L. Dawson, "Molecular pathways of neurodegeneration in Parkinson's disease," *Science*, vol. 302, pp. 819–822, 2003.

[6] L. Zuo and M. S. Motherwell, "The impact of reactive oxygen species and genetic mitochondrial mutations in Parkinson's disease," *Gene*, vol. 532, pp. 18–23, 2013.

[7] A. Nunomura, G. Perry, G. Aliev et al., "Oxidative damage is the earliest event in Alzheimer disease," *Journal of Neuropathology & Experimental Neurology*, vol. 60, pp. 759–767, 2001.

[8] K. Leuner, W. E. Müller, and A. S. Reichert, "From mitochondrial dysfunction to amyloid beta formation: novel insights into the pathogenesis of Alzheimer's disease," *Molecular Neurobiology*, vol. 46, pp. 186–193, 2012.

[9] A. Ferri, M. Cozzolino, C. Crosio et al., "Familial ALS-superoxide dismutases associate with mitochondria and shift their redox potentials," *Proceedings of the National Academy of Sciences of the United States of America*, vol. 103, pp. 13860–13865, 2006.

[10] R. Franco and J. A. Cidlowski, "Apoptosis and glutathione: beyond an antioxidant," *Cell Death and Differentiation*, vol. 16, pp. 1303–1314, 2009.

[11] G. N. Babu, A. Kumar, R. Chandra et al., "Oxidant-antioxidant imbalance in the erythrocytes of sporadic amyotrophic lateral sclerosis patients correlates with the progression of disease," *Neurochemistry International*, vol. 52, pp. 1284–1289, 2008.

[12] V. Calabrese, R. Sultana, G. Scapagnini et al., "Nitrosative stress, cellular stress response and thiol homeostasis in patients with Alzheimer's disease," *Antioxidants & Redox Signaling*, vol. 8, pp. 1975–1986, 2006.

[13] R. K. B. Pearce, A. Owen, S. Daniel, P. Jenner, and C. D. Marsden, "Alterations in the distribution of glutathione in the substantia nigra in Parkinson's disease," *Journal of Neural Transmission*, vol. 104, pp. 661–677, 1997.

[14] M. Garrido, Y. Tereshchenko, and Z. Zhevtsova, "Glutathione depletion and overproduction both initiate degeneration of nigral dopaminergic neurons," *Acta Neuropathologica*, vol. 121, pp. 475–485, 2011.

[15] M. Hsu, B. Srinivas, J. Kumar, R. Subramanian, and J. Andersen, "Glutathione depletion resulting in selective mitochondrial complex I inhibition in dopaminergic cells is via an NO-mediated pathway not involving peroxynitrite: implications for Parkinson's disease," *Journal of Neurochemistry*, vol. 92, pp. 1091–1103, 2005.

[16] H. Muyderman, P. G. Hutson, D. Matusica, M. L. Rogers, and R. A. Rush, "The human G93A-superoxide dismutase-1 mutation, mitochondrial glutathione and apoptotic cell death," *Neurochemical Research*, vol. 34, pp. 1847–1856, 2009.

[17] T. Du, G. D. Ciccotosto, G. A. Cranston et al., "Neurotoxicity from glutathione depletion is mediated by Cu-dependent p53 activation," *Free Radical Biology and Medicine*, vol. 44, pp. 44–55, 2008.

[18] Y. Iguchi, M. Katsuno, S. Takagi et al., "Oxidative stress induced by glutathione depletion reproduces pathological modifications of TDP-43 linked to TDP-43 proteinopathies," *Neurobiology of Disease*, vol. 45, pp. 862–870, 2012.

[19] A. K. Jaiswal, "Nrf2 signaling in coordinated activation of antioxidant gene expression," *Free Radical Biology and Medicine*, vol. 36, pp. 1199–1207, 2004.

[20] L. Sun, L. Gu, S. Wang, J. Yuan, H. Yang, and J. Zhu, "N-acetylcysteine protects against apoptosis through modulation of group I metabotropic glutamate receptor activity," *PLoS One*, vol. 7, article e32503, 2012.

[21] O. A. Andreassen, A. Dedeoglu, P. Klivenyi, M. F. Beal, and A. I. Bush, "N-acetyl-L-cysteine improves survival and preserves motor performance in an animal model of familial amyotrophic lateral sclerosis," *Neuroreport*, vol. 11, pp. 2491–2493, 2000.

[22] S. A. Farr, H. Fai Poon, D. Dogrukol-Ak et al., "The antioxidants α-lipoic acid and N-acetylcysteine reverse memory impairment and brain oxidative stress in aged SAMP8 mice," *Journal of Neurochemistry*, vol. 84, pp. 1173–1183, 2003.

[23] G. D. Zeevalk, L. Manzino, P. K. Sonsalla, and L. P. Bernard, "Characterization of intracellular elevation of glutathione (GSH) with glutathione monoethyl ester and GSH in brain and neuronal cultures: relevance to Parkinson's disease," *Experimental Neurology*, vol. 203, pp. 512–520, 2007.

[24] L. K. Mischley, J. B. Leverenz, R. C. Lau et al., "A randomized, double-blind phase I/IIa study of intranasal glutathione in Parkinson's disease," *Movement Disorders*, vol. 30, pp. 1696–1701, 2015.

[25] P. C. Chen, M. R. Vargas, A. K. Pani et al., "Nrf2-mediated neuroprotection in the MPTP mouse model of Parkinson's disease: critical role for the astrocyte," *Proceedings of the National Academy of Sciences of the United States of America*, vol. 106, pp. 2933–2938, 2009.

[26] M. R. Vargas, D. A. Johnson, D. W. Sirkis, A. Messing, and J. A. Johnson, "Nrf2 activation in astrocytes protects against neurodegeneration in mouse models of familial amyotrophic lateral sclerosis," *The Journal of Neuroscience*, vol. 28, pp. 13574–13581, 2008.

[27] A. Neymotin, N. Y. Calingasan, E. Wille et al., "Neuroprotective effect of Nrf2/ARE activators, CDDO ethylamide and CDDO trifluoroethylamide, in a mouse model of amyotrophic lateral sclerosis," *Free Radical Biology and Medicine*, vol. 51, pp. 88–96, 2011.

[28] K. Kanninen, R. Heikkinen, T. Malm et al., "Intrahippocampal injection of a lentiviral vector expressing Nrf2 improves spatial learning in a mouse model of Alzheimer's disease," *Proceedings of the National Academy of Sciences of the United States of America*, vol. 106, pp. 16505–16510, 2009.

[29] B. Olsson, M. Johansson, J. Gabrielsson, and P. Bolme, "Pharmacokinetics and bioavailability of reduced and oxidized N-acetylcysteine," *European Journal of Clinical Pharmacology*, vol. 34, pp. 77–82, 1988.

[30] W. Y. Tsai, W. Chang, C. Chen, and F. Lu, "Enhancing effect of patented whey protein isolate (Immunocal) on cytotoxicity of an anti-cancer drug," *Nutrition and Cancer*, vol. 38, pp. 200–208, 2000.

[31] P. Micke, K. M. Beeh, and R. Buhl, "Effects of long-term supplementation with whey proteins on plasma glutathione levels of HIV-infected patients," *European Journal of Nutrition*, vol. 41, pp. 12–18, 2002.

[32] V. Grey, S. R. Mohammed, A. A. Smountasm, R. Bahlool, and L. C. Lands, "Improved glutathione status in young adult patients with cystic fibrosis supplemented with whey protein," *Journal of Cystic Fibrosis*, vol. 2, pp. 195–198, 2003.

[33] G. Bounous and P. Gold, "The biological activity of undenatured dietary whey proteins: role of glutathione," *Clinical and Investigative Medicine*, vol. 14, pp. 296–309, 1991.

[34] D. A. Linseman, T. Laessig, M. K. Meintzer et al., "An essential role for Rac/Cdc42 GTPases in cerebellar granule neuron survival," *The Journal of Biological Chemistry*, vol. 276, pp. 39123–39131, 2001.

[35] S. Baruchel and G. Viau, "In vitro selective modulation of cellular glutathione by a humanized native milk protein isolate in normal cells and rat mammary carcinoma model," *Anticancer Research*, vol. 16, pp. 1095–1100, 1996.

[36] S. Baruchel, G. Viau, R. Olivier, G. Bounous, and M. A. Wainberg, "Nutraceutical modulation of glutathione with a humanized native milk serum protein isolate, Immunocal®: application in AIDS and cancer," in *Oxidative Stress in Cancer, AIDS, and Neurodegenerative Diseases*, L. Montagnier, R. Olivier and C. Pasquier, Eds., vol. 1, Chapter 42, pp. 447–462, Marcel Dekker, Inc., New York, NY, USA, 1998.

[37] A. K. Zimmermann, F. A. Loucks, E. K. Schroeder, R. J. Bouchard, K. L. Tyler, and D. A. Linseman, "Glutathione binding to the Bcl-2 homology-3 domain groove: a molecular basis for Bcl-2 antioxidant function at mitochondria," *The Journal of Biological Chemistry*, vol. 282, pp. 29296–29304, 2007.

[38] H. M. Wilkins, K. Marquardt, L. H. Lash, and D. A. Linseman, "Bcl-2 is a novel interacting partner for the 2-oxyglutarate carrier and a key regulator of mitochondrial glutathione," *Free Radical Biology and Medicine*, vol. 52, pp. 410–419, 2012.

[39] R. Drew and J. O. Miners, "The effects of buthionine sulphoximine (BSO) on glutathione depletion and xenobiotic biotransformation," *Biochemical Pharmacology*, vol. 33, pp. 2989–2994, 1984.

[40] M. Arciello, G. Rotilio, and L. Rossi, "Copper-dependent toxicity in SH-SY5Y neuroblastoma cells involves mitochondrial damage," *Biochemical and Biophysical Research Communications*, vol. 327, pp. 454–459, 2005.

[41] I. L. Yurkova, J. Arnhold, G. Fitzl, and D. Huster, "Fragmentation of mitochondrial cardiolipin by copper ions in the Atp7b$^{-/-}$ mouse model of Wilson's disease," *Chemistry and Physics of Lipids*, vol. 164, pp. 393–400, 2011.

[42] T. Fukushima, M. Koide, Y. Ago, A. Baba, and T. Matsuda, "T-817MA, a novel neurotrophic agent, improves sodium nitroprusside-induced mitochondrial dysfunction in cortical neurons," *Neurochemistry International*, vol. 48, pp. 124–130, 2006.

[43] T. Wei, C. Chen, J. Hou, B. Zhao, W. Xin, and A. Mori, "The antioxidant EPC-K1 attenuates NO-induced mitochondrial dysfunction, lipid peroxidation and apoptosis in cerebellar granule cells," *Toxicology*, vol. 134, pp. 117–126, 1999.

[44] V. Kumar and K. D. Gill, "Aluminum neurotoxicity: neurobehavioural and oxidative aspects," *Archives of Toxicology*, vol. 83, pp. 965–978, 2009.

[45] P. Y. Niu, Q. Niu, Q. L. Zhang et al., "Aluminum impairs rat neural cell mitochondria in vitro," *International Journal of Immunopathology and Pharmacology*, vol. 18, pp. 683–689, 2005.

[46] E. R. Whittemore, D. T. Loo, J. A. Watt, and C. W. Cotman, "A detailed analysis of hydrogen peroxide-induced cell death in primary neuronal culture," *Neuroscience*, vol. 67, pp. 921–932, 1995.

[47] C. J. Eggett, S. Crosier, P. Manning et al., "Development and characterization of a glutamate-sensitive motor neuron cell line," *Journal of Neurochemistry*, vol. 74, pp. 1895–1902, 2000.

[48] P. Mao and P. H. Reddy, "Aging and amyloid beta-induced oxidative DNA damage and mitochondrial dysfunction in Alzheimer's disease: implications for early intervention and therapeutics," *Biochimica et Biophysica Acta*, vol. 1812, pp. 1359–1370, 2011.

[49] G. Bounous and S. Baruchel, "Whey proteins as a food supplement in HIV-seropositive individuals," *Clinical and Investigative Medicine*, vol. 16, pp. 204–209, 1993.

[50] J. H. Jang and Y. J. Surh, "Bcl-2 attenuation of oxidative cell death is associated with upregulation of gamma-glutamylcysteine ligase via constitutive NF-kappaB activation," *The Journal of Biological Chemistry*, vol. 279, pp. 38779–38786, 2004.

[51] M. J. Meredith, C. L. Cusick, S. Soltninassab, K. S. Sekhar, S. Lu, and M. L. Freeman, "Expression of Bcl-2 increases intracellular glutathione by inhibiting methionine-dependent GSH efflux," *Biochemical and Biophysical Research Communications*, vol. 248, pp. 458–463, 1998.

[52] A. Hochman, H. Stemin, S. Gorodin et al., "Enhanced oxidative stress and altered antioxidants in brains of Bcl-2 deficient mice," *Journal of Neurochemistry*, vol. 71, pp. 741–748, 1998.

[53] J. H. Freedman, M. Ciriolo, and J. Peisach, "The role of glutathione in copper metabolism and toxicity," *The Journal of Biological Chemistry*, vol. 264, pp. 5596–5605, 1989.

[54] L. M. Sayre, G. Perry, P. L. Harris, Y. Liu, K. A. Schubert, and M. A. Smith, "In situ oxidative catalysis by neurofibrillary tangles and senile plaques in Alzheimer's disease: a central role for bound transition metals," *Journal of Neurochemistry*, vol. 74, pp. 270–279, 2000.

[55] A. R. White and R. Cappai, "Neurotoxicity from glutathione depletion is dependent on extracellular trace copper," *Journal of Neuroscience Research*, vol. 71, pp. 889–897, 2003.

[56] K. A. Trumbull and J. S. Beckman, "A role for copper in the toxicity of zinc-deficient superoxide dismutase to motor neurons in amyotrophic lateral sclerosis," *Antioxidants & Redox Signaling*, vol. 11, pp. 1627–1639, 2009.

[57] M. Di Filippo, D. Chisserini, A. Tozzi, B. Picconi, and P. Calabresi, "Mitochondria and the link between neuroinflammation and neurodegeneration," *Journal of Alzheimer's Disease*, vol. 20, pp. S369–S379, 2010.

[58] J. E. Yuste, E. Tarragon, C. M. Campuzano, and F. Ros-Bernal, "Implications of glial nitric oxide in neurodegenerative diseases," *Frontiers in Cellular Neuroscience*, vol. 9, p. 322, 2015.

[59] C. Dias, C. F. Lourenco, E. Ferreiro, R. M. Barbosa, J. Laranjinha, and A. Ledo, "Age-dependent changes in the glutamate-nitric oxide pathway in the hippocampus of the

triple transgenic model of Alzheimer's disease: implications for neurometabolic regulation," *Neurobiology of Aging*, vol. 46, pp. 84–95, 2016.

[60] E. Fernández, J. M. Garcia-Moreno, A. Martin de Pablos, and J. Chacón, "May the evaluation of nitrosative stress through selective increase of 3-nitrotyrosie proteins other than nitroalbumin and dominant tyrosine-125/136 nitrosylation of serum α-synuclein serve for diagnosis of sporadic Parkinson's disease?," *Antioxidants & Redox Signaling*, vol. 19, pp. 912–918, 2013.

[61] K. Murakami and M. Yoshino, "Aluminum decreases the glutathione regeneration by the inhibition of NADP-iscocitrate dehydrogenase in mitochondria," *Journal of Cellular Biochemistry*, vol. 93, pp. 1267–1271, 2004.

[62] C. Shaw and M. S. Petrik, "Aluminum hydroxide injections lead to motor deficits and motor neuron degeneration," *Journal of Inorganic Biochemistry*, vol. 103, pp. 1555–1562, 2009.

[63] R. W. Haley, "Excess incidence of ALS in young Gulf War veterans," *Neurology*, vol. 61, pp. 750–756, 2003.

[64] N. R. Cashman, H. D. Durham, J. K. Blusztain et al., "Neuroblastoma x spinal cord (NSC) hybrid cell lines resemble developing motor neurons," *Developmental Dynamics*, vol. 194, pp. 209–221, 1992.

[65] J. Lewerenz and P. Maher, "Chronic glutamate toxicity in neurodegenerative diseases – what is the evidence?," *Frontiers in Neuroscience*, vol. 9, p. 469, 2015.

[66] C. Caspersen, N. Wang, J. Yao et al., "Mitochondrial Abeta: a potential focal point for neuronal metabolic dysfunction in Alzheimer's disease," *The FASEB Journal*, vol. 19, pp. 2040-2041, 2005.

[67] M. Manczak, M. J. Calkins, and P. H. Reddy, "Impaired mitochondrial dynamics and abnormal interaction of amyloid beta with mitochondrial protein Drp1 in neurons from patients with Alzheimer's disease: implications for neuronal damage," *Human Molecular Genetics*, vol. 20, pp. 2495–2509, 2011.

[68] K. C. Walls, P. Coskun, J. L. Gallegos-Perez et al., "Swedish Alzheimer mutation induces mitochondrial dysfunction mediated by HSP60 mislocalization of amyloid precursor protein (APP) and beta-amyloid," *The Journal of Biological Chemistry*, vol. 287, pp. 30317–30327, 2012.

[69] W. Song, A. Tavitian, M. Cressatti, C. Galindez, A. Liberman, and H. M. Schipper, "Cysteine-rich whey protein isolate (Immunocal®) ameliorates deficits in the GFAP.HMOX1 mouse model of schizophrenia," *Free Radical Biology and Medicine*, vol. 110, pp. 162–175, 2017.

[70] E. K. Ross, A. N. Winter, H. M. Wilkins et al., "A cystine-rich whey supplement (Immunocal®) delays disease onset and prevents spinal cord glutathione depletion in the hSOD1G93A mouse model of amyotrophic lateral sclerosis," *Antioxidants*, vol. 3, pp. 843–865, 2014.

Hindawi
Oxidative Medicine and Cellular Longevity
Volume 2017, Article ID 3160360, 10 pages
https://doi.org/10.1155/2017/3160360

Research Article

HIV-1 Transactivator Protein Induces ZO-1 and Neprilysin Dysfunction in Brain Endothelial Cells via the Ras Signaling Pathway

Wenlin Jiang,[1] Wen Huang,[1] Yanlan Chen,[2] Min Zou,[1] Dingyue Peng,[1] and Debing Chen[1]

[1]*Department of Neurology, First Affiliated Hospital, Guangxi Medical University, Nanning 530021, China*
[2]*Nanxishan Hospital of Guangxi Zhuang Autonomous Region, Guilin 541000, China*

Correspondence should be addressed to Wen Huang; hwen1229@163.com

Received 29 November 2016; Revised 9 February 2017; Accepted 1 March 2017; Published 2 May 2017

Academic Editor: Anna M. Giudetti

Amyloid beta (Aβ) deposition is increased in human immunodeficiency virus-1- (HIV-1-) infected brain, but the mechanisms are not fully understood. The aim of the present study was to evaluate the role of Ras signaling in HIV-1 transactivator protein- (Tat-) induced Aβ accumulation in human cerebral microvascular endothelial cells (HBEC-5i). Cell viability assay showed that 1 μg/mL Tat and 20 μmol/L of the Ras inhibitor farnesylthiosalicylic acid (FTS) had no significant effect on HBEC-5i cell viability after 24 h exposure. Exposure to Tat decreased protein and mRNA levels of zonula occludens- (ZO-) 1 and Aβ-degrading enzyme neprilysin (NEP) in HBEC-5i cells as determined by western blotting and quantitative real-time polymerase chain reaction. Exposure to Tat also increased transendothelial transfer of Aβ and intracellular reactive oxygen species (ROS) levels; however, these effects were attenuated by FTS. Collectively, these results suggest that the Ras signaling pathway is involved in HIV-1 Tat-induced changes in ZO-1 and NEP, as well as Aβ deposition in HBEC-5i cells. FTS partially protects blood-brain barrier (BBB) integrity and inhibits Aβ accumulation.

1. Introduction

Human immunodeficiency virus-1- (HIV-1-) related cognitive impairment and dementia are more prevalent in older HIV-1-infected individuals [1, 2]. Amyloid beta (Aβ) deposition is a characteristic in the HIV-1-infected brains [1, 3, 4]. Reportedly, exposure to HIV-1 increases brain Aβ levels by stimulating Aβ formation [5], upregulating amyloid precursor protein expression [6], inhibiting Aβ degradation [7], or altering Aβ transport across the blood-brain barrier (BBB) [8]. The BBB plays a critical role both in HIV-1 trafficking into the brain [9] and in Aβ pathology [1]. The major components of the BBB are brain microvascular endothelial cells [10] joined by tight junctions (TJs) [11]. TJ proteins such as occludin, claudin, and zonula occludens (ZO) play a critical role in maintaining BBB integrity and low permeability [12]. ZO-1 linking the transmembrane TJs (occludin) to actin cytoskeleton plays an important role in barrier resistance and permeability [13, 14].

HIV-1 transactivator of transcription (Tat) protein is essential for HIV infection and virus replication [15]. HIV-1 Tat is involved in several cellular processes including inducing angiogenesis, modulating cytokine expression, and activating cellular signaling pathways [16]. Tat protein is actively secreted by HIV-1-infected cells [10, 15] and may cross the BBB [10] and be taken up by astrocytes and neurons, resulting in neuronal apoptosis and BBB disruption by increasing intracellular calcium and reactive oxygen species (ROS) levels and stimulating inflammation [16]. HIV-1 Tat also inhibits the Aβ-degrading enzyme neprilysin and restricts its ability to degrade Aβ, resulting in increased soluble Aβ levels in cell culture [7]. Cerebral clearance of soluble Aβ involves both degradation in the brain and transport across the BBB to systemic circulation. Neprilysin-degraded Aβ is partially removed from the brain by efflux transport at the BBB [17]. The Ras family of small GTPases transmits extracellular signals involved in many cellular processes that regulate cell growth, differentiation, motility, and death. Ras

is a major hub of many signaling pathways [18]. For example, activation of the Ras/mitogen-activated protein kinase pathway is involved in HIV-1 Tat-induced disruption of TJ proteins in brain endothelial cells [19]. Ras signaling induces the generation of ROS via activating the downstream effector mitogen-activated protein kinase (MEK)/extracellular signal-regulated kinases (ERK), resulting in the alteration of TJs and BBB permeability [20]. Farnesylthiosalicylic acid (FTS) is a synthetic and functional Ras inhibitor [21] that has been successfully used in phase II clinical trials of patients with pancreatic and non-small-cell lung cancer [22]. Inhibition of Ras by FTS may ameliorate inflammatory conditions [23]. Ras signaling can be a target for HIV-1 Tat-induced changes of TJ proteins [3], and inhibition may be an appropriate therapeutic intervention [21].

Whether the Ras signaling pathway is involved in HIV-1-induced BBB disruption and Aβ deposition is not fully understood. The aim of the current study was to evaluate the role of Ras signaling in HIV-1-induced ZO-1 and neprilysin disruption and Aβ accumulation in HBEC-5i cells.

2. Materials and Methods

2.1. Cell Cultures and Treatment. Human cerebral microvascular endothelial cells (HBEC-5i) were purchased from American Type Culture Collection (ATCC, Manassas, VA, USA). The cells were cultured on 0.1% gelatin solution (ATCC)-coated flasks in DMEM:F12 medium (ATCC) supplemented with 10% foetal bovine serum (Gibco/Thermo Fisher, Waltham, MA, USA), 40 μg/mL endothelial growth supplement (ECGS, ATCC), and 1% penicillin-streptomycin (Beyotime, Shanghai) according to the manufacturer's instructions. HBEC-5i cells were incubated at 37°C in a humidified atmosphere of 5% CO_2.

Recombinant HIV-1 Tat clade-B protein (amino acids 1 to 86) was purchased from Prospec (Rehovot, Israel). The previous literature indicated that concentrations of Tat in HIV-infected patients could reach the range of 0.5 μg/mL of serum [24], so this concentration was used in subsequent experiments. Controls consisted of cells treated with 0.02% DMSO or heat-inactivated Tat (1 μg/mL). Before exposure to 1 μg/mL HIV-1 Tat for 12 or 24 h, confluent HBEC-5i cells were pretreated with 5 μmol/L FTS for 3 h and FTS was retained in the serum-free cell culture medium during Tat treatment as previously described [25].

2.2. Cell Viability Assay. A density of 1×10^4 cells/well of HBEC-5i cells were seeded onto 96-well plates. After 12 h, HBEC-5i were treated with Tat at 0, 0.25, 0.5, 1, or 1.25 μg/mL and heat-inactivated Tat for 24 h or the Ras inhibitor FTS (Sigma-Aldrich, St. Louis, MO, USA) at 0, 5, 10, 20, 30, 40, or 50 μmol/L for 12, 24, and 48 h. The cells were then incubated with 20 μL 3-(4,5-dimethylthiazol-2-yl)-2,5-diphenyltetrazolium bromide solution (MTT, 5 mg/mL; Sigma-Aldrich) for another 4 h. Optical density was measured at 570 nm using a microwell plate reader (Thermo Scientific). Neither Tat at 1 μg/mL nor FTS at 20 μmol/L for 24 h had a significant effect on HBEC-5i cell viability.

2.3. Western Blot Analysis. Following treatment, cells were washed three times and lysed using radioimmunoprecipitation assay cell lysis buffer (Beyotime) containing protease inhibitor cocktail tablets (Beyotime). The lysates were collected and centrifuged at 12,000*g* for 15 min, and protein levels were quantified using a BCA Protein Assay Kit (Beyotime). Next, 30 μg proteins were separated by SDS-PAGE and transferred onto polyvinylidene fluoride membranes (0.45 μm; Millipore, Billerica, MA, USA). Membranes were blocked for 1 h with 5% fat-free milk at room temperature and then incubated with primary antibodies against ZO-1 (1 : 400, rabbit polyclonal; Abcam, Cambridge, UK), NEP (1 : 400, rabbit polyclonal; Abcam), and GAPDH (1 : 5000; Proteintech Group, Chicago, IL, USA) at 4°C overnight. The next day, the membranes were washed and incubated with IRDye 680 RD goat anti-rabbit immunoglobulin (Ig) G (1 : 10,000; LI-COR Biosciences, Lincoln, NE, USA) secondary antibody for 1 h at room temperature. The detected proteins were then visualized using an Odyssey Infrared Imaging System (LI-COR Biosciences). Band density was analysed by ImageJ software (National Institutes of Health, Bethesda, MD, USA), and signal density was calculated as the ratio of signal intensity to that of GAPDH.

2.4. Real-Time Reverse Transcription Polymerase Chain Reaction. After treatment, cells were harvested, total RNA was extracted using TRIzol reagent (TakaraBio, Dalian, Japan), and cDNA was generated from 1 μg RNA using the Prime-Script RT reagent kit (Takara) according to the manufacturer's instructions. cDNA was used for quantitative RT-PCR using a Taq PCR Master Mix kit (Takara) and conducted on the StepOnePlus Real-Time PCR System (Applied Biosystems, Foster City, CA, USA) using RT Reaction Mix in a total volume of 20 μL at 95°C for 30 s, followed by 95°C for 5 s, and 60°C for 30 s for 40 cycles. The primer sequences were as follows: ZO-1 (Takara): 5′-GACCAATAGCTGATGTTGCCAGAG-3′ and 5′-TGCAGGCGAATAATGCCAGA-3′; NEP (Takara): 5′-TAAGCAGCCTCAGCCGAACC-3′ and 5′-TTGACATAG TTTGCACAACGTCTCC-3′; and GAPDH (Takara): 5′-GCACCGTCAAGGCTGAGAAC-3′ and 5′-TGGTGAAG ACGCCAGTGGA-3′. GAPDH was used to normalize target gene mRNA levels, which were analysed using the $2^{-\Delta\Delta Ct}$ method.

2.5. Immunofluorescence Microscopy. HBEC-5i cells were seeded onto gelatin-coated circular glass slips in 24-well plates and incubated for 24 h. After treatment, the cells were fixed with 4% paraformaldehyde (Solarbio, Beijing, China) on ice for 30 min and permeabilised with 0.1% TritonX-100 (Beyotime) for 10 min. They were then blocked with 3% bovine serum albumin (Sigma, St. Louis, MO, USA) for 1 h at room temperature before overnight incubation with a primary antibody against NEP (1 : 100, rabbit polyclonal; Abcam) at 4°C. After washing with phosphate-buffered saline (PBS), the slides were incubated with the Alexa Fluor-488 donkey anti-rabbit (1 : 500; Invitrogen, Thermo Fisher, Waltham, MA, USA) secondary antibody for 2 h at room temperature. After washing and staining with

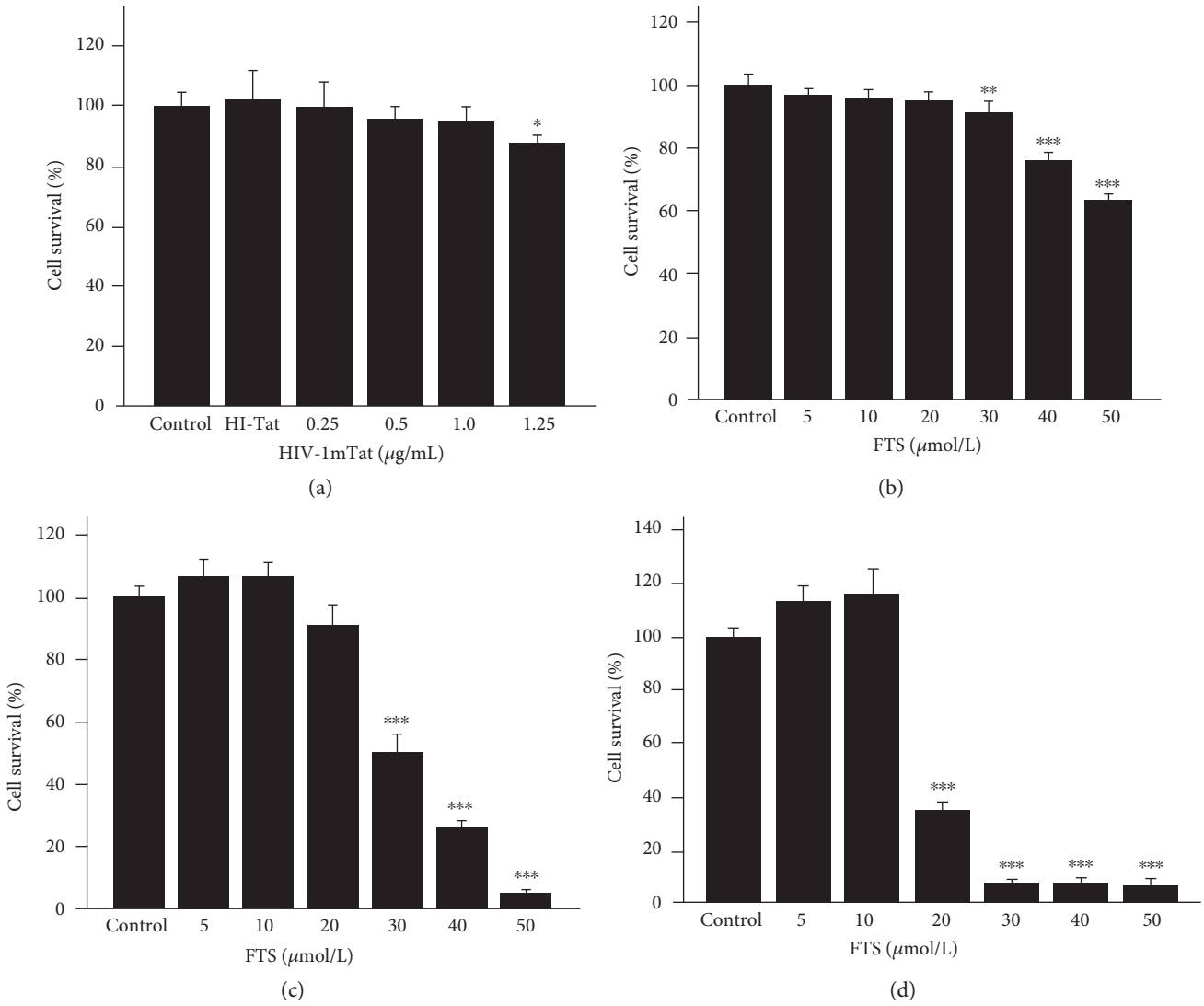

Figure 1: Cell viability assay. HBEC-5i cells were treated with HIV-1 Tat at 0, 0.25, 0.5, 1, or 1.25 μg/mL and heat-inactivated Tat for 24 h (a) or FTS at 0, 5, 10, 20, 30, 40, or 50 μmol/L for 12, 24, or 48 h (b, c, d). Cell viability was not affected by 1 μg/mL HIV-1 Tat or 20 μmol/L FTS for 24 h. Results are expressed as means ± standard error of the mean ($n = 5$). $^{*}p < 0.05$, $^{**}p < 0.01$, and $^{***}p < 0.001$ versus that in the control.

4′,6-diamidino-2-phenylindole (Invitrogen), samples were visualized using a fluorescence microscope (OlympusBX53, Tokyo, Japan).

Aβ (1–40) HiLyte (a fluorescently labelled Aβ) was purchased from AnaSpec (San Jose, CA, USA). Aβ (1–40) HiLyte was first dissolved in PBS and then diluted in cell culture medium as suggested by the manufacturer. Cells were treated with Aβ (1–40) HiLyte at the concentration of 1 μmol/L for 10 min in serum-free medium as previously described [1]. The cells were then fixed, washed, and mounted. The fluorescence signal from Aβ (1–40) HiLyte was directly acquired with a fluorescence microscope (OlympusBX53). Both acquisition and quantification were performed using Olympus cellSens Dimension software.

2.6. Aβ (1–40) Transport across HBEC-5i Monolayers. Confluent HBEC-5i cells cultured on Transwell filter inserts (pore size 0.4 μm, 24-well cell culture plate; Corning, Corning, NY, USA) were pretreated with 5 μmol/L FTS for 3 h and exposed to 1 μg/mL HIV-1 Tat for 24 h. For the last 20 min of HIV-1 Tat exposure, 1 μmol/L Aβ (1–40) HiLyte was added to the upper chamber incubated at 37°C in the dark. The fluorescence signal from Aβ (1–40) HiLyte as the indicator of transendothelial Aβ transfer was measured using a multidetection microplate reader (Bio-Rad, Hercules, CA, USA) in the lower chamber at 503 nm (excitation) and 528 nm (emission).

2.7. Detection of Intracellular ROS. Intracellular ROS levels were quantified using the Reactive Oxygen Species Assay Kit (Beyotime). Cells were washed with PBS, and then, a final concentration of 10 mmol/L DCFH-DA was added for 30 min incubation at 37°C in the dark. After washing with PBS, the stained cells in the 24-well plate were visualized by

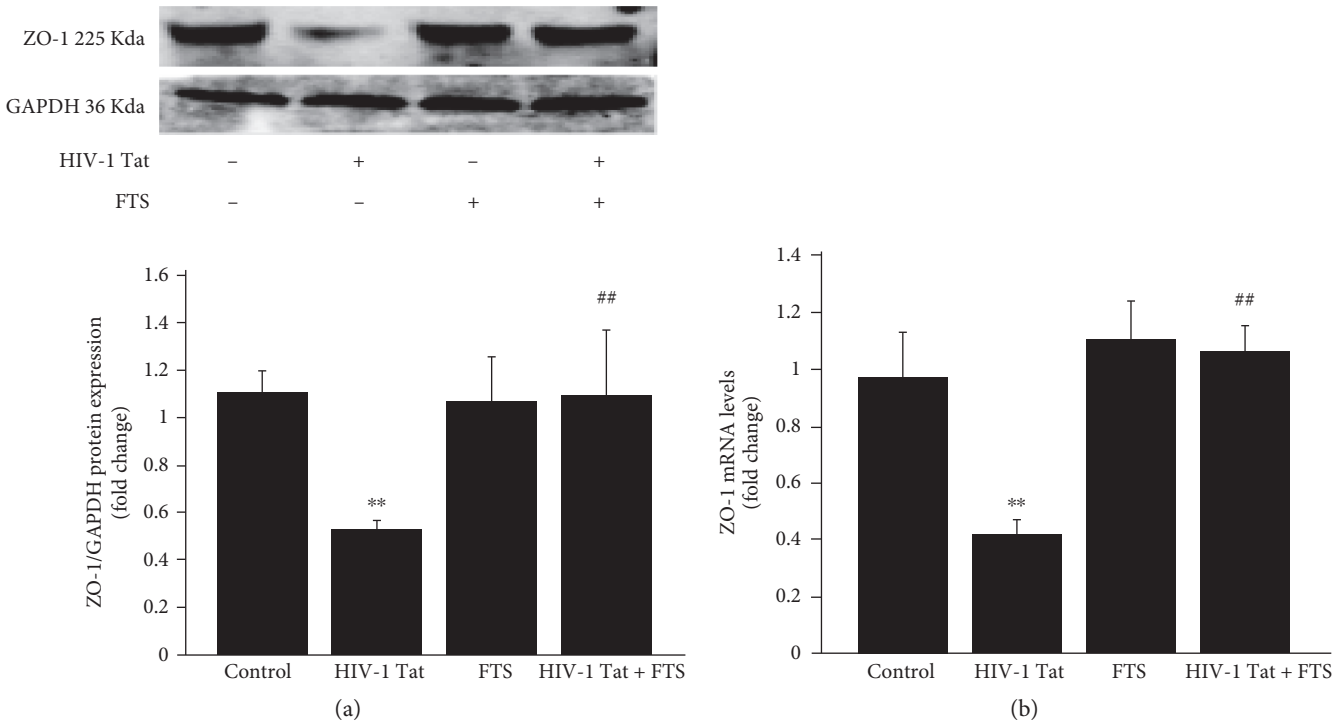

Figure 2: Role of Ras signaling in HIV-1 Tat-induced disruption of ZO-1. Before HIV-1 Tat exposure, HBEC-5i cells were pretreated with 5 μmol/L FTS for 3 h. FTS remained in the culture medium during Tat exposure. The time of Tat exposure was 24 h for western blotting (a) and 12 h for RT-PCR (b). HIV-1 Tat exposure induced decreased ZO-1 protein and mRNA levels in HBEC-5i cells. Following cotreatment with FTS and HIV-1 Tat, ZO-1 protein and mRNA levels were significantly increased compared with those in the HIV-1 Tat group. Data are shown as means ± standard error of the mean ($n = 3$ for (a), $n = 5$ for (b)). $^{**}p < 0.01$ versus control; $^{\#\#}p < 0.01$ versus HIV-1 Tat.

inverted fluorescence microscopy (Nikon, Tokyo, Japan). Relative levels of fluorescence in cells were measured with a multidetection microplate reader (Bio-Rad) at 488 nm (excitation) and 525 nm (emission). Intracellular ROS level was expressed as the percentage of the control group.

2.8. Statistical Analysis. The data are shown as means ± standard deviations. Data were analysed using SPSS version 17.0 (SPSS, Chicago, IL, USA). One-way ANOVA was used to compare responses between groups. Differences were considered statistically significant at $p < 0.05$.

3. Results

3.1. Cell Viability. HBEC-5i viability was tested with MTT assays. Neither HIV-1 Tat at 1 μg/mL nor FTS at 20 μmol/L for 24 h had a significant effect on HBEC-5i cell viability (Figure 1).

3.2. Ras Signaling Is Involved in HIV-1 Tat-Induced Disruption of ZO-1. To observe the effects of HIV-1 Tat on the TJ protein ZO-1, HBEC-5i cells were exposed to 1 μg/mL HIV-1 Tat for 24 h (for western blotting) or 12 h (for real-time RT-PCR). Both protein and mRNA levels of ZO-1 were significantly lower in the HIV-1 Tat group compared to the control group (Figures 2(a) and 2(b)).

To determine if Ras signaling is involved in HIV-1 Tat-induced ZO-1 downregulation, HBEC-5i cells were pretreated for 3 h with 5 μmol/L FTS, followed by cotreatment with FTS and 1 μg/mL HIV-1 Tat for 24 or 12 h. ZO-1 protein and mRNA levels were significantly increased following coexposure to FTS and HIV-1 Tat compared with the HIV-1 Tat group (Figures 2(a) and 2(b)).

3.3. Ras Signaling Is Involved in HIV-1 Tat-Induced Regulation of NEP Expression. To investigate whether HIV-1 Tat could affect the expression of NEP in HBEC-5i cells, its expression was detected with western blotting, real-time RT-PCR, and immunofluorescence. Treatment with 1 μg/mL HIV-1 Tat for 24 h (for western blotting and immunofluorescence) or 12 h (for real-time RT-PCR) significantly downregulated NEP protein and mRNA levels (Figures 3(a) and 3(b)) and resulted in markedly weaker NEP immunoreactivity compared with the control group (Figure 3(c)).

To evaluate whether Ras signaling affects HIV-1 Tat-induced changes in NEP expression, HBEC-5i cells were pretreated with 5 μmol/L FTS for 3 h and then cotreated with FTS and HIV-1 Tat for 24 or 12 h. FTS increased NEP protein levels (Figure 3(a)). These results were consistent with the NEP mRNA levels in the groups cotreated with FTS and HIV-1 Tat versus the HIV-1 Tat group (Figure 3(b)), and markedly stronger NEP immunoreactivity was noted

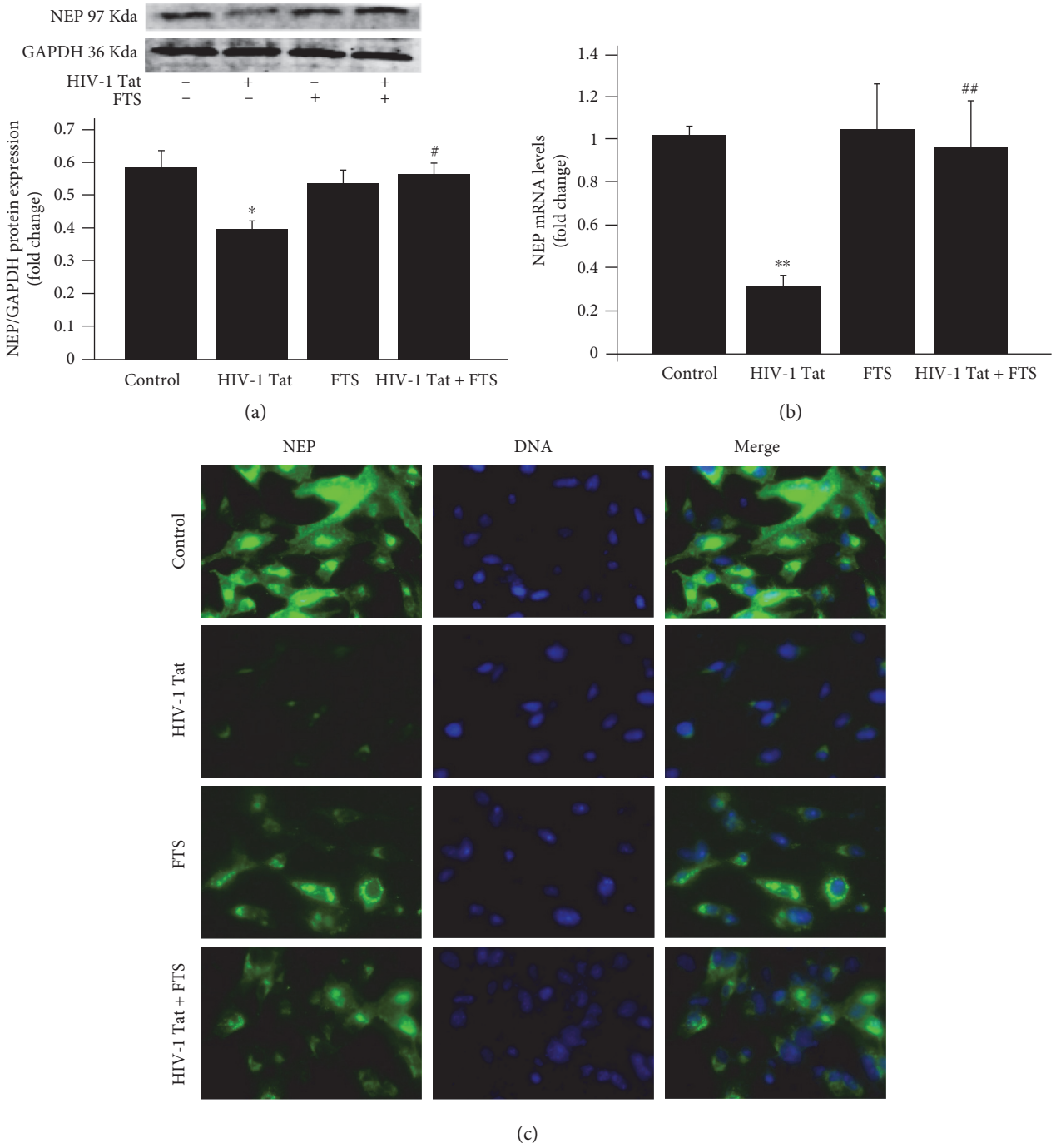

FIGURE 3: Role of Ras signaling in HIV-1 Tat-induced changes in NEP. Exposure to HIV-1 Tat resulted in marked decreases in NEP protein (a) and mRNA (b) and weaker immunoreactivity (c) compared with the control group. Prior to HIV-1 Tat exposure, cells were pretreated with 5 μmol/L FTS for 3 h with FTS in the culture medium. NEP protein and mRNA levels and immunoreactivity significantly increased with coexposure to FTS and HIV-1 Tat compared with the HIV-1 Tat group. Data are expressed as means ± standard error of the mean ($n = 3$ for (a), $n = 5$ for (b)). $^{*}p < 0.05$, $^{**}p < 0.01$ versus that in the control; $^{\#}p < 0.05$, $^{\#\#}p < 0.01$ versus that in HIV-1 Tat.

in the FTS-treated cells compared with the HIV-1 Tat group (Figure 3(c)).

3.4. Ras Signaling Is Involved in HIV-1 Tat-Induced Accumulation of Exogenous Aβ. To observe the combined effects of HIV-1 Tat and exogenous Aβ on intracellular Aβ levels, HBEC-5i cells were exposed to 1 μg/mL HIV-1 Tat for 24 h. For the last 10 min of HIV-1 Tat treatment, Aβ (1–40) HiLyte was added to the culture medium. As shown in Figure 4(a), green fluorescence from Aβ (1–40) HiLyte was significantly increased in the presence of HIV-1 Tat compared with the control group treated with Aβ (1–40) HiLyte alone.

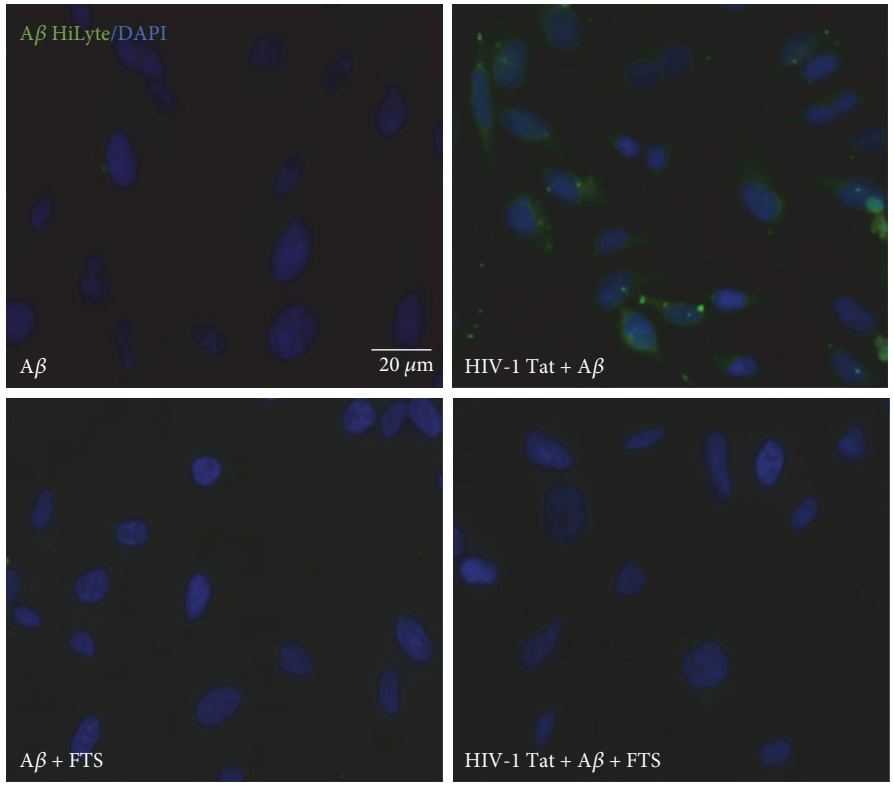

(a)

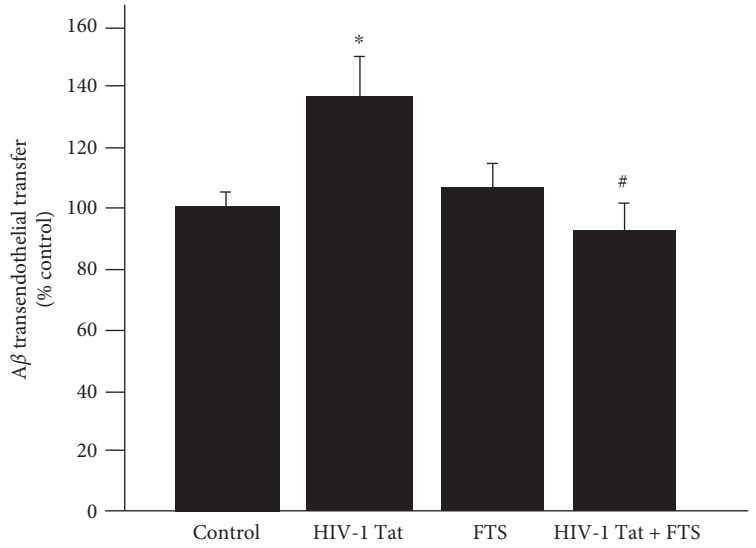

(b)

Figure 4: Role of Ras signaling in HIV-1 Tat-induced accumulation of exogenous Aβ in HBEC-5i. HIV-1 Tat exposure markedly increased the accumulation of Aβ (1–40) HiLyte in HBEC-5i. Pretreatment with 5 μmol/L FTS for 3 h followed by coexposure to HIV-1 Tat and FTS significantly decreased Aβ (1–40) HiLyte accumulation (a). FTS inhibited HIV-1 Tat-induced transendothelial transfer of Aβ. Confluent HBEC-5i cells in Transwell filter inserts were exposed to 1 μmol/L Aβ (1–40) HiLyte for the last 20 min of HIV-1 Tat exposure in the upper chamber, mimicking the blood side of the BBB. The fluorescence signal of Aβ (1–40) HiLyte was measured in the lower chamber, equivalent to the brain side of the BBB (b). Data are expressed as means ± standard error of the mean ($n = 4$). $^{*}p < 0.05$ versus that in the control; $^{\#}p < 0.05$ versus that in HIV-1 Tat.

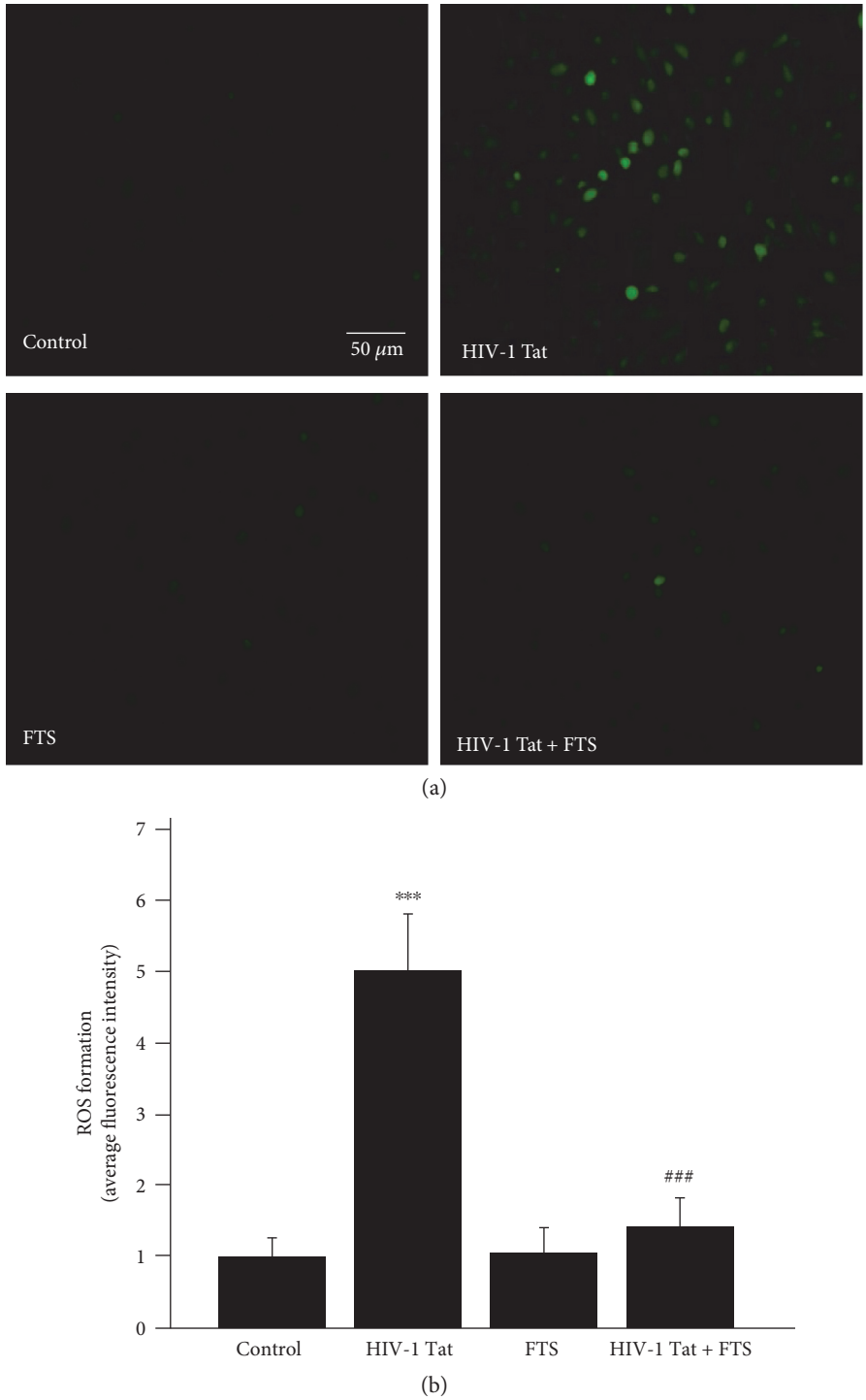

Figure 5: Role of Ras signaling in HIV-1 Tat-induced changes in intracellular ROS levels. Exposure to HIV-1 Tat for 24 h significantly increased intracellular ROS levels in HBEC-5i cells. Pretreatment with 5 μmol/L FTS and then coexposure to HIV-1 Tat and FTS markedly attenuated HIV-1 Tat-induced intracellular ROS production. Results are shown as means ± standard error of the mean ($n = 4$). $^{***}p < 0.01$ versus that in the control; $^{###}p < 0.01$ versus that in HIV-1 Tat.

To explore whether Ras signaling is involved in HIV-1 Tat-induced effects of exogenous Aβ, HBEC-5i cells were pretreated with 5 μmol/L FTS for 3 h followed by coexposure to FTS and 1 μg/mL HIV-1 Tat for 24 h. As shown in Figure 4(a), FTS pretreatment prior to coexposure to HIV-1 Tat and FTS markedly decreased HIV-1 Tat-induced accumulation of Aβ (1–40) HiLyte.

To evaluate the effect of HIV-1 Tat and/or FTS on Aβ transfer across HBEC-5i monolayers, HBEC-5i cells were exposed to 1 μmol/L Aβ (1–40) HiLyte during HIV-1 Tat

treatment in a Transwell model system. This led to significant transendothelial Aβ transfer, which was significantly attenuated by a 3 h pretreatment with 5 μmol/L FTS before cotreatment with HIV-1 Tat and FTS (Figure 4(b)).

3.5. ROS Production Induced by HIV-1 Tat in HBEC-5i Is Attenuated by Ras Inhibition. To observe the effects of HIV-1 Tat on intracellular ROS levels, overall intracellular ROS production in HBEC-5i cells was assessed with DCFDA staining. Exposure to HIV-1 Tat significantly increased intracellular ROS levels, but this was ameliorated by pretreatment with 5 μmol/L FTS (Figure 5).

4. Discussion

HIV-1 Tat protein is regarded a pathogenic factor in HIV-associated neurocognitive disorders (HAND) [26–29]; however, how HIV-1 Tat induces the development of AD-like pathology in HIV-1-infected patients is not fully understood. HAND in older patients seems to be linked to early beta-amyloidosis [3, 8]. HIV-1 Tat is reportedly both neuroexcitatory and neurotoxic [30] and can enhance the adhesion of monocytes and T cells to the endothelium both in vivo and in vitro [31]. A previous study found that two mechanisms underlying HIV-1 Tat-induced BBB destruction were elevated cellular oxidative stress and stimulated inflammatory responses [32]. Our previous study reported that HIV-1 Tat disrupted the TJ protein occludin, downregulated low-density lipoprotein receptor-related protein 1 expression, and even upregulated the expression of a receptor for advanced glycation end products, but all of these outcomes were attenuated by inhibiting Rho/ROCK signaling [33]. A functionally impaired BBB with deficient Aβ clearance could lead to brain Aβ accumulation [11]; therefore, the BBB is critical for preventing Aβ deposition in the HIV-infected brain.

HIV-1 Tat activates Ras and then leads to ERK phosphorylation in endothelial cells [34]. Ras signaling induces ROS generation via the downstream effector MEK/ERK [20], and oxidative stress may be an early step in Tat-induced neurotoxicity [35]. The elements of the Ras signaling cascade are involved in proinflammatory signal transduction [36]. Ras proteins can also activate the immune system [23]. Inhibition of the Ras pathway by FTS was previously found to protect brain endothelial cells from Tat-induced disruption of TJ proteins [25]. ZO-1 acts as a scaffold protein linking occludin to the actin cytoskeleton, and it plays a critical role in maintaining BBB resistance and permeability [14]. Knocking down ZO-1 with siRNA leads to barrier hyperpermeability [36]. HBEC-5i cells have major characteristics of cerebral endothelial cells, such as high transendothelial electrical resistance (TEER) and low permeability [37]. A previous study demonstrated that exposure to HIV-1 Tat increased permeability and decreased TEER of brain microvascular endothelial cells [38]. In accordance with the earlier study [25], in the present study, HIV-1 Tat-mediated downregulation of ZO-1 protein and mRNA levels was attenuated by inhibiting Ras signaling with FTS. Collectively, these findings indicate that FTS protected against HIV-1 Tat-induced BBB dysfunction partly by inhibiting Ras signaling.

NEP is considered a critical Aβ-degrading enzyme in the brain [39] that can degrade both extracellular and intracellular Aβ [4]. Levels were increased obviously in the brains of NEP knockout mice [40]. However, the mechanisms of Tat-induced inhibition of NEP are relatively unknown. A previous study reported that the regulation of NEP activity may involve MEK/ERK signaling; specifically, MEK inhibition increases NEP activity [41]. In addition, increasing intracellular ROS production may also downregulate NEP expression in vascular endothelial cells [42]. In the present study, HIV-1 Tat treatment reduced NEP protein and mRNA levels; however, these effects were diminished by FTS treatment, and the effect of HIV-1 Tat on weaker NEP immunoreactivity was reversed by FTS. Exposure to HIV-1 Tat also significantly elevated intracellular ROS levels, which were decreased by FTS. These results suggest that FTS may partly protect against HIV-1 Tat-induced inhibition of NEP by ameliorating oxidative stress (decreased ROS formation) and inhibiting Ras cascades.

A previous study demonstrated that Tat clade-B may possess a unique ability to directly stimulate both Aβ formation and cell-bound Aβ accumulation [5]. Exposure to HIV-1 also increases Aβ transendothelial transfer [1]. Aβ is a proinflammatory factor that may induce chronic neuroinflammatory responses and damage the endothelium [8]. Aβ toxicity in the brain vasculature seems to induce ROS production [1]. In accordance with the earlier findings [3], we showed that treatment with exogenous Aβ (1–40) HiLyte increased intracellular Aβ levels, and this effect was further enhanced by the presence of HIV-1 Tat. Notably, inhibition of Ras by FTS effectively prevented HIV-1 Tat-mediated Aβ accumulation. In addition, Tat treatment enhanced transendothelial transfer of Aβ (1–40) HiLyte; this finding is in conformity with the earlier findings [8]; however, this effect was attenuated by Ras inhibition. These data suggest that inhibiting Ras may attenuate HIV-1 Tat-induced Aβ accumulation and transendothelial transfer.

In summary, inhibition of Ras signaling in HBEC-5i cells significantly attenuated HIV-1 Tat-induced disruption of ZO-1 and NEP, decreased HIV-1 Tat-induced intracellular ROS formation, and protected against HIV-1 Tat-induced Aβ accumulation. These findings clarify the possible mechanisms involved in HIV-1-induced Aβ accumulation in the brain. They also indicate a potential protective effect of FTS on HIV-1 Tat-mediated BBB dysfunction and Aβ accumulation. Targeting the Ras signaling pathway may be a promising approach for HAND.

Conflicts of Interest

The authors declare that they have no conflicts of interest.

Acknowledgments

This work was supported by the National Nature Science Foundation of China (81371333, 81160152, and 2013GXNSFCA019013).

References

[1] I. E. Adrás and M. Toborek, "HIV-1 stimulates nuclear entry of amyloid beta via dynamin dependent EEA1 and TGF-beta/Smad signaling," *Experimental Cell Research*, vol. 323, no. 1, pp. 66–76, 2014.

[2] V. Valcour, C. Shikuma, B. Shiramizu et al., "Higher frequency of dementia in older HIV-1 individuals: the Hawaii Aging with HIV-1 Cohort," *Neurology*, vol. 63, no. 5, pp. 822–827, 2004.

[3] I. E. András, S. Y. Eum, and M. Toborek, "Lipid rafts and functional caveolae regulate HIV-induced amyloid beta accumulation in brain endothelial cells," *Biochemical and Biophysical Research Communications*, vol. 421, no. 2, pp. 177–183, 2012.

[4] C. L. Achim, A. Adame, W. Dumaop, I. P. Everall, E. Masliah, and Neurobehavioral Research Center, "Increased accumulation of intraneuronal amyloid beta in HIV-infected patients," *Journal of Neuroimmune Pharmacology*, vol. 4, no. 2, pp. 190–199, 2009.

[5] M. Y. Aksenov, M. V. Aksenova, C. F. Mactutus, and R. M. Booze, "HIV-1 protein-mediated amyloidogenesis in rat hippocampal cell cultures," *Neuroscience Letters*, vol. 475, no. 3, pp. 174–178, 2010.

[6] J. Zhang, J. Liu, B. Katafiasz, H. Fox, and H. Xiong, "HIV-1 gp120-induced axonal injury detected by accumulation of beta-amyloid precursor protein in adult rat corpus callosum," *Journal of Neuroimmune Pharmacology*, vol. 6, no. 4, pp. 650–657, 2011.

[7] H. C. Rempel and L. Pulliam, "HIV-1 Tat inhibits neprilysin and elevates amyloid beta," *Aids*, vol. 19, no. 2, pp. 127–135, 2005.

[8] I. E. András, S. Y. Eum, W. Huang, Y. Zhong, B. Hennig, and M. Toborek, "HIV-1-induced amyloid beta accumulation in brain endothelial cells is attenuated by simvastatin," *Molecular and Cellular Neurosciences*, vol. 43, no. 2, pp. 232–243, 2010.

[9] W. Huang, S. Y. Eum, I. E. András, B. Hennig, and M. Toborek, "PPARalpha and PPARgamma attenuate HIV-induced dysregulation of tight junction proteins by modulations of matrix metalloproteinase and proteasome activities," *The FASEB Journal*, vol. 23, no. 5, pp. 1596–1606, 2009.

[10] S. M. Woollard, B. Bhargavan, F. Yu, and G. D. Kanmogne, "Differential effects of Tat proteins derived from HIV-1 subtypes B and recombinant CRF02_AG on human brain microvascular endothelial cells: implications for blood-brain barrier dysfunction," *Journal of Cerebral Blood Flow and Metabolism*, vol. 34, no. 6, pp. 1047–1059, 2014.

[11] I. E. András and M. Toborek, "Amyloid beta accumulation in HIV-1-infected brain: the role of the blood brain barrier," *IUBMB Life*, vol. 65, no. 1, pp. 43–49, 2013.

[12] A. Banerjee, X. Zhang, K. R. Manda, W. A. Banks, and N. Ercal, "HIV proteins (gp120 and Tat) and methamphetamine in oxidative stress-induced damage in the brain: potential role of the thiol antioxidant N-acetylcysteine amide," *Free Radical Biology & Medicine*, vol. 48, no. 10, pp. 1388–1398, 2010.

[13] P. Dalvi, K. Wang, J. Mermis et al., "HIV-1/cocaine induced oxidative stress disrupts tight junction protein-1 in human pulmonary microvascular endothelial cells: role of Ras/ERK1/2 pathway," *PloS One*, vol. 9, no. 1, article e85246, 2014.

[14] H. Alluri, R. L. Wilson, C. Anasooya Shaji et al., "Melatonin preserves blood-brain barrier integrity and permeability via matrix metalloproteinase-9 inhibition," *PloS One*, vol. 11, no. 5, article e0154427, 2016.

[15] I. E. András, G. Rha, W. Huang et al., "Simvastatin protects against amyloid beta and HIV-1 Tat-induced promoter activities of inflammatory genes in brain endothelial cells," *Molecular Pharmacology*, vol. 73, no. 5, pp. 1424–1433, 2008.

[16] J. Kim, J. H. Yoon, and Y. S. Kim, "HIV-1 Tat interacts with and regulates the localization and processing of amyloid precursor protein," *PloS One*, vol. 8, no. 11, article e77972, 2013.

[17] S. Ito, K. Matsumiya, S. Ohtsuki, J. Kamiie, and T. Terasaki, "Contributions of degradation and brain-to-blood elimination across the blood-brain barrier to cerebral clearance of human amyloid-beta peptide (1-40) in mouse brain," *Journal of Cerebral Blood Flow and Metabolism*, vol. 33, no. 11, pp. 1770–1777, 2013.

[18] E. Schmukler, E. Grinboim, S. Schokoroy et al., "Ras inhibition enhances autophagy, which partially protects cells from death," *Oncotarget*, vol. 4, no. 1, pp. 142–152, 2013.

[19] Y. Zhong, B. Hennig, and M. Toborek, "Intact lipid rafts regulate HIV-1 Tat protein-induced activation of the Rho signaling and upregulation of P-glycoprotein in brain endothelial cells," *Journal of Cerebral Blood Flow and Metabolism*, vol. 30, no. 3, pp. 522–533, 2010.

[20] D. A. Mayes, T. A. Rizvi, H. Titus-Mitchell et al., "Nf1 loss and Ras hyperactivation in oligodendrocytes induce NOS-driven defects in myelin and vasculature," *Cell Reports*, vol. 4, no. 6, pp. 1197–1212, 2013.

[21] E. Schmukler, E. Wolfson, R. Haklai, G. Elad-Sfadia, Y. Kloog, and R. Pinkas-Kramarski, "Chloroquine synergizes with FTS to enhance cell growth inhibition and cell death," *Oncotarget*, vol. 5, no. 1, pp. 173–184, 2014.

[22] E. Bustinza-Linares, R. Kurzrock, and A. M. Tsimberidou, "Salirasib in the treatment of pancreatic cancer," *Future Oncology*, vol. 6, no. 6, pp. 885–891, 2010.

[23] E. Aizman, E. Blacher, O. Ben-Moshe, T. Kogan, Y. Kloog, and A. Mor, "Therapeutic effect of farnesylthiosalicylic acid on adjuvant-induced arthritis through suppressed release of inflammatory cytokines," *Clinical and Experimental Immunology*, vol. 175, no. 3, pp. 458–467, 2014.

[24] A. Poggi, R. Carosio, D. Fenoglio et al., "Migration of V delta 1 and V delta 2 T cells in response to CXCR3 and CXCR4 ligands in healthy donors and HIV-1-infected patients: competition by HIV-1 Tat," *Blood*, vol. 103, no. 6, pp. 2205–2213, 2004.

[25] Y. Zhong, E. J. Smart, B. Weksler, P. O. Couraud, B. Hennig, and M. Toborek, "Caveolin-1 regulates human immunodeficiency virus-1 Tat-induced alterations of tight junction protein expression via modulation of the Ras signaling," *The Journal of Neuroscience*, vol. 28, no. 31, pp. 7788–7796, 2008.

[26] L. Agrawal, J. P. Louboutin, B. A. Reyes, E. J. Van Bockstaele, and D. S. Strayer, "HIV-1 Tat neurotoxicity: a model of acute and chronic exposure, and neuroprotection by gene delivery of antioxidant enzymes," *Neurobiology of Disease*, vol. 45, no. 2, pp. 657–670, 2012.

[27] L. Buscemi, D. Ramonet, and J. D. Geiger, "Human immunodeficiency virus type-1 protein Tat induces tumor necrosis factor-alpha-mediated neurotoxicity," *Neurobiology of Disease*, vol. 26, no. 3, pp. 661–670, 2007.

[28] J. E. King, E. A. Eugenin, C. M. Buckner, and J. W. Berman, "HIV tat and neurotoxicity," *Microbes and Infection / Institut Pasteur*, vol. 8, no. 5, pp. 1347–1357, 2006.

[29] X. Chen, L. Hui, N. H. Geiger, N. J. Haughey, and J. D. Geiger, "Endolysosome involvement in HIV-1 transactivator protein-induced neuronal amyloid beta production," *Neurobiology of Aging*, vol. 34, no. 10, pp. 2370–2378, 2013.

[30] F. Niu, H. Yao, W. Zhang, R. L. Sutliff, and S. Buch, "Tat 101-mediated enhancement of brain pericyte migration involves platelet-derived growth factor subunit B homodimer: implications for human immunodeficiency virus-associated neurocognitive disorders," *The Journal of Neuroscience*, vol. 34, no. 35, pp. 11812–11825, 2014.

[31] K. Matzen, A. E. Dirkx, M. G. Oude Egbrink et al., "HIV-1 Tat increases the adhesion of monocytes and T-cells to the endothelium in vitro and in vivo: implications for AIDS-associated vasculopathy," *Virus Research*, vol. 104, no. 2, pp. 145–155, 2004.

[32] M. Toborek, Y. W. Lee, H. Pu et al., "HIV-Tat protein induces oxidative and inflammatory pathways in brain endothelium," *Journal of Neurochemistry*, vol. 84, no. 1, pp. 169–179, 2003.

[33] Y. Chen, W. Huang, W. Jiang, X. Wu, B. Ye, and X. Zhou, "HIV-1 Tat regulates occludin and Abeta transfer receptor expression in brain endothelial cells via Rho/ROCK signaling pathway," *Oxidative Medicine and Cellular Longevity*, vol. 2016, Article ID 4196572, p. 9, 2016.

[34] R. F. Wu, Z. Ma, D. P. Myers, and L. S. Terada, "HIV-1 Tat activates dual Nox pathways leading to independent activation of ERK and JNK MAP kinases," *The Journal of Biological Chemistry*, vol. 282, no. 52, pp. 37412–37419, 2007.

[35] W. Huang, L. Chen, B. Zhang, M. Park, and M. Toborek, "PPAR agonist-mediated protection against HIV Tat-induced cerebrovascular toxicity is enhanced in MMP-9-deficient mice," *Journal of Cerebral Blood Flow and Metabolism*, vol. 34, no. 4, pp. 646–653, 2014.

[36] M. Strazza, V. Pirrone, B. Wigdahl, and M. R. Nonnemacher, "Breaking down the barrier: the effects of HIV-1 on the blood-brain barrier," *Brain Research*, vol. 1399, pp. 96–115, 2011.

[37] S. C. Wassmer, V. Combes, F. J. Candal, I. Juhan-Vague, and G. E. Grau, "Platelets potentiate brain endothelial alterations induced by plasmodium falciparum," *Infection and Immunity*, vol. 74, no. 1, pp. 645–653, 2006.

[38] R. Mishra and S. K. Singh, "HIV-1 Tat C phosphorylates VE-cadherin complex and increases human brain microvascular endothelial cell permeability," *BMC Neuroscience*, vol. 15, no. 80, p. 12, 2014.

[39] B. Spencer, R. A. Marr, R. Gindi et al., "Peripheral delivery of a CNS targeted, metalo-protease reduces Ab toxicity in a mouse model of Alzheimer's disease," *PloS One*, vol. 6, no. 1, article e16575, 2011.

[40] N. Iwata, S. Tsubuki, Y. Takaki et al., "Metabolic regulation of brain Abeta by neprilysin," *Science*, vol. 292, no. 5521, pp. 1550–1552, 2001.

[41] N. Kakiya, T. Saito, P. Nilsson et al., "Cell surface expression of the major amyloid-beta peptide (Abeta)-degrading enzyme, neprilysin, depends on phosphorylation by mitogen-activated protein kinase/extracellular signal-regulated kinase kinase (MEK) and dephosphorylation by protein phosphatase 1a," *The Journal of Biological Chemistry*, vol. 287, no. 35, pp. 29362–29372, 2012.

[42] P. A. Fitzpatrick, A. F. Guinan, T. G. Walsh et al., "Down-regulation of neprilysin (EC3.4.24.11) expression in vascular endothelial cells by laminar shear stress involves NADPH oxidase-dependent ROS production," *The International Journal of Biochemistry & Cell Biology*, vol. 41, no. 11, pp. 2287–2294, 2009.